

TOMSK POLYTECHNIC UNIVERSITY

P.V. Efimov, V.K. Kuleshov

RADIATION TESTING

Study Aid

Tomsk Polytechnic University Publishing House
2008

UDC 620.179.152(075.8)

BBC 31.42я73

E91

Efimov P.V.

E91 Radiation testing: study aid / P.V. Efimov, V.K. Kuleshov. – Tomsk: TPU Publishing House, 2008. – 295 p.

ISBN 5-98298-236-9

Principles of the radiation testing, receiving and registration of different kinds of radiation, radiation testing methods, problems of work safety in the radiation defectoscopy and the main applications of the radiation testing are considered and discussed. Some features of the most widespread methods and devices are also shown.

The textbook is developed in the framework of Innovative Educational Programme of the TPU on the direction “Nondestructive testing”. The study aid is designed at the Physical methods and Instruments of Quality Control Department of the TPU. The manual is intended for training students majoring in the specialties 200102 “Quality Control and Diagnostic Methods and Instruments” and 220501 “Quality management”.

UDC 620.179.152(075.8)

BBC 31.42я73

It is recommended for publishing as a study aid
by the Editorial Board of the Tomsk Polytechnic University

Reviewer

Doctor of Engineering,
Professor of the Tomsk State University of Architecture and Building
O.I. Nedavny

ISBN 5-98298-236-9

© Efimov P.V., Kuleshov V.K., 2008

© Tomsk Polytechnic University, 2008

© Design. Tomsk Polytechnic University
Publishing House, 2008

PREFACE

At present, the industrial development level of the foremost countries is characterized not only by the whole volume of industrial production and its big variety but also by the quality indexes of the production. The problem of the total quality improvement is realized by means of improvement of the quality of used raw materials, stuff, articles and objects. That, in its turn, allows to prolong the period of service of devices, machines and mechanisms as well as to decrease their material- and power-consuming and to increase the labor productivity.

An important role in the solution of this problem of the production quality improvement is assigned to the methods and means of nondestructive testing. Their development is attributed to a number of the most important directions of the scientific and technical progress.

Among the physical methods of nondestructive testing, the largest application (upwards of 80 %) at present got the radiation testing methods. The origin of the idea of nondestructive testing and the radiation testing too, can be related to the time of the discovery in 1895 by C.W. Roentgen the “roentgen” or “X-rays” which had allowed to detect not only a metal object inside a closed wooden box but also the non-uniformity of the internal structure of a metal.

The roentgen testing methods are based on the registration and analysis of the penetrating ionizing radiation. The penetrating radiation (roentgen, gamma-radiation, neutron flows and others), being passed through the thickness of an article, is weakened differently within the defective and non-defective cross-section and so give information about the internal structure of the matter and the presence of defects inside the tested objects. Radiation testing is used for the defectoscopy of the welded and soldered joints, iron casts, rolled metal, in medical diagnostics, in roentgenostructural and element analysis of substances, in dosimetry and radiometry and so on. A wide introduction and development of the radiation testing requires the training of skilled specialists. The quality of such specialists training depends much on the availability of special training appliances, which would set forth all the material of interest on the modern level and would choose the most essential moments for the given kind of testing.

The proposed textbook is an attempt to set forth systematically the basic theoretical and practical information in radiation nondestructive testing

corresponding to the requirements of the State educational standard for training the bachelors and masters in the specialty 200102 “Devices and methods of quality testing and diagnostics” and 220501 “Quality management”.

The following problems are considered in the textbook: physical bases of the radiation quality testing; the construction, characteristics and spheres of the application of ionizing radiation sources of different kinds; principles of the radiation image forming and their characteristics; the construction and main parameters of the ionizing radiation detectors; methods of the radiation image transformation into the visual one; different methods of the radiation testing; methods and means for providing labor safety conditions in radiation testing; some practical applications of the radiation testing.

The textbook is intended for students and instructors of technical universities.

Chapter 1

PRINCIPLES OF THE RADIATION TESTING

1.1. The spectrum of the electromagnetic radiation

The spectrum of the electromagnetic radiation is spread from the long radiowaves with wave lengths in meter-and-kilometre-zones up to high-energy gamma-radiation with wave lengths of a few picometers.

Table 1.1. gives a review of all electromagnetic spectrum.

It is clear from table 1.1 that the visible light envelopes only the very narrow wave zone of this spectrum, namely the zone from 350 to 700 nanometers. If the wave length achieves the sizes which are commensurable with the interatomic distances of the solid bodies, then the bodies become transparent for the electromagnetic radiation. Electromagnetic radiation of the similar wave length is generated owing to two mechanisms. Firstly, owing to the physical nuclear processes. In this case, the photons are emitted from the atomic nuclei. The similar radiation is the component part of the radioactive radiation and is called “gamma-radiation”. Secondly, because of the deceleration of the accelerated particles and also owing to the electron transfers, the high-energy photons are generated in the electron shell.

This radiation was called “the roentgen radiation” in honour of the first discoverer, and soon after its discovery in 1895 by the physicist Roentgen the radiation was used in the nondestructive testing.

The electromagnetic radiation has the wave and the corpuscular nature. The relationship between the radiation wave length and frequency is the following:

$$c = \lambda \cdot \nu, \quad (1.1)$$

where c is the propagation velocity; λ is the wave length; ν is the frequency of radiation.

The photon energy is connected by the Plank constant h with the frequency of radiation:

$$E = h \cdot \nu. \quad (1.2)$$

In accordance with the Einstein equation, there is the connection between the energy and proton mass:

$$E = m \cdot c^2, \quad (1.3)$$

i. e. protons have the mass m . The distinctive feature from the other elementary particles is that protons propagate with the light speed c .

Table 1.1

Spectrum of the electromagnetic radiation

Kind of wave	Mechanism of origin	Photon energy, eV	Wave length, m
Long waves, middle waves, short waves, ultrashort waves	Radiation by dipoles	$10^{-8} \dots 10^{-4}$	$10^2 \dots 10^{-2}$
Superhigh- frequency waves	Radiation by antenna	$10^{-4} \dots 10^{-2}$	$10^{-1} \dots 10^{-4}$
Infrared radiation	Thermal emission; transfers between the excited states of the molecules	$10^{-2} \dots 1$	$10^{-4} \dots 7 \cdot 10^{-7}$
Visible light	Light emission; electron transfers of the electrons from the external atomic electron shell	≈ 1	$7 \cdot 10^{-7} \dots 4 \cdot 10^{-7}$
Ultraviolet light	Electron transfers of the electrons from the external atomic electron shell	$1 \dots 100$	$4 \cdot 10^{-7} \dots 10^{-8}$
X-radiation	Deceleration of the accelerated electrons (bremsstrahlung radiation);	$10^2 \dots 10^3$	$10^{-8} \dots 10^{-15}$
	Electron transfers of the electrons from the internal atomic electron shell (characteristic radiation)	$10^4 \dots 10^5$	$10^{-10} \dots 10^{-12}$
Gamma-radiation	Transfers between the excited states of the atomic nuclei	$10^4 \dots 10^6$	$10^{-10} \dots 10^{-13}$

1.2. The formation and properties of the X-radiation

1.2.1. The formation

The X-radiation was discovered in 1895 by the German physicist Wilhelm Konrad Roentgen (1845–1923). He found that at the working out of the cathode-ray tube its screen emitted some invisible rays capable to spoil

photoplates through the black paper. Roentgen called the detected radiation “the X-rays”. Today the roentgen rays, as they are called in present time, are got by the help of the special electron-ray devices mainly by means of the roentgen tubes. Within the tube the beam of the accelerated in the electric field electrons is formed. This beam is directed on to anode and the electrons are decelerated in the material of the anode. At this process the roentgen rays are excited containing the hard electromagnetic radiation of the two kinds: the bremsstrahlung radiation and the characteristic radiation.

The roentgen radiation originates from the deceleration of the accelerated electrons in the solid body. The electrons are generated as the result of the thermal emission on the cathode and accelerated by the high tension added on the section between the cathode and anode (Fig. 1.1).

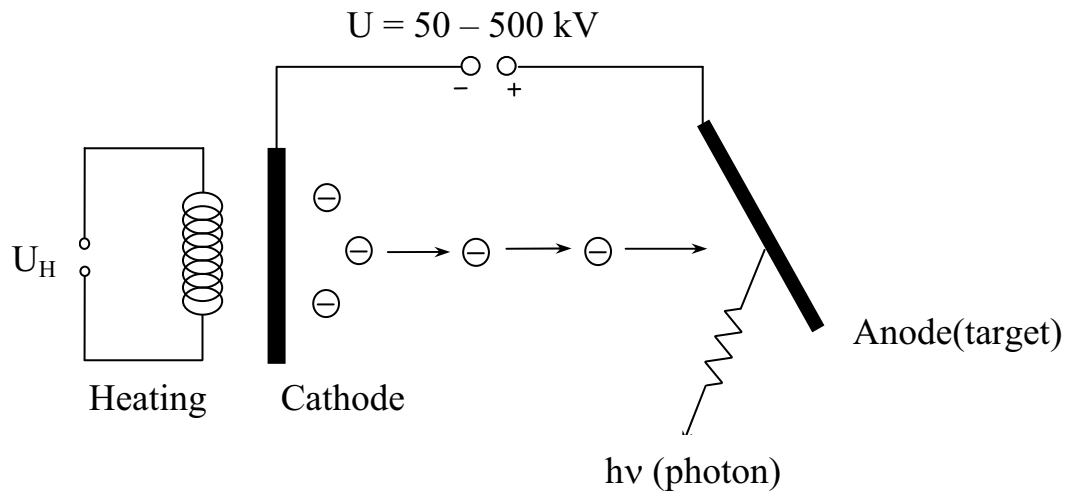


Fig. 1.1. The formation of X-radiation

At the collision with the anode electrons are decelerated. Owing to the electrons deceleration in the atomic nucleus field, a certain part of its kinetic energy is transformed into photons. The prevalent part of the electron kinetic energy is converted into the anode heating. Only a very small part of the kinetic energy is transformed into the X-radiation. The part of the kinetic energy of the electron which is transformed into the X-radiation is proportional to the accelerating voltage and to the ordinal number of the anode material. This part is within 1 % for the ordinary X-ray arrangements. The material of the roentgen tube anode must have as high the ordinal number as possible and must stand the high thermal loads. Tungsten corresponds most of all to these demands so that explains its application as the material of the roentgen tube anodes.

Since a large quantity of the thermal energy is formed and a good heat removal is required, only the target from the tungsten, i. e. that part of the

anode on which electrons fall, is suitable, and the remaining part of anode is made from copper, which can be cooled additionally by water or oil.

The bremsstrahlung radiation is the consequence of the deceleration of the electrons penetrating into anode at their interactions with the matter of nuclei through the electrostatic field (Coulomb interaction). At the deceleration process electrons lose the kinetic energy, which is transformed partially into the bremsstrahlung radiation energy. The maximally possible photons energy, i. e. the shortest wave length, occurs when the total kinetic energy of the electron is transformed into one (single) electron at collision.

The energy spectrum of the bremsstrahlung radiation is the continuous energy distribution of the emitted bremsstrahlung photons. It is explained by the fact, that electrons (in the beam) have different speeds and are decelerated mostly by multi-stage way having consecutive interactions with a large number of nuclei. The view of the energy spectrum of the bremsstrahlung radiation of different values of the accelerating tension U added to the roentgen tube is given in Fig. 1.2.

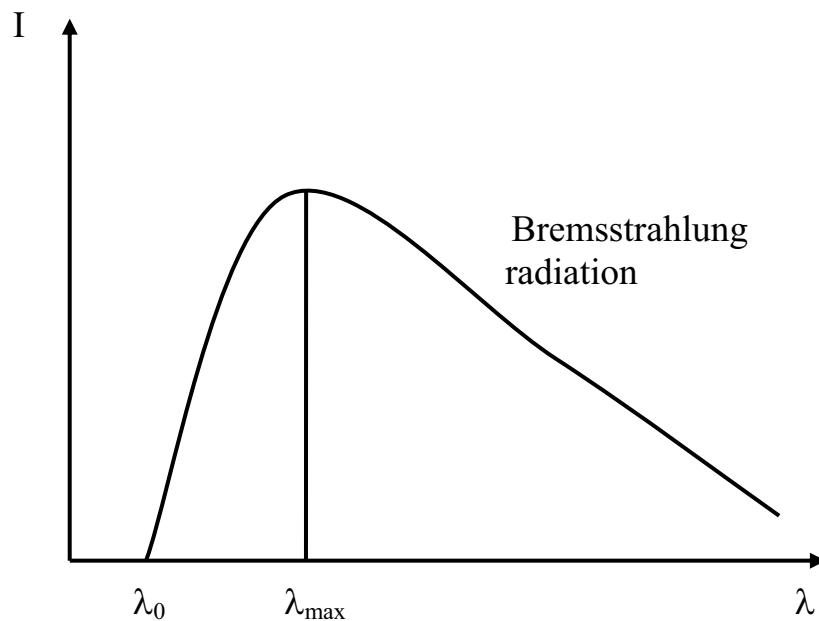


Fig. 1.2. Bremsstrahlung radiation spectrum

The wave length λ of radiation is on the abscissa axis and the intensity of radiation is on the ordinate axis. One can see that the radiation is emitted at all possible wave lengths, beginning with some minimum value λ_{\max} which determines the spectrum boundary. This value corresponds to the maximum kinetic energy of the electrons in the beam. The gradual decrease of the intensity in the long-wave part of the spectrum is stipulated mainly by the photon absorption in the wall of the glass envelope of the roentgen tube. The

absorption is the more the less the photon energy. The increase of the accelerating tension shifts the spectrum boundary towards the area of the short-wave radiation. Therefore, the hardness of the bremsstrahlung radiation may be controlled.

At passing the accelerating part with the accelerating tension (U_a) electrons get the energy $E = U_a \cdot e$, where e is the charge of electron. At total transformation of this energy into photon, the energy of the photon is equal to the energy of the accelerated electron. It follows from this that

$$h \cdot \nu_{\max} = U_a \cdot e, \quad (1.5)$$

where ν_{\max} is maximally possible frequency or the boundary frequency of the bremsstrahlung radiation spectrum and h is Plank constant. Taking into account the connection between the frequency and the photons wavelength ($c = \lambda \cdot \nu$), one can get the following relationship:

$$\lambda_{\max} = \frac{h \cdot c}{e \cdot U_a} = \frac{1.24}{U_a (keV)} \text{ [nm]}. \quad (1.6)$$

The wave length for maximum radiation intensity λ_{\max} is equal to $\lambda_{\max} = 1,5\lambda_0$.

For an ordinary X-ray installation one can change the X-ray spectrum by means of the variations of the accelerating tension U_a or the current passed in the roentgen tube. At this, the current in the tube may be changed with the help of the cathode tension change and it is accompanied by the increase or by the decrease of the thermoelectron emission in the cathode. The current increase in the roentgen tube does not mean that the energy of the accelerated electrons will be higher.

The spectrum of the tube radiation remains the same but the intensity of the radiation will increase.

On the contrary to this, the increase of the accelerating tension gives the rise of the electron energy and the roentgen radiation spectrum shifts towards the shorter wave lengths. Since the output of the roentgen radiation increases at the tension increase, so the radiation intensity increases at the accelerating tension increase.

Side by side with the bremsstrahlung radiation, the characteristic roentgen radiation is excited. The characteristic radiation is emitted by the anode material atoms. If the energy of the electrons penetrating into the anode is high enough, then they knock out the electrons from the internal atomic electron shells towards the external shell i. e. they excite atoms. Returning in the stable energy state, the atoms irradiate the gained energy surplus as the photons of electromagnetic radiation. Since the energy state of atoms is quantized, the spectrum of the characteristic radiation is discrete.

It consists of the lines of the so called K-, L-, M- and N- series which correspond to the values of the energy at transfer from the external shell of the excited atom on the stable internal K-, L-, M- and N-shells.

One must notice that the part of the characteristic radiation in total X-radiation is very small – it is not more than 1 %. Therefore this kind of radiation has no practical significance for the defectoscopy. However, the characteristic radiation is used successfully for roentgenospectral analysis of the matter at which the mentioned spectral lines are the distinctive sign of presence of the concrete chemical element in the analysed matter.

1.2.2. Properties

Since X-radiation is electromagnetic it spreads with the light speed. It can pass through any materials. At this, the penetrating capacity depends on the material properties and on the radiation wave length. The roentgen radiation can lead to the ionization, at the interaction with gases. Therefore, one often speaks about the ionizing radiation. The high energy of photons is the cause of the photons giving rise to the chemical reactions and their ability to destroy molecules especially the long organic molecules. Hence, the danger of the X-radiation for the living organisms generates. The roentgen rays can provoke damages in organism. Therefore, when handling the roentgen radiation it is very important to follow directions for the protection from the radiations.

1.3. X-ray and gamma-radiation interaction processes

1.3.1. X-ray and gamma-radiation

At passing the X-radiation with the intensity I_0 through the material the interaction of the radiation with this material occurs (see Fig. 1.3) This interaction leads firstly to the absorption of the X-radiation and, secondly, the scattered radiation is generated. This scattered radiation spreads in all directions. At using the collimator for the received roentgen radiation, the scattered radiation may be excluded. For narrow (pencil) beams one can get the absorption relationship, i. e. the intensity decrease normed on the path unit d_x in the matter is proportional to the initial intensity I . In this case:

$$dI / dx = - \mu \cdot I, \quad (1.7)$$

where the proportionality coefficient μ is called the weakening coefficient and it depends on the examined material and also on the wave length or the spectrum of the applied roentgen radiation. From the formula (1.7) the law of weakening for the “narrow beams” at passing through the material with the thickness d follows:

$$I(d) = I_0 \cdot \exp (- \mu \cdot d). \quad (1.8)$$

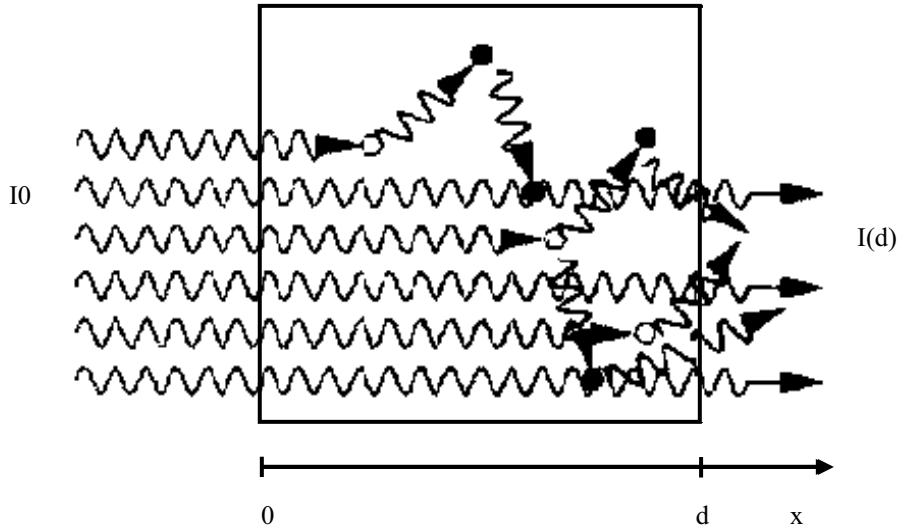


Fig. 1.3. The weakening of the roentgen and gamma-radiation

As a rule, the radiation testing is not conducted with the narrow beam for the image receiving. Side by side with the weakened primary radiation, the additional scattered radiation is registered and it can constitute a very large part of the total radiation at certain conditions. The registered by the detector intensity of the X-radiation at weakening in material with the thickness d will be higher in this case than at the collimated X-radiation (narrow beam). At this so called “broad beam”, the additional coefficient B is introduced by which the intensity I of the passed radiation increases:

$$I(d) = B \cdot I_0 \cdot \exp(-\mu \cdot d). \quad (1.9)$$

B is called “the build-up (accumulation)” factor and it depends on the ordinal number and thickness of the material, and also on photons energy and weakening coefficient. The law of weakening for the “narrow beams” has the same mathematics form as the law of the radioactive decay. One can calculate the thickness at which the intensity of the passed radiation will be 50 % from the input (initial) intensity I_0 . This thickness is called “the half-value layer” and is equal:

$$\Delta 1/2 = \ln 2 \cdot \mu^{-1}. \quad (1.10)$$

Fig. 1.4 gives the dependence of the half-value layer as well as the tenth-value and hundredth-value weakening layers on the photon energy at which the one /tenth or one/ hundredth part of input intensity is registered. Besides, for any energy of photons the corresponding X-rayed steel thickness is shown by the stroke.

The weakening of X-radiation is provoked by different mechanisms of the interactions between the radiation and the material. For nondestructive testing the most important processes are the following ones: the photoeffect,

the Compton scattering and the pair formation effect. Different mechanisms of the interactions are shown schematically in Fig. 1.5.

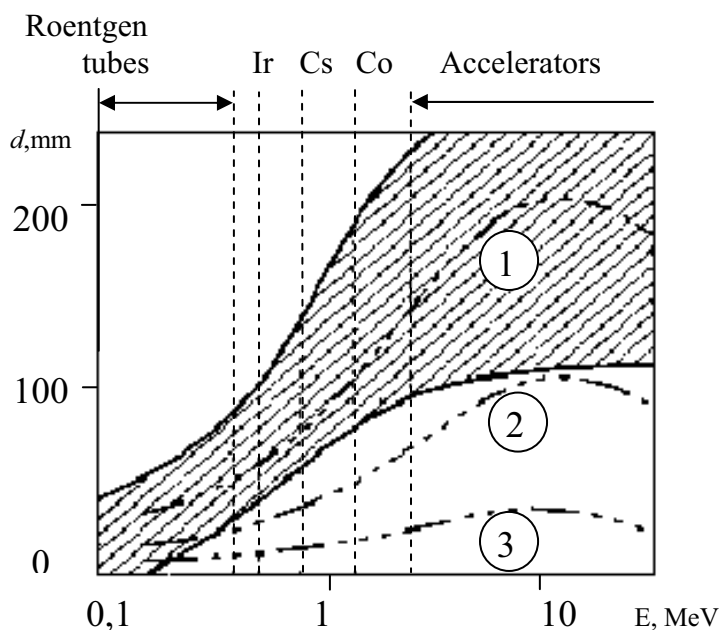
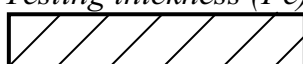


Fig. 1.4. Thickness of half-value, one /tenth, one/ hundredth layers of weakening for steel
 1 – one / hundredth part of thickness;
 2 – one / tenth part of thickness; 3 – half value layer;
 Testing thickness (Fe)



At the photoeffect the X-ray quantum is absorbed on the atomic electron shell and then an internal electron of the atom is knocked out owing to the inelastic collision between the roentgen quantum and the electron of the shell. In this case the energy of photon must be higher than the electron binding energy.

Since the free shell vacancy for the electron occurs owing to the photoeffect, then at the vacancy replacement by the external electron of the atom the secondary roentgen radiation (characteristic radiation) is generated. The contribution of the photoeffect in weakening coefficient is described by the factor τ . The weakening of the radiation at the expense of the photoeffect is strongly reduced with the photons energy increase.

On the external weakly-bound electrons of the atom the Compton scattering occurs. Photon transfers some part of its energy to the shell electron which is knocked from the shell. The energy loss by the photon leads towards the change of the wave length. The contribution of the Compton scattering described by the scattering factor σ , in the total

weakening coefficient falls with the rise of photon energy in slighter way than for the photoeffect.

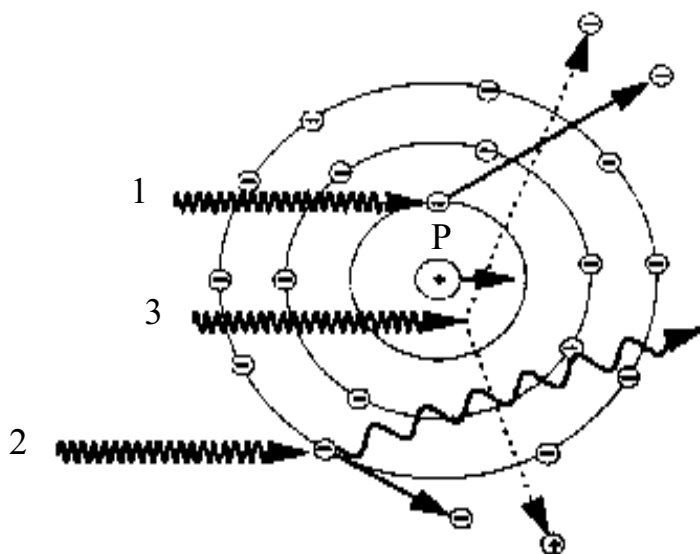
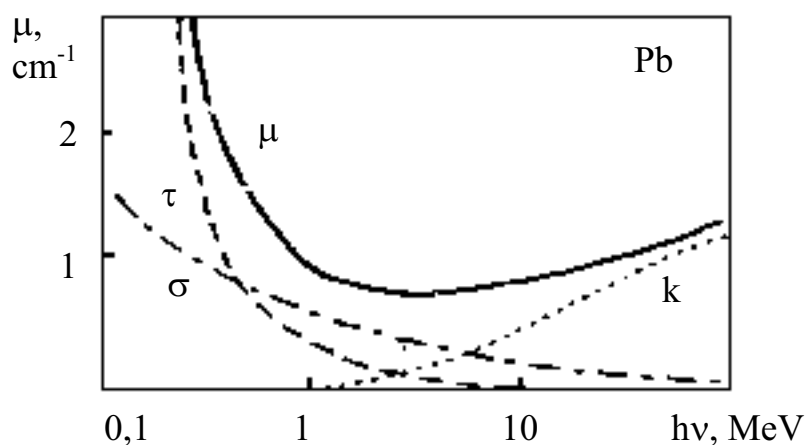


*Fig. 1.5. Mechanisms of the interactions of the roentgen radiation with the material:
1 – photoeffect (τ); 2 – Compton scattering (σ); 3 – pair formation effect (κ)*

High photons energies which are more than the double rest energy of a single electron, i. e. more than 1.022 Mev, can lead to the formation of the electron-positron pair in the area of the atomic nucleus. The photon energy is transformed into the mass of two elementary particles. The photon impulse is transferred on the atomic nucleus and a pair is formed near it. This effect is more effective the higher the photon energy. At the energies in a few MeV which are available in the accelerators the pair formation effect is described by the pair formation factor which introduces the largest contribution in total weakening coefficient. The prevailing in the weakening

of the X-radiation effect depends on the photon energy and on the ordinal number of the examined material (see Fig. 1.6)

For comparison of different materials the weakening factor μ is correlated with the density ρ and the mass weakening factor μ/ρ is determined. The advantage of the mass weakening factor is that for the material composed from several elements this factor can be calculated as the sum of the mass weakening factors of all separate elements. The roentgen radiation with the relatively short wave lengths is named as “the hard roentgen radiation” and on the contrary, the long-wave X-radiation is named “the soft roentgen radiation”.

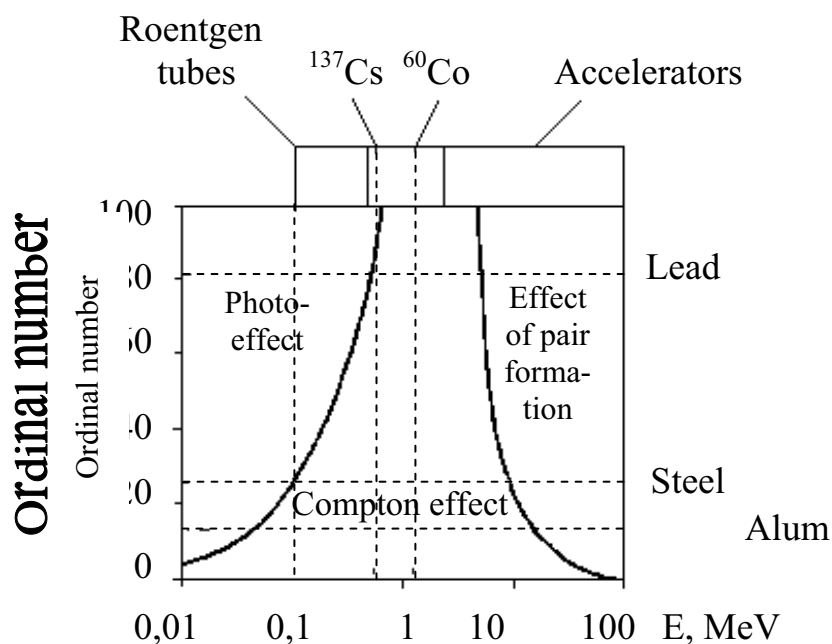


Fig. 1.6. The prevailing mechanisms of the X-radiation weakening

In the area of the X-radiation energies and for the isotopes, i. e. up to 1 MeV, the weakening factor is strongly reduced with the energy gain. It leads to the state that at passing of the X-radiation through the material the parts with high energy appear in the radiation spectrum because the short-wave radiation will be weakened less than the long-wave components of the spectrum.

Also the spectrum maximum shifts in the direction of the short wave lengths when the intensity of the X-radiation decreases in a common way.

The effect of the change of the X-ray spectrum form at passing through material is named “the hardening of X-radiation spectrum”. This change of the spectrum leads to the increase of the penetrating capacity of the X-radiation at passing through the tested material. This effect is applied solely in practice for example for filtering the low-energy part of the roentgen spectrum. More in detail the physics of the radiation interactions with the material is examined in the Appendix.

1.4. Physical principles of the radiation image formation and basic characteristics

1.4.1. Radiation contrast

The weakening of the X-radiation depends on the thickness of examining material. In the defects area the examining thickness of the material is less. Defects may be either the emptinesses as pores or they may be filled by the absorbing materials, for example, by slag. If the sources of the X-radiation are considered approximately as the point, then the process of the radiation intensity relief appearance at the examining can be understood from Fig. 1.7. At this, the X-radiation intensity in the defect area I_d will be higher than in other zones if the weakening factor of the defect is less than that of the examining material. And, on the contrary, the intensity will be less if the defect is filled by the material with the weakening factor higher than it is for the tested material. It is possible at steel testing when there are inclusions of heavy metals, e.g. tungsten, in the testing object.

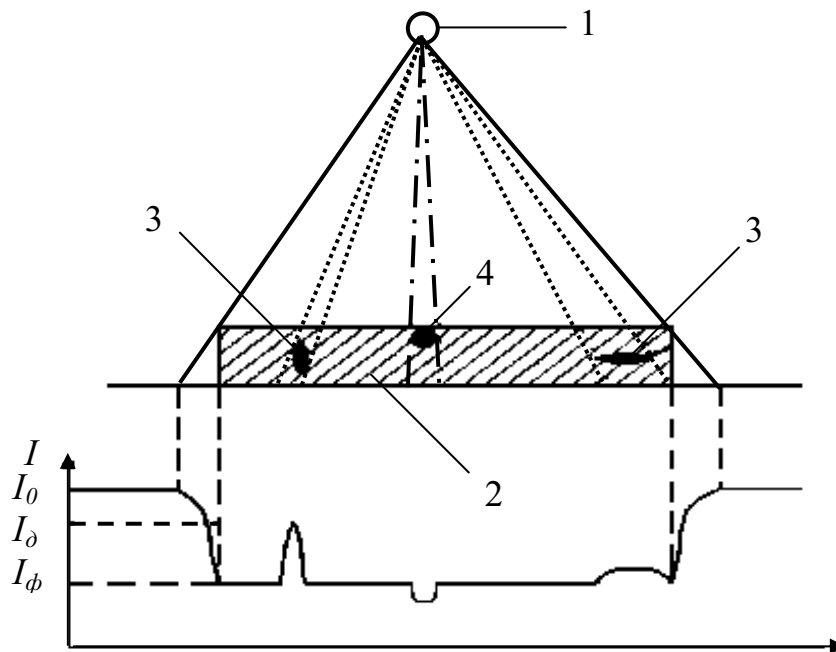


Fig. 1.7. The appearance of the examining picture:

1 – Irradiator (source); 2 – testing object;

3 – nonuniformity with $\mu d < \mu$; 4 – nonuniformity with $\mu d > \mu$

This energy distribution at the radiation testing becomes visible owing to a certain registering material. One must notice that at the examining the question is always about the central projection, i. e. on the base of the geometric relationships the appearance of the shift or the gain of the imaged defect is possible. Defects oriented along the examining direction give more

values of contrast than the defects disposed perpendicularly to the examining direction. Hence, at the determination of such critical (minimum) lengthy defects as cracks the problem appears to orientate the testing object in such a way that the defects will be oriented better in the direction of examining.

The ratio of the difference between intensities I_d and I_{ph} ($I_d - I_{ph}$) to the passed radiation intensity outside the defect area I_{ph} is called “the radiation contrast” K_r . At this, I_{ph} is composed from the intensity of the passed primary radiation I_{uns} and the intensity of the scattered radiation I_{sc} . Since the scattered radiation is distributed uniformly onto all image, the difference $I_d - I_{ph}$ can be considered only as the difference between the unscattered radiation passed through the defect and passed through the area without defects:

$$K_r = \frac{I_d - I_{ph}}{I_{ph}} = \frac{\Delta I}{I_{uns} + I_{sc}} \frac{I_{uns}(defect) - I_{uns}}{I_{uns} + I_{sc}}. \quad (1.11)$$

Taking into account the law of the X-radiation weakening (1.8) the following expression may be written for the image contrast:

$$K_{sc} = \exp[\Delta d (\mu - \mu_d)], \quad (1.12)$$

where Δd is the change of the sample thickness in the defect area and μ is the weakening factor of the material; μ_d is the weakening factor of the defect. In the case of gas-filled defect, i. e. at $\mu_d = 0$, the approximate relationship is established:

$$\Delta I = I_{uns}(defect) - I_{uns} = I_{uns} \cdot \mu \cdot \Delta d. \quad (1.13)$$

By substitution (1.13) and (1.11) one can get the following:

$$K_r = I_{uns} \cdot \mu \cdot \Delta d / I_{uns} + I_{sc} = \mu / (1 + I_{sc} / I_{uns}) \cdot \Delta d. \quad (1.14)$$

The value C_{sp} which is equal

$$C_{sp} = \mu / (1 + I_{sc} / I_{uns}) \quad (1.15)$$

is called “the specific contrast”.

The image contrast K_r is proportional to the defect lengthy Δd and to the specific contrast C_{sp} :

$$K_r = C_{sp} \cdot \mu \cdot \Delta d. \quad (1.16)$$

Fig. 1.8 shows the contrast dependence on the examining thickness of the steel sample at different energy values.

The contrast increases at lower energies as a result of the weakening factors gain and also at reduction of the sample thickness. It is interesting that at very high energies achieved by means of the accelerators and at big thickness one can achieve a better contrast than at the low examining energies with isotopes. It occurs because at such a high energy another weakening mechanism prevails, namely the pair formation effect.

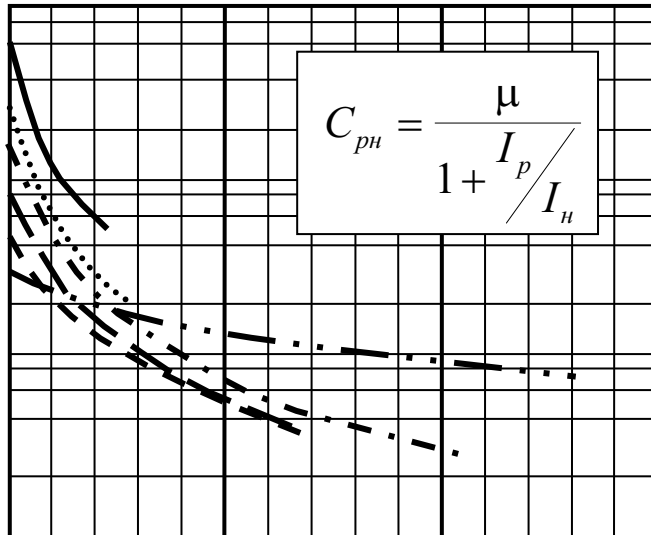


Fig. 1.8. Specific contrast

- 100 kV
- 200 kV
- · - · - · 400 kV
- Ir 192 (0,1 mm Pb)
- · - · - · Co 60 (0,1 mm Pb)
- 15 MeV (1.5 + 0.5 mm Pb)

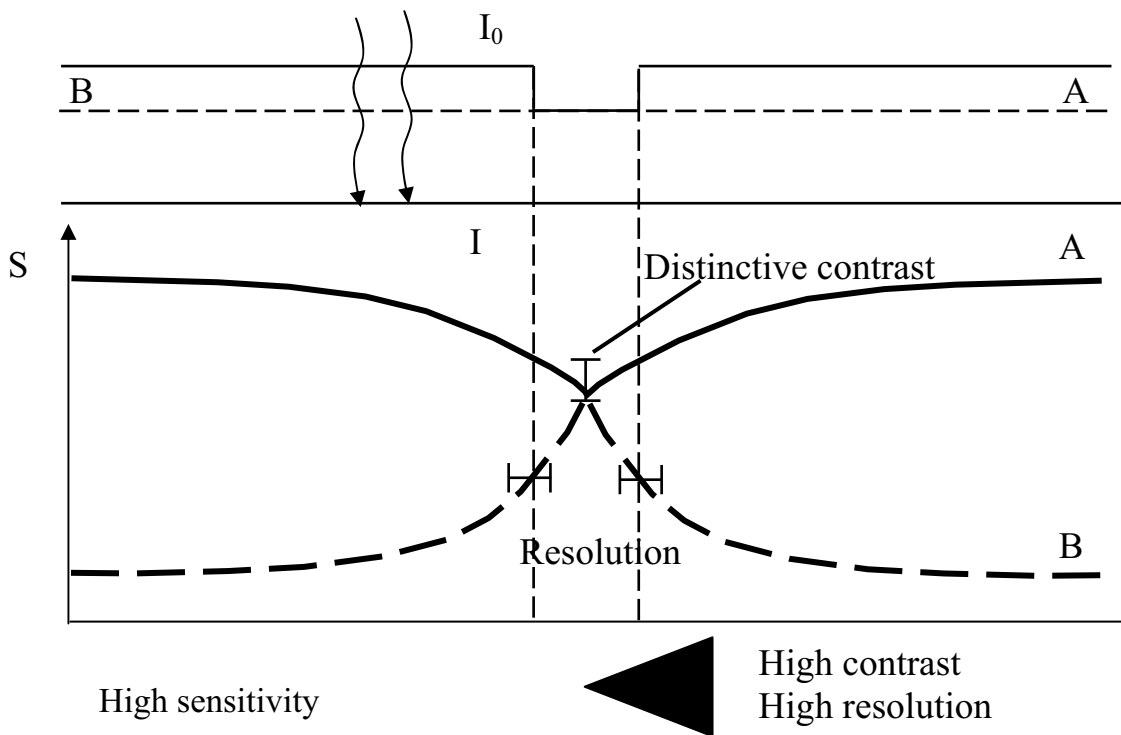


Fig. 1.9. Contrast and unsharpness

One more effect leading to the contrast decrease must be taken into account at the receiving of the defect image. The roentgen sources can not be

the point ones and have limited length in a few millimetres. It leads to the unsharpness of the defects boundary, as it is given in Fig. 1.9. The unsharpness reduces the contrast. Therefore, at testing particularly thick-walled components, as accurate as possible orientation is required in the examining direction.

1.4.2. Geometrical unsharpness

Geometrical unsharpness U_g is stipulated by the limited sizes of the focal spot (optical focus), i. e. the projection of the irradiator section emitting the ionizing radiation on the plane which is perpendicular to the beam axis (to “central ray”). It follows from the geometrical considerations that

$$U_g = F \cdot l_c / l_f, \quad (1.17)$$

where F is effective linear size of the focal spot, l_f and l_c are the distances between the object and tube focus and between the object and image converter. It follows from here that for the geometrical unsharpness reduction one must seek to use the irradiators with the minimum focal spot size and to dispose the object as close as possible to the image converter and farther from the radiation source. If the roentgen tube is used as the irradiator, the problem how to combine as high as possible tube power with a rather small size of the focal spot appears. Taking this into account, the anode slant (the angle α between the anode surface and the beam axis) is chosen so that at the relatively large square of the anode section (electron focus), onto which the electron flow is directed, the tube optical focus will be minimum. In reality, the size and the form of the optical focus are not the same for the different sections of the image converter. This distinction is reduced at distance f from focus to converter gain and at decrease of the working field. One must also take into account that electrons are decelerated in some depth inside the anode so the radiation passing from it at small angles to the anode surface is weakened more by the anode material than the radiation passing out at big angles. This state limits the possibilities of the angle α reduction and stipulates the non-uniformity of the radiation distribution on the surface of the image converter, which is developed the more, the less the ratio between f and the surface sizes.

The additional source of the unsharpness may be the afocal (extrafocal) radiation which appears owing to the fact that about one-half of electrons number reaching the anode either refract from the anode or cause the emission of the secondary electrons decelerated out of the electron focus. With the help of the special catcher of such electrons this effect may be reduced to a minimum so that the part of the afocal radiation is decreased from 8–10 to 3 %. One must also take into account that this radiation has lower energy than the radiation created by the primary electrons deceleration. One usually seeks to do so that along the beam axis the optical focus will have the square form whose side is assumed as the size of the focal spot. At a deviation from this form, F is

considered equal to the one-half of the maximum and minimum size sum. The decrease of the focal spot of the X-ray tubes is limited by the temperature increase of the anode section bombarded by electrons and above 99 % of their energy is transformed into heat. In order to reduce the anode heating for the tubes applied in the defectoscopy where the exposure time is determined in a few minutes, the water cooling is used and for the medical tubes a special anode construction is applied and, partially, the rotating anode. The electron focus of this anode is shifted by the ring and at the same time the optical focus remains immobile. Having in view that for different problems the focus of the different size is needed, the two-focus tubes are made. The long focus of this tube is used for the study of the mobile objects when short exposures are needed and the small (short) focus is used for the roentgenography of the immobile objects with thin structure, and partially for the receiving of the shootings with the so called direct (geometrical) gain which is achieved by removal of the cassette with screens and film from the study object (it is clear that the image size relates to the object size as l_c / l_f). The typical sizes of the long focus spot for medical tubes are 1,2 mm and the small focus – 0,3...0,6 mm. Hence, for direct gain the focus of less size is used sometimes. In the tubes applied in defectoscopy the focus spot achieves the 4 mm – size. The typical values of the unsharpness are equal to $U_g = 0.1...0.5$ mm.

If the focus size is bigger than the size of the detail which must be regenerated on the image (e.g. at detection of the pores in welded joint, the details of the bone structure, the microcalcionats in the mammography of the milk gland, etc.) so, in case of dependence on distance between the objective and the film (Fig. 1.10) the full shadow with the size less than the detail is formed or the pseudo-shadow (disposed lower the plane II) with the lower contrast is formed. The pseudo-shadow contrast ratio to the full-shadow contrast can be determined on the base of geometrical considerations.

At the radiation passing through the small hole the image of the radiation source focus but not the image of the hole appears on the film remote from the hole. The application of the so called “lokh-chambers” for measuring the focus spot sizes is based on this principle.

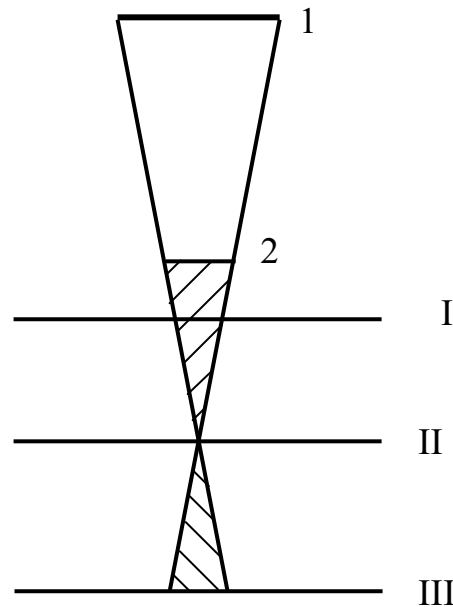


Fig. 1.10. The formation of the image:
1 – focal spot; 2 – article

1.4.3. Dynamic unsharpness

The dynamic unsharpness U_d appears at receiving the mobile objects shootings. U_d is stipulated by the displacement of the object at the exposure time t . The value of U_d may be determined by the formula

$$U_d = (l_c / l_f) \int_0^t V(t) dt, \quad (1.18)$$

where $V(t)$ is the component of the motion speed directed parallel the film. If the object performs oscillations, then the value of U_d is not higher than the amplitude of oscillation multiplied by the image gain factor $m = l_c / l_f$.

In medical practice it is necessary to take into account the involuntary movements connected with the physiological functions of the human organs: the heart pulsation, the stomach peristalsis, etc.

For the haemorrhage rate, the heart walls motion and for the area of the lung fit close to the heart, the values of the $V = 50\text{--}500 \text{ mm}\cdot\text{cm}^{-1}$, and taking into account the non-uniformity of these organs motion, the exposure is recommended not more than 5 microseconds (for the lung parts remote from the heart the exposure can be raised up to 20 microsecond); for the gullet $V=50\div 200 \text{ mm}\cdot\text{cm}^{-1}$ and the recommended value $t=10$ microseconds; for the stomach and the bowels the data of different authors as related to the peristalsis rate are from $1.5\div 15 \text{ mm}\cdot\text{cm}^{-1}$ up to $50 \text{ mm}\cdot\text{cm}^{-1}$ and even higher and the values of the optimal exposure will be from $10\div 20$ to $100\div 200$ microseconds.

Besides the involuntary motions of the human body organs one must take in account the vibration of the radiation sources and cassette especially at the tomography and also the motion of the articles studied in the defectoscopy. A lot of designs conducted in the roentgenotechnic sphere are directed on the guaranteeing of the mentioned short exposures and, partially, the construction of the roentgen apparatus of the higher power with the small tension pulsation. The transfer from the single-phase to the three-phase apparatus allows to increase the radiation output by one-third at the same tension and current. The semi-wave apparatus gives no possibility to get shootings at the exposure less than the duration of the alternative tension period with frequency 50 hertz, i. e. less than 20 microseconds. Therefore, the six-pulse and twelve-pulse apparatus were designed allowing to reduce the exposure time up to 5...10 microseconds in the first case and up to 2 microseconds in the second case. In order to achieve such a short exposure at really achieved apparatus power in 50...100 kW, the high-effective gained screens, which have been constructed in recent time, are used. At the high-speed processes study, for example, at the detonation wave motion or the missile

motion the exposure shorter than 1 microsecond is needed. The impulse roentgen apparatus are designed for this purpose. They are used in combination with the screen and films composition having a high sensitivity.

1.4.4. The screen or own unsharpness

Owing to the granular structure of the most luminescent screens applied in defectoscopy and medicine and owing to sufficient thickness of the illuminating layer the reduction of which is limited by the reduction of the screens efficiency and by the increase of the structural granularity, most of the light coming into the detector, including the boundary of the irradiated part of the screen, deviates from the normal to the screen surface. The larger is the angle characterising this deviation, the longer the light path and the stronger it deviates. At the same time the illumination is weakened in the area close to the boundary of the irradiated section because part of light is getting out the section limits.

As a result, the light flow distribution is maintained and provokes the so called “screen unsharpness” of the image.

As distinct from the geometrical and dynamic unsharpness, it is difficult to determine the boundaries of the screen unsharpness because the curve of the brightness B distribution on the screen or the blackening S on the film approach asymptotically towards their extreme values.

If the steepest part of this curve is rectilinear, then by its continuation up to the intersection with the horizontal straight lines concerning the maximum and minimum values of B or S one can determine the distance on the abscissa axis between the intersection points. This distance is taken as the measure of the screen unsharpness U_s . Sometimes it is recommended to lead the straight line through the points concerning 16 and 84 % of the maximum value of B or S. In both cases it is assumed that it is the steepest part of the boundary curve that determines the subjective perception of the unsharpness.

In order to get the reproducible results, one must conduct the measuring very scrupulously. If the boundary curve is plotted by the results of the shootings photometry of the edge of the non-transparent for the ionizing radiation object, for example, a lead plate, then the receiving conditions must be strongly standardized. One must seek to achieve the same maximum blackening density in all shootings, with the error not more than ± 0.05 , because at the gain of the blackening density overfail the measured value of the U_s increases. It may be stipulated that a corresponding increase of the exposure dose leads to the appearance of the blackening on the parts behind the object edge where there was no blackening at lower doses, because for blackening generation, some minimum (threshold) illumination must be exceeded.

In order to minimize the influence of the film properties and the phototreatment conditions, it is recommended to plot the boundary curve

in the $B(x)$ or $I(x)$ – coordinates by using the characteristic curve received at the same conditions.

Arrangements for the direct microphotometry of the image on the screen are available and they are used mainly in the roentgen image intensifier (RII) study and in the study of the screens for roentgenoscopy and fluorography. Hence, one must have in view that in the case of applying the combination of the gain screens set with the two-sided film this method is difficult for using, because the unsharpness appearing in this case is stipulated not only by the screens but also by the film, owing to the effect of the intersection spoiling (cross-over). This effect consists in that the light emitted by the screen (including the light belonging to the photoactinic area of its spectrum) is passed partially by the emulsion layer fit close to the screen and then comes onto the second emulsion layer, which is the reason of its blackening. This light can also scatter mainly owing to the refraction. As a result, the additional component of the unsharpness appears and it is similar to the component observed at the incompact screens pressure to the film. It is to be taken into account especially in recent time in connection with the tendency of the decrease of the silver layer thickness for its economy (the corresponding decrease of film sensitivity is overlapped by the increase of the screen efficiency).

Besides the thickness of the luminescent layer, the size of the luminophor granule and the intersection spoiling effect, the screen unsharpness is also influenced by the following factors: the granule's form and the density of its packing; the luminophor refraction factor; the presence of the reflecting layer and the pigment added specially for the unsharpness and granularity reduction; the disposition of the screen in the cassette (the front, i. e. the first along the radiation spreading screen provokes a bigger unsharpness, than the back screen); the chemical content of the luminophor and the spectrum of the applied ionizing radiation, on which the generation of the characteristic and scattered radiations depend, and the path of the photoelectrons in the screen luminescent layer.

Depending on the screen types, its using conditions and measuring method, the values of the screen unsharpness usually given in the literature range within (0.2...0.4) mm for the luminescent intensifying (gained) and up to 0.7 mm for the roentgenoscopic screens.

1.4.5. Other sources of the image unsharpness. The sum unsharpness

In the case when the ionizing radiation is directed not perpendicularly to the screens and film surface (e.g. in tomography and oblique projections) or when the direction of the observation of the image received on the monocrystalline screen does not coincide with the direction of the luminescence exciting radiation spreading (for example, at the viewing of image close to the screen edges), then the unsharpness appears which is called “parallaxic” U_p . In the first case it is

determined by the roentgen ray path section on both screens of the set and in the film projection on the plane in which they are disposed. Therefore U_p depends on the tomography angle or the oblique projection angle on the screens and film thickness. In the second case, as it follows from the geometrical considerations,

$$U_p = d_s \cdot \cos(90^\circ - \alpha - \beta) \cdot (\cos \beta)^{-1},$$

where d_s is the thickness of the monocrystalline screen; α and β are the angles between the normal to the screen surface and the directions of the observation and of the incidence of the ionizing radiation correspondingly.

In using the roentgenographic films without screens and also with the metal foils the unsharpness appears stipulated by the action of the photo- and Compton-electrons moving in different directions.

At $E_{\text{eff}} = 250$ keV it is only about (0.05...0.1) mm for the film without screens and about (0.15–0.2) mm in the case of the lead foils using. However, the unsharpness raises fast at the further gain of the quantum energy, reaching 0.17 mm for the film without screens and 0.5 mm at the film combination with foils at $E_{\text{eff}} = 1$ MeV.

A special kind of the unsharpness is connected with the phenomenon near the edge of the detail disposed inside the scattering body: a gradual change of the scattered radiation intensity occurs (The study object is here in the role of the radiation source with a large focal spot). This effect is reduced at the transfer from the roentgen to the high-energy gamma-radiation owing to increase of the scattered radiation part whose spreading direction is near the direction of the primary beam.

The image is received unsharp because of the decrease of the primary radiation weakening near the object edge, which is connected either with its form or with the radiation beam being divergent. This so called “absorption” or “morphological” unsharpness characterizes the features of the object structure and therefore, in the general case, it is not the factor decreasing the image informativity. But in some cases, for the more reliable recognition of the small-contrast details, for example, the pathological formations in the milk gland, one resorts to the artificial gain of the detail contours by using the xeroroentgenography where it is achieved owing to the edging effect or by using the television facilities of the image harmonisation.

The sum image unsharpness U_{sum} is determined mainly by its biggest component. In the cases when the basic components of the unsharpness have similar (almost the same) values, their added action is often determined by using the approximate equations:

$$U_{\text{sum}} \approx \sqrt{U_g^2 + U_d^2 + U_s^2} ; U_{\text{sum}} \approx 3\sqrt{U_g^3 + U_d^3 + U_s^3} . \quad (1.19)$$

However, the difference of the boundary curve form stipulated by the screen unsharpness from the curves forms connected with the geometrical and dynamic unsharpness leads to the fact that in reality their relative contribution to the sum unsharpness and unsharpness influence on the contrast is strongly dependent on the detail size because the increase of the size reduces the role of the U_g and U_d in comparison with the U_s .

When comparing the U_{sum} measuring results with the subjective perception of the unsharpness one must take into account the Max effect consisting in the phenomenon that near the boundary between the dark and light fields the dark field seems even darker and the light field seems even lighter. As a result of this the impression of the non-uniform illumination of each field is made and the boundary between the fields seems the sharper the higher the contrast. So, by means of the visual analyzer the same image contour gain is realized as it is achieved by the application of the above-mentioned television harmonizers.

1.4.6. The frequency-contrast characteristics

In the case of small details, the overlapping of the unsharp image instalments leads towards the decrease of contrast which is the more, the less is the size of the detail. In order to determine the character of the detail image contrast dependence on its size, test objects are in used most cases; they are the lead foils with thickness 0.05...0.1 mm and with the row of slits divided by the intervals with the width which is equal to the slit width. The number of slits normed on the length unit (usually one speaks about strokes number, number of line pairs or the number of periods on 1 mm or 1 cm) is called "the space frequency of the mira ν ". Instead of the miras set with different ν one can use the single mira with the fine changed ν .

The dependence of the test object image contrast k_t is called the contrast transfer coefficient M_{tr} which has the following form in this case:

$$M_{tr} = \frac{(B_{max} - B_{min}) / (B_{max} + B_{min})}{[(B_{max} - B_{min}) / (B_{max} + B_{min})]_{\nu \rightarrow 0}}. \quad (1.20)$$

The maximum value of the k_b placed in the denominator of this expression is achieved practically at $\nu=0,05 \text{ mm}^{-1}$ and rarely at smaller values of ν . The function $M_{tr}(\nu)$ is called the amplitude characteristic, or the function of contrast transfer (FCT) or the rectangular frequency-contrast characteristic.

In order to determine the loss of the involuntary form detail image contrast one must, however, use the test objects of the sinusoidal form but not the rectangular. It is connected with the fact that the space distribution of the ionizing radiation intensity passed through any object (radial profile) in using the Fourier analysis may be presented as the sum of the sinusoidal form

components different from each other by the frequency ν and the amplitude (in practice, for this purpose the Fourier conversion is added to the object shooting on the out-screen film conducted under conditions of the small geometrical and dynamic unsharpness). The space-frequency spectrum of the object received by this way is compared with the function $M(\nu)$ of the sinusoidal mira contrast transfer which is called “the space frequency contrast characteristic” (FCC) or the function of the modulations transfer. This function characterizes the system of the image formation (independently on the study object properties) as the filter at passing through which the components amplitude of the space-frequency spectrum of the object decreases to a different degree depending on their frequency ν , i. e. the FCC is:

$$FCC = \frac{\text{space - frequency spectrum of the image}}{\text{space - frequency spectrum of the object}}. \quad (1.21)$$

The connection between the FCC, FCT, the function of the line scattering and the edging function. It is quite difficult to make the sinusoidal mira from the strongly weakening the roentgen radiation materials. Therefore in practice the FCT is measured by using the following formula for the transfer towards the FCC:

$$M(\nu) = \frac{\pi}{4} \left[M_{tr} + \frac{M_{tr}(3\nu)}{3} - \frac{M_{tr}(5\nu)}{5} + \frac{M_{tr}(7\nu)}{7} - \dots \right]. \quad (1.22)$$

Besides, the FCC is received as a result of the line scattering function transformation, i. e. the distribution of the light intensity on the narrow slit $\Lambda(x)$ image which is connected, in its turn, with the edging function $I(x)$, i. e. stipulated by the unsharpness of the light distribution on the edge image (Fig. 1.11).

$$\Lambda(x) = \frac{dI}{dx} \quad I(x) = \int_{-\infty}^x \Lambda(x) dx$$

$$M(\nu) = \sqrt{\left(\int_{-\infty}^{\infty} \Lambda(x) \cos 2\pi \cdot \nu \cdot x \cdot dx \right)^2 + \left(\int_{-\infty}^{\infty} \Lambda(x) \sin 2\pi \cdot \nu \cdot x \cdot dx \right)^2} \quad (1.23)$$

In this case the condition of the normalization is

$$\int_{-\infty}^x \Lambda(x) dx = 1.$$

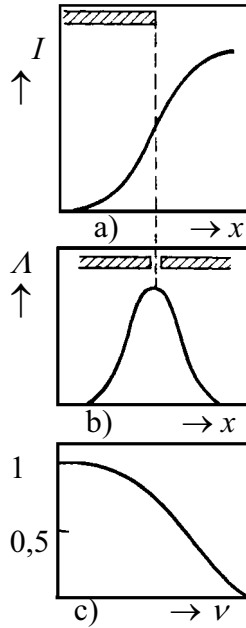


Fig. 1.11. The binding between the edge function a), the line scattering function b) and the frequency-contrast characteristic c)

It follows from equations (1.22) and (1.23) that $M(v) = 1$. The mentioned relationships are the base for the three methods of the FCC measuring: by means of the mira image, by means of the narrow slit and by means of the plate edge. In all cases the strong diaphragming is conducted and also some measures are taken in order to minimize the influence of FCC of the measuring facilities. In case of need, the corresponding corrections are made partially in the FCC of the measuring slit of the microphotometer. From the considerations which have been stated at the unsharpness determination methods consideration it is expedient at the radiography and fluorography to do the transfer from the blackening density distribution to the shooting towards the illumination intensity distribution on the screens with the help of the film characteristic curve, or, at the fluorography, to measure directly by means of the scanning microphotometers.

In order to determine the FCC by the experimentally measured FCT, the calculation is fulfilled in accordance with the formula (1.22) for several values of v . At this, for the highest v all members of the series, except the first one are cast away and at the transfer towards the lower v the number of the series members is increased with the decrease of v . For example, if the $M_{tr}(v)$ is measured up to $v = 6 \text{ mm}^{-1}$, then $M(5) = (\pi/4) M_{tr}(5)$,

$$M(2) = (\pi/4)[M_{tr}(2) + (1/3)M_{tr}(6)];$$

$$M(1) = (\pi/4)[M_{tr}(1) + (1/3)M_{tr}(3) - (1/5)M_{tr}(5)]; \quad (1.24)$$

$$M(0,5) = (\pi/4)[M_{tr}(0,5) + (1/3)M_{tr}(1,5) - (1/5)M_{tr}(2,5) + (1/7)M_{tr}(3,5)].$$

At the direct measuring of the line scattering function (LSD), the slits with the width in 5...10 micrometers are used for the out-screen film; with the width in 1...200 micrometers for the combination of the gained screen with the film, and wider for R I I. The value of M for several ν is calculated by the formula (1.23) with the account of the normalization condition. If the LSF is approximated by the exponential function, the calculation becomes essentially simpler. Taking into account the difficulty of the diaphragm making with such a narrow slit and the above-mentioned difficulties of the edging unsharpness measuring, the FCC is determined more often with the help of the lead miras. Since the values of the M_{tr} are averaged for every frequency and repeatedly at the graph $M_{tr}(\nu)$ plotting, a better reproducibility than for other methods is achieved.

The basic components of the space FCC of the image formation system. The FCC of the complete systems. The FCC is simply connected with the edging function. Therefore FCC as well as the image unsharpness may be divided into the geometrical $M_g(\nu)$, dynamic $M_d(\nu)$ and screen $M_s(\nu)$ components. Their independence from each other allows to determine the total FCC of the system as the multiplication of these components:

$$M(\nu) = M_g(\nu) \cdot M_d(\nu) \cdot M_s(\nu). \quad (1.25)$$

At this, as distinct from the relationships above, this equation is preserved in the wide range of the ν values. By the similar way one calculates the FCC of the complete system of the image formation, for example the radiotechnical system by the data of FCC of its elements which allows to estimate the relative influence of every element. In the production of the FCC of the system elements the FCC of the measuring facility also comes. In order to exclude its influence, the measuring result must be divided by it.

The geometrical and dynamic components of FCC are connected with the corresponding unsharpnesses by formulas

$$M_g = [\sin(\pi\nu U_g)]/(\pi\nu U_g); M_d = [\cos(\pi\nu U_d)]/(\pi\nu U_d). \quad (1.26)$$

The connection of the screen component of the FCC with the U_s is written satisfactorily by the equation

$$M_s(\nu) = 1 / (1 + 7.5 U_s^2 \cdot \nu^2). \quad (1.27)$$

In some cases $M_s(\nu)$ may be conveniently approximated by the exponential function

$$M_s(\nu) = \exp(-2 \pi \cdot \alpha \cdot \nu), \quad (1.28)$$

where α is the parameter simply connected with the $M_p(\nu)$ at the given frequency. At the close values of the U_g and U_s the influence of the M_d and M_s on the small details contrast is non-uniform: at $\nu = 0.5 \div 1.5 \text{ mm}^{-1}$ the

influence of the M_s is considerably higher and only for the smallest details the roles of the M_g and M_s are the same. It is stipulated by the difference of the form of the geometrical and screen components of the FCC. Often, especially in the technical documentation, the FCC is characterized by a single value, e.g. by value M or M_p at the certain ν (2 mm^{-1} for the combination of the screens with the film or by the value ν at $M = 0.1$; $M = 0.5$ or $M = t/e$).

The value ν_{exp} , which is equal to that space frequency at which M is reduced by e times, is called the effective width of the space transmission strip.

One must notice that the FCC for the (Zinc Sulphur · Cadmium Sulphur – Argent) – screen for the roentgenoscopy and fluoroscopy is near the FCC of the photochannel of the R II and, so, it is better than FCC of the television channel of the RII though in the reality the detail discerning at the roentgenoscopy with using of such a screen without the image gain is worse than at the examining with the roentgen image intensifier because of the low contrast sensitivity of the human eye under the twilight vision conditions.

But also at the optimal illumination one must take in account the properties of the eye and its FCC, $M(\nu)$, partially. The feature of the visual analyzer FCC is the presence of the maximum on the curve at $\nu_{\text{max}} = 11.4 \text{ mm}^{-1}$ connected with the so called lateral deceleration leading towards the weakening of the light action on the central receptors of the retina at the simultaneous exciting of the receptor calls in the neighbour areas. Taking in account the fact that the reduced image is projected on the retina, for the chosen observation distance I_{obs} one must use the FCC of the eye counted again from the relationship

$$\nu_{\text{obs}} / \nu_{\text{ret}} = I_{\text{vis}} / I_{\text{obs}}, \quad (1.29)$$

where ν_{obs} , ν_{ret} are the frequencies in the plane of the observed image and retina, correspondingly: $I_{\text{vis}} = 1.67 \text{ cm}$ is the average distance from the centre of the crystalline lens to the retina. The FCC of the eye for $I_{\text{obs}} = 20 \text{ cm}$ and $B = 343 \text{ cd}\cdot\text{m}^{-2}$ (it depends sufficiently on the brightness) is given in Fig. 1.12. At the determination of the sum FCC of the image formation system the contribution of the visual analyzer in FCC must be accounted by using a rule of the production of the FCC components. However, if the observation distance is chosen so that the size of the details of interest corresponds to the area of ν_{obs} in which M_{obs} is maximum or fits closely the maximum value, the influence of eye FCC is practically excluded. So, in the case shown in Fig. 1.12, the account of $M_{\text{obs}}(\nu)$ is sufficient only for $\nu > 2\nu_{\text{max}} = 2 \text{ mm}^{-1}$, i. e. only for the smallest details.

Therefore, it is important to choose I_{obs} property proceeding from the expected sizes of the defect (pathological formations). For example, large low

contrast formations may be not detected if the formations are looked at from a short distance and, on the contrary, small formations are not detected at long I_{obs} . However, the reduction of I_{obs} is limited within the eye accommodation limit.

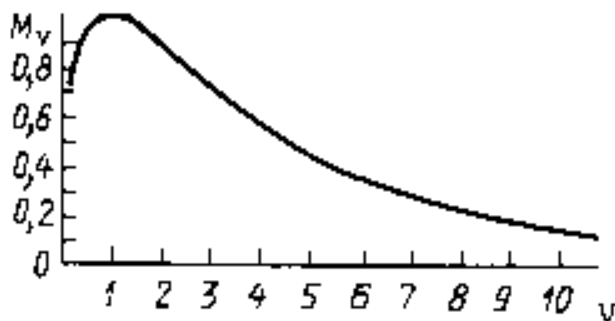


Fig. 1.12. The FCC of the eye for the observation distance

$$I_{\text{obs}} = 20 \text{ cm and brightness } B = 343 \text{ cd}\cdot\text{m}^{-2}.$$

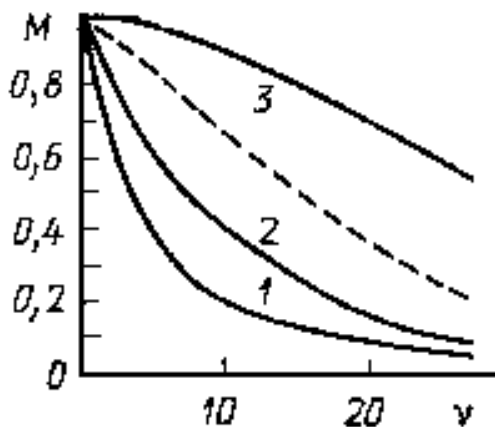


Fig. 1.13. The time FCC of the television channel of the roentgen image intensifier (1) and its components stipulated by inertness of the vidicone with the target from Sb_2S (antimony-two sulphur-three) (2), and time of the scanning of the electrostatic image on the target (3). The time FCC for the roentgen image intensifier with the plumbicone (the target from Plumbum Oxygen) is shown by the stroke

1.4.7. Quantum fluctuations of the ionizing radiation and their influence on the threshold contrast

The idea about quantum fluctuations and their connection with the threshold contrast. Static fluctuations in the space-time distribution of the photon radiation are the consequence of its two main features: the quantum nature and the probable character of the photons generation process and interactions with absorbers.

In accordance with the last circumstance, in using the absorbers with uniform composition and thickness a number of the ionizing radiation

photons oscillates around some average value in all its path. Let's assume for the observed stage of the process that the average number of photons which occurs on the unit of the beam cross-section square in the time unit is N .

The real number of photons in different parts of the section and in different time moments N_i differs from N by some value ΔN_i which may be positive and negative, and $\Sigma \Delta N_i \rightarrow 0$ at $i \rightarrow \infty$. Therefore the statistic mean measure of the deviation of N_i from N (the fluctuation of N_i) is the root-mean-square deviation $\sigma = [(\Delta N)^2]^{1/2}$. At this, as it may be shown, $[(\Delta N)^2]^{1/2} = N^{1/2}$. From here, the mean relative fluctuation normed on the square unit and time unit is

$$\sigma = \frac{[(\Delta N)^2]^{1/2}}{N} = \frac{1}{\sqrt{N}}. \quad (1.30)$$

Let's examine the image element with the square Ω at the time t_Σ of photons action summing. In this case, the relative fluctuation of the photons number taking part in such element formation may be performed in the form

$$\sigma = \frac{1}{\sqrt{N t_\Sigma \Omega}}. \quad (1.31)$$

In radiography t_Σ is equal to exposure time and in radioscopy t_Σ is equal to the effective time of the visual sensation integration whose damping may be described by exponential function

$$E_c = \exp(-t/\tau). \quad (1.32)$$

At this, the value $t_z = 3\tau$ is taken as the integration time depending on the brightness for which the eye is adapted and consisting about 0.1 second in radioscopy with the roentgen image intensifier and about 0.2 second in radioscopy without gain.

In radioscopy with the use of roentgen image intensifier, the connection between the image brightness B on output screen and the ionizing radiation intensity I in the working (linear) part of the gradation curve is expressed by the equation

$$\lg B = \gamma \cdot \lg I + C. \quad (1.33)$$

By its differentiation one can find that

$$dB/B = \gamma (dI/I), \quad (1.34)$$

or by the transfer to the finite differences

$$\Delta B/B = \gamma (dI/I). \quad (1.35)$$

It follows from here that the fluctuations of the photons number (if all other noise sources are neglected) provoke the fluctuations of the relative

brightness which are proportional to δ with the proportionality factor γ . However, taking in account the influence of FCC on the contrast of the small detail image and therefore on the brightness oscillations caused by the quantum fluctuations, one can receive

$$\Delta B/B = \gamma \cdot M(\nu)(\Delta I/I) = \gamma \cdot M(\nu) \cdot \delta. \quad (1.36)$$

In order to detect the detail image against the background of such fluctuations of the illumination brightness, its contrast must be more by certain times ψ_{th} than the fluctuations, i. e. the threshold contrast is

$$K_{th} = \psi_{th} \cdot \gamma \cdot M(\nu) \cdot \delta. \quad (1.37)$$

Factor ψ_{th} is named the threshold signal/noise ratio. Usually it is taken equal to 3 or 5 depending on the desirable probability P of the detail detection (defect or the pathological formation). At the same probability of the false-positive and false-negative interpreting $P = 0,93$ at $\psi_{th} = 3$ and $P = 0,99$ at $\psi_{th} = 5$. From the considerations analogous to those mentioned above, for the threshold photographic contrast of the image one can receive

$$\Delta S_{th} = 0.434 \psi_{th} \cdot \gamma \cdot M(\nu) \cdot \delta. \quad (1.38)$$

In the calculations in accordance with the obtained formulas, a question about the connection between Ω and ν appears. This connection is maintained by means of Fourier transformation. At the simplest and in the same time the spreading case of the details having the form of the sphere with diameter d , one can assume as for the mira with the slit width d that

$$\nu = 1 / (2d). \quad (1.39)$$

1.4.8. The information capacity of the image formation system

In order to express the image informativity by a single number it is convenient to use the number of the contrast steps (brightness gradation) p as the gradation characteristic of the system. For its determination one must know the maximum B_{max} and minimum B_{min} of the brightness really achieved under the study conditions (for image perceptible by the eye – with taking in account the dynamic range of the vision) and the dependence of the threshold contrast K_{th} on the brightness B for the image cell of the given size.

Let's assume in the first approach that K_{th} is not changed in all the interval from B_{min} to B_{max} . Then ρ may be found by the consecutive adding of $\Delta B = K_{th}$ and B_{min} :

$$\begin{aligned} B_1 &= B_{min} + K_{th} \cdot B_{min} = B_{min} (1 + K_{th}); \\ B_2 &= B_1 + K_{th} \cdot B_1 = B_{min} (1 + K_{th})^2; \\ B_3 &= B_2 + K_{th} \cdot B_2 = B_{min} (1 + K_{th})^3, \end{aligned} \quad (1.40)$$

and so on. As the result may be found that

$$B_{\max} = B_{\min} (1 + K_{\text{th}})^m, \quad (1.41)$$

where $m = \rho - 1$, because B_{\min} is the first step of the brightness. From here

$$\rho = [(\lg B_{\max} - \lg B_{\min}) / \lg (1 + K_{\text{th}})] + 1. \quad (1.42)$$

For the photographic image it may be found that

$$\rho = (\Delta S / S_{\text{th}}) + 1. \quad (1.43)$$

The simplest image that may be suggested is the one consisting from a single element for which only two steps are possible; for example, it can be either white or black. The information given by such image is taken as the unit the information named the binary unit (bit). If the image consists of two elements, then at two steps of the contrast there are four possibilities (2^2); for four elements – $2^4=16$ (possibilities) and so on. In the general case at $\rho -$ steps of the contrast from $n -$ elements the system can give the $z = \rho^n$ different images and, namely, it must be taken as the measure of the information capacity, if one comes from the assumption about the equivalence of the gradation and space-frequency information. However, at the increase of the surface square of the image converter by two times, the number of the images becomes equal to $z = \rho^{2n}$ in the time when, following the logic, the informativity increases by two times only. Therefore it is more correctly to use the logarithm z as the measure of the information capacity C . At this, it is convenient to take 2 as the logarithm basis as it is taken in the theory of the information. Then

$$\rho^n = 2^c \text{ and } c = \log_2 z = n \log_2 \rho. \quad (1.44)$$

For calculation of the maximum value of C for the used system, the parameter n must be determined with taking into account its resolution capacity R , i. e. the space frequency ν (the number of lines pairs) at which the optical contrast of the test object image, characterized by the radiation contrast $k_r=1$ achieves the value of K_{th}

$$N = 4R^2\Omega. \quad (1.45)$$

Since in reality ρ is the function of n , then instead of (1.44) one must write

$$c = \int_0^n \log_2 P(n) dn. \quad (1.46)$$

For the calculations simplification the dependence $\rho(\nu)$ is plotted proceeding from the data about $M(\nu)$ and $K_{\text{th}}(\nu)$ and mean value of ρ is

$$\bar{P} = \frac{1}{R} \int_0^{v=R} \rho(\nu) d\nu. \quad (1.47)$$

In this case from (1.44) – (1.46) it may be received that

$$c = 4R^2 \Omega \log_2 \bar{P}. \quad (1.48)$$

For example, in accordance with the approximate data, the information capacity of the television channel of the roentgen image intensifier with the 625 -line expansion of the image is 2 megabit on each sequence, i. e. the speed of the information transfer at the frequency 50 hertz is 50 megabit/second. Such data are useful for determination of the demands for the technical facilities of the videomagnetic recording of the image and for the estimation of the time expenditure on the radiation testing by the radioscopy.

Apart from the examined, the other complex characteristics of the image formation systems were offered. In substance, the resolution capacity may be taken to be a complex characteristic, thus it takes into account the added influence of the FCC, image noise and visual analyzer parameters (the idea of the “resolution capacity” is widely used because of its direct measurements by simple ways). However, all these characteristics have a limited applicability, since depending on the object features and study problems, the priority is given to the different parameters of the image quality. For example, at the roentgen image intensifier application the threshold contrast, as related to the large low-contrast detail, is often more important than the space resolution capacity. Therefore, as a rule, the systems of the image formation are characterized by a set of parameters.

1.5. Control tasks

There are at least three basic elements used in the radiation testing (RT) procedure:

- a) the source of the ionizing radiation;
- b) the testing object (at defectoscopy);
- c) the detector or the converter (transformer) for registration of the receiving defectoscopic, dosimetric or radiometric information.

The source of ionizing radiation is characterized by some basic physical parameters: the kind of radiation; the energy of radiation, power (yield) or activity and by exploitation and construction characteristics: sizes of active part, the duration of life or the working resource, the intake power, overall dimensions and the mass, the exploitation safety and so on.

For the testing object, the most important physical parameters on which the ionizing radiation weakening index depends are as follows: the atomic number or the isotopic composition, the density of the object matter.

The most important exploitation and construction parameters are the configuration and sizes of the object and the dynamics of its motion.

The basic characteristics of the detector (transformer) are the response function, the registration efficiency, the image own unsharpness (the resolution capacity).

The final results of the RT, besides the complex of characteristics of the testing main elements, depend much also on the testing geometry.

Roentgen and gamma-radiation are most widely adopted in the radiation testing. Therefore the main attention in the first section of the training appliance is given to these kinds of the ionizing radiation. The processes of formation and properties of radiations were considered as well as the main processes of the radiation interaction with the matter which play the main role in the radiation image formation, and basic characteristics of radiation and visual images: the radiation contrast, dynamic, and geometric unsharpnesses of the image; the own unsharpness of the converter; the summing unsharpness; the threshold contrast, the information capacity, etc.

In order to consolidate the studied material of the first section, a row of control tasks is offered to fulfill.

Answers to the set control problems are given in the final part of the working note-book.

The list of basic formulas and theoretical propositions needed for the solutions of tasks is given for making easier the fulfillment of control tasks:

- the boundary of the roentgen bremsstrahlung radiation spectrum:

$\lambda_{\min} = 1,23/V$, where V is the tension on the roentgen tube, kV;

λ_{\min} is measured in nanometers;

- the flow of the roentgen radiation $\Phi = k \cdot T \cdot V^2 \cdot z$, where I and V are the current and the tension on the roentgen tube, z is the ordinal number of the element of the anode matter, $k = 10^{-9} \cdot V^{-1}$;

- the mean length of the free path of gamma-quanta in ratio in the matter; $l = 1/n \cdot \sigma$, where n is the nuclei concentration in the matter; σ is the microscopic cross-section (barn/atom) of gamma-quanta interaction with the matter as the result of following processes: photoeffect, the Compton scattering, the pair formation process;

- the length of the free path at the presence of all three processes is determined from the relationship:

$$l^{-1}_{\text{total}} = l^{-1}_{\text{ph}} + l^{-1}_{\text{comp}} + l^{-1}_{\text{pair}};$$

- the probability of the photoabsorption is determined by the formula:

$$\omega_{\text{ph}} = \frac{\sigma_{\text{ph}}}{\sigma_{\text{total}}} (1 - e^{-\mu d}),$$

where $\mu = n \cdot \sigma_{\text{total}}$;

- the frequency-contrast characteristic (FCC) by the contrast transfer function (CTF) can be determined by the formula:

$$M(\nu) = \frac{\pi}{4} \left[M_{tr}(\nu) + \frac{M_{tr}(3\nu)}{3} - \frac{M_{tr}(5\nu)}{5} + \frac{M_{tr}(7\nu)}{7} - \dots \right];$$

- the number of photons fallen on the single square of the image formation system consisting of the luminescent screen and roentgen film combination can be found by the formula:

$$Nt_{exp} = \alpha \frac{87P_{exp}}{\mu_{km} \cdot E_{eff}},$$

where N is the number of quanta fallen on the single square at the time unit, α is the absorbed dose of the falling radiation; P_{exp} is the exposure dose of the radiation; μ_{km} is the mass factor of the energy transfer in the air; E_{eff} is the effective energy of the radiation; t_{exp} is the exposure time;

- the threshold photographic contrast of the image can be calculated by the formula:

$$\Delta S_{th} = 0.434 \cdot \psi_{th} \cdot \gamma \cdot M(\nu) \cdot \delta,$$

where ψ_{th} is the threshold relationship signal/noise; γ is the contrastness factor; $M(\nu)$ is the frequency-contrast characteristic (for articles, having the sphere form, the space frequency may be assumed equal to $\nu = 1/(2d)$), δ is the relative fluctuation of the photons number ($\delta = 1/\sqrt{N \cdot t_{exp} \cdot S}$); S is the square of the image element;

- the illumination of the eye retina is determined by the formula:

$$E_{ret} = \frac{\pi \cdot B_{sc} \cdot \tau \cdot Q^2}{4(1+m)^2},$$

where B_{sc} the brightness of the fluoroscopic screen luminescence; τ is the production of the transmission coefficient of the eye crystalline on the quantum efficiency of the retina receptors; m is the scale of the image increase; $Q = \pi \cdot d_p^2 / 4 \cdot l_{obs}^2$ is the relative hole of the human eye optical system (d_p is the diameter of the pupil of the eye; l_{obs} is the distance of the observation);

- the threshold contrast of the light and shade image:

$$K_{th} = \psi_{th} \cdot \gamma \cdot M(\nu) \cdot \delta.$$

1. Find the boundary of the roentgen bremsstrahlung radiation (the frequency and the wave length) for tensions $V_1 = 2$ kV and $V_2 = 20$ kV on the tube. How many times is the energy of photons of these radiations greater than the energy of the photon corresponding to $\lambda = 760$ nanometers (red color)?
2. In what case will a greater increase of the roentgen radiation flow take place: at the increase of the current by two times at the constant tension on the tube, or, on the contrary, at the increase of the tension by two times with the

constant current? How can one increase the current intensity without changing the tension on the roentgen tube? Give the analysis of processes occurred at the change of the current intensity and at the change of the tension.

3. Find the flow of the roentgen radiation at $V = 10 \text{ kV}$, $I = 1 \text{ mA}$. The anode is made of the tungsten. How many photons per second is this flow, if one can assume that the electromagnetic wave is emitted with the wave length equal to $3/2$ (three second) of the length of the wave corresponding to the spectrum boundary of the roentgen bremsstrahlung radiation?
4. With the help of graphs given in the Appendix 1, find the mean length of λ free path of gamma-quanta with energy 2.0 Mev , in the lead, and also the mean free path of these quanta for cases of the Compton scattering, the photoeffect and the effect of the electron-positron pair formation. By what relationship are these free paths connected?
5. With the help of graphs of the Appendix 1 find the probability of the absorption of the gamma-quantum with the energy 2.0 Mev in the lead plate with the thickness 2.0 mm .
6. The beam of the monochromatic gamma-radiation at passing the lead plate with the thickness 3.2 cm is attenuated 6 times. Calculate the mass factor of the Compton scattering of these rays in lead with the help of graphs of the Appendix 1.
7. The total cross-section of the gamma-quantum Compton scattering on the free electron is described by the formula:

$$\sigma_{\text{comp}} = \frac{3}{4} \sigma_{\text{T}} \left[\frac{\epsilon^2 - 2\epsilon - 2}{2\epsilon^3} \ln(1 + 2\epsilon) + \frac{\epsilon^3 + 9\epsilon^2 + 8\epsilon + 2}{\epsilon^2 \{1 + 2\epsilon\}^2} \right],$$

where $\epsilon = h\nu/mc^2$ is the energy of the gamma-quantum in the terms of the electron rest energy; σ_{T} is the cross-section of the Thomson (classic) scattering.

- a) Simplify this formula for the case of $\epsilon \ll 1$ and the case of $\epsilon \gg 1$;
 - b) calculate the linear factor of the Compton scattering of gamma-quanta with the energy $\epsilon = 3.0$ at the interaction with beryllium;
 - c) find the mass factor of the Compton scattering of gamma-quanta with the energy $\epsilon = 2.0$ for light media.
8. With the help of graphs of the Appendix 1, calculate the cross-section of the electron-positron pair formation by the gamma-quantum with the energy 6.0 MeV in the lead plate with the thickness equal to the layer of the half-value weakening.
 9. At what thickness of the lead plate is the probability of the electron-positron pair formation by the gamma-quantum with the energy 7.0 MeV equal to 0.1 ?

10. Show that a gamma-quantum can not form a pair outside the nucleus field even if this process is energetically possible.
11. Find the coefficient of the image increase if it is known that the distance from the source to the object and from the object to the converter **a** and **b** are equal to 10 cm. The radiation source is the point one.
12. Determine the image contrast with the accounting of the own unsharpness $U_{\text{own}} = 5$ mm at the roentgen contrast $K_r = 1$, at the object size $l = 2$ mm and the scale of the increase $m = 2$.
13. Determine the roentgen image contrast in the area of the pseudo-shade at the object size $l = 2$ mm, the focal distance $F = 100$ mm, the focus spot size $\varnothing = 6$ mm and the distance from the object to the converter **b** = 40 mm.
14. Find the focal distance F , at which the resolution capacity $R=5$ (pairs of lines/mm) is received on the converter, if it is known that the focus spot of the radiation source $\varnothing = 1$ mm, the distance from the object to the converter **b** = 220 mm and the geometrical unsharpness of the image is not more than the own unsharpness.
15. Determine the frequency-contrast characteristic ($M(\nu)$) by function of the contrast ($M_{\text{tr}}(\nu)$). $M_{\text{tr}}(\nu)$ is measured up to $\nu = 6$ mm⁻¹.
16. Receive the optimal relationship between the weakening factor μ and the testing object thickness x , with taking into account that for the relationship “the signal/noise” one can write the following expression:

$$\Psi = \mu \cdot \Delta x \cdot \sqrt{n_0 \cdot S_d \cdot t_{\text{exp}} \cdot e^{-\mu \cdot x}},$$

where Δx is the meaning of the defect in the direction of the examining; n_0 is the number of quanta of the ionizing radiation hitting the single square of the surface of the testing object at the time unit; S_d is the defect square; t_{exp} is the exposure time.

17. Find the threshold contrast (ΔS_{th}) for the image formation system consisting from the combination of the CaWO₄-screen with the medium increase and the roentgen film of the medium sensitivity (e. g. type PM-1). Determine the threshold contrast at following conditions:
 - the effective radiation energy $E_{\text{eff}} = 50$ keV;
 - the exposure time $t_{\text{exp}} = 0.02$ s;
 - the exposure dose needed for the shooting receiving $D = 1.1$ mR;
 - the threshold relation “signal/noise” $\Psi_{\text{th}} = 5$;
 - the contrast factor $\gamma = 2,5$;
 - the defect is the sphere-shaped article with $d = 0.5$ mm ($\nu = 1$ mm⁻¹, $M(\nu) = 0.6$).
18. Determine the threshold contrast for the radioscopy without any increase at the visual observation of the image having the view of the sphere-shaped

detail with the diameter $d = 3$ mm and $\Psi_{th} = 5$. The exposure dose rate in the screen plane is 0.2 R/min; the part of the absorbed energy of the radiation in the screen $\alpha = 0.35$; the effective energy of the radiation $E_{eff} = 50$ keV. In the above-mentioned conditions every photon of the ionizing radiation gives 2500 (two thousand and five hundred) light photons. The visualizer – the human eye has the following parameters: the image scale $m \ll 1$; the diameter of the pupil of eye $d_p = 7$ mm, the observation distance $l_{obs} = 20$ cm; the production of the crystalline transparency on the quantum efficiency of the eye receptors in equal to 0.8 %.

Appendix to sect. 1

Weakening and absorption factors for gamma-quanta

Energy, MeV	Aluminum		Lead		Water		Air	
	μ/p	τ/p	μ/p	τ/p	μ/p	τ/p	μ/p	τ/p
0.1	0.169	0.0371	5.46	2.16	0.171	0.0253	0.155	0.0233
0.2	0.122	0.0275	0.942	0.586	0.137	0.0299	0.123	0.0269
0.4	0.0927	0.0287	0.220	0.136	0.106	0.0328	0.0953	0.0295
0.6	0.0779	0.0286	0.110	0.0684	0.0896	0.0329	0.0804	0.0295
0.8	0.0683	0.0278	0.0866	0.0477	0.0786	0.0321	0.0706	0.0288
1.0	0.0614	0.0269	0.0703	0.0384	0.0706	0.0310	0.0635	0.0276
1.5	0.0500	0.0246	0.0550	0.0280	0.0590	0.0283	0.0515	0.0254
2.0	0.0431	0.0227	0.0463	0.0248	0.0493	0.0260	0.0445	0.0236
3.0	0.0360	0.0201	0.0410	0.0238	0.0390	0.0227	0.0360	0.0211
4.0	0.0310	0.0188	0.0421	0.0253	0.0339	0.0204	0.0307	0.0193
6.0	0.0264	0.0174	0.0436	0.0287	0.0275	0.0178	0.0250	0.0173
8.0	0.0241	0.0169	0.0459	0.0310	0.0240	0.0163	0.0220	0.0163
10.0	0.0229	0.0167	0.0189	0.0328	0.0219	0.0154	0.0202	0.0156

Here μ/p and τ/p – mass factors of the weakening (for narrow beam) and of the absorption, cm^2/gram .

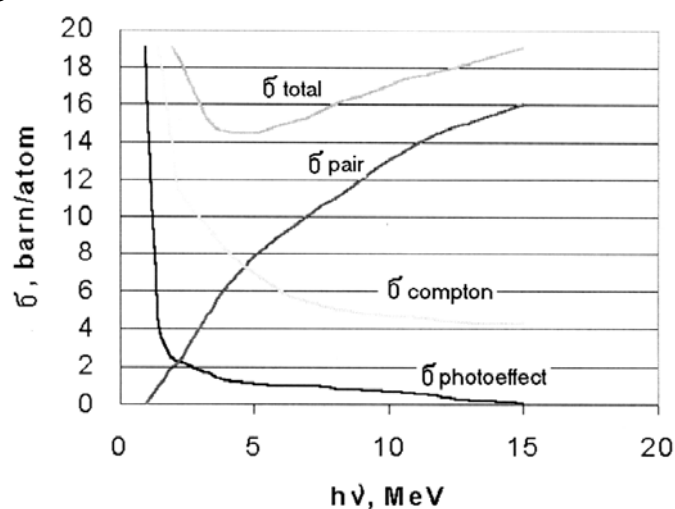


Fig. 1.14. Cross-section of the gamma-quanta interactions in lead

Chapter 2

RECEIVING AND REGISTRATION OF ROENTGEN AND GAMMA-RADIATION

2.1. Sources of X-ray and gamma-radiation

2.1.1. X-ray apparatus

X-rays occur at the deceleration of the accelerated electrons. In practice of testing, the voltage of accelerating is mostly in interval from 50 kV up to 500 kV. The accelerating of electrons occurs inside a vacuum tube with a heated cathode. Emitted owing to thermal emission electrons are accelerated between the anode and the cathode and then are focused on the anode with the help of electromagnets system. There is the target in the area of the anode focal spot. The target is usually made from tungsten. Since at the electrons deceleration side by side with the roentgen radiation a large quantity of the heat is produced, then the anode at the high power must be cooled. Depending on the tube type this cooling is fulfilled with water or oil.

Since the X-ray images occur as shade projections, the size of the focal spot of the roentgen tube is decisive for the reproducible sharpness of the image. However, a small focal spot means a high energy concentration on the anode, therefore the achieved roentgen currents and the intensity decrease. The present-day roentgen tubes have different sizes of the focal spot but for ordinary radiation testing it is a generally accepted practice to apply tubes with the focal spots having sizes from a few millimeters up to 0.2 mm. There are microfocal tubes with the focal spot sizes about 10 micrometers for very small structures testing. The similar focal spots of the microfocal tubes allow to conduct 10–50 – multiplied geometrical magnification with sufficient image resolution.

An ordinary X-ray arrangement consists of an irradiator, a source of high voltage power and a control unit. The power source and the irradiator joined in one housing are called the single-frame facility (monoblock). The irradiator frame, however, is relatively compact. For the high voltage receiving in the single-frame arrangements simple switching schemes are used, as a rule, in which the alternating voltage is got with the help of the high voltage transformer, as it is given in Fig. 2.1. From the point of view of the electricity, the roentgen tube is itself a rectifier passing only the positive

semi-wave of the alternating voltage. But since the anode is heated due to high temperature occurring at the electrons deceleration, then thermal emission is generated on the anode which needs additional rectifying of the voltage. Such high-voltage sources are called single-half-period generators.

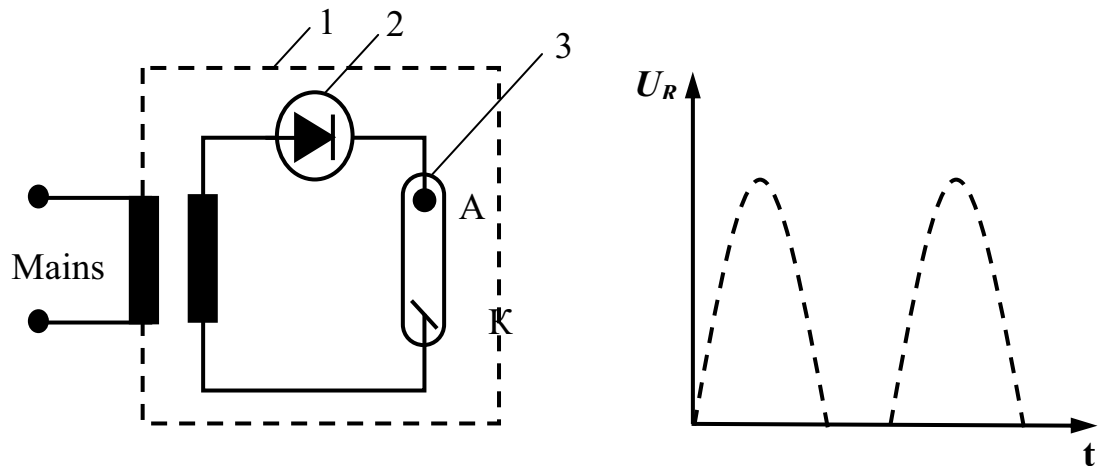


Fig. 2.1. The principle of the single-half-period generator

In practice, more and more the direct voltage facilities are applied in which schemes on tiristors and transistors are used. As distinct from the single-half-period generators, in the given case the direct voltage is applied to the X-ray tube (Fig. 2.2).

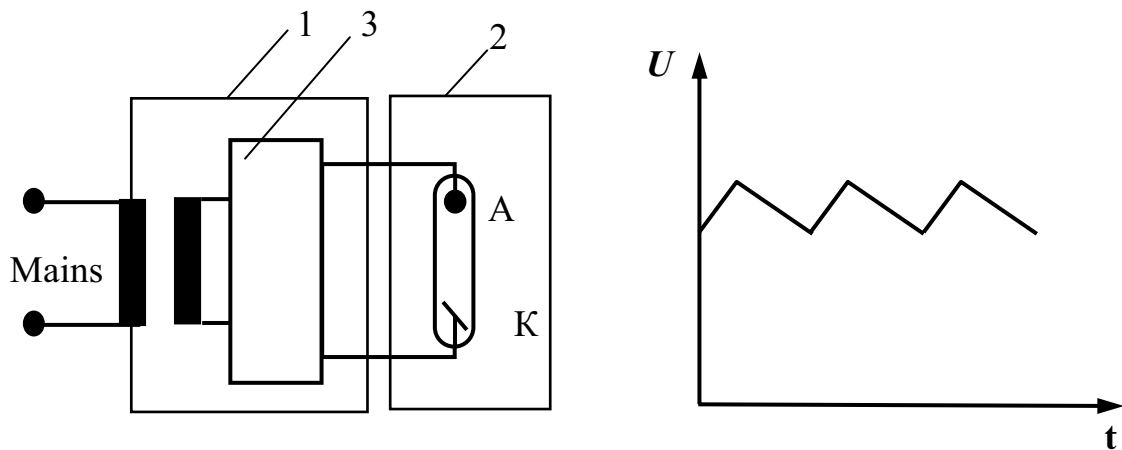


Fig. 2.2. The principle of the direct voltage arrangement

It means that in the time of measuring, the energy of the direct voltage generators is higher than the energy of the single-impulse generators. In the direct voltage arrangements, as a rule, the power source and the radiation source are divided. This arrangement is called two-frame. It has the advantage consisting in that the roentgen radiation sources have small sizes.

In spite of large expenditures for the direct voltage receiving, the number of such apparatus is much greater.

In the unipolar tubes, the anode (target) is grounded and all voltage of the acceleration is applied to the cathode. In this case a simple enough cooling of the anode with water is possible. Besides, such tubes can be made unsymmetrical and can be adjusted for the geometry of the testing detail. This kind of tubes is usually applied at the low accelerating voltages up to 160 kV. The efficiency coefficient of the roentgen tubes is approximately 1 per cent.

Accelerators are applied for the high energy production. One of the variants is a linear accelerator with accelerating sections following each other. Betatrons are the small-sizes accelerators in which electrons are accelerated by the circle. The circle of the acceleration acts as a transformer secondary winding in whose electrons are accelerated in a time of a quarter-period. The magnetic field of the primary winding is used firstly for the electrons acceleration and, in the second, for the stabilization of the electrons acceleration trajectory.

The number of electrons accelerated in the betatron is essentially less than in the ordinary roentgen tubes. But because of electrons high energies, the betatron efficiency factor as related to the bremsstrahlung radiation output is much higher and is approximately 40 %. The accelerators are used for producing the energy from several MeV up to 70 MeV.

2.1.2. Radioisotopic sources

2.1.2.1. Isotopes for the materials testing

For the roentgen radiation to be brought about, high voltage sources are needed. But sometimes there are no such power sources at one's disposal. In this case one uses radioactive isotopes. The origin of gamma-radiation is the effect of the radioactive decay, in which side by side with protons the electrons, positrons (positive charged electrons) and alpha-particles (helium nuclei) are also let out. The long life isotopes are needed for the nondestructive testing. At this the consideration is, as a rule, about the beta-irradiators, i. e. the isotopes which side by side with gamma-radiation emit electrons.

Mainly, Cobalt-60 and Iridium-192 are applied.

Table 2.1 gives a review of the properties of some isotopes applied in the nondestructive testing. The given isotopes are received by the neutron irradiation in the reactor. At this, from the stable Cobalt-59 the radioactive Cobalt-60 is formed transforming after certain time into the stable Nickel-60 and emitting in that time electrons and protons as it is given in Fig. 2.3.

The time of one-single decay of the nucleus can not be set accurately. There is the so called "decay probability". During the decay the nucleus can

firstly take the different energy levels and then at the transfer from one level to the next, protons (gamma-quantums) of certain energy are emitted. The spectrum of the isotope radiation is firstly linear (discrete). Then it is transformed into the continuous spectrum owing to interaction processes inside the source (see Fig. 2.4).

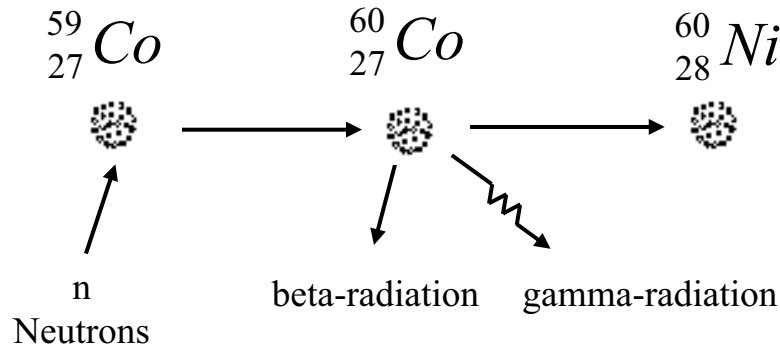


Fig. 2.3. Receiving and the decay of ${}^{60}\text{Co}$

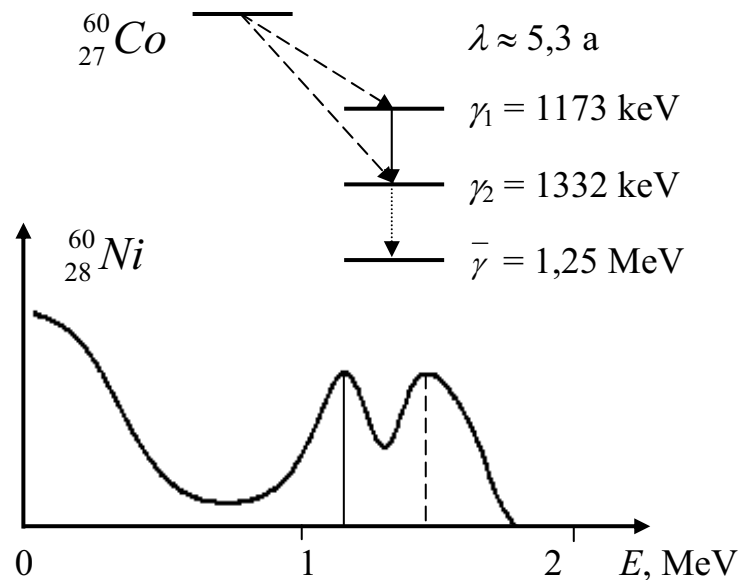


Fig. 2.4. Spectrum of the ${}^{60}\text{Co}$ radiation

For the description of the photons number formed in the unit of time, the concept of the “Activity” (A) is introduced. The activity A is the number of decays in the source occurring in one second. The dimensionality of the activity is Becquerel (B_q) determined as one decay in one second. In the nondestructive testing very high-power sources with the activity up to several hundred Gigabecquerel (GBq) are applied.

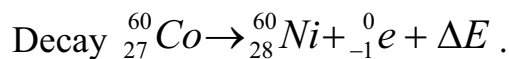
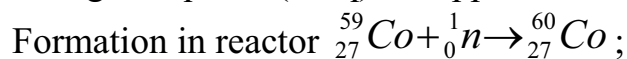


Table 2.1

Isotopes for the material testing

Isotope	Photon Energy, MeV	Half-decay Period	Thickness of tested materials, mm Fe
60 Co	1.17/1.33	5.3 years	40 ... 160
192 Ir	0.3 ... 1.06	74.5 days	6 ... 100
170 Tm	0.084	127 days	0 ... 5
137 Cs	0.66	30 years	30 ... 100

The decay time of one-half of the total number of the radioactive nuclei can be determined for a large number of nuclei containing in single source. This time is called “the half-decay period” ($T_{1/2}$). During this time activity is decreased two times. The reduction of activity is described by the law of the radioactive decay

$$A = A_0 \cdot e^{-\lambda t} = A_0 \cdot e^{(-0,693 / T_{1/2}) \cdot t}, \quad (2.1)$$

where A_0 is the activity in time moment $t = 0$ and λ is the decay constant.

The knowledge of the activity has important significance for the defectoscopist, as owing to this knowledge he can calculate the exposure time for the roentgen film at the examining.

2.1.2.2. Equipment for the testing by isotopes

Isotopes used in the nondestructive testing have photons energy up to 1.3 MeV. Therefore, special facilities are needed for testing which can fulfil functions of the transportation container and the irradiator at the same time. The radioactive isotope is inside the soldered capsule which is inserted into the protective container. The container has a round form and is made of a heavy metal (for example, Lead or Uranium). Uranium has the property of a very high shielding effect at high thermal stability and high density.

Shielding containers made from Uranium are sufficiently compact and simple in manufacture which is of prime importance in practical application.

With the help of a mechanical distant control the irradiator is extracted from the container and transferred into the collimated cap within which the radiation is emitted. In order to direct the radiation in the direction of the testing detail one uses collimators which also are made, as a rule, of heavy metals, e.g. tungsten.

The work with the arrangement for the isotope testing requires special training and special measures concerning protection from the radiation. This arrangement is subject to strict control quaranteeing that even in the extreme conditions, for example, in an accident of the vehicle transporting the devices, the radioactivity will not be spread into the environment.

2.1.3. Betatrons

Betatron is the inductive cyclic accelerator of electrons and is one of the first high-energy sources of the bremsstrahlung radiation which begins to be applied in the industrial defectoscopy. This accelerator finds a wide application owing to its relative simplicity as related to the linear accelerators and microtrons though the dose rate of the bremsstrahlung radiation of the betatron is by one-two orders less. Recently, small-sizes betatrons with energy (3–6) MeV receive especially wide application; they have small mass and admit the possibility of the manual transport towards the testing object, which is especially important in working on the assembly sites, building slips, at the repair of the boiler-houses and energy arrangements, testing of the reinforced concrete piers of bridges and other building constructions.

Betatron acts in accordance with the following principle. Electrons injected into the vacuum chamber are accelerated under the action of the vertical electric field created by the alternative magnetic flow which, in its turn, is created with the help of a special system of electromagnets. At this, during all the acceleration cycle electrons move by the circular orbit of a constant radius. The plane of the orbit is perpendicular to the axis of the symmetry of the magnetic field. In order to preserve the constancy of the radius of the orbit on which electrons move in the acceleration process, it is needed that the velocity of the electron energy increase be equal to the rate of the magnetic field increase. This condition is achieved by that the relationship of the magnetic flow value within the round of the equilibrium orbit to such cycle square is equal to the doubled voltage of the magnetic field on the orbit itself.

In modern betatrons the voltage of the electric field on the orbit achieves the values about 0.2–0.25 V/cm. In order to obtain the final energy of several millions electron-volts, electrons must do more than one million turns by the equilibrium orbit in the acceleration process. For providing a stable movement of the electron beam during the total cycle of the acceleration, the voltage of the magnetic field in the electromagnet gap in the orbit plane decreases with the distance from the orbit center to the periphery. Such space distribution of the magnetic field in the area of the equilibrium orbit excites the appearance of the focusing forces in the case of the electrons deviation from the equilibrium orbit (for example, owing to electrons collision with the air molecules) which compel the electrons to come back into the equilibrium orbit in automatic way.

At the end of the acceleration cycle the electrons are shifted from the equilibrium orbit by means of special facilities and then hit the target where the bremsstrahlung radiation is generated.

The inductive accelerator (Fig. 2.5) usually consists of the electromagnet 4, power unit 3, the acceleration chamber 1 disposed in the

interpolar space. The injector 7 is mounted in one of the branch pipes of the vacuum acceleration chamber. The injection scheme 6 is disposed in the separate unit or directly on the betatron electromagnet under the facing housing. The control panel 5 of the betatron is manufactured as a separate unit.

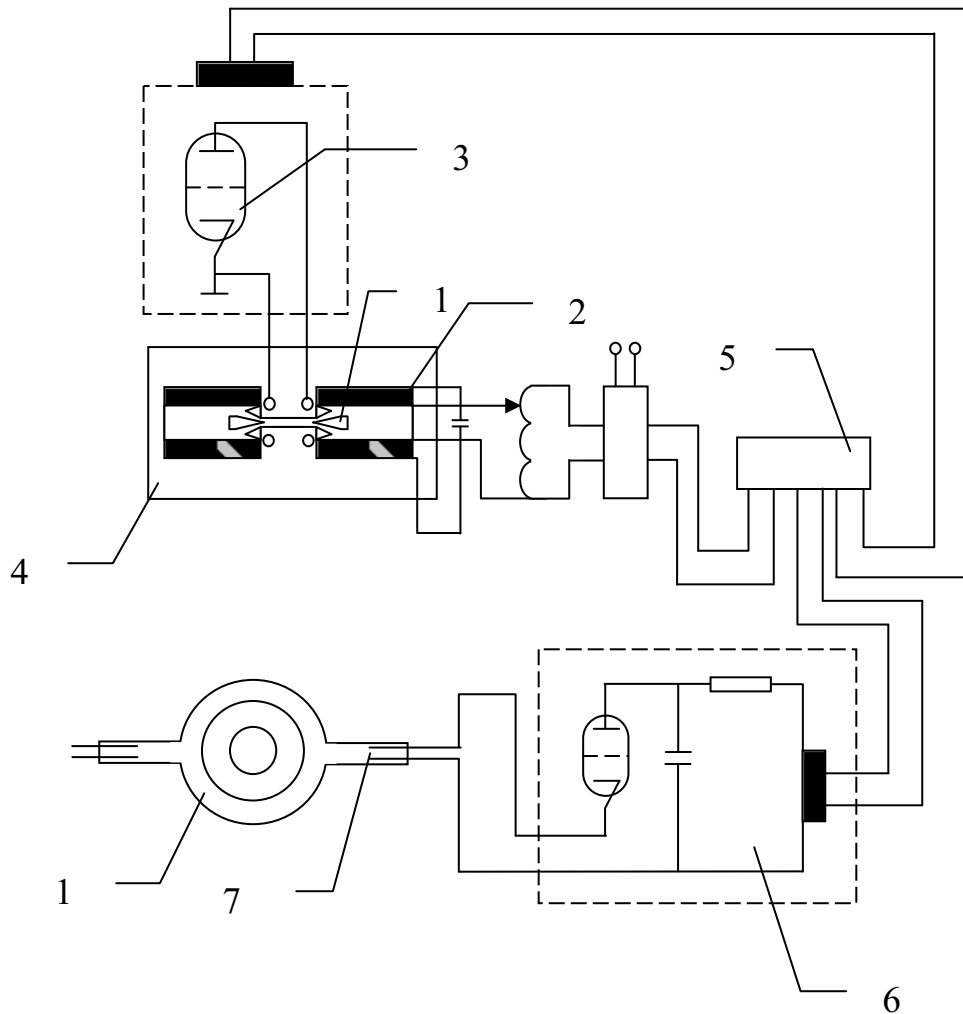


*Fig. 2.5. Structural scheme of the betatron:
 1 – Accelerating chamber; 2 – Exciting coils; 3 – Power unit;
 4 – Electromagnet; 5 – Control panel; 6 – Injection scheme; 7 – Injector*

The electromagnet, applied in the betatron, consists of a III-shaped or the multi-post, or the armored type magnetolead, and of the poles between which a round vacuum chamber is placed, and central insets. Central insets and the magnetolead of poles are made of the transformer steel. The electromagnet poles have usually a cylinder form. The configuration of the poles surface, where the vacuum chamber is disposed, is made in a way that the interpolar gap is increased at the increase of the distance from the center in accordance with the law

$$h \sim R^{\nu}; n = -R/B \cdot (\partial R/\partial)_{z=0}, \quad (2.2)$$

where n is the slump index of the magnetic field B , which is chosen in the range $0 < n \leq 1$.

The feeding of the betatron electromagnet is produced from the industrial mains of the alternative current with the frequency 50 hertz or from the power source generating the voltage of higher frequency. Practically in all applied betatrons the resonance scheme is used (see Fig. 2.5) in which the power circuit of the excitation winding is in sequence switching on with the condenser battery. The capacity of the condenser battery is chosen so that the resonance frequency of the received contour would be equal to the frequency of the power current. In order to maintain the constancy of the magnetic field induction in the electromagnet gap at certain moments of the time and to provide a stable regime of the accelerator working, special elements are used for the betatron power voltage stabilization.

The acceleration of electrons occurs in the vacuum chamber made of glass or porcelain and having a toroidal form. It may be the sealed off or can work at the continuous pumping out. In the betatron defectoscopes the sealed off chambers are usually applied (Fig. 2.6). For the normal work of the accelerator the pressure of the residual gas in the vacuum chamber must be not more than 10^{-4} Pa. The raise of the pressure leads to the reduction of the particles number reaching the end of the acceleration. For the vacuum improvement in the sealed off chambers, a getter is used. In the collapsible chambers with the continuous pumping out the needed vacuum is provided by the pumps.

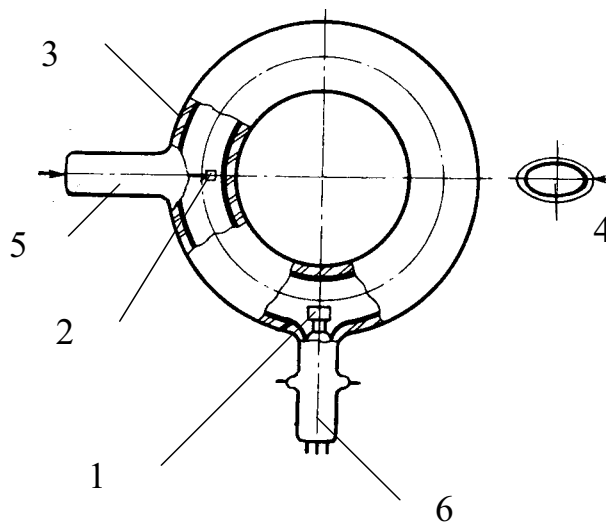


*Fig. 2.6. The external view and the construction of the betatron vacuum chamber:
 1 – Injector of the electrons; 2 – Bremsstrahlung target; 3 – Conductive cover;
 4 – The cross-section of the chamber; 5 and 6 – Branch pipes*

In order to avoid the formation of the surface charge on the chamber walls owing to the setting of the part the accelerating electron beam, the

surface of the chamber is covered by a conductive layer with the resistance 30...100 Ohm and is grounded. In Fig. 2.6 the external view of the sealed-off vacuum chamber of betatron purposed for the bremsstrahlung radiation generation is shown. In one of the branch pipes of the chamber the injector of electrons is mounted and the deceleration target and the gas absorber are mounted in other branch pipe. The injector is disposed in the plane of the equilibrium orbit near the external wall of the chamber and the target is on the other side of the orbit—near the internal wall.

In the acceleration process the amplitude of the cross-sectional oscillations of electrons is damped as related to the equilibrium orbit and the electron beam on the target has small diametric sizes. The flow of the generating bremsstrahlung radiation comes out from the chamber through its walls.

The high voltage electron sources are used as the injector in betatrons. One of the possible injector constructions is shown in Fig. 2.7. The thorium-oxide rectiheated cathodes having a tungsten or tantalum kern or the cathodes from pure tungsten are used as the cathodes. The first have a high specific emission, are easily activated and have a low sensitivity to the poisoning but the shorter life than the cathodes from tungsten which have a lower efficiency.

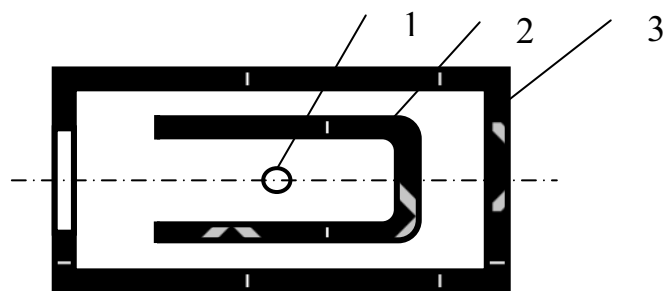


*Fig. 2.7. The injector construction:
1 – Cathode; 2 – Focussing electrode; 3 – Anode*

The cathode itself is manufactured as the helical spiral. The injection of the electrons into the vacuum chamber is realized at the putting the negative impulse of high voltage with the duration in a few microseconds on the cathode.

The needed focusing of the injecting electrons is achieved by the selection of the focusing electrode potential and by the depth of the cathode settling in it. The anode of the injector is grounded in order to avoid its influence on the orbital motion of the particles. In betatron the electrons are accelerated in the time duration when the magnetic flow is changed from the null up to the maximum value, i. e. in the time of the single quarter-period of the sinusoidal change of the magnetic flow. The electrons injection and the capture in the acceleration process are fulfilled in a short time interval during which the

magnetic induction has a value needed for the electrons rejection onto the orbit. The choice of the injection moment in the betatron and the corresponding electron trajectories at different time moments is given in Fig. 2.8. The electron beam on the betatron output is the clots of the particles of short length having repetition rate equal to the exciting frequency of the electromagnet.

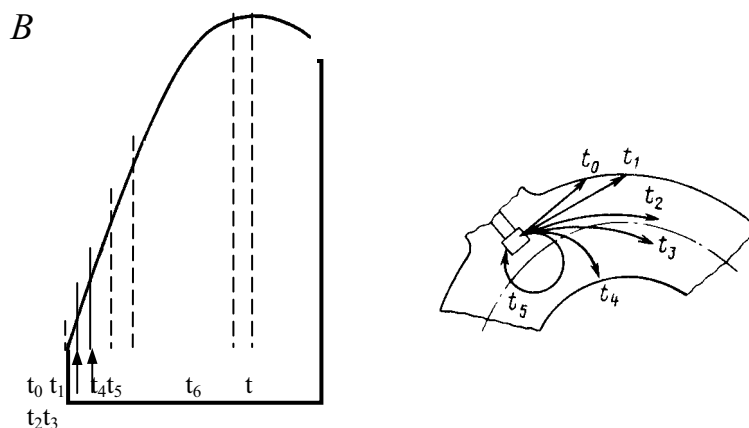


Fig. 2.8. The choice of the injection moment in betatron and the trajectories of electrons injected in different time moments: the time interval of the electrons capture in the acceleration process $\Delta t = t_3 - t_2$; t_6 is the moment of time of U the particles dropping on target or the moment of the particles rejection from the accelerator

Depending on the purpose, electrons at the end of the acceleration cycle (working quarter-period) are shifted from the orbit and then, having fallen on the deflector, are extracted outside from the vacuum chamber or are extracted on the bremsstrahlung target. The shifting of the electrons is fulfilled by means of the shift windings mounted on the electromagnet poles through which the short impulse of the current with needed polarity is transmitted at the needed time moment. So the equilibrium value of the magnetic field on the orbit is changed.

In recent years, in the Scientific-Research Institute of Introscopy (НИИ ИИ) of the Tomsk Politechnical University small-size betatrons for the defectoscopy were designed in which the operating magnetic field with the space orientation is applied, as related to the above considered betatron with the azimuthally-uniform field. The electromagnet of the betatron with the azimuthal field variation is given in Fig. 2.9. The gap between the betatron poles is changed periodically along the azimuth and owing to this the azimuthal components of the leading magnetic field and the additional focusing forces appear. It allows to increase the number of particles captured in the acceleration process and, correspondingly, the intensity of the bremsstrahlung radiation generated by the betatron. The magnetolead of the magnet has six locking posts

and on the poles of the magnet six ridges are mounted which change the gap and, so, the magnetic field by the azimuth with the step in 60° . In Fig. 2.9 the direction of the plates from the transformer steel is also shown. The post and the ridges of the back magnetolead are set up from the transformer steel. For the given considered arrangement the mean radius of the equilibrium orbit is 6 cm, the interpolar gap on this radius is approximately 4 cm and the slump index of the mean magnetic field on the orbit, $n \cong 0.6$. The injection energy is 25 keV and the final energy of the accelerated electrons is 6 MeV. The accelerators of such type are manufactured serially.

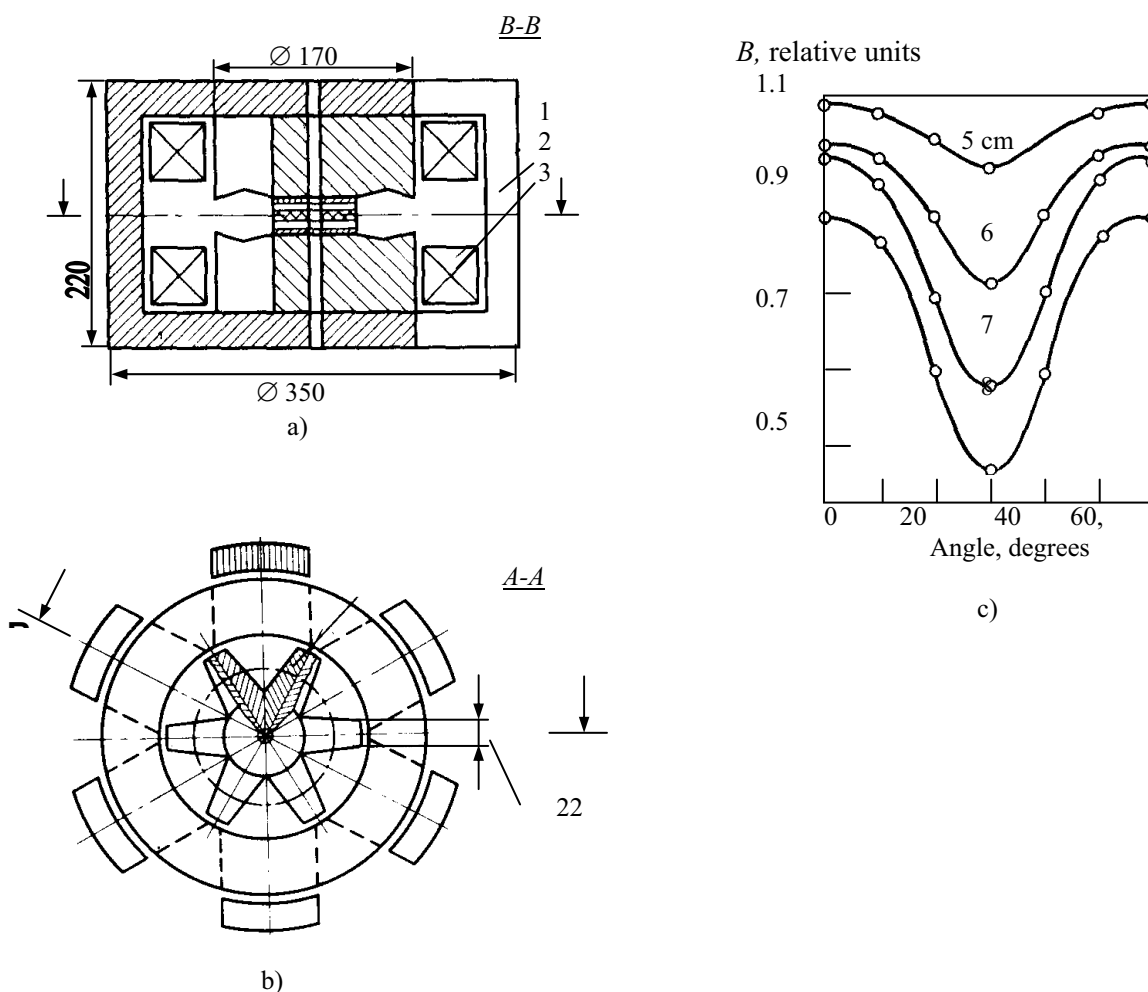


Fig. 2.9. The magnet of the betatron with the azimuthal variation of the field:

- a) Diametric section by B-B; b) Section by A-A;
 c) Distribution of leading magnetic field B by azimuth in the median plane at single period of variation at the difference values of the radius;
 1 – Magnetolead; 2 – Locking yoke of the magnetolead; 3 – Winding; 4 – Ridge

The designed constructions of the radially-ridged electromagnets of the small-size betatrons which form the operating field with the space variation have less mass and consumptive power in comparison with the electromagnet

of the classical betatrons and also the above-mentioned constructions provide the working of the betatron at higher power frequencies. The using of the time correction of the magnetic field at the injection moment by means of the additional winding allows to increase the efficiency of the electrons capture in the acceleration process by several times and so to raise the radiation intensity of these devices.

The brief technical characteristics of betatrons for the industrial defectoscopy designed in this country and abroad are given in Table 2.2 (see Appendix 1)

The distinctive features of the type ПМБ and МИБ betatrons in comparison with the stationary electron accelerators for the defectoscopy are the mass, the possibility of the manual transport towards the testing object, operation in any weather conditions and the possibility of the testing of every sort and kind of constructions and materials having place at the assembly works in the field conditions.

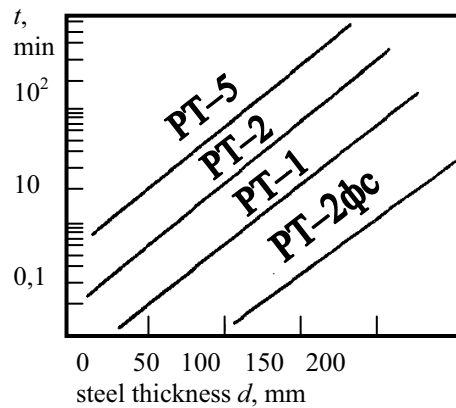


Fig. 2.10 a. Exposure graphs at the steel sample examining by the betatron МИБ-4: examining condition $E_{max} = 4 \text{ MeV}$; $I_j = 1 \text{ R/min}$; $F = 1 \text{ m}$; lead screen width = 0.5 mm; blackening density 1.7 – 1.9 units

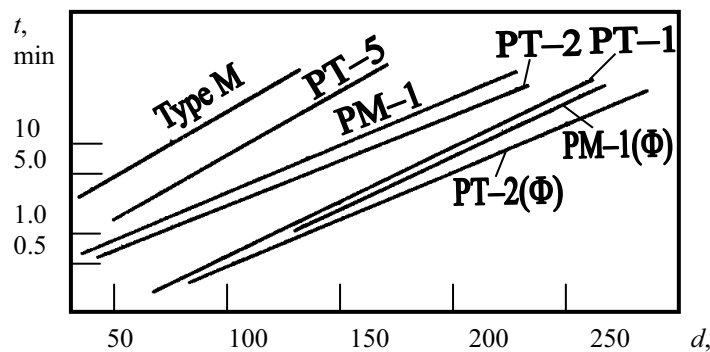


Fig. 2.10 b. Exposure graphs at the steel absorber examining by the betatron МИБ-6: $F = 60 \text{ mm}$; blackening density $D = 1.5 - 1.7$; dose rate $P = 220 \text{ R/h}$; screens from Pb: 1.22 mm (front) and 2.0 mm (back)

The small-size betatrons consumption power is from 2 to 4 kW and they may be connected to the ordinary mains with voltage 220/127 V.

The betatron МИБ-6 consists constructively of three units: the irradiator with mass 100 kg, the power unit with mass 80 kg and the control panel unit with mass 20 kg. The length of the connective cable between the control unit and the irradiator is 35 meters.

At the radiographic testing by means of МИБ-4 and МИБ-6 betatrons the different types of the films and the intensifying screens applied in roentgeno- and gammagraphy can be used. The exposures graphs at the steel samples examining are given in Fig. 2.10 (a, b). The defectoscopic sensitivity achieved at the using of these arrangements is 1...2 % at the radiography with the steel thickness range 20...150 mm.

2.1.4. Linear accelerators

Linear accelerators. In the practice of the radiation defectoscopy a wide application was found for the resonance linear electrons accelerators with the energy from ones to tens of Megaelectronvolt. The principle of the resonant acceleration of the charged particles is in the base of action of all modern high-energy accelerators. It consists in that the particle passes repeatedly through the areas of the alternating electric field getting in it every time at one and the same phase of the voltage at which a certain raise of the particle energy occurs. A wide development of accelerators based on the resonant method began with the discovery of the autophasing phenomenon consisting in that the stable regime of the particle acceleration is possible not only for the separate equilibrium particles but also for particles hitting into the accelerating field within a certain phase interval. The particles with the phases in this interval can be in the acceleration regime for a long time performing at this stable oscillations by the phase and collecting, in multipassing the accelerating field, approximately the same mean energy as the equilibrium particles.

The principle of the linear resonant accelerator action is a follows. Electrons, which are preliminary accelerated in the injector (for example, the electron gun) are then inserted into the accelerating system made as a cylindrical diaphragming wave-guide (Fig. 2.11) in which the travelling electromagnetic wave of E_{oi} type with the phase speed V_{ph} (the linear accelerator with the travelling wave) is excited.

Electrons getting in the accelerating half-wave then will be accelerated along the wave-guide axis under the action of the force of the longitudinal component of the electric field. At this, the energy of electrons will be raised continuously if the speed of the electromagnetic wave v_{ph} is equal to the electrons speed v_e in the process of all the acceleration time.

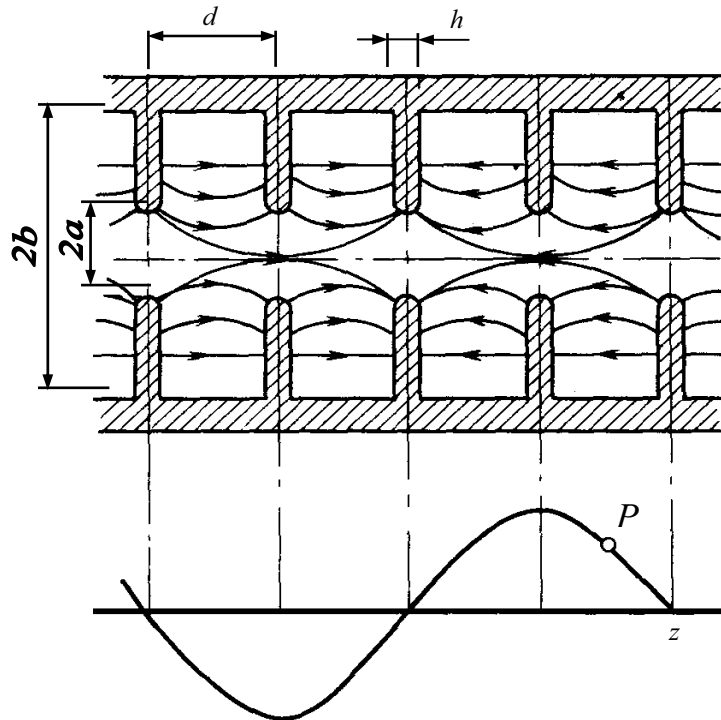


Fig. 2.11. The electrical field in the diaphragming wave-guide

The phase speed of the electromagnetic oscillations spreading in the wave-guide depends on the type, wave length and the construction of the wave-guide.

In the smooth cylindrical wave-guide the phase speed of the electromagnetic wave is higher than the light speed and the acceleration is impossible. In the linear accelerators the metal smooth cylindrical wave-guide is usually applied in which the systems of the round conductive diaphragm are mounted for moderation of the electromagnetic wave speed towards the needed value. The cells of the diaphragming wave-guide may be considered as a set of the volumetric resonators connected through the central hole. The phase speed of the wave spreading through the diaphragming wave-guide depends on its parameters: wave-guide radius b , the diaphragm hole radius a , the distance between diaphragms (structure period) d and the diaphragm thickness h .

The schematic draft of the linear accelerators with the travelling wave is shown in Fig. 2.12. Electrons from the injector 1 come into the diaphragming wave-guide 3. The regime of injection is the impulse one: the energy of electrons is usually 30...100 keV. At the motion along the wave-guide the electrons are grouped in the clusters 4 and their energy increased continuously. At the end of the diaphragming wave-guide the electrons are hitting onto the target or move outside through special windows. For the wave-guide feeding, powerful generators of the

superhigh-frequency-oscillations are used: the impulse magnetrons or the keystrons working in the wave length range 10...25 cm. The superhigh-frequency electromagnetic oscillations are getting into the diaphragmed wave-guide by the smooth power wave-guide 2. In the end of the accelerator the unused capacity of the superhigh-frequency-oscillations of the travelling wave is removed by the wave-guide 5 into the absorbing loading. During the operation of the accelerator, high vacuum is maintained inside the accelerating section.

Owing to the action of the autophasing mechanism the majority of electrons injected into the accelerating system are captured in the acceleration process and grouped into compact clusters around the resonant particles, whose speed at any time moment coincides with the phase speed of the accelerating wave. On every impulse with duration T of the superhigh-frequency-oscillations with frequency f there are Tf electron clusters.

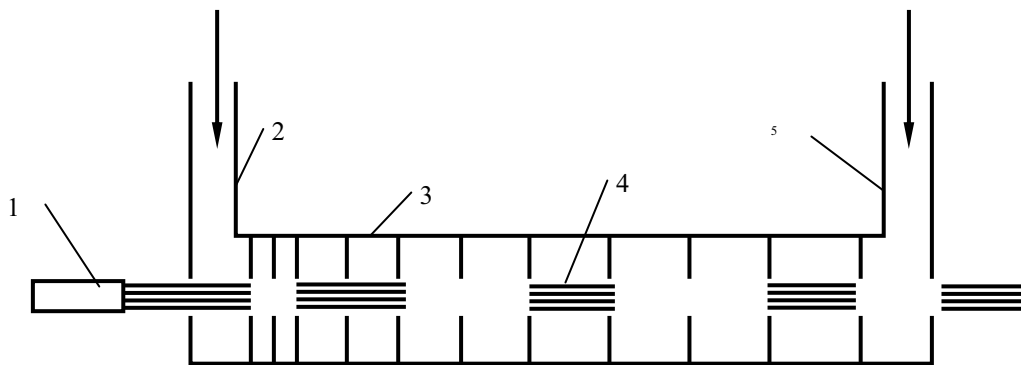


Fig. 2.12. A schematic drawing of the linear resonant electrons accelerator with the travelling wave

In recent years the accelerating structures working with the standing electromagnetic waves are used in the linear accelerators. If in the accelerator with a travelling wave the superhigh-frequency is added to one end of the diaphragming wave-guide and the loading is mounted on the other end of the wave-guide, the unused power is absorbed in the loading. The wave-guide with a standing wave is short locked from both sides and the energy of the superhigh-frequency-oscillations is inserted in the middle part of the wave-guide. The diaphragming wave-guide with the standing wave may be considered as a group of the connected resonators in which there are travelling waves with the different phase speeds. At this, acceleration is fulfilled in the field of the main harmonic with the phase speed coinciding with the speed of the particles. Today the accelerating structures with the standing wave are proposed and used in which one can receive the same energy of the accelerated electrons as in an ordinary diaphragming wave-guide but at a shorter total length of the wave-guide.

Table 2.3

Linear accelerators of electrons used for defectoscopy

Name of accelerator	Firm, country	Energy of electrons	Dose rate of bremsstrahlung radiation at distance 1 m from the target, R/min	Diameter of irradiation field at distance 1 m from the target, mm	Diameter of focal spot at the target, mm	Size of irradiation unit, mm ³	Mass of irradiation unit, kg
LUE-10-1 (Linear Accelerator of Electrons)	НИИ ЭФА (Scientific research institute of electrophysics and automatics)	8	1800	200	1.5	2750×100×800	—
LUE-10-2Д	-/-	10	2500 5000	300 —	3.0	4170×1250×1000	2000
LUE-15-1.5	-/-	15	10000	300	2.5	4500×1500×2000	—
LUE-5-500Д	-/-	5	500	360	2.0	2880×850×1160	2000
LUE-8-2000Д	-/-	8	2000	235	2.0	2880×850×1110	2000
LUE-15-1500Д	-/-	18.5	5600 15000	400(filter) —	2.3	4300×900×1150	2500
LUE-5-1500Д	-/-	6	1370 rad·m ² /min	535	2.0	2120×920×830	900
LUE-10-5000	-/-	3	4100 rad·m ² /min	350	3.0	2120×920×830	950
LUE-15-10000	-/-	13	8650 rad·m ² /min	210	3.0	1358×1000×2030	1500
Linatron-200	“Varian” USA	2	200	830×830	2.5	1030×760×840	816
Linatron-400	-/-	4	500	400×400	2.0	1680×710×740	900
Linatron-2000	-/-	8	2000	535	2.0	1680×710×740	900
Linatron-3000	-/-	9	3000	535	2.0	2520×1320×1520	—
Linatron-6000	-/-	16	6000	350×260	3.0	2520×1320×1520	3900

One of the advantages of the linear accelerators is the possibility of receiving a high power of the accelerated electrons beam and the possibility of the adjustment of the current and the output electrons energy in a wide range. The simplicity of the electrons withdrawal from the accelerator allows to get on the bremsstrahlung target the focused good and powerful beams of the accelerated electrons, and so high intensities of the bremsstrahlung radiation at the small focal spot. In most cases the dose rate of the bremsstrahlung radiation in the linear electrons accelerator is limited by the capacity for work of the bremsstrahlung target but not by the possibilities of the linear accelerator. The technical characteristics of the modern linear electrons accelerators allow to conduct the radiographic testing of the steel articles with the thickness from 50 to 600 mm at the sensitivity 0.5–1 % and short exposure time. The pulsed character of the linear electrons accelerator allows to use these arrangements for the pulsed radiography of the fast-passing processes and also in the study of the objects moving periodically.

The technical characteristics of the accelerators are given in Table 2.3.

2.1.5. Microtrones

At present the effective electrons accelerator called microtron finds more and more considerable application for purposes of radiation nondestructive testing of the thick-walled and large-sized articles.

Microtron as a cyclic accelerator is an accelerator of the parallel action (a single accelerating cell repeatedly accelerates the electrons) and its effective impedance is higher than in the linear accelerators. Therefore the power of superhigh-frequency (SHF) generators for the microtron power may be much less. In accordance with the above-mentioned reasons the microtron has a simpler construction, less overall dimensions and mass than the linear accelerators, approaching it by intensity of the bremsstrahlung radiation.

In comparison with the betatron having an ordinary construction the microtron has a bremsstrahlung radiation intensity 10–100 times higher. Besides, the strong-current betatrons have more complicated construction, larger overall dimensions and mass than the microtron.

The above-mentioned reasons side by side with the small cross-section size of the microtron electron beam, its monoenergy character and the stability stipulate the using of this type of the accelerator for the defectoscopy. Technical characteristics of the modern microtrons for the defectoscopy are given in Table 2.4, and in Fig. 2.13 the most common structural scheme of the microtron is given, showing the basis parts of the accelerator and the interconnections between the separate parts.

The structure of the microtron consists functionally of the irradiator unit, the control system, the signalization, the blocking and defence, the

control panel, the pulsed modulator, systems of the transformation of the power three-phase voltage, cooling, the formation and maintenance of the needed vacuum.

The principle of the accelerator action. In the microtron, electrons are accelerated by the alternating electric field with constant frequency in the in time-constant and the radially uniform magnetic field, and are moved in the vacuum chamber by the orbits-circles having the common point of tangency (Fig. 2.14). The resonator is disposed in this place and its SHF-field accelerates the electrons.

The resonator is excited by the powerful source of the SHF-oscillations, namely the magnetron of pulsed action (in principle it is possible to excite the resonator by the source of continuous action).

Table 2.4

Technical characteristics of the microtros for defectoscopy

№	Type of accelerator *	Energy of radiation, MeV	Mean current of beam, micro A	Radiation exposure dose rate, R/(min·m)	Size of focal spot, mm	Increment of energy at single turn, MeV	Mass of irradiation unit, kg	Overall dimensions of irradiation unit, m
1	Graficon RM-8	8	50	1500	Ø2 with focusing	0.5	1500	1.1×0.8×1.8
2	Graficon RM-8S	8	250	3600	-»-	0.5	1750	1.7×0.9×2.4
3	PMD-10T	8.12	Up to 50	1000; 2000	2×3	0.6 – 0.9	1200	1.0×1.0×1.5
4	MP-1	7	Up to 35	500	2×3	0.6	1500	1.0×1.5×1.5
5	MD-10	7	50	2000	Ø2...3	0.6	2000	1.2×1.5×1.5
6	MMT-501	5	3	15	1.5×2	–	80	Linear sizes are not more than 0.5 m
7	MP-10	10	20	800	–	–	–	

*1–5;7 – microtrons of $\lambda=10$ cm diapason; 6 – microtron of $\lambda=3$ cm diapason; 1,2 – made in Sweden; 3–6 – made in USSR (Russia); 7 – made in PPR (Poland).

At this the accelerating field is formed in the resonator with the voltage of several hundred kilovolts on one cm (kV/cm), at the voltage of the leading magnetic field of the microtron within 900...2000 Oersted.

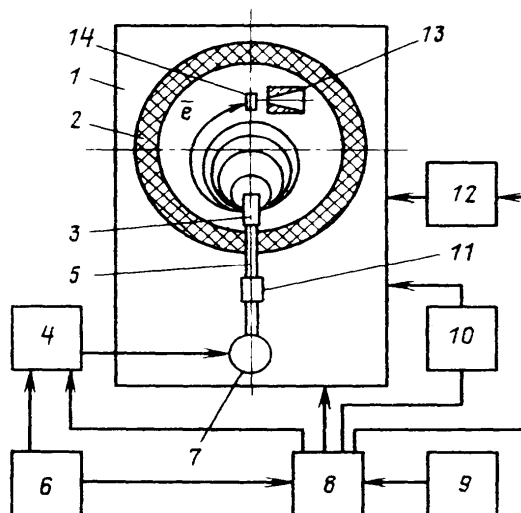


Fig. 2.13. Structural scheme of the microtron:

- 1 – Irradiator unit; 2 – Electromagnet with vacuum chamber; 3 – Accelerating resonator; 4 – Impulse modulator; 5 – Wave-guide loop; 6 – System of transformation of the power three-phase voltage; 7 – Source of the high-frequency power; 8 – Control system; 9 – Control panel; 10 – Cooling system; 11 – High-frequency upshot; 12 – System of needed vacuum formation and maintenance; 13 – Collimator; 14 – Bremsstrahlung target

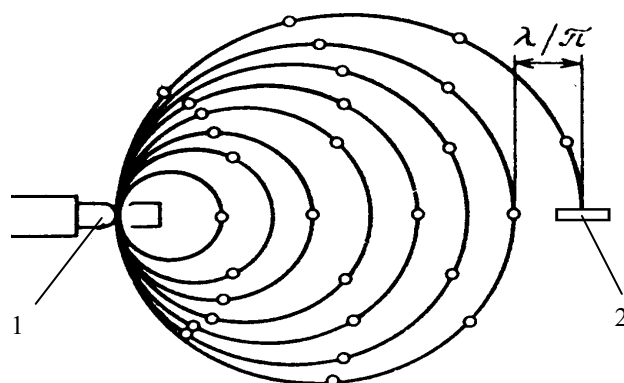


Fig. 2.14. Scheme of the electron acceleration in microtron:

- 1 – Irradiator unit; 2 – Target

At every passing through the resonator, electrons gain a certain energy ΔU and then transfer onto orbit of the large radius. The synchronism of the electron motion and the change of the accelerating SHF-field is achieved owing to the fact that every next turn is longer than the previous one by the integral number g of the SHF-oscillations. At the fulfilment of the above-mentioned condition the electrons pass through the resonator in one and the same phase of the SHF-field.

In practice those acceleration regimes are realised for which $g=1$ and the period of the electrons motion on the first orbit is equal to two periods of the SHF-field in the resonator. In this case the electrons energy on the n -orbit is (Fig. 2.15):

$$U_n = (n+1) \Delta U. \quad (2.3)$$

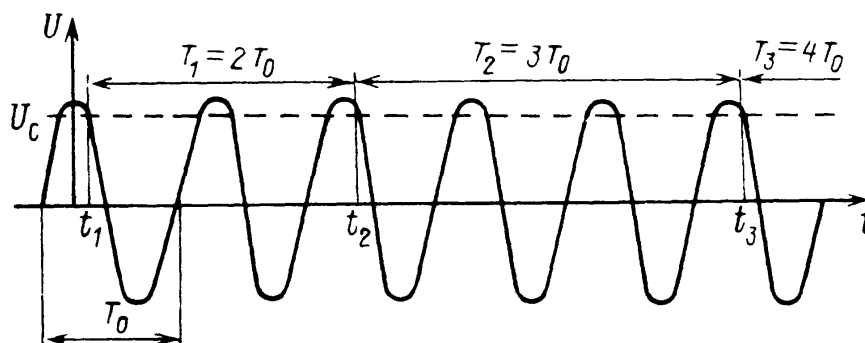


Fig. 2.15. The simplest regime of electrons divisible acceleration:
 T_0 – the period of SHF-oscillations of electromagnetic field in resonator

Electrons reaching the last orbit either move out from the vacuum chamber through the magnetic channel or hit the target.

The beam of the accelerated electrons consists of the separate clusters following each other at the distance equal to the wave length of the accelerating field. The clusters length is approximately $1/20\lambda$ (one/twentieth of lambda).

The accelerator works in the pulsed regime and the direction of impulses in the microtrons of the 10-centimeter range for the defectoscopy is several microsecond, the repetition rate may be 50, 100, 200, 400 hertz.

Microtrons may be used mainly for the radiographic testing of the welded joints, forging, castings and other steel articles with the wall thickness up to 400 mm.

The experimental results achieved by means of the microtron allow to estimate its efficiency of the using at the testing of the articles from steel with wall thickness 70...400 mm with the sensitivity at the radiography not less than 1 %.

2.2. The receiving of the examining picture by means of the X-ray film

The distribution of the roentgen radiation occurring at the examining of the test specimem must be visualised by a proper method. One of these methods is the application of the X-ray film. Since the X-radiation has a high penetrating capacity for the solid bodies, only a very small part of the radiation is absorbed on the film. Therefore, special requirements are put forward to the film sensitivity for the X-radiation. The silver content in the roentgen films is much higher than in the ordinary photofilm.

The roentgen films are covered with a sensitive layer from both sides, i. e. on the base there are emulsion layers from both sides. These layers are pasted on the substratum (the base) by a special glue layer and are protected from the external actions as it is shown in Fig. 2.16.

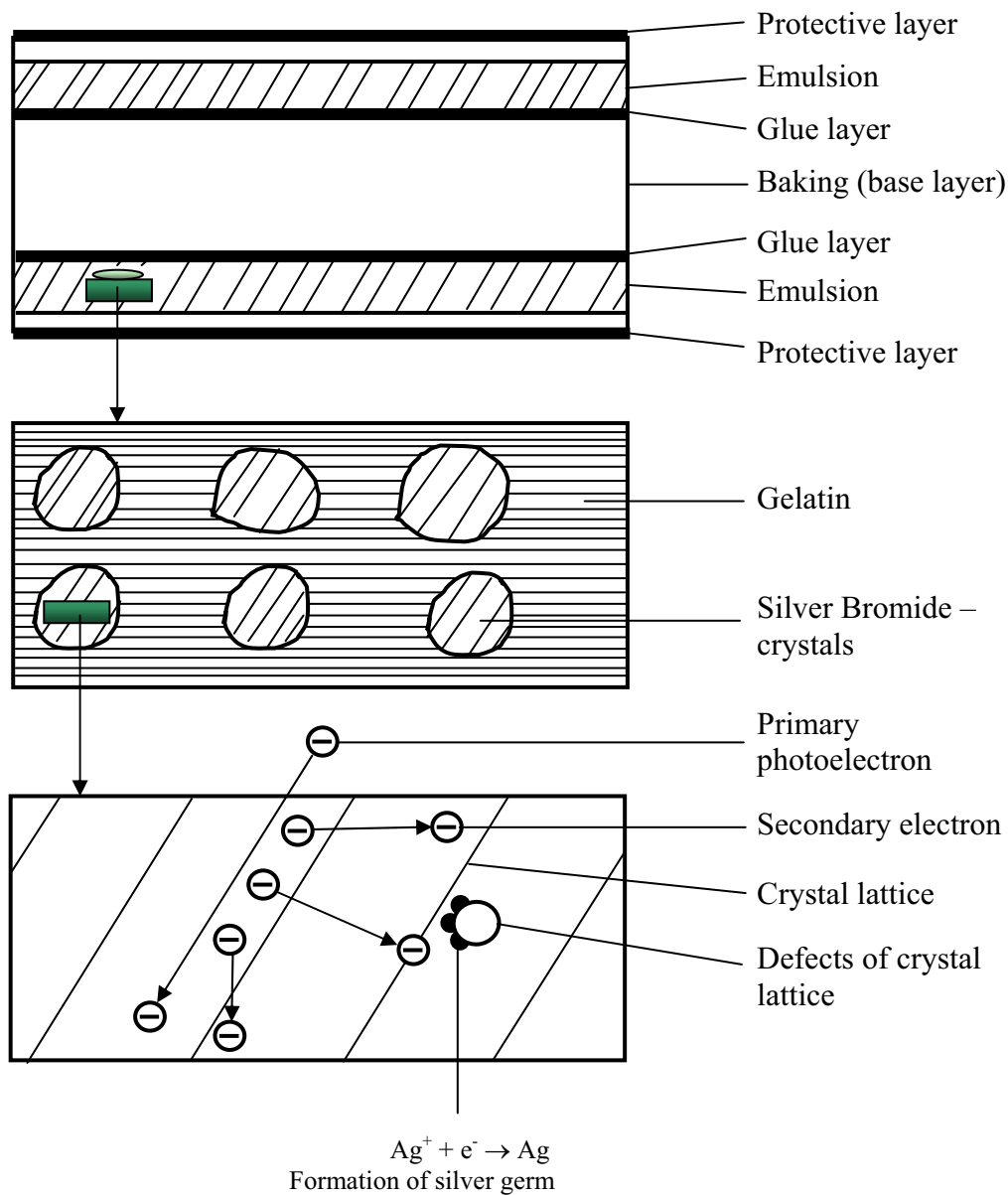


Fig. 2.16. The structure of the roentgen film layers

The crystals of the silver bromide are disposed in the emulsion layer in the gelatine matrix. A roentgen quantum can generate an electron in such a crystal of the silver bromide which will set free secondary electrons at the interaction with crystal. These secondary electrons are collected on the defects of the crystallic lattice and then led to the formation of the metallic granules of silver. In the process of the development, the visual image is received from the

negative image in which only a few granules of silver are presented. At this the metallic atoms of silver are the catalyzer for the formation of the further silver,so the available crystals may be transformed into the metallic silver.

The transparency of the emulsion layer is falling depending on how many granules of silver were available, i. e. how much of the X-radiation was absorbed in every area of the image. For the X-ray film it is described by means of optical blackening densities. At this, S is understood as the decimal logarithm of the ratio of the input light intensities to the light passed through the X-ray film:

$$S = \lg \frac{I_0}{I}, \quad (2.4)$$

where I_0 is the light intensity at input; I is the intensity at output. The illumination B is understood as the product of the intensity and the time:

$$B = I \cdot t. \quad (2.5)$$

In accordance with the Bunsen law:

$$S - S_0 \approx I \cdot t^P. \quad (2.6)$$

The connection between the natural logarithm of the illumination and the blackening received on the X-ray film is described by the curve plotted in Fig. 2.17.

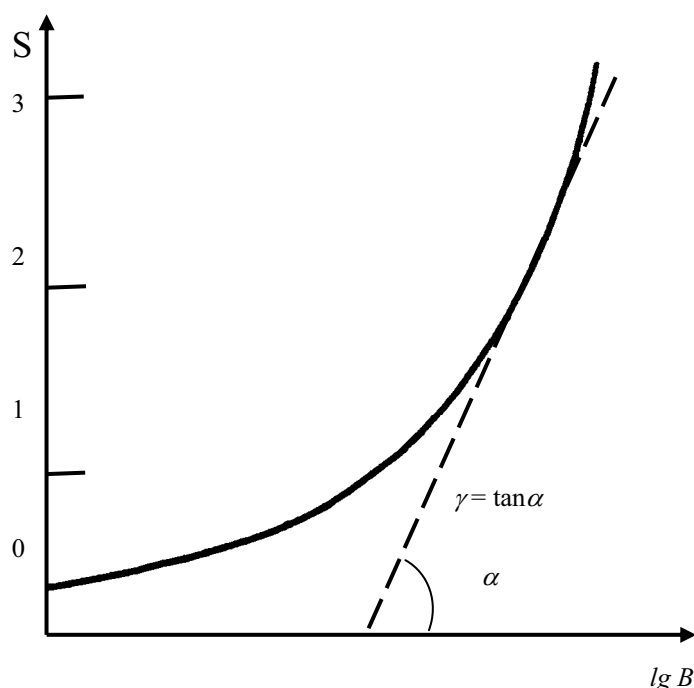


Fig. 2.17. The graduating curve

This connection has a parabolic form for modern X-ray films. It begins at the absent radiation from the fog and then transfers into a straight line at high

energies. The tangent of the slope angle of this straight line is marked as the gamma (γ) – (coefficient of the contrast). On the contrary to the obsolete roentgen films, modern films achieve the blackening of about 6–7 units and no any saturation effect occurs, determined as the “solarization” of the blackening.

The optical density of the blackening for the roentgenography must be not less than 2 in order to guarantee a sufficient contrast.

The area of the blackening, performed with the film whose low boundary value (for example, $S = 2$) is set by the norms and the upper boundary value is given through the transparency for the visual light sufficient for the image observation, is designated as the dynamic range. It is usually in the blackening area between 2 and 4. With the help of the contrast coefficient one can receive the exposures area belonging to the dynamic range and the corresponding area of the roentgen radiation intensities. Further, by means of the weakening coefficient one can calculate the maximum change of the testing sample thickness which one can still picture within the dynamic range (Table 2.5).

In order to increase the sensitivities of the roentgen films and the reduction of the exposure time, the intensifying foils are used. The metallic foils are closely set from both sides onto the roentgen film. Roentgen quanta are knocking out the photoelectrons at the passing through the foil which then can penetrate into the film from the foil and further can lead to the silver granules formation by means of the secondary electrons.

Table 2.5

The testing thickness of Fe, mm

Irradiator	$\Delta S = 1.5$	$\Delta S = 2.5$
Roentgen up to 100 kV	2	3
Roentgen up to 300 kV	10	16
¹⁹² Ir	12	22
⁶⁰ Co	24	40

The gain coefficients of the metallic foils are very low (see Table 2.6). However, these foils don't lead to a decrease of image sharpness. Another advantage is the capacity for the absorption of the low-energy scattered radiation which then leads to the contrast improvement on the film. The fluorescent screens have much more coefficients than the metallic foils. The consideration is about the fluorescent materials which emit ultraviolet radiation at passing the roentgen radiation through them. The films applied in this case have sensitivity to the ultra-violet radiation. With the help of fluorescent screens it is possible to achieve an increase of the sensitivity gain with the factor from 30 to 100. The shortcoming is that the sharpness is reduced in this case. It is the reason for

which the fluorescent screens are not permitted for the radiation testing. The single exclusion is the testing of the thick-walled parts from the iron cast in which it is needed to detect the defects having a very large volume.

Table 2.6

The intensifying foils

Irradiator	Foil	Gain factor
Roentgen 80...250 kV	Lead 0.02 mm	1...2
Roentgen above 250 kV	Lead 0.1 mm	2...3
¹⁹² Ir	Lead 0.1 mm	2...3
⁶⁰ Co	Steel 0.5 mm	1...1,5 (improvement of contrast)

2.3. Fluoroscopy and the roentgen radiation intensifiers

The advantage of the X-ray films is easy availability and the possibility of the received results storage. The shortcomings are the high costs at the very frequent testing fulfilment, a large expense of silver and chemicals for the image treatment and also the impossibility of the radiation testing automation. Therefore, in practice the other methods of the image receiving are finding much more application.

One of these methods is the using of fluorescent screens in which the X-radiation leads to the emission of visual light. For receiving a sufficient light intensity, a high intensity of the X-radiation is needed. One of the ways out is proposed by the application of the fluorescent screens in combination with the high-sensitive television chambers, the so called chamber of the residual illumination (isocones).

Still, today the fluorescent screens don't have the quality of the image needed for most of applications in radiation testing. Another case is with the roentgen radiation intensifiers. The roentgen radiation falls onto the primary fluorescent screen which is connected with the photocathode (see Fig. 2.18). From the photocathode the photoelectrons are emitted depending on the fluorescent radiation, i. e. depending on the falling roentgen radiation too. These photoelectrons are accelerated in the accelerating tube at the voltage of several tens kilovolts and then hit the second fluorescent screen.

This second image is characterised by the sufficiently higher light force than the primary one and can be observed by the eyes directly. But all the same today mainly the connection with the videochamber is used. Since the possibilities of the resolution for the X-radiation intensifier are better than for the ordinary television chamber, so the combinations with the high-resolution videosystems are used.

Since the own unsharpness of the X-radiation intensifier is higher than for the radiographic film, so the work with the roentgen radiation intensifiers is conducted at the direct magnification with the factor equal to 2–3, and the roentgen tubes with a very small focal spot are applied.

For receiving a contrast noise less image the intensifier is needed with a high intensity of the X-radiation which are not available in an ordinary application of the radiation testing methods. Therefore the noise is placed on the image received by the chamber. At using the technique of the images treatment in which the integration of a certain number of the videoimages (for example, 250) is fulfilled, one can receive the contrast and unnoised picture of the examining which corresponds to the requirements of such responsible problems as the welded joints testing. Owing to this, the systems of the X-radiation gain are forcing out ever more the application of the X-ray films. Together with the television chambers using and the image treatment, the digitised image may be received which can further be treated with the help of the computer and then be stored in the file form.

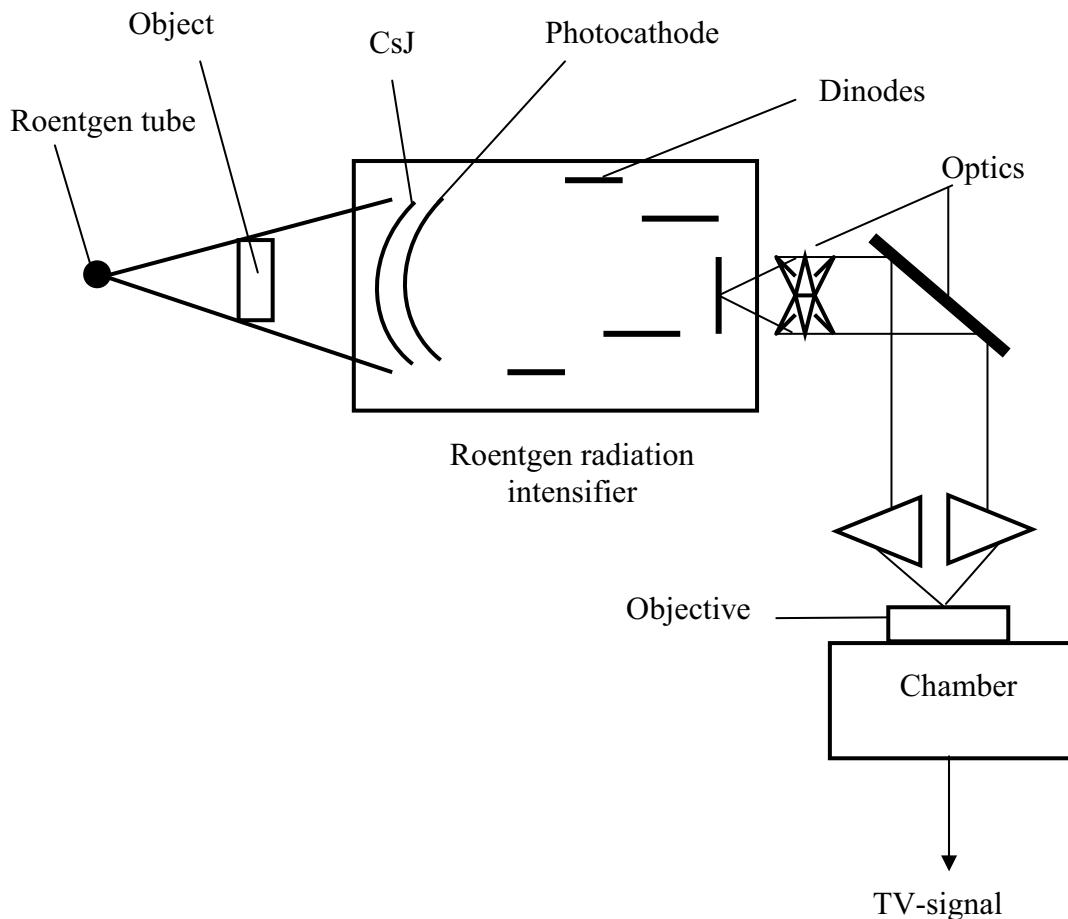


Fig. 2.18. The principle of the roentgen radiation intensifier action

2.4. Detectors of the X-radiation

2.4.1. The semi-conductive detector

The semi-conductive detector (SCD) is assigned to the class of the ionizing detectors. Requirements to the working matter of SCD and its principle of action may be considered easily on the base of the uniform (homogeneous) solid-body conductive detector. By the construction such a detector is a plate made from the dielectric and placed between two plane electrodes. The difference of the potentials created by the electric field inside a dielectric is added to the electrodes. We shall analyse the case when the dielectric has the ohmic contact with electrodes, i. e. the contact at which the free charge is realised between carriers of the charge of any pole between the dielectric and electrodes.

The charged particle being passed through a dielectric forms free electrons and holes on its path. Under the action of the electric field the formed free carriers are shifted towards electrodes and, at this, induce a charge on the electrodes that leads to the appearance of a current impulse in external circuit.

The choice of dielectric as the working matter of the homogeneous conductive detector is not casual since this matter must satisfy several requirements at the same time:

1. If the charged particle has lost the energy E_n in the material, then the mean number of the formed charges pairs N_0 is $N_0 = E_n/W$, where W is the mean energy required for the formation of one pair of the charges carriers. The less W , the more carriers appear in the working matter and the bigger the signal amplitude taken from the detector. Dielectrics have comparatively small value of W whose magnitude is in the range from units to several tens electron-volts.
2. At the motion of charges formed by the charged particles towards electrodes their number may decrease owing to the recombination or to the capture by the catcher. The process of change of the free charges number is characterised by the value of the mean life time τ which shows the time in which the number of free charges is reduced by e times.
3. It is obvious that the signal amplitude in the external circuit depends not only on the initial number of the carriers formed by the particle N_0 , but also on their mean life time τ . Therefore the bigger the value of τ (more exactly, the relationship of value τ and time of charges collecting), the greater the signal amplitude. In some dielectrics the life time of electrons and holes may achieve the magnitudes of about $\tau = 10^{-3} - 10^{-4}$ seconds and be sufficiently above the time of their collecting onto the electrodes.

4. The time of charges collecting on the electrodes is determined by the carriers transfer speed (drift speed) V_{dr} in the electric field which, in its turn, is connected with the field tension E by the relationship: $V_{dr}^+ = \mu_0 E$, where μ_+ , μ_- are mobilities of the positive and negative charges. The higher mobilities of charges, the shorter the time of their collecting on the electrodes and the higher resolution time of the detector. In a number of dielectrics, electrons and holes have approximately equal and sufficiently high values of mobilities and, therefore, detectors on their base may have sufficiently good time characteristics.
5. A very important requirement is set for the value of the specific electric resistance of the working matter of the detector in question. Since any material has a finite electroconductivity, then under the action of the electric field the current flows through this material. The number of the charge carriers drifting between electrodes and generating the direct current I_0 is the subject to the statistical fluctuations whose absolute magnitude is the bigger the bigger the current. If the number of the current fluctuations is comparable with the carriers number N_0 formed by the particle, then the extraction of the useful signal on the phone of this fluctuations (on the phone of noises) becomes impossible. In order to estimate the accepted value of the specific resistance of the working matter of the homogeneous solid-state conductive detector, let's find the ratio of the carriers number N_0 to the direct current fluctuations I_0 .

Let's characterise the direct current fluctuations by the value of the root-mean-square deviation $\sigma(N)$ from the mean number of carriers forming the direct current.

Considering that the number of direct current carriers crossing the distance d between electrodes in the time of carriers collecting $T = d/V_{dr}$ is described by the Poisson distribution, the value $\sigma(N) = \sqrt{I_0 T / e}$, where e is the carrier charge. Then the ratio of the number of carriers pairs formed by the charged particle with energy $E_{\bar{i}}$ and the $\sigma(N)$

is $N_0 / \sigma(N) = \frac{E_{\Pi}}{W} \sqrt{\frac{e}{I_0 \cdot T}}$. Let's choose the ratio $N_0 / \sigma(N) = 10^2$, i. e. let's

give the value of the signal from the charged particle bigger by two orders (by 100 times) than the direct current fluctuations in the external circuit of the detector. So, for the mean value of the direct current through the detector the following condition must be fulfilled:

$$I_0 \leq (E_{\Pi} / W)^2 \cdot \frac{e}{T} \cdot 10^{-4}. \quad (2.7)$$

Taking into account that the specific resistance of the material ρ is connected with the current by the relationship $I_0 = \frac{E \cdot S}{\rho}$, where E is the tension of the electric field in the detector volume, S is the detector square, and assuming that $\mu_- \cong \mu_+ = \mu$, we shall receive that

$$\rho \geq \left(\frac{W}{E_{\Pi}}\right)^2 \cdot \frac{E \cdot S \cdot T}{e} \cdot 10^{-4} = \left(\frac{W}{E_{\Pi}}\right)^2 \cdot \frac{V \cdot 10^{-4}}{e \cdot \mu}, \quad (2.8)$$

where $V = S \cdot d$ is the detector volume.

For the quantitative estimation of the ρ value let's assume that in the detector with the volume 1 cm^3 the charged particles completely lose their energy; $E_n = 1 \text{ MeV}$; $W \cong 5 \text{ eV}$; $\mu = 10^3 \frac{\text{cm}^2}{\text{V} \cdot \text{S}}$. The order of magnitude of W and μ corresponds to their values in dielectrics. Then the minimum accepted specific resistance is approximately equal to $\rho = 10^9 \text{ Ohm} \cdot \text{cm}$. Therefore the above-fulfilled analysis of ω , τ , μ and the estimation of the accepted magnitude of ρ strongly narrows the range of materials (even between dielectrics) which can be used as the working matter of the homogeneous solid-state conductive detector.

Insulators have a high specific resistance ($\approx 10^{16} \Omega \cdot \text{cm}$), comparatively small ω and big μ . However, the life time of the carriers in them is too short and also the carriers capture in the crystal volume leads to the appearance of the volumetric charge, to the polarisation and, finally, to the disruption of the detector working.

Silicon and germanium have the needed magnitudes of ω , τ , μ for the formation of the homogeneous conductor SCD from the semi-conductor (see Table 2.7). However, at the room temperature the specific resistance of silicon and especially, of germanium is sufficiently less than it is needed in accordance with above-fulfilled calculations for the formation of the type of detector in question. Let's take silicon as an example. It is known that the specific resistance of dielectrics is determined through using the density of electrons in the zone of the conductivity and holes in the valent zones and their mobilities by the following expression:

$$\rho = \frac{1}{e} (n\mu_- + p\mu_+), \quad (2.9)$$

where n and p are the electrons density and holes density. In the silicon crystal having its own type of conductivity (i. e. in crystal in which structural defects and impurities are absolutely absent) the densities of electrons and holes are equal $n = p = n_i(S_i)$ and determined from the formula:

$$n_e(Si) = 2.8 \cdot 10^{16} T^{3/2} e^{-E_g/2KT}, \quad (2.10)$$

where T is the temperature; $E_g = 1.1$ eV is the width of the forbidden zone, K is the Boltzmann constant. Let's consider the case of a homogeneous conductive detector with the ohmic contacts when the semi-conductor is freely changed by the free charges with electrodes, the density of carriers in the zones in the presence of electric field remains the equilibrium and equal to $n_e(Si)$. Calculating the value of $n_e(Si)$ for silicon at the room temperature ($T = 300$ K) and using the data of Table 2.7, we get the magnitude of ρ for a crystal with no impurities $\rho(Si) = 2.4 \cdot 10^5$ Ohm·cm. The analogous calculation for germanium $n_i(Ge) = 9.7 \cdot 10^{15} \cdot T^{3/2} \cdot e^{-E_g/26T}$; $E_g(Ge) = 0.67$ eV; gives $\rho(Ge) = 65$ Ohm·cm.

Table 2.7

Material	W, eV	μ , cm ² /V·S		τ_p , second	
		μ_-	μ_+	e^-	e^+
Diamond	15...20	1800	1200	—	—
Silicon telluride	4.65	600	45	$>10^{-5}$	$4 \cdot 10^{-5}$
Silicon	3.7	1350	480	$3 \cdot 10^{-3}$	$3 \cdot 10^{-3}$
Germanium	2.94	3800	1820	10^{-3}	10^{-3}

Besides, the specific resistance of silicon and germanium depends very strongly on the presence of impurities in them. Therefore the specific resistance of real crystals even at very high degree of the purification from impurities is significantly less than the calculated above meanings of $\rho(Si)$ and $\rho(Ge)$.

Therefore at present the development of detectors on the base of silicon and germanium goes in the direction of the creation of the nonuniform (heterogeneous) SCD. In such SCD the properties of the transfer between semi-conductors with different type of conductivity or the transfer between the semi-conductor and the metal are applied.

Let's consider processes taking place in the transfer formed between the semi-conductors of n-type and p-type or, briefly, p-n transfer (examples of methods of transfers formation are given below). Let's choose the frequently encountered in practice case when one of the semiconductors (for example, of p-type) is strongly alloyed, i. e. the concentration of the acceptor impurities in it is sufficiently higher than the concentration of impurities in the n-type crystal. In n-area of the semi-conductor the main carriers are electrons, in p-area the main carriers are holes. At the moment of the contact appearance between n ~ and p-semiconductors the diffusion of carriers towards the decrease of their concentration gradient occurs because of the concentration

difference. Since the ionizing atoms of donor and acceptor impurities can not move, then in n-area of the semi-conductor near the contact a non-compensated positive volumetric charge appears and in p-area – a negative charge of ions of acceptor. At the accumulation of volumetric charges on the transfer a potential jump appears, performing the role of the potential barrier and preventing the electrons diffusion in the p-area and the holes in the n-area.

In the state of dynamic equilibrium coming in, the current (flow) of the main carriers of each pole at the expense of the residual diffusion will be balanced by the current of the secondary carriers diffused from the other area, and the mean value of the current through the transfer occurs, equal to null, and the carriers concentration in the transfer area will be sharply decreased (Fig. 2.19).

In principle, such a detector with p-n transfer may be already used for the charged particles registration even in the absence of the external tension source, since in the semiconductor it is the area in which the electric field tension is different from the null. If the charged particle passes through this area and forms free carriers, they will be transferred under the action of the field of the volumetric charge and will induce the charge on the electrodes.

However, the area of volumetric charge in p-n transfer (the thickness of the transfer area d) makes up less than 10^{-4} cm. Since the paths of the charged particles are usually greater than this value, such regime has no practical interest.

Therefore at the application of the heterogeneous SCD the transfer thickness is raised by adding the back shift tension V_{sh} to the detector electrodes, i. e. the “plus” of the tension source is added to the electrode from the n-area side and the “minus” of source is added to the electrode from the p-area. In this case the value of the potential barrier is increased, the external field rolls out the main carriers from the transfer area increasing thus the length of the volumetric charge and the transfer thickness correspondingly (Fig. 2.19, II). The conductivity of the transient area to which the back tension of the shift is applied is different from zero, since at the transfer area there is a certain density of the free charge carriers and so the current flows continuously through the transfer. Really, as distinct to the case of p-n transfer without the external electric field, the current of the secondary carriers is not already balanced by the current of the main carriers, since none of the main carriers can practically overcome the high potential barrier created by the external electric field in the transfer area.

Therefore, the current will flow through the transfer owing to the secondary carriers diffusion in the transfer area (diffusion current). Besides, in the transfer zone the thermal generation of electrons and holes takes place

constantly. These carriers, being transferred under the action of the electric field, are the current source too (generation current).

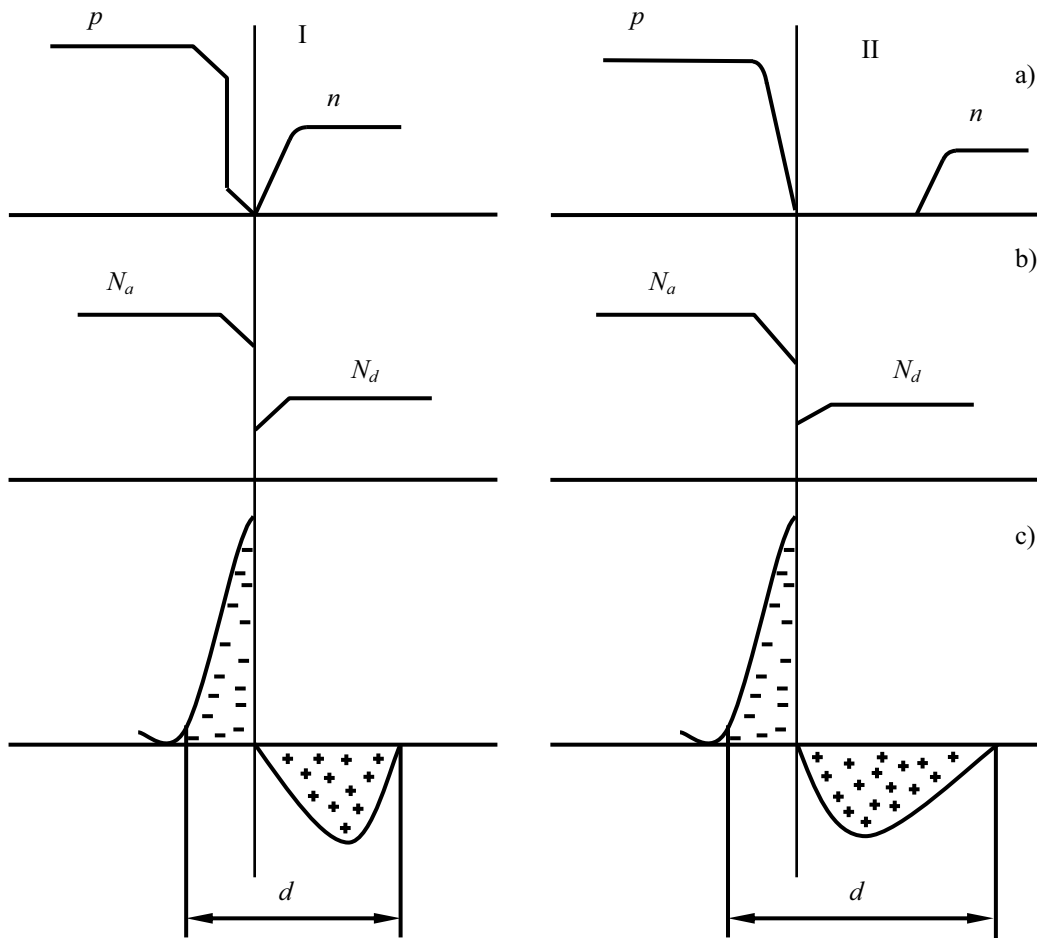


Fig. 2.19. Characteristics of the equilibrium (I) and p-n transfer with back shift (II):
 a) – concentration of electrons and holes; b) – concentration of ionizing atoms of impurities; c) – distribution of the volumetric charge

Since the generation speed of secondary carriers outside the transfer is $g \cong 1/\tau_r$, where τ_r is the life time of the free carrier before the recombination and the time of their drift through the transfer (the collecting time) is equal to value T , then the density of the secondary carriers in the transfer area and their density outside the transfer are in the ratio T/τ_p .

By the analogous way at the thermal generation speed of carriers in the transfer $\approx n_i/\tau_p$, their density in the p-n transfer area as related to the density outside the transfer is proportional to the ratio T/τ_p . So, for example, in the SCD with p-n transfer on the base of silicon the collecting time T depends on the transfer area sizes and has magnitudes in the range of $10^{-6} \dots 10^{-9}$ seconds. It is seen from the comparison of T with τ_p in silicon given in Table 2.7, that $T \ll \tau_p$. Therefore the carriers density in the transfer is by several orders

(several tens times) less than the carriers density outside the transfer. Hence, a sufficiently lower current will flow through the transfer than in the case of the homogeneous conductive detector with the same geometric dimensions. In other words, since the specific resistance is inversely proportional to the density of the free carriers, the value of ρ of semi-conductor material in the transfer area is, as related to the τ_p/T ratio, approximately higher than the specific resistance value outside the transfer, i. e. than the value of initial semi-conductor matter. Modern industry produces many different types of heterogeneous silicon and germanium SCD. As distinct from the heterogeneous SCD on the base of germanium, the silicon SCD usually work at the room temperature. Depending on the way of the transfer formation the following types of silicon detectors are distinguished: the diffusion detectors, the ion-alloyed, the surface-barrier detectors. In the diffusion detectors the transfer is formed by the diffusion of donor atoms (mainly phosphorus) into the semi-conductor of p-type or by diffusion of acceptor atoms (mainly Boron) into the semiconductor of n-type.

In the ion-alloyed detectors the transfer is formed by the insertion of the impure atoms into the semi-conductor at its irradiation by the ions beam.

In the surface-barrier detectors the transfer appears on the silicon surface at the covering on it by the evaporation in the vacuum of some metals or by the surface oxidation on the air. The silicon surface-barrier SCD have found a especially wide application for the registration of the charged particles of different types. The transfer thickness of such SCD is comparatively short, they are usually applied for the spectrometry of heavily charged particles (protons with energy up to 5 MeV, alpha-particles with energy up to 20 MeV, heavy ions, fission fragments), electrons with energy up to 200 keV, for the registration of flows of low-energy roentgen – and gamma-quanta.

The main exploitation parameters of the silicon surface-barrier semi-conductor detectors. At present, such SCD are manufactured mainly from the silicon of n-type. After a corresponding treatment on the surface a very thin layer of the silicon of n-type the layer with high density of holes is formed, similar by its properties with the diffusion layer of p-type.

The electric contact with the formed on the surface transfer layer is realised most often with the help of a thin film of gold covered in vacuum. On the other side of the crystal the ohmic contact is created by the aluminum sputtering in vacuum or by the nickel application. In the process of ionizing radiation registration the back tension of the shift is added on the detector.

In accordance with the state standard such surface-barrier silicon detectors are marked by the following way: ДКПс – 100 (Detector Silicic Semi-conductor-100). The small letter behind ДКП shows the type

of the constructive mounting, figures designate the square of the sensitive surface of detector in the square millimetres. Usually the SCD characteristics are divided into the geometric, electric and radiometric ones.

Geometric parameters of SCD are the thickness of the sensitive area, the thickness of the dead layer and the square of the sensitive surface.

The sensitive area is that part of the SCD volume in which the interaction of ionizing radiation with the semi-conductive material leads to the appearance of the useful signal on the output electrodes of the detector. The thickness of the sensitive area is the length of the transfer area measured at the normal to the SCD surface. For the surface-barrier detectors the thickness of the area may be expressed by the equation:

$$d = \sqrt{2 E_0 \cdot E \cdot M \cdot V_\rho (V_0 + V_{sh})},$$

where E_0 is the electric constant; E is the dielectric penetrability of silicon; μ is the mobility of the main carriers of the slightly alloyed semi-conductor; ρ is the specific resistance of the initial material – Silicon of n-type, which is used for the detector creation; V_0 is the difference of potentials in the transfer area in the absence of the external tension; V_{sh} – is the back tension of the shift applied to the SCD.

The silicon of n-type obtained at present allows to make the industrial detectors of DKP-type with the thickness of the sensitive area not more than 300 micrometers.

The dead layer thickness is determined as the insensitive part of SCD disposed between the input window and the sensitive part of the detector. For the surface-barrier detectors of DKP-type the dead layer is determined by the gold film thickness only put on the silicon surface and it is equal $\leq 20 - 50$ microgram/cm (≤ 0.03 micrometers).

The sensitive surface square is the part of the detector surface through which the radiation gets into the sensitive volume. Silicon manufactured at present by the industry allows to make detectors with the sensitive surface square not more than 5 cm^2 .

The main electric parameters of SCD are the detector capacity; the back dark current; the energy equivalent of the noise level.

Detector capacity. The surface-barrier detector with shift tension applied to it may be approximately considered as two metallic electrodes with the insulator between them.

So, the detector capacity C_{det} and the sensitive area thickness d are connected by the relationship: $C_{det} = E_0 \cdot E \cdot S / d$, where S is the sensitive surface square. It is the value of d that comes into the formula but not the total thickness of the silicon crystal itself from which the detector is made.

It is connected with the fact that, as it was mentioned above, the resistance of the transfer area is sufficiently higher than the resistance of the semiconductor initial material and, therefore, the tension applied to the electrodes is then reduced mainly on the transfer.

The back dark current of the silicon surface-barrier detector at adding to it the shift tension is connected with the current passing through the transient area having the finite conductivity (the volumetric current of leakage) and with the leakage current passing through the SCD surface (surface current of leakage).

The volumetric current has diffusion and generation components whose nature was considered above. It is practically impossible to estimate the surface current of leakage by the calculation though in many cases it makes the main contribution to the back dark current. Therefore, the value of the back dark current is measured usually in the experiment and then is given in the specifications of the given specimen of the detector for the optimal shift tension. Since the back current gives as a rule, the main contribution in the SCD noises, this characteristic is an important electric parameter of the detector. For detectors of DKP-type the typical value of the back current of leakage is in the interval of values of (0.05...0.5) microAmper.

The energy equivalent of the SCD noise level characterises the impulses amplitude spread on the detector output connected with the passing of the back dark current at the adding of the shift tension and with the presence of the thermal noises. The energy equivalent of the noise level is typically described by the value $\Delta E_{\text{det-n}} = 2.35 \cdot \sigma_{\text{det-n}}$, where $\sigma_{\text{det-n}}$ is the mean-root-square fluctuations of the impulses amplitudes on the detector output expressed in the energy units (usually-in keV). Having determined by the experiment the $\Delta E_{\text{det-n}}$ value, one can draw a conclusion about the SCD noises contribution to the own energy resolution of the detector.

The radiometric parameters of SCD are parameters connected with the registration of the ionizing radiation, partially the own energy resolution, the detector proportionality, the charge collecting efficiency formed by the ionizing radiation, the efficiency of the registration.

Side by side with the own energy resolution the idea of the total energy resolution is applied as the characteristic of the spectrometric arrangement in total, i. e. the detector in the combination with the electronic loop. This value accounts also for the contribution of the electronic loop to the impulses energy spread.

It is known that the total energy resolution of the spectrometric arrangement with the SCD as the detector depends on the magnitude of the V_{sh} . Therefore, at the exploitation of the SCD of DKP (silicic surface detector) – type a great role is performed by the right choice of the shift tension.

2.4.2. The gas ionization detectors

2.4.2.1. Impulsed ionization chamber

The pulsed ionization chamber is a detector whose action is based on the measuring of the charge created by the charged particles in its working matter. The gas ionization chamber is a closed volume filled with the working material – gas with two or several electrodes of the different configuration disposed in it. The pulsed ionizing chambers are applied usually for the registration of the strongly-ionizing short-path particles.

In passing through gas, a charged particle loses its energy on the medium atoms ionization and excitation. At this, a number N of electron-positron pairs is formed. The mean energy ω which is expended on the single electrons-ion pair formation is independent practically from energy and particle type and for the most of gases used as the working matter of the ionization chambers, is in the values interval $\omega = 20 \dots 40$ eV. The mean number of charges pairs created in the gas at the deceleration of particles with the energy E is $N_0 = E/\omega$. Because of the accidental character of the charged particle interaction with the matter atoms the value of N is fluctuating. The fluctuations of the number of the charges pairs N are characterised by the dispersion $D(N)$.

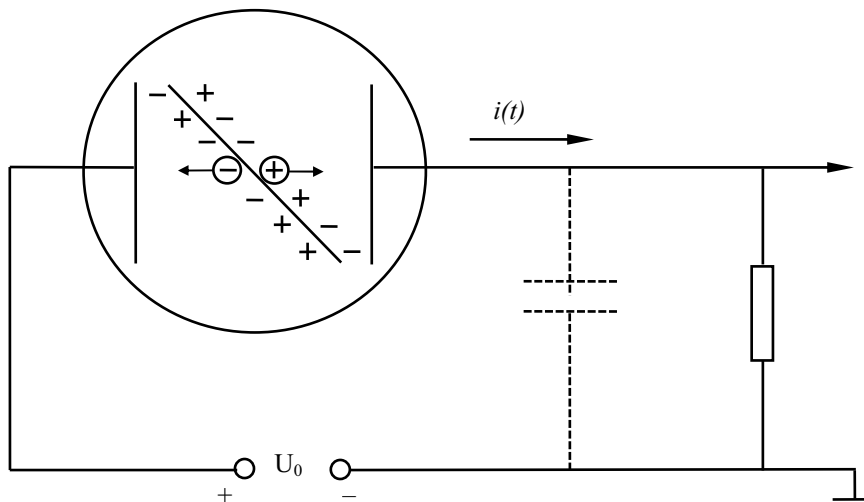


Fig. 2.20. The scheme of the pulsed ionizing chamber switching on

The dispersion of the number of charges pairs is proportional to their mean number: $D(N) = F \cdot N_0$. The proportionality factor F has the name of Fano factor. If the ionization fluctuation is occurring in accordance with the Poisson law, the value of F will be equal to 1. In reality it is $F < 1$. It has been shown that the ionization fluctuations are described by a more complex law. The reason consists in the fact that the ionization acts are not independent if the particle at the deceleration in the matter process loses all

its kinetic energy and the relationship between the energy expended on the ionization and the excitation of the matter is not maintained strictly determined in every ionization act. The created as the result of ionization charges $q_0=eN_+=eN_-=eN_0$ under the action of the external electric field pass towards the corresponding electrodes. The motion of the positive and negative charges leads to the change of the induced charge appearing on the electrodes. Its value is determined by the primary disposition of the drifting charges and by their number $e \cdot N_+(t)$ and $e \cdot N_-(t)$.

While charges pass between electrodes, at the external circuit of the chamber the electric current flows. The value of the electron $i_-(t)$ and ion $i_+(t)$ components of the electric current impulse is maintained by the Ramo – Shokley formula:

$$i(t) = q(t) \cdot \frac{E}{V_0} \cdot \frac{dx}{dt} \quad (2.11)$$

where $q_+(t)=e \cdot N_+(t)$ and $q_-=e \cdot N_-(t)$ are the meanings of the charges drifting in the chamber; $E=V_0/d$ is the electric field tension in the chamber with the distance d between electrodes on which the difference of the potential V_0 is added; $dx/dt=V_{\pm}$ is the charges drift speed.

It is seen from formula (2.11) that the current amplitude and the form, its duration depend on the charges drift speed in the chamber and on where and how the particle has passed in the interelectrode space. Really, if the charged particle has flown in parallel to the chamber electrodes at the distance x from the high-voltage electrode (the left in Fig. 2.20), then the components of the induced current, under the condition that the number of electrons and positive ions in the drift process is not changed, have the following form:

$$i_-(t) = \begin{cases} eN_- \frac{v_-}{d}, & 0 \leq t \leq \frac{x}{v_-}; \\ 0, & t > \frac{x}{v_-}, \end{cases} \quad (2.12)$$

$$i_+(t) = \begin{cases} eN_+ \frac{v_+}{d}, & 0 \leq t \leq \frac{d-x}{v_+}; \\ 0, & t > \frac{d-x}{v_+}. \end{cases} \quad (2.13)$$

If the particle of the same energy has passed perpendicularly to electrodes and its path is equal to the interelectrode distance d , the number of electrons and ions in the chamber is reduced in time by the following laws:

$$N_-(t) = N_0 \left(1 - \frac{v_-}{d} t \right); \quad (2.14)$$

$$N_+(t) = N_0 \left(1 - \frac{v_+}{d} t \right); \quad (2.15)$$

in the time interval $0 \leq t \leq d/v_-$ and $0 \leq t \leq d/v_+$ correspondingly, on condition that the ionization density is constant along the track. In Fig. 2.19 the forms of the electron and ion components of the current impulses in the external circuit of the chamber are given for tracks oriented in parallel (a) and perpendicularly (b) to the electrodes.

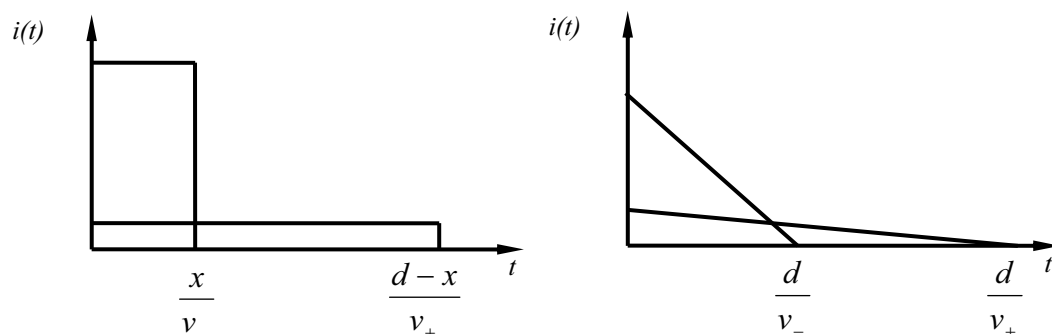


Fig. 2.21. The components of the current impulses in the external circuit of the chamber

The charges' collecting time in the pulsed chamber determines its time resolution, i. e. that minimum time interval which must differ two following each other particles in order to avoid the overlapping of the current impulses and change of the impulses amplitude. Speeds of ions drift (positive and negative) in gases are by 2–3 orders (in 100...1000 times) less than electrons speeds. Therefore the full charges' collecting time (electrons and ions) is usually $10^{-2} \dots 10^{-3}$ seconds. This circumstance places a limitation on the intensity of the studied particles flow. The flow must be not more than $\sim 10^{+2} \text{ s}^{-1}$, since the time intervals between the particles hits into the detector must be not less than 10^{-2} s .

One can provide a high time resolution of the chamber by the registration of the electron component of the current impulse only. Since the current impulse amplitude $i_-(t)$ is the function of the drifting electrons number $N_-(t)$, it is necessary that the electrons in the drift process are not captured by molecules or by the gas atoms with the creation of the negative

ions. The long life time of electrons in the free state may be achieved in pure inert gases which are applied often for the filling of the impulsed ionization chambers. By the registration of the current impulses, one can measure the particle energy (if the particle loses its energy fully in the chamber); receive the information about the moment of its passing; determine the orientation of the particle trace as related to the electrodes.

However, the registration and the treatment of the short current impulses with the amplitude $10^{-7} \dots 10^{-9}$ Amper has certain difficulties. Therefore, the charge is usually measured which is accumulated on the capacity C (see Fig. 2.20). The capacity C is added from the own capacity of the chamber, the capacity of the loading resistor R , the assembling capacity and the capacity of the electron block added to the detector.

The magnitude of the charge $Q(t)$ which is accumulated on the capacity C , for the scheme with such external circuit, is determined by the equation:

$$\frac{dQ(t)}{dt} + \frac{Q}{RC} = i(t). \quad (2.16)$$

The solution of this equation at the initial condition $Q(0)=0$ has the following form:

$$Q(t) = e^{-t/RC} \int_0^t i_-(t') e^{-t'/RC} dt' + e^{-t/RC} \int_0^t i_+(t') e^{-t'/RC} dt'. \quad (2.17)$$

The first term of the formula (2.17) $Q_-(t)$ describes the charge accumulation on the capacity C from the electron component of the current in the time interval $0 \div T^-$; the second term $Q_+(t)$ describes the charge accumulation from the ion component of the current in the interval $0 \div T^+$, where T^- and T^+ is the time of electrons and ions collecting in the chamber. For $t > T^-$, $i_-(t)=0$ and the first term in the expression (2.17) in the accordance with the solution of the equation (2.16) with the null right part, becomes

equal to $Q_-(t) = Q_-(T^-) e^{-\frac{t-T^-}{RC}}$. By the analogous way, for $t > T^+$ the second

term in the formula (2.17) is transformed: $Q_+(t) = Q_+(T^+) e^{-\frac{t-T^+}{RC}}$, i. e. both cases describe the process of the capacity C discharge through the resistor R .

If $RC \gg T^+$ (T^+ is ions collecting time), the solution of the equation (2.16) is given by the expression:

$$Q(t) = \int_0^t i_-(t') dt' + \int_0^t i_+(t') dt' \quad (2.18)$$

Such regime of the chamber working is named **the regime of the full collecting** at which the maximum charge induced on the capacity C independently from the particle track orientation in the chamber is determined by the number of charges N_0 only and $Q(T^+) = e \cdot N_0$. So, by substitution the expression for the current (2.12) and (2.13) in the equation (2.18) one has

$$Q_{\max} = eN_- \frac{x}{d} + eN_+ \frac{d-x}{d} = eN_0.$$

By the analogous way the solution of the equation (2.18) for the case of track perpendicular to electrodes gives $Q_{\max} = e \cdot N_0$. Since $N_0 = E/w$, so $Q_{\max} = e \cdot E/w$ is a handy characteristic of the particle energy lost in the chamber.

In those cases when the main demand is the providing of a high time resolution of the chamber, the condition $T^- \ll RC \ll T^+$ is chosen. Then, the expression (2.17), with a high accuracy, is transformed:

$$Q(t) = e^{-t/RC} \int_0^t i_-(t') e^{t'/RC} dt'.$$

The chamber with such working regime is called the chamber with the electron collecting. If $T^- \ll RC \ll T^+$, so

$$Q(t) = \int_0^t i_-(t') dt'. \quad (2.19)$$

In practice the needed regime of the chamber working is provided not by the change of RC but by the choice of the passing band of the amplifier. A significant defect of the ionization chamber with the electron collecting is the dependence of the charge $Q(t)$ not only on the particle energy but on its track orientation, too. The considered effect considerably complicates the problem of measuring the energy of the studied particles. One of the methods of its elimination is the insertion into the chamber of the third electrode, i. e. grid. The gas pressure in the chamber with the grid is chosen by the way that paths of the registered particles are fully kept within the interval “the high-voltage electrode – the grid” (the auxiliary volume of the chamber). The particles – electrons created on the track drift in the direction of the collecting electrode, then passed through the grid and induce the charge in the external circuit at the motion in the interval “the grid – the collecting electrode” (the working volume of the chamber), only, since the grid screens one volume of the chamber from the other practically fully. It is obvious that in this case the maximum amplitude of the charge induced in the external circuit does not depend on the track orientation. Thus, the chamber with the grid can provide a sufficient energy resolution at a sufficiently high time resolution.

The low limit of the absolute energy resolution ΔE_{abs} of the spectrometer on the base of the chamber with the grid is connected with the fluctuations in the number of the formed pairs of the charges carriers and for the absorbed energy E it is equal to the value $\Delta \varepsilon_u = 2,36\sqrt{F\varepsilon\omega}$. This resolution will be achieved if the other factors worsening the energy resolution are eliminated fully. These worsening factors are the input noises of the amplifier; the presence of the leakage currents around the chamber; fluctuations in the number of collected electrons stipulated by the nonuniformity of the grid and by the electron capture by the electronegative impurities; the incomplete shielding (screening) of the working volume of the chamber from the auxiliary volume and some dependence of the induced charge amplitude on the particle track orientation connected with the incomplete screening; the dependence of the induced charge form on the particle orientation in the auxiliary volume of the chamber which leads to fluctuations of the impulses amplitude on the spectrometric loop output because of the different conditions of their formation.

2.4.2.2. Gas-filled proportional detector

The gas-filled proportional detector is attributed to the ionization detectors working in the regime of gas amplification.

In passing through the gas the charged particle, having lost the energy E, creates on its track N_0 of electron-ion pairs, on average (the primary ionization), determined by the relationship $N_0=E/w$, where w is the mean energy spent on the single pair formation. Electrons and ions drift through the gas under the action of the external electric field. If the strength of the electric field inside the detector is sufficiently high, the electrons created by the particle in the working volume collect the energy on the free path length which is enough for the molecules or atoms of the gas ionization at the collisions with them (the secondary ionization).

If on the path of 1 cm in the direction of the electric field electrons experience the α intercollisions led to the ionization, the number of ions pairs created by N electrons in the layer dx

$$dN = N \cdot \alpha(x) dx,$$

where α is the coefficient of the collision (impact) ionization.

So the total number of 'ions pairs in the avalanche is

$$N = N_0 \exp\left(\int_{x_1}^{x_2} \alpha(x) dx\right), \quad (2.20)$$

where x_1 is the coordinate of the primary ionization location; x_2 is the coordinate of the avalanche end.

The increase of the number of the ions pairs owing to the impact ionization is characterized by the gas amplification factor m which is equal to the ratio of the total number of ions pairs N in the avalanche to the number of ions pairs N_0 created initially by the registered particle: $m = N/N_0$.

It is seen from the formula (2.20) that the number of ions pairs formed inside the avalanche is determined not only by the values of N_0 and α but also by the location of the primary ionization. So, the value of the charge Q induced in the external circuit of the ionizing detector with the gas amplification, which is proportional to the number of the drifted charges $Q \sim m \cdot N_0 \sim N$, will depend on the particle track coordinate too.

It is obvious that in a detector with the gas amplification the amplitude of the charge Q induced in the external circuit will be proportional to the energy E lost by the particle only in the case if every primary electron creates in the amplification process one and the same number of ions pairs on average and independently in the place of its formation. Such condition is fulfilled in the detector of cylindrical form in which the diameter of the cathode, i. e. the cylinder, is much bigger than the diameter of the anode, i. e. the metal filament stretched by the cylinder axis (Fig. 2.22).

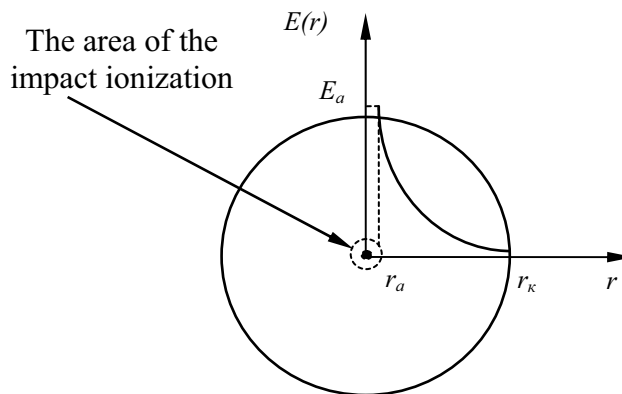


Fig. 2.22. The dependence of the electric field strength by the radius in the cylindrical detector

Really, because of the sharp nonuniformity of the electric field E along the direction r ($E = v_0/r \ln(r_k/r_a)$, where v_0 is the difference of the potentials on electrodes, r_c is the cathode radius, r_a is the anode radius) the factor of the impact ionization α is different from zero in a very small volume only fitted closely to the filament. So, for all primary electrons the conditions of the avalanche formation are the same and independent from the place of the particle passing.

In this case for sufficiently high coefficients of the gas amplification m the induced charge stipulated by electrons and ions motion towards the place

of the impact ionization may be neglected. The charge Q in the external circuit will be determined by the number of electrons and ions drifting from the area of the impact ionization and, so, by the particles energy only:

$$Q \sim mN_0 = m \cdot E/w.$$

Therefore detectors with the gas amplification, having a cylindrical form, are named the proportional counters.

The form and the charge impulse amplitude Q in the external circuit of the proportional counter, the time characteristics of the counter depend on the value of loading resistor R and the equivalent capacity C (the sum capacity of the counter and circuits added to it).

Since the avalanche development takes place near the anode at the distances equal to several filament diameters, the electrons drift paths towards the anode happen to be small. Therefore the main contribution in the charge value Q is given by the current appearing in the external circuit owing to the drift of ions to the cathode.

If we choose $RC \gg T^+$ (T^+ is the time of ions drift from the impact ionization area to the cathode), the maximum value of the charge in the external circuit $Q_{\max} = m \cdot N_0$. However, it is not necessary to choose $RC \gg T^+$ since the main contribution into the induced charge amplitude Q gives the ions motion in the strong field near the anode. It has been found that at the values of RC in several microseconds the charge amplitude is about 50 % of the maximum value. At this, naturally, the proportional properties of the counter are preserved and its time resolution is improved sufficiently.

On the other hand, the RC must be at least ten times bigger than T^- , i. e. the time of the primary ionization electrons drift from the cathode towards the anode. Really, if $RC \sim T^-$, so in that case when the primary ionization is conducted by particles with paths comparable with the counter sizes, the charge Q amplitude will depend on the path length of the ionizing particle and on its direction and thus the proportional properties of the counter will be disturbed. It must be notified that in practice the pulse forming from the detector is achieved not by change of RC but by the choice of the amplifier passing band.

The effect of the impact ionization is the main but not the only effect determining the avalanche development in the detector. At the electrons drift in the strong electric fields, side by side with the impact ionization process the molecules excitation or gas atoms excitation take place. Coming back into the ground state, molecules are emitting photons which can provoke the photo effect on the counter cathode.

The photoelectron coming from the cathode surface creates additional ionization in the anode area. Besides, if the positive ion coming up to the

cathode from the impact ionization area, has the potential energy above the doubled exit work from the cathode surface, another free electron can appear. This electron on the path towards the anode, in its turn, forms the electron-ion avalanche.

The probability of the similar processes in the proportional detector is characterised by the production $\gamma \cdot m$, where γ is the factor depending sufficiently on the cathode material and on the properties of the gas filling the counter ($\gamma \sim 10^{-4}$). The gas amplification coefficient with the accounting of the secondary processes M is determined as $M = m / (1 - \gamma m)$.

The gas amplification factor M depends on the voltage v_0 applied to the electrodes of the proportional detector in such a way that an insignificant nonstability (the drift) of the feeding source can lead to a considerable change of the factor M .

The gas amplification factor is determined usually by experiment using the method of the comparison of the value of the charge of the gas-filled proportional detector $Q_{p.d.}$ and the same detector working in the ionization chamber regime in the absence of the gas amplification $Q_{i.ch.}$:

$$M = Q_{pd} / Q_{i.ch.} \quad (2.21)$$

The gas-filled proportional detectors have found a wide application in the technique of the nuclear-physical experiment.

2.4.2.3. The Geiger-Muller counter

The Geiger-Muller counter is attributed to the ionization detectors working in the regime of the self-dependent gas discharge.

The counter is applied for the registration of the charged particles as well as uncharged ones. The registration of the uncharged particles is conducted by the secondary charged particles appearing at the interaction of the uncharged particles with the working matter of the detector.

The Geiger-Muller counter has a cylindrical form: metal or glass cylinder with a metallic covering performs the role of the cathode and the thin metal filament stretched along the cathode axis is the anode.

The self-dependent gas discharge can be used for the ionizing radiation's registration only under the condition that the discharge provoked by the particle in the working volume of the detector must be quenched before the hit into the working volume of the next particle. The Geiger-Muller counters are divided into the non-self-quenched and the self-quenched counters.

In the non-self-quenched counters for the secondary effects elimination on the cathode provoking the repeated development of the discharge, special schemes of quenching are applied or the loading resistor with the value $10^8 - 10^9$ Ohm is switched on the external circuit. The resistor is chosen from the condition

that in the time of several avalanches development, such decrease of the tension will be applied to it at which the counter will come out from the regime of the self-dependent gas discharge. The non-self-quenched counters have the resolution time $\sim 10^{-2}$ seconds and, at present, are not used in the physical experiments.

In the self-quenched counters the secondary effects are eliminated owing to special additions to the main gas. For filling the counter volume the gas mix is used composed from the main gas (usually – argon $\sim 90\%$) and the impure (quenching) gas ($\sim 10\%$) consisting of a complex organic combination (the alcohol vapors, ether, etc.). The components of the working mix of the counter must satisfy the following condition: the potential of the ionization of the quenching gas must be less than the first potential of the excitation of the main gas (Argon).

Electrons formed on the trace of the charged particle in counter gas interval drift towards the anode under the action of the external electric field. The cylindrical configuration provides the strength of the electric field in the area near the filament which is enough for the impact ionization. The electron-ion avalanches appear around the anode filament. Side by side with the ionization, the excitation of molecules and atoms of the gas takes place near the anode location. The excited atoms of argon emit photons which are absorbed intensively by molecules of the impure gas (the pressure of the quenching gas is chosen so that the path length of the photon before the absorption will be not bigger than 1 mm). This state leads to the photo-ionization of the impure molecules in the area around the anode, to the formation of the additional free electrons giving a start to the new electron-ion avalanches. Thus, the spreading of avalanches along the filament takes place while the counter in all is enveloped by the discharge.

For counters of the middle sizes filled by ordinary gas mixes the speed of the discharge spreading along the filament is $10^6 \dots 10^7$ cm/s and, so, the spreading time is $10^{-5} \dots 10^{-6}$ seconds.

Electrons having a high mobility are collected fast on the anode and ions create a volumetric positive charge near the filament. This charge reduces, in the final analysis, the strength of the electric field near the filament up to the value at which the impact ionization is already impossible and the active stage of the discharge is finished. At the drift from the area of the impact ionization of electrons and ions, the electric current flows through the counter and the tension impulse appears in the external circuit.

Ions of argon at the drift towards the cathode undergo many intercollisions with molecules of the quenching gas. Since the ionization potential of the quenching addition is less than the ionization potential of argon, in the end the ion of argon captures the electron from the quenching gas molecules and then the ion is neutralised. Therefore, mainly ions of the

quenching gas come towards the cathode which, as distinct from ions of argon, don't escape free electrons capable of provoking the repeated stage of the discharge from the cathode surface.

Since the stopping of the discharge in the self-quenched counter is connected with the processes in its working volume, it is not necessary to use an extra much loading resistor. In making a choice of the loading resistor R one comes usually from the comparison of the discharge spreading time along the filament with the time constant RC of the external circuit, where C is the capacity of the counter and of, added to it, circuits of the electronic facilities. For the counter of the middle sizes the optimal magnitude of the loading resistor is in the range of $10^5 \dots 10^6$ Ohm. At such choice of the resistor value, the time of the rise and the drooping time of the impulse are approximately the same.

It is obvious that in the self-quenched Geiger-Muller counter the formation of a single electron-ion pair is enough for the appearance of a discharge. The amplitude of the tension impulse on the output does not depend on the primary ionization created by the charged particle in the gas. Therefore the Geiger-Muller counter is not suitable for the spectrometry of the ionizing radiations.

The fundamental characteristic of the Geiger-Muller counter is the count one, i. e. the dependence of impulses number n registered by the counter in the time unit on the tension V_0 applied to the electrodes at the constant radiation intensity. In Fig. 2.23 the count characteristic of such a counter is plotted. In the tensions area from V_b to V_{end} (i. e. on the "plateau") the counting rate is practically constant. In the tensions area $V_0 < V_b$ the counting rate sharply droops and at the tension on the counter $V_0 = V_f$, called the firing potential the counting rate is equal practically to null. In the area $V_0 < V_b$ the tension impulses amplitudes from the counter are comparatively small (volts and parts of volt) and still depend on the initial ionization. Some tension impulses become less than the sensitivity threshold of the counting facility and, therefore, can not be registered by the latter.

At $V_0 > V_{end}$ the number of the registered impulses sharply rises owing to the so called false impulses which stipulate some slope of the "plateau". The presence of the false impulses (nonconnected with the particle passing) is stipulated by the fact that the possibility of the discharge active stage repetition owing to the secondary effects on the cathode is not excluded absolutely. Really, though there is small enough probability of the free electron appearance related to the single positive ion neutralised on the cathode, this probability still has a finite magnitude. The secondary electrons can appear at the positive ions of the main gas coming in to the cathode, which have avoided the neutralisation at the drift as well as a result of the

photoeffect at the de-excitation of the quenching gas molecules turned out in the excited state after the ions neutralisation. Since the number of the positive ions formed in the discharge is large ($10^9 \dots 10^{10}$), the probability of the free electron appearance on the cathode with the accounting of all positive ions can compose an appreciable value.

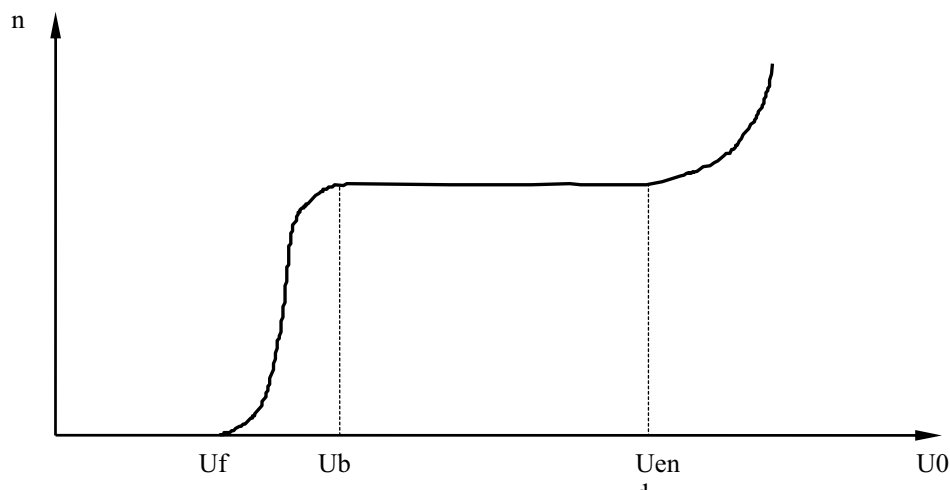


Fig. 2.23. The count characteristic of the Geiger-Muller counter

As it was mentioned above, the de-excitation of the gas discharge in the Geiger-Muller counter is finished by the appearance of the positive volumetric charge near the anode filament. The registration of the next particle is possible only after the moment when the positive ions come away from the anode at some critical distance at which the electric field strength in the area of the impact ionization (in the anode area) will be restored up to the value corresponding to the firing potential of the gas filling the counter. The time during which the counter does not register particles getting into it, is called the dead time τ_{dead} (Fig. 2.24).

After the moment when positive ions come away from the anode at a distance longer than the critical one, the counter will begin to registrate ionizing particles getting into its working volume, but the tension impulse amplitude on the detector output will be less than the nominal. The nominal tension impulse amplitude can be obtained only after the full neutralisation of positive ions on the cathode and after the full restoration of the field strength in the area of the impact ionization. The time during which positive ions pass the path from the anode where they have been formed owing to the gas discharge development, to the cathode is called the restoration time τ_r . The triggering threshold of the sensitive electronic counting systems used usually at working with the Geiger-Muller counters is small enough (parts of volt), therefore the ionizing particles getting into the working volume of the counter at the time

of the process of the restoration of the potentials difference up to nominal value can be registered by the counter. The minimum time interval between two following each other particles when they are registered separately by the counter is called the resolution time τ_{res} . It is obvious, that $\tau_{res} \geq \tau_{dead}$ and the relationship between them depends on the triggering threshold.

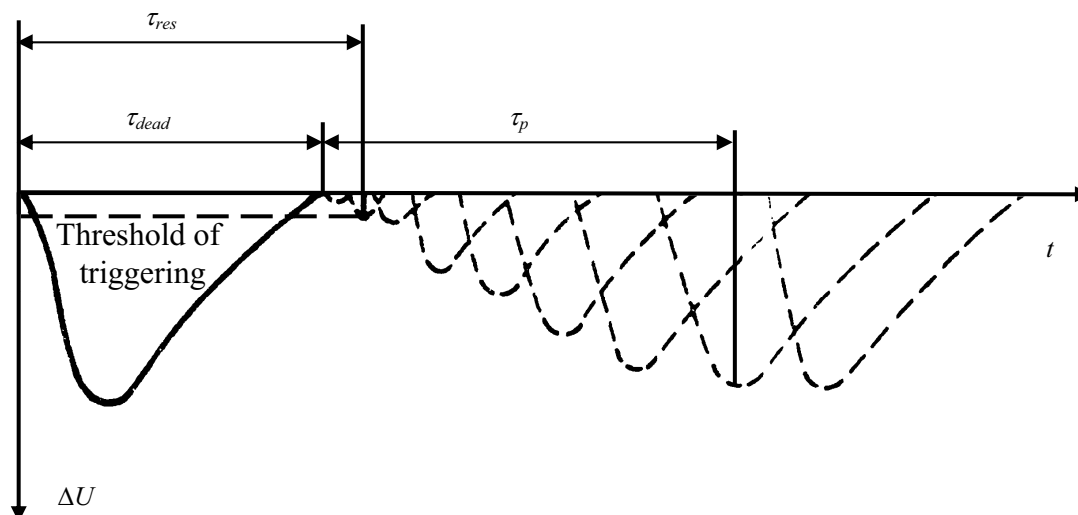


Fig. 2.24. The time characteristics of the Geiger-Muller counter: τ_{res} – the resolution time; τ_r – the restoration time; τ_{dead} – the dead time

The self-quenched counters are applied widely for the registration of particles of different kind. At this, the registration efficiency depends strongly on the nature of the registered radiation. For example, any charged particle getting into the working volume of the counter and creating in it at least a single ions pair will be registered with the probability fitted closely to 1, i. e. the efficiency is near 100 %. This probability is calculated by the formula:

$$\eta = 1 - \exp\left(-v_0 l \frac{p}{p_0}\right),$$

where V_0 is the primary specific ionization carried out by the particle on the path of one centimetre at the normal pressure p_0 ; l is the particle path in the counter; p is the gas pressure in the working volume of the counter.

The registration of the uncharged particles is conducted by the secondary charged particles appearing owing to the interaction of the uncharged primary particles with the working matter of the detector. Thus, for example, at the interaction of gamma-quanta with the working material of the detector (mainly with the material of the cathode) a charged particle appears, i. e. electron (or the photoelectron, or the Compton-electron, or the

electron-positron pair) which having got into the working volume of the detector filled by gas, produces ionization there.

It is obvious that the probability of the free electron appearance and its getting into the working volume of the counter depend on the thickness and the material of the cathode and on the energy of gamma-quanta. Therefore, as distinct from the efficiency of the charged particles registration, the efficiency of the gamma-quanta registration in the energy range $E_\gamma \sim 0.1 \dots 3$ MeV is only from several tenth to a few units per cent.

2.4.3. Scintillation detector

The scintillation method is based on the registration of short light flashes, i. e. scintillations appearing in some materials after the charged particles passing through them. Scintillation differs from other kinds of the luminescence formed at the particles interaction with the matter (for example, the Vavilov-Cerenkov luminescence) by that they appear owing to the electron transfers inside the luminescence centres. The luminescence centre can be an atom or a molecule, or an ion, or more complex formation.

The scintillation process can be divided into three stages:

- 1) the excitation of the fundamental matter being in solid, liquid or gaseous phase, by the charged particles (generation stage);
- 2) the transfer of the energy lost by the charged particle in the matter towards the luminescence centres (migration stage);
- 3) the excitation and the de-excitation of the luminescence centre (intercentre stage).

For the registration of the scintillation appearing under the action of separate ionizing particles the electron photomultiplier (EPM) is usually applied. Photons of the scintillation flash hit onto the photocathode of the EPM, forming photoelectrons as a result of the photoeffect. Photoelectrons pass under the action of the external electric field and then hit onto dinodes of EPM. As a result of the secondary electron emission in dinodes, the number of electrons is increased $10^6 \dots 10^9$ times. Thus, on the anode of the EPM the electric signal is created which is registered then by different electronic schemes.

At the ionizing radiation detection with the help of the scintillation detector it is necessary to apply namely such type of the scintillator whose main parameters allow to solve the raised problem in the most optimal way. The main parameters of the scintillator are: the conversion efficiency η_k ; the mean energy w_{ph} expended on the single photon formation; the time of the de-excitation τ ; the efficiency of the ionizing radiation registration η . Values of these parameters for the most widely used scintillators are given in Table 2.8.

Table 2.8

Main characteristics of some scintillators

Scintillators	Density, g/cm ³	Mean atomic number	De-excitation time	Energy hv, eV	Efficiency η c.p. for electrons	ω_{ph} , eV	α/β
Inorganic							
Na J (Tl)	3.67	32	250	3	0.153	19.6	0.5
Cs J (Tl)	4.51	54	700	2.2	0.06	36.6	0.5
ZnS(Ag)	4.09	23	1000	2.7	0.1	27	1
Bi ₄ Ge ₃ O ₁₂	7.13	28	300	2.6	0.02	163.5	0.2
Organic							
Anthracene	1.25	6	25...30	2.77	0.034	81.4	0.1
Naphthalene (C ₁₀ H ₁₈)	1.45	6	70...80	3.6	0.017	176.4	0.1
Stilbene (C ₁₄ H ₁₂)	1.16	6	–	3.5	0.03	116.6	0.1
Tolane (C ₁₄ H ₁₀)	1.18	6	–	3.16	0.032	98	0.1
Plastics							
Terphenyl in polystyrene	1	6	5	3/1	0.015	210	0.1

The physical conversion efficiency of the scintillator (or the energy output) is the ratio of the light flash energy $E_{e.f.}$ to the energy of the charged particle absorbed within the scintillator volume E_{abs} :

$$\eta_{cp} = E_{ef} / E_{abs} = N_p h \bar{\nu}_{ef} / E_{abs} , \quad (2.22)$$

where N_p is the total number of photons formed in the scintillator by the charged particle; $h\nu_{ef}$ is the mean energy of the scintillation. The value of the physical conversion efficiency is connected with the mean energy spent by the particle on single photon creation by the relationship:

$$w_p = \frac{E_{abs}}{N_p} = \frac{h \bar{\nu}_{ef}}{\eta_{cp}} . \quad (2.23)$$

The meanings of $h\nu_{e.f}$ and ω_{ph} for some types of scintillators are given in Table 2.8.

Side by side with the idea of the physical conversion efficiency the value of the **technical conversion efficiency** is introduced:

$$\eta_{ct} = f \eta_{cp} .$$

where \underline{f} is the factor accounting for the part of photons hitting onto the photocathode of EPM, from the total number of photons N_p formed by the particle inside the scintillator.

The physical conversion efficiency of the scintillator for the particles of one and the same type usually slightly depends on their energy. With the due account of the written relationships the amplitude of the impulse on the EPM output in the number of electrons is

$$V = Mf\gamma \frac{\eta_{cp}}{h\nu} E_{abs}, \quad (2.24)$$

where M is the gain coefficient of EPM; γ is the quantum efficiency of the photocathode of EPM equal to the probability of photons to pull out the electron from the photocathode. Thus, the impulse amplitude on the EPM output depends linearly on the energy lost by the particle in the scintillator. This testifies the fact that the scintillation detector for particles of the same type is proportional. However, the physical conversion efficiency depends on the specific ionization losses of the registered particles and is different for different types of particles. This dependence, for example, for the alpha particles and electrons is characterised by the value α/β which is the ratio of the physical conversion efficiencies at the irradiation of the scintillator by alpha-particles and electrons with the same energy.

The de-excitation time τ of the scintillator is usually taken as the time during which the intensity of the scintillation luminescence n_p , i. e. the number of photons created inside the scintillator in the time unit, is reduced by e times. If, for example, the number of photons in the scintillation is distributed at the time t by the exponential law, then

$$n_p = \frac{N_p}{r} \cdot e^{-t/\tau}.$$

The meaning of τ depending on the scintillator type may be changed from a few nanoseconds up to microseconds (see Table 2.8).

The registration efficiency η of the radiation is the probability with which a particle may be registered by the detector, i. e. it is the ratio of the number of the registered particles to the number of particles hitting into the scintillator: $\eta = N/N_0$. For the charged particles the registration efficiency is equal to 1, practically.

One of the main advantages of scintillation detectors, as compared to detectors of other types, is a high efficiency of the registration of neutral radiations (gamma-quanta and neutrons). As it is known, the interaction of this radiation with the matter leads to the formation of charged particles

which then are registered by the detector. Thus, the efficiency of the registration of gamma-quanta and neutrons will be determined by the probability of their interaction with the detector material. For gamma-quanta the registration efficiency may be estimated as

$$\eta = 1 - e^{-\mu x}, \quad (2.25)$$

where μ is the total linear coefficient of the gamma-quanta absorption; x is the scintillator thickness. The value of the registration efficiency depends on the mean atomic number of the absorber \bar{Z} (increases with the increase of \bar{Z}), therefore for obtaining a higher efficiency of the gamma-quanta registration the scintillators of NaJ(τ) or CsJ(τ) types are applied. The classification of scintillators can be fulfilled in accordance with different indications. Two large groups, organic and inorganic, have the most clear distinctions in their characteristics (see Table 2.8).

Organic scintillators are characterised by the comparatively small atomic numbers ($\bar{Z} \sim 6...7$) and by the small density ($\rho \sim 1...2 \text{ g/cm}^3$). Organic scintillators have high time resolution ($10^{-7}...10^{-9} \text{ s}$). Efficiency of the gamma-radiation registration by such scintillators is small, therefore they are applied most often for the charged particles registration. Organic scintillators are organic crystals, liquid and solid solutions of the scintillating materials in monomers and polymers and also organic gases.

Inorganic scintillators are characterised by the big atomic numbers ($Z \sim 25...50$) and by the high density ($\rho \sim 4 \text{ g/cm}^3$). The registration efficiency of the gamma-radiation by such detectors is enough high. The time resolution is worse as compared to the organic scintillators ($\tau \sim 10^{-7}...10^{-6} \text{ s}$).

Inorganic scintillators are alkaline-haloid zinc-sulphide and oxide scintillators and also scintillators on the base of the noble gases (solid-state, liquid and gaseous).

In physical experiment scintillation detectors are applied most often for the spectrometry of ionizing radiations, and partially, of the gamma-radiation. The spectrometry of gamma-quanta is conducted by the measuring of the energy of secondary electrons formed at the interaction of gamma-quanta with the scintillator material.

As it is known, gamma-quanta passed through the material are interacting with it owing to one of three processes: photo effect, Compton-effect and the effect of the pair formation. The probability of these processes depends significantly on the gamma-quanta energy as well as on the properties of the material with which these gamma-quanta interact.

At the photo effect, the gamma-quantum with the energy $h\nu$ pulls out from the atom one of the internal (K, L, M...) electrons and spends at this the energy which is equal to the energy of the binding of the corresponding

electron (E_K, E_L, E_M, \dots) whose value is some tens kiloelectron-volts. The residual energy is transferred into the kinetic energy of the photoelectron E_p :

$$E = h\nu - E_k. \quad (2.26)$$

At the Compton scattering the gamma-quantum transfers to the electron only a part of its energy. At this, the energy of the Compton-electron E_e is connected with the energy of the gamma-quantum $h\nu$ by the relationship:

$$E_e = \frac{h\nu}{1 + \frac{m_0 c^2}{h\nu(1 - \cos \Theta)}}, \quad (2.27)$$

where Θ is the angle of the scattering gamma-quantum leaking-out as related to the direction of primary gamma-quantum motion; $m_0 c^2 = 0.511$ MeV is the electron rest mass.

In the process of the pair appearance two particles are created – the electron and the positron, for whose formation it is needed to spend the energy $2m_0 c^2 = 1.02$ MeV. The residual energy of gamma-quanta transfers into the kinetic energy of the electron and the positron.

In Fig. 2.25, as an example, the impulses amplitude distribution is given from the secondary electrons in the scintillation detector of NaJ(Tl) type at the registration in it of the monoenergetic quanta with the energy 0.5 MeV. From (2.26) it is seen that the maximum energy of Compton electrons is always less than the energy of photoelectrons and

$$E_{e \max} = \frac{h\nu}{1 + \frac{m_0 c^2}{2h\nu}}. \quad (2.28)$$

Therefore, there is a principal possibility to release the peak corresponding to the total energy absorption in the scintillator – the peak of the total absorption (the area 1 in Fig. 2.25). The formation of the total absorption peak is connected with the processes of the photo electric interaction and multiple scattering of gamma-quanta in the scintillator. Usually, the location of the total absorption peak is applied for the gamma-quantum energy determination. Since at the Compton scattering the energy of the Compton electron $E_e = f(\Theta)$, such events lead to the appearance of the continuous Compton distribution in the spectrum (area 2). In the low-energy part of the Compton distribution a wide asymmetrical peak is often released stipulated by the scattering of gamma-quanta at angles fitted closely to 180° from the EPM window, shielding housing walls and the container glass window in which the scintillator is packed. This peak is called the back scattering peak (area 3 in Fig. 2.25).

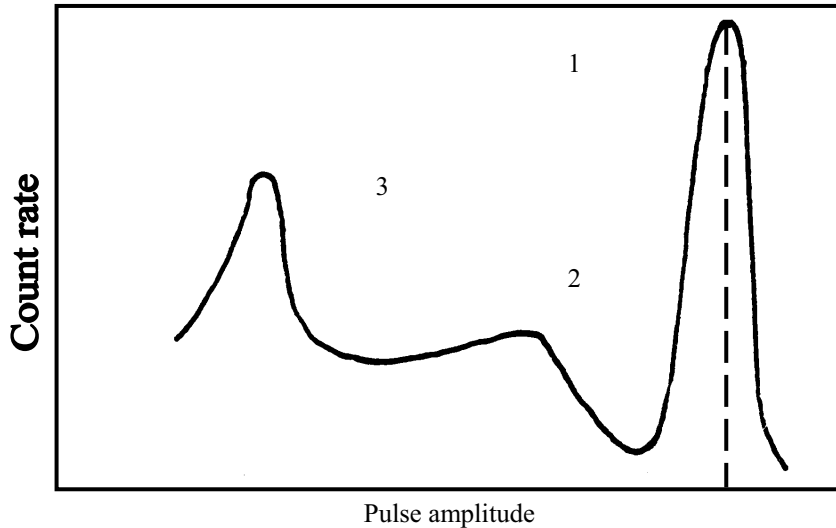


Fig. 2.25. Pulses amplitude distribution at registration of the gamma-quanta with $E_\gamma = 0.5 \text{ MeV}$

The form of the pulse amplitudes distribution at the gamma-quanta registration by scintillation detector depends essentially on the scintillator type (unorganic or organic), its geometric dimensions and also on the irradiation conditions. For example, in large-sized crystal a considerable suppression of the continuous spectrum of Compton electrons is observed due to the repeated Compton scattering, as well as the corresponding increase of the peak intensity corresponding to the total gamma-quantum energy absorption.

The accuracy of the ionizing radiation spectral structure measurement and the possibility of a separate registration of the closely disposed energy lines is determined by the energy resolution of detector, which usually means the ratio of the width ΔE on the half-height of the amplitudes distribution received with mono-energy particles, to the average (middle) value of energy in this distribution: $\eta = \Delta E/E$.

At the gamma-quanta registration by the scintillation detector within the energy area up to 1.5...2 MeV, the dependence of the energy resolution on the quantum energy can be described accurately enough by means of relationship:

$$\eta^2 = \left(\frac{\Delta E}{E} \right)^2 = \delta^2 + \frac{C_1}{E}. \quad (2.29)$$

The value δ depends essentially on the quality of photomultiplier making, especially on whether the photocathode properties are as far as the same in different points, how much effective is the electrons collecting onto the first dinode, what are the quality and the uniformity of the light collecting inside the scintillator and the optical contact with the photomultiplier, etc. The value C_1 is determined mainly by the number of the formed photons

of scintillation and by their losses inside the scintillator itself, on the photocathode, and at collecting onto the first dinode of the photomultiplier. For a few choice scintillation detectors with the NaJ(Tl) crystal the meaning of the value C_1 may achieve $1.5 \cdot 10^{-3}$ MeV, and the value of $\delta^2 \sim 2 \cdot 10^{-4}$. At such values of C_1 and δ^2 the energy resolution η for gamma-quanta with energy 1 MeV is approximately equal to 4.5 %.

In the area of high magnitudes of gamma-quanta energies the radiation leakage from the crystal becomes essential, i. e. the going out of electrons, forming nearly the crystal surface, from the scintillator bounds. This phenomenon leads to the appearance of pulses with lower amplitudes and to a change for the worse of the energy resolution.

At using the organic scintillators which have usually a small mean atomic number ($\bar{Z} \sim 6$), the photopeak is practically absent, as the photoeffect cross-section σ depends on Z for gamma-quanta, as $\sigma \sim Z^5$.

2.5. Control tasks

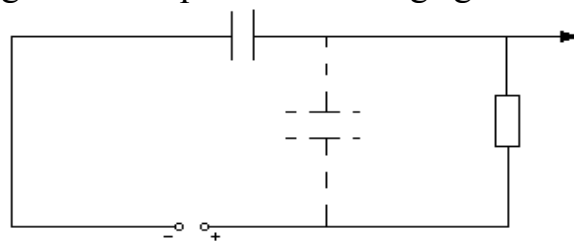
- The root-mean-square disassembly of the ion cloud in the diffusion process $\delta = \sqrt{2D \cdot t}$. Taking this into account, the pulse-decay time may be determined by the formula: $\Delta t = 2\sqrt{2Dt}/U$, where $t = d^2/\mu$; $D = kT\mu/e$; D is the diffusion coefficient; T is the thermodynamic temperature; μ is the mobility factor; k is the Boltzmann constant.
- The density of the current in the parallel-plate ionizing chamber is: $j = j_+ + j_- = e(n_+ \cdot U_+ + n_- \cdot U_-)$, where $n_+(x) = n_0 \cdot x/U$; $n_-(x) = n_0(d - x)/U$; n_+ and n_- are concentrations of positive and negative ions; U_+ and U_- are velocities of positive and negative ions correspondingly.
- The threshold tension is the tension at which electrons receive enough energy for the ionization on the distance from the anode which is equal to the mean length of the free path. The condition of the collision (impact) ionization can be written in a view:

$$W_i = e \int_{r_a}^{r_a + \lambda_e} E(r) dr = \frac{U_{th}}{\ln(r_c/r_a)} (1 + \lambda_e/r_a),$$

where $E(r)$ is the intensity of the electrical field in the cylindrical counter; r_c and r_a are radii of the cathode and anode; λ_e is the electron free path length; U_{th} is the threshold tension; W_i is the energy of the ionization.

- The own capacity of the detector with the p-n transfer from the Silicon of the p-type is calculated by means of formula: $C_{det} = 3.3 \cdot 10^{-9} \cdot S \sqrt{U \cdot \rho}$, where U is the tension of shift in volts; ρ is the conductivity in Ohm·cm; S is the square of the transfer in cm^2 .

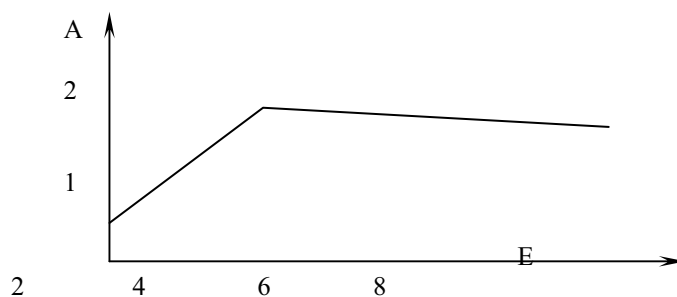
- The mean energy needed for the single photon formation in the scintillator is $\overline{W}_{ph} = \overline{h\nu} / \kappa$, where κ is the conversion efficiency, and the mean energy of the photon can be calculated by the position of maximum of the strip (band) of the radiation: $\overline{h\nu} = h_c / \lambda_0$.
 - The spectrum of the deexcitation (fluorescence) of many scintillators, given in the scale of waves lengths, is describes satisfactorily by the Gaussian: $L(\lambda) = L_0 \cdot \exp[-(\lambda_0 - \lambda)^2 / 2\delta^2]$, where $\delta = G / (2\sqrt{2\ln 2})$, G is the full Gaussian width on the one-half of the height. At the spectrum transfer from the scale of waves lengths into the scale of photons energies the following equations are composed: $L(\lambda) \cdot d\lambda = L(E) \cdot dE$.
 - In order to estimate the connection between the integral sensitivity of the photoelectron multiplier and the quantum efficiency, one can use the definition of the light flow. For the maximum visibility the following relationship is true: $1A / \text{lumen} = 683 \text{electron/eV}$.
 - The fluctuation of the multiplication factor of the photo-multiplier connected with fluctuation of the feeding tension and the factor of the secondary election emission can be determined with the help of the formula: $dM / M = n(dm / m) \cdot (dU / U)$.
1. In the space between two electrodes having the constant difference of potentials U there is a charge q moving under the action of the field. Receive the expression for the current induced in the external loop (chain) at the charge motion.
 2. In the parallel-plate ionizing chamber there is the alpha-particle passing in the immediate nearness from the positive electrode in parallel to its surface. Calculate the duration of the pulse-decay time of the current connected with the diffusion of the ions cloud at its drift inside the chamber. The chamber is filled with pure Argon up to the pressure 0.1 Mpa. The distance between electrodes is 1 cm and the potentials difference 500 V is added to electrodes.
 3. Indicate the polarity of the signal on the output of scheme given in the figure. In what way must one change the scheme in order to receive the impulse of the contrary sign on the output without changing the added tension polarity?



Calculate the induced charge and the amplitude of the tension pulse in the parallel-plate ionizing chamber, normed on 1 MeV of the energy

of the particle passing parallel to the electrodes plane at the distance 1 cm from the negative electrode. The distance between electrodes is 3 cm and the tension 600 V is added to electrodes. The chamber is filled with pure Argon up to the pressure 0.2 MPa. The equivalent capacity is 20 picoFarad.

4. The flat ionizing chamber is irradiated in such a way that charges are formed uniformly by the whole volume of the chamber at a constant velocity. Neglect the processes of re-combination, diffusion and volumetric charges formation and receive the expression for the current density of positive and negative charges.
5. The gas-amplification factor of the proportional counter filled with a mix of Argon and Methane, is 10^3 . Calculate the mean number of ionizing collisions of electrons at passing the area of the impact ionization up to the anode surface.
6. Calculate the threshold tension, i. e. such tension at which the gas amplification begins, in the proportional counter filled with pure Argon up to the pressure $1.33 \cdot 10^4$ Pa. At this, radius of the anode is $1.25 \cdot 10^{-2}$ cm and the cathode – 1.1 cm.
7. The back shift (displacement) 10 Volts is added to the semi-conductive detector (SCD) with the area 1 cm^2 made of the P- type Silicon with the specific resistance $10^3 \text{ Ohm}\cdot\text{cm}$. Calculate the tension pulse amplitude stipulated by the proton with the energy 1 MeV. Assume that $RC \gg T_-$; $RC \gg T_+$ and the assembly capacity is 11 picoFarad.
8. The dependence of the pulse amplitude in the silicon surface-barrier counter on the energy of protons hitting the counter normally to its surface from the side of the transfer, is given in figure. Determine the width of the transfer.



9. Calculate the medium energy needed for the formation of the single photon in anthracene if the conversion efficiency is known.
10. Estimate the number of photons emitted by the crystal of NaJ (Tl) at the registration of gamma-quanta of ^{137}Cs if the known technical conversion efficiency of NaJ(Tl) is approximately 10 %.

11. For many scintillators the spectrum of the luminescence in the scale of the wave lengths may be satisfactorily described by the Gaussian. So, for example, the spectrum of NaJ(Tl) is the Gaussian with the maximum at 410 nanometers. What is the view of the luminescence spectrum of NaJ(Tl) on the scale of photons energies?
12. It is needed to apply the scintillation detector for the fission fragments registration. What type of the scintillator must one choose if the main problem is the fragments spectroscopy?
13. The practically point source of alpha-particles is placed on the butt-end surface of a cylindrical scintillator with the nonrefracting walls. The cylinder radius is 0.5 cm and the cylinder length is 2 cm. Calculate the number of photons coming out from the scintillator butt-end opposite the source if the alpha-particle forms 10^5 photons in the single scintillation. One can neglect the luminescence light absorption.
14. The main parameter which characterizes the photocathode of the photo multiplier purposed for working in scintillation detectors is the quantum efficiency and its spectral distribution. However, only the integral sensitivity of the photocathode is shown, as a rule, in the photomultiplier passport. Show the connection between the quantum efficiency and the integral sensitivity of the photocathode.
15. What defines the short-wave and the long-wave boundary of the spectral sensitivity of the photomultiplier?
16. Show and explain the sign (polarity) of the signal taken from the anode of the photomultiplier.
17. What is the value of fluctuations of the amplification factor of the fourteen-cascades photomultiplier if the feeding tension is stabilized with the error up to 0.1 % and in the working regime the coefficient of the secondary electron emission is changed up to 0.9 % at the tension change of 1 %?

2.6. Set of tests on sections: "Principles of radiation testing; sources of radiation; detectors of ionizing radiation"

1. Which kinds of particles are called "ionizing radiation"?
 - A only electrons and protons;
 - B only protons;
 - C only particles of corpuscular radiation;
 - D particles of corpuscular radiation and photons.
2. Isotop is:
 - A radionuclide;

- B** nuclide with number of protons within nucleus attributed to given element;
- C** isoton.
3. Distinctly to beta- and alpha-particles, neutrons have no:
- A** charge;
- B** mass;
- C** spin;
- D** B and C.
4. Positron is coupled with _____, forming photons:
- A** neutron;
- B** proton;
- C** electron;
- D** alpha-particle.
5. The thin layer of matter with thickness dx removes the part $n\sigma dx$ of number of photons passing through it. If n is a density of a matter's particles in a volume unit, then the value σ is:
- A** linear weakening coefficient;
- B** mass weakening coefficient;
- C** interaction cross-section;
- D** number of photons in a beam.
6. Interaction cross-section is changed approximately as Z^2 . Which kind of interaction has place?
- A** photo-effect;
- B** Compton-effect;
- C** pair formation effect.
7. Which of particles has the highest ionizing effect (number of ion pairs, generated at passing the 1 cm of air):
- A** alpha-particles;
- B** beta-particles;
- C** neutrons;
- D** photons.
8. If photoelectric interaction has place, what has happened with atom?
- A** electron is removed from internal atomic levels;
- B** photon of characteristic radiation is emitted;
- C** electron is withdrawn from external atomic shells;
- D** whole of above-mentioned is true.
9. Neutrons are interacted with the matter by means of following processes:
- A** Ionization;

- B** scattering on nuclei;
 - C** absorption by nuclei;
 - D** B and C.
10. Which value of energy have photons of gamma-source Thulium-170:
- A** 1,33 and 1,17 MeV;
 - B** 0,084 and 0,052 MeV;
 - C** 0,31 and 0,47 MeV.
11. Which of radionuclidic sources for radiation testing, having one and the same activity, will need the least mass of shielding material?
- A** cobalt-60;
 - B** Thulium-170;
 - C** Iridium-192;
 - D** Californium-252.
12. Half-decay period is one of several main parameters of radionuclide. Which percent of initial quantity is the approximate decrease of decayed atoms after four half-decay periods?
- A** 2 %;
 - B** 3 %;
 - C** 6 %;
 - D** 1 %.
13. Electrons are accelerated in betatron by means of:
- A** electric SHF- field;
 - B** raising(increase) of magnet induction of eddy current electric field;
 - C** high tension between the cathode and the target.
14. Which kind of sources are used for generation the photon radiation with energy within several MeV:
- A** microtron;
 - B** betatron;
 - C** linear accelerator;
 - D** all of above-mentioned facilities.
15. The current of ionizing chamber is amplified for measurement:
- A** by electronic amplifier;
 - B** by gas non-self-maintained discharge;
 - C** by gas self-maintained discharge;
 - D** is measured without any amplification.
16. Scintillator on the base of LiI(Eu) is used mainly for detection:
- A** photons;
 - B** beta-particles;

- C** neutrons;
 - D** A and C.
17. The particle that made sensitive the germ of photo-emulsion, is:
- A** photon;
 - B** electron;
 - C** proton;
 - D** B and C.
18. The energy of electrons interacted with germs of emulsion of X-ray film, is influenced mainly on:
- A** own unsharpness of the film;
 - B** film's contrast factor;
 - C** shape of the characteristic curve;
 - D** geometry unsharpness of shoot.
19. The granularity of X-ray film increases at:
- A** increased time of film development;
 - B** increased energy of ionizing particles;
 - C** using the luminescent screens;
 - D** A, B and C.
20. Linear dependence of exposure time on blackening density is expressed mostly for:
- A** fine-grained films at short exposures;
 - B** fine-grained films at long-time exposures;
 - C** coarse-grained films;
 - D** screen films.
21. The most appropriate device for energy spectrum analysis of the photon radiation is:
- A** ionizing chamber;
 - B** scintillation detector;
 - C** proportional counter;
 - D** Geiger-M. counter.
22. Gases aren't used in sensitive volumes of:
- A** proportional chambers;
 - B** semiconductor detector;
 - C** ionizing chambers;
 - D** Geiger-M. counters.
23. The contrast coefficient of X-ray film is:
- A** gradient of rectilinear region of the characteristic curve;
 - B** gradient of any region of characteristic curve;

- C** blackening densities difference for two regions(squares) of film;
 - D** ratio of blackening densities for two squares of film.
24. Geiger-Mueller counters have:
- A** complete electronic loops(chains) of amplification;
 - B** low level of reliability;
 - C** small sizes;
 - D** are very expensive.
25. Gamma-exposure may be expressed:
- A** in mA·min;
 - B** in mA·sec;
 - C** in Bq·sec;
 - D** in kV.
26. The accumulation(built-up) factor is:
- A** ratio of sum of flows of particles of primary and secondary radiation over the flow of primary radiation particles;
 - B** ratio of radiation weakening factor of tested object material over the half-weakening layer thickness;
 - C** part of flow of primary radiation.
27. Non-sufficient sharpness of the defect image on X-ray shoot may be resulted from:
- A** large size of the focus spot of the radiation source;
 - B** increased distance between the object and the film;
 - C** low contrast level of the film;
 - D** A, B and C.

Chapter 3 RADIOGRAPHY

3.1. Bases of radiography

Radiography means the method (techniques) of receiving the Roentgen radiation intensity distribution image on the radiographic film. At present radiography occupies a substantial part in radiation control in general. The principle scheme of radiographic control execution is given in Fig. 3.1.

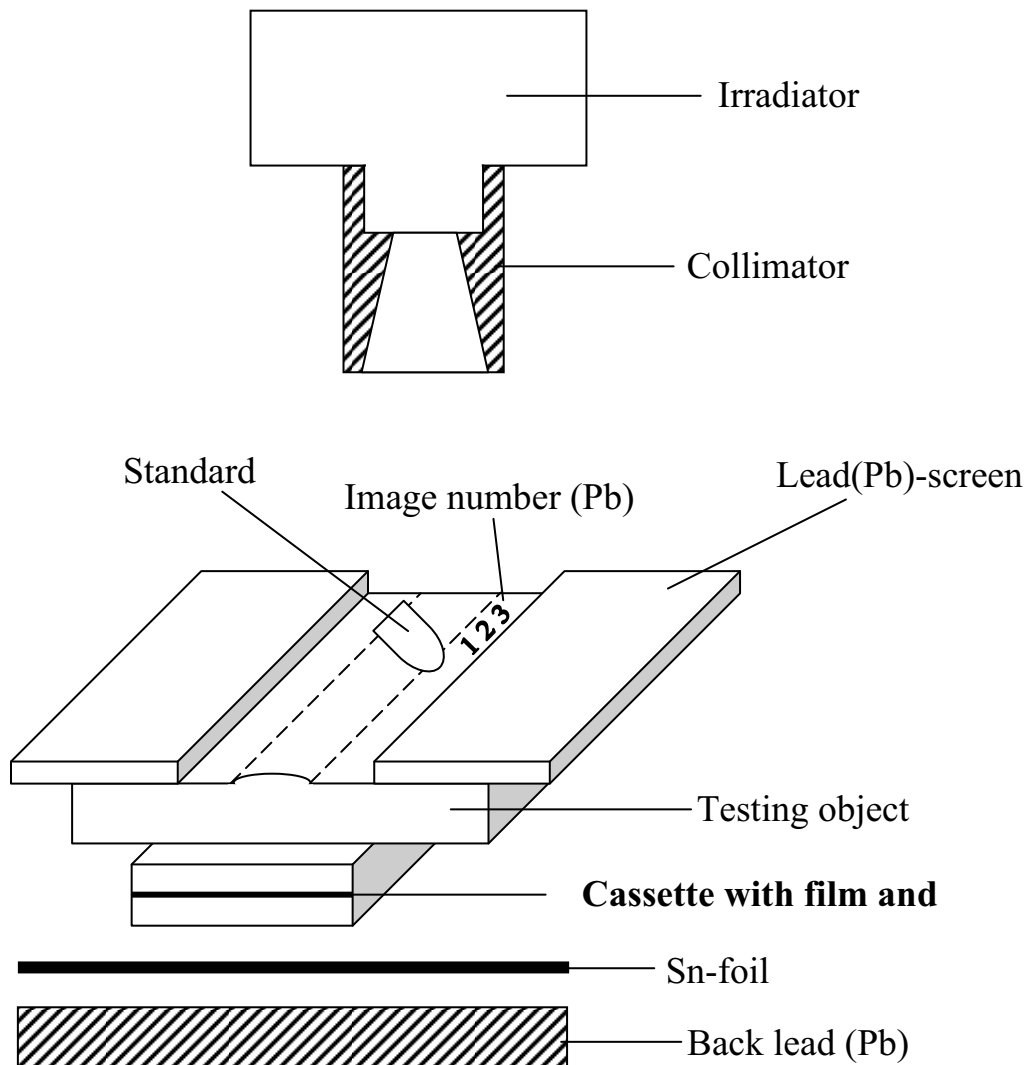


Fig. 3.1. The disposition at the radiation radiographic testing of an object

The testing detail is placed on the table. The surface of the table is covered with Pb and usually with additional Sn-foil in order to prevent back-scattered radiation. The cassette with film-foil combination is placed between the object of control (detail) and the table. The cassette is nontransparent and, therefore, after cassette loading one can work with cassette in daylight. The modern radiographic films are supplied at once in cover as film-foil combinations and so they can be applied without any previous cassette loading in a darkroom.

For reducing the scattering radiation effect it is required that the primary radiator from irradiation will be collimated in order to irradiate only that square (zone) which is essential for testing. Those zones, which will not be examined with X-ray, must be covered by Pb-screen.

Nota bene: In order to identify any image, the image marking is required, and this marking is fulfilled by means of lead letters placed on the detail surface. The test specimen allows determining the quality of developed film and the correctness of the chosen examining regime.

If the extensive surfaces or long welded joints are subject to control, then films must be placed in a way to overlap each other. It is important in this case to designate the overlapping by means of lead arrow placed on the testing detail.

Choosing the distance between the source of radiation and the film, if enlargement techniques is used, as well as between the detail and the film, one must take into account that the geometrical unsharpness, generated on the basis of projection relationships, will not be more than the internal unsharpness in imaging media (in a film). The relationship is schematically given in Fig. 3.2. If Φ is the diameter of Roentgen tube anode spot and d_d is the diameter of defect, then on the film the geometrical or boundary unsharpness (U_g) is coming into being:

$$U_g = l_e * \Phi / F - l_e, \quad (3.1)$$

where F is the distance between the film and the source of radiation and l_e is the film – defect distance. If the enlargement technique is not used, then the maximum film-defect distance is approximately equal to detail thickness d . Let us assume that the average distance between the radiation source and film (F_{min}) is given. If the geometrical unsharpness U_g is equal to its own unsharpness U_i , one can obtain the average radiation source – film distance F_{min} :

$$f_{min} = l_e * \Phi / u_i. \quad (3.2)$$

A distance bigger than F_{min} will not bring any additional gain in sharpness. The X-ray radiation intensity is decreasing proportionally to squared distance.

Choosing the control geometry, one must take in consideration the area of the examine zone and the angle of the Roentgen tube irradiating cone enveloped during examination. Usually the angle of irradiation makes up 40° . Hence, for X-ray examination of 40 cm – film the distance should not be less than 50 cm. In practice it is normal to work with a focal distance 50 or 70 cm and this focal distance is maintained even if the calculated F_{\min} indicates a shorter distance. These cases with a constant distance allow to easily define exposure time by means of exposure nomographs.

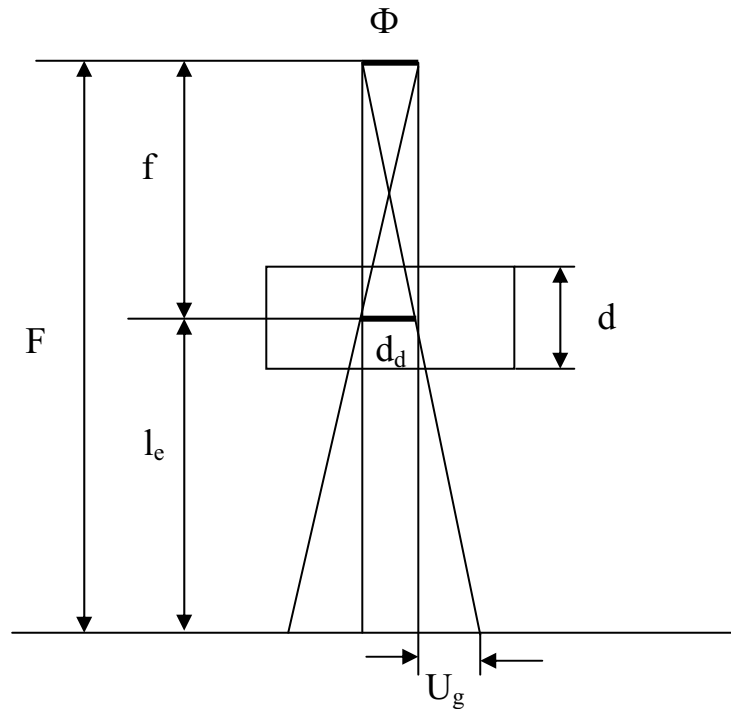


Fig. 3.2. The setting-up of the focal distance

At control procedure organization one must take into account the X-ray examining directions. The testing detail must be oriented as possible in such ways that the expected (planned) defects were lying in examining direction. This state requires, particularly, in welding joints testing, to use side by side with perpendicular examining, also the examination at another angle in order to have a possibility to distinguish extensive defects orientated in the same direction.

The choice of examining parameters depends on testing geometry and on examining detail weakening properties. The examination rules give the values for minimum blackening which the exposure film must achieve. In order to obtain those values without making a lot of experiments, the exposure nomographs that act only for concrete Roentgen apparatus, concrete detail material and film-foil combination are used. The exposure nomograph presented in Fig. 3.3 gives the relation (connection) between examining detail

thickness W and exposure B depending on X-ray tube tension required for certain minimum blackening achievement.

The exposure B is the product of Roentgen current I (mA) and exposure time t (min):

$$B = I \cdot t \text{ (mA min)}, \quad (3.3)$$

By means of nomograph at the given thickness of object of control and for certain tension on X-ray tube one can obtain the exposure value. If the constant Roentgen current is used, one can calculate the exposure time. According to the rule the examination tension must be chosen at the least possible value and the exposure time must be within several minutes.

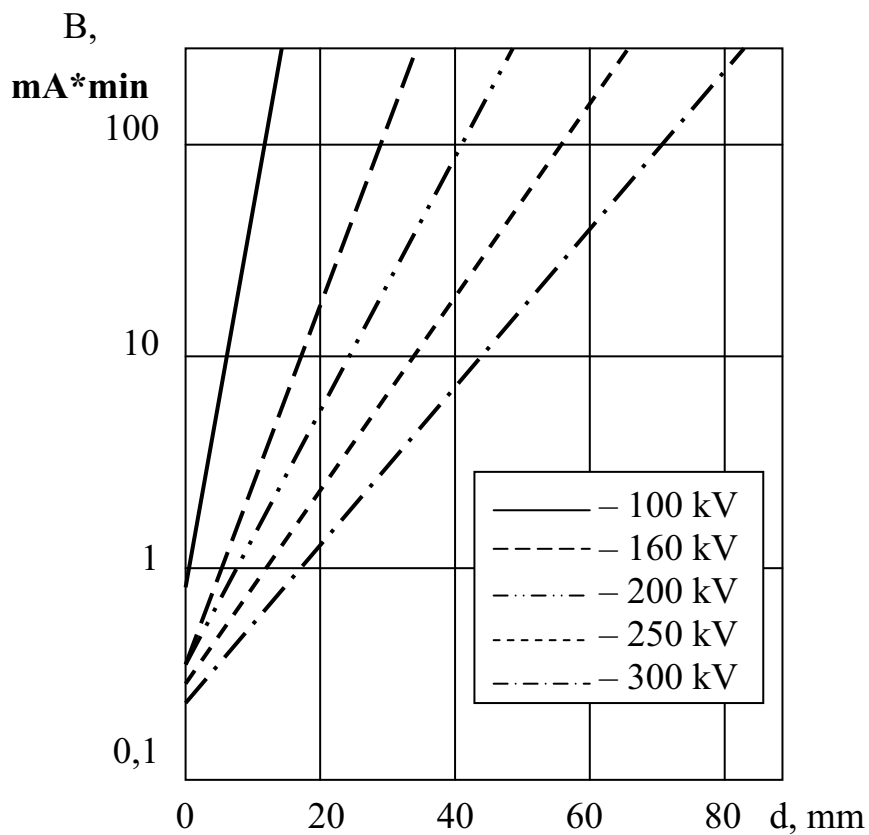


Fig. 3.3. The nomograph of the irradiation

If values of blackening, focal distance and film-foil combination are already given and are different from those in nomograph, then the exposure must be corrected.

In case of isotope application the exposure is understood as the product of isotope activity and irradiation time. In this case, the focal distance between the radiation source and film is used instead of tension on the tube, because the inspector can only change this focal distance.

One must take into account that nomograph acts only for a single film-foil combination and that the film developing procedure must be kept accurately.

Image quality obtained is adjusted by means of cassette disposition, chosen examination, parameters and a type of film. Review of some factors, which can influence the image quality, is given in Table 3.1. The image quality is determined by means of standards used as quality testing indicators.

The image quality, is characterized by means of two parameters: contrast and unsharpness. Contrast depends on material decreasing factor, examination energy, back-scattered radiation values and photographic contrast on the base of parameters γ for the used radiographic film. Unsharpness depends on geometrical unsharpness and on the film own unsharpness. Wire standards DIN 54109 consist of a set of wires with decreasing diameters numbered in order. The thickest wire has number 1 and its diameter is 3.2 mm. The thinnest wire has number 19 and its diameter is 0.05 mm. 7 wires with numbers one after another are joined in a single gelatinous unit (frame). The number of the thinnest wire that can be seen on the film is the index of quality of the obtained figure. The standard wires must be made of the same material as the testing one. Therefore there are standards for fermium, aluminium, copper and titanium.

Table 3.1

Image quality influence factors

	Influences on contrast	Influences on unsharpness
Scheme and procedure of control conducting	<ul style="list-style-type: none"> – radiation spectrum; – scattered radiation; – detail and geometry for X-ray input; – material 	<ul style="list-style-type: none"> – dimensions of focal spot; – geometrical disposition irradiator/detail/film
Films and foils	<ul style="list-style-type: none"> – blackening; – film processing; – foil type and thickness; – haze 	<ul style="list-style-type: none"> – radiation spectrum; – foil type and thickness; – contact between film and foil; – film granularity

For image quality determination the state standard (ГОСТ) 7512–82 (seven thousand five hundred twelve – (dash) -eighty-two) recommends to apply wire,- ditched,- and stepped standards. The wire length in wire standards is (20 ± 0.5) (twenty plus/minus zero point five) mm. and the thickest wire has the diameter of 4.0 mm.

Sensitivity standards are made from different materials and alloys. The inset and cover for wire standards are made from flexible transparent plastics. Each wire standard has seven wires. In accordance with wire diameter joined in a standard, it is given a number from 1 to 4. The standard number and wire

material are indicated by means of lead-made sign (symbol) inserted in standard cover (for example, Fe 4 or by means of figures: the first figure is standard material, the next one or two figures – standard number, where 1 – designate Fe-based alloys, 2 – Al-based or Mg-based, 3 – Ti-based, 4 – Cu-based, 5 – Ni-based alloys).

Ditched standards have six ditches (standard numbers from 1 to 3). Ditch depth is changing from 0,1 mm. (zero point one) to 4,0 mm. Ditched standards are also made from different materials and also have symbols.

The lamellated (stepped) standards with numbers from 1 to 2 have thickness from 0,1 up to 2,5 mm. This standard has two holes on lamel surface and hole diameters are equal to standard thickness and to double thickness of standard.

Control (testing) sensitivity is determined as the least diameter of unmasked wire on the radiograph, or as the least depth of unmasked ditch on the radiograph for ditched standard or as the least thickness of lamellate standard for which the unmasked on radiograph hole has a diameter equal to doubled standard thickness.

The control sensitivity E determination is also carried out, where E is determined as relation between the least visible wire diameter (d), or the minimum visible ditch depth (h_d) or minimum visible lamellated standard thickness (h_e) to the thickness of examined testing object (d). This value d is defined by the formulas:

$$\begin{aligned} E_w &= d * 100 \% / d; \\ E_d &= h_d * 100 \% / d; \\ E_e &= h_e * 100 \% / d, \end{aligned} \tag{3.4}$$

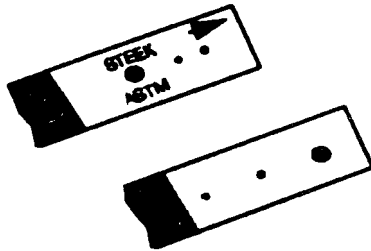
where E_e is sensitivity for wire standard, E_d is sensitivity for ditched standard, E_e is sensitivity for lamelled (stepped) standard.

Other types of international standards are given in Fig. 3.4. In this case, as a rule, the interconnection is used between testing object thickness and any still visible structure consisting, for example, of a set of holes. At present, greater significance receive the CERL-B- standards – the double platinum (Pt) wires placed in plastic frame in such a way that each of two Pt-wires with the same diameters are disposed at the distance equal to the wire diameter. In order to define the image qualities one must determine the minimum diameter at which two separate wires are still visible.

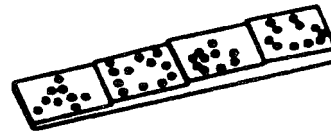
The determinant factor for a high-quality control is a careful developing of the film. Since the material defects being tested are often sited on the sensitivity boundary, even a slight scratch or damages can change the defect data (readings) in the film. Film is developed in a dark room, subsequently, in different photo-baths.

The film development process:

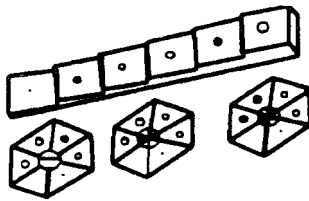
1. Developing in the bath with developer.
 2. Stoppage of developing process in bringing to a stop bath.
 3. Dissolution of non-irradiated argent bromide (AgBr) in fixing bath.
 4. Washing out of chemicals still remaining in emulsion.
 5. Film drying.
- Only after film drying the image deciphering (interpreting) is permitted.



American (US)–standards



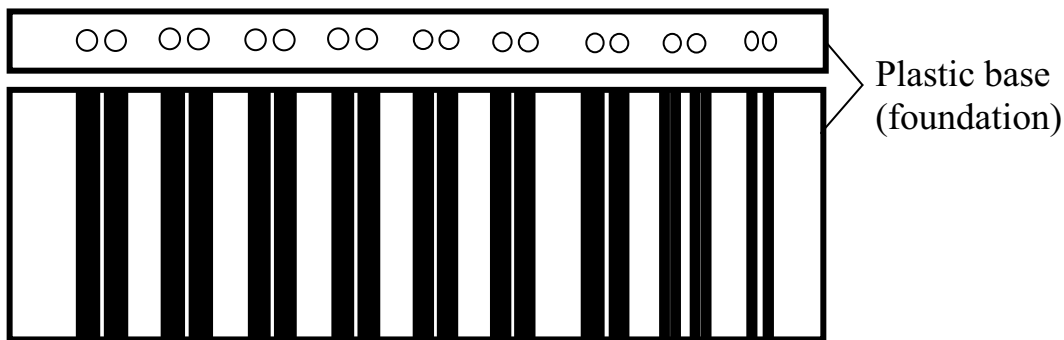
English (GB) – standards



French standards

AFNOR

∅ diameter of hole=thickness of steps



The wire standard – CERL B

Fig. 3.4. The International indicators of image quality

The image interpretation. In order to interpret the film it must be placed on a special device called negatoscope, which illuminates the film from the backside. The rules (normative) have directions concerning minimum permissible illumination force for similar devices depending on film optical density.

The interpretation takes place in the following order:

Firstly, with the help of standard image the required sensitivity testing is fulfilled. If the needed value is not obtained, then one must develop a new radiograph (photo). If the film is fit for interpretation, then by means of careful survey one can try to distinguish the possible defects. Since determined defects, particularly those critical defects as cracks or inclusions in construction details, are often only just visible on the film, a particular care is required, as well as defectoscopist (defector) with a proper experience.

If the defects on the film are visible, then one must determine the disposition, dimension and orientation of the defect. By means of defects catalogue and on the base of the defectoscopist's own experience, defects are classified as, for example, gas-filled pores or cracks. Defects are classified by their dimensions and frequency of occurrence. In accordance with norms and instructions and with inspector experience the testing conclusion is required as the result of control, i. e. decision that the given detail is either suitable or must be improved (or rejected as defective).

3.2. TYPE METHODS OF RADIOGRAPHIC TESTING

Interconnected regimes of radiographic testing of the object, needed for making the technological cards of the testing and for fulfillment the testing procedures in proper consequence.

In practice, the usage of the radiation defectoscopy is regulated by the certain testing instructions, technological cards and other documentation which must meet the acting standards. This documentation determines the means of checking, the consequence of operations, testing modes for concrete articles and assemblies. The base of the technological documentation is formed by methods of radiation-defectoscopic testing, allowed to provide the accordance of the testing object quality to the demands of technical norms, rules and conditions concerning the manufacturing and exploitation of the objects.

The present type methods doesn't substitute the acting standards and meet them and allow to define the total chain of the interconnected modes of testing, needed for developing the technological cards of testing followed by the testing proceeding:

1. Material and the thickness d of the testing object.
2. So, in any case, you must know beforehand, at least, the density, thickness, weakening coefficient and other parameters of the object.
3. Main demands (requirements) for testing (for example, sizes of the permitted defect δ). The object having this defect is considered as the check passed.

4. Sensitivity of testing k and the element of the sensitivity standard (quality indicator) which is the subject to revealing (ordinal number of the wire, ditch or hole).
5. Energy of the source of radiation.
6. Type of the radiation source (taking into account the anode current at the roentgen tube, or the source activity and the size of the focal spot of source).
7. Geometry of the exposure (including the focus distance).
8. Type of the X – ray film and type of the amplifying screen.
9. Exposure time.
10. Sizes (dimensions) of the area tested at single procedure.
11. Number of tested sections or number of shots needed for checking the object totally.

The structure of type techniques is so that any of regimes selected is chosen separately but in accordance with the native or international standards, depending on the object purpose and the requirements for objects checking.

Main standards:

In Russia – GOST 7512, GOST 20426, GOST 23055.

In Europe – EN 444, EN 584 -1.

In Germany – DIN 54109.

In USA – ASTM E94, ASTM E142, ASTM E 1255.

3.2.1. Types regimes

Material and thickness of the object tested are the initial parameters determining all another regimes of the radiographic testing. So, those parameters must be known beforehand the testing operation.

Norms of defects permitted (requirements for the quality of the object). In Russia, the permitted sizes of defects are shown usually on plots of details or articles or may be received from the technical conditions, rules of checking and approving or in other documentation and instructions. If the sizes of defects permitted can't be found in the documentation accompanied the object, they can be estimated in accordance with the State standard 23055 “Non-destructive testing. The welding of metals by smelting. Classification of welded joints after the radiographic testing” or by the class of the sensitivity of testing (the least diameter of wire of wire standard, detected on the shot; the least depth of ditch of groove standard, detected on the shot; and so on for other indicators. At this, one can detect on the shot the image of the hole having the diameter equal to double thickness of the standard.

Size of defect $\geq 2k$: this is the condition for guarantee the revealing the defects, having size more than double sensitivity of testing along the examining direction.

In Europe (EN 444 and other): the tested objects are divided on two classes: A – ordinary or common used objects (technique); B – improve or responsible technique (objects).

Class B is applied if the procedure concerning the A – class can't meet the needed sensitivity of the defects detection. The determining of the class of the objects is gotten usually in contracts or technical demands for delivery or producing the object.

Sometimes, one can combine the requirements for class A and class B at testing the object, if any difficulties occur at fulfillment of the conditions concerning the certain class of the object.

For example: Decrease of sensitivity of testing may be compensated by the increase of the minimum of optical density of the shots or by choosing the more contrast type of the X – ray film. In the USA practice, the required level of the radiography quality is equal usually to the sensitivity 2 %, which corresponds to level 2 – 2T in accordance with the standard ASTM E142.

Determination of the testing sensitivity and choice of type and number of standards (indicators): K(mm) is the least diameter, depth, thickness, at which at radiographic shot the revealed hole diameter, equal to doubled thickness of the indicator, is not more than one-half of the defect size, permitted in the object tested.

In Germany the quality of radiography is estimated with the help of wire standard according the DIN 54109 system and with the help of lamellate standards according the MIL – STD – 453 system. In the DIN 54109 system, the model (penetrometer) consists from 7 wires having length 50 or 25 mm and the gap in 5 mm between wires. Wires are inserted into the flexible plastic housing with marking signs made from lead (system DIN, year of inculcation, type of material – Fe, Cu, Al, numbers of the most thick and thin wires). Numbers of wires (units of radiography quality BZ) are given in Table 3.2.

They use the following materials for wires: aluminum (testing of objects from Al – alloys), steel (alloys on base of Fe and Ni), copper (testing of copper, brass and their alloys). The quality level is estimated by the number of wire (BZ). In aerospace industry of Germany, they use the quality level, corresponding to the sensitivity 1 % of total thickness of tested object. This level corresponds to European class B (responsible technique). Lamellate standards MIL – STD-453 are identical to ASTM-standards of the USA.

ASTM standards E 94: in the USA levels of radiographic sensitivity were set for lamellar models of sensitivity, inculcated by the ASTM standard E 142. Lamellar penetrometer is the plate from material similar to material of tested object having thickness T and with holes having diameters 1T, 2T and 4T. Levels of radiographic quality corresponding to the detection of one or another hole of penetrometer, are given in Table 3.3.

Table 3.2

*Numbers of wires (BZ) and their diameter
in penetrometers in DIN 54109 system*

Diameter, mm	3.20	2.50	2.00	1.60	1.25	1.00	0.80	0.63
Number of wire (BZ)	1	2	3	4	5	6	7	8
Diameter, mm	0.50	0.40	0.32	0.25	0.20	0.16	0.125	0.100
Number of wire (BZ)								

Numbers of penetrometers and numbers of wires (BZ) in DIN 54109 system

Number of penetrometer	Numbers of wires (BZ)							
	DIN 1/7	1	2	3	4	5	6	7
DIN 6/12	6	7	8	9	10	11	12	
DIN 10/16	10	11	12	13	14	15	16	

Table 3.3

Level ¹ of radiographic quality	Thickness T of penetrometer in % of thickness of object	Minimum distinctive diameter of hole	Equivalent sensitivity ² by penetrometer, %
2 – 1T	2	1T	1,4
2 – 2T	2	2T	2,0
2 – 4T	2	4T	2,8
Special levels of testing			
1 – 1T	1	1T	0,7
1 – 2T	1	2T	1,0
4 – 2T	4	2T	4,0

¹ First cipher means thickness of plate in % from thickness of object tested: second cipher is the diameter of revealing hole in units of thickness of model.

² Level of sensitivity, using single model, is correct for materials with thickness more than 6 mm; level of sensitivity for thinner materials requires for using of different penetrometers.

In the USA they used to settle the quality level equal to 2 % (2 – 2T) if, in accordance with agreement between the customer and the manufacturer of tested objects they need not in higher or lesser level of quality.

If the material for penetrometers, similar to tested object's material, is not available, they permit the usage of penetrometers having the same sizes as the needed one, but made from lesser absorbing material.

3.2.2. Selection of radiation energy (tension between electrodes of X-ray tube, accelerator energy or energy of radionuclidic source)

In Russia, in accordance with the State standard 20426, the voltage on the tube type of source or the energy of accelerated electrons are chosen depending upon the thickness and density of material exposed (see Tables 3.4, 3.5, 3.6):

Table 3.4

Area of usage of radiographic method at applying the X-ray apparatus

Thickness of examining metal mm				Thickness of examining non-metal with mean atomic number Z and density ρ g/cm ³ , mm			Voltage on X-ray tube, kV, not more
Iron	Titanium	Aluminum	Magnesium	Z = 14, $\rho = 1.4$	Z = 6.2 $\rho = 1.4$	Z = 5.5 $\rho = 0.9$	
0.04	0.1	0.5	1.5	1	10	15	20
0.4	1	5	14	8	70	100	40
0.7	2	12	22	17	95	135	50
1	3	20	35	25	120	170	60
2	6	38	57	–	–	–	80
5	10	54	80	–	–	–	100
7	18	59	105	–	–	–	120
10	24	67	120	–	–	–	150
21	47	100	160	–	–	–	200
27	57	112	200	–	–	–	250
33	72	132	240	–	–	–	300
46	106	210	310	–	–	–	400
150	265	430	650	–	–	–	1000

Table 3.5

Area of usage of radiographic method at applying the γ -defectoscopes

Thickness of examining material, mm				Sealed radioactive sources
Iron	Titanium	Aluminum	Magnesium	
1...20	2...40	3...70	10...200	¹⁷⁰ Tm
5...80	10...120	40...350	70...450	¹⁹² Ir
10...120	20...150	50...350	100...500	¹³⁷ Cs
30...200	60...300	200...500	300...700	⁶⁰ Co

Table 3.6

Area of usage of radiographic method at applying betatrons

Thickness of examining material, mm				Energy of accelerated electrons, MeV
Iron	Titanium	Aluminum	Lead	
50...100	90...190	150...310	30...60	6
70...180	130...350	220...570	40...110	9
100...220	190...430	330...740	40...110	18
130...250	250...490	480...920	60...120	25
150...350	290...680	570...1300	60...150	30
150...450	290...880	610...1800	60...180	35

At source type selection, one must pay into attention that industrial X-ray apparatus are the most available, reliable and simple at service.

Gamma-defectosopes are recommended to apply for testing:

- thick articles, impossible for examining by X-ray devices because of insufficient penetrating capacity of X-rays;
- complicated aggregates, welded and another articles and patterns having construction inaccessible for examining by optimal way and scheme;
- aggregates, welded and another indivisible joints at field conditions, where applying of X-ray apparatus is impossible because of absence of power supplies.

Note: the objects with the same thickness may be tested often by means of different sources of radiation, that why it is the problem for operator to select the source providing the best ratio between the sensitivity, productivity, quality and radiation safety at composing the examining scheme.

Accelerators are used mainly for testing the thick objects with thickness inaccessible for examining by other sources of radiation.

If the material of the object is not listed in Tables given above, the needed value of thickness corresponds the energy of radiation, listed in Tables, may be determined with the help of formulae:

1. For X-rays and bremsstrahlung radiation of betatrons:

$$d = \mu_t (E_{eff}) \times d_t / \mu (E_{eff}), \quad (3.5)$$

where E_{eff} – effective energy of examining radiation; $E_{eff} = 2/3 U_{anode}$ of X-ray tube; $E_{eff} = 1/2 E_{ac.el.}$ at $E_{ac.el.} \leq 10$ MeV; $E_{eff} = 1/3 E_{ac.el.}$ at $E_{ac.el.} > 10$ MeV; $\mu_t (E_{eff})$ – weakening coefficient of material, listed in Table; $\mu (E_{eff})$ – linear absorption coefficient of given tested material, listed in GOST 20426 or references; d – thickness of examining material absent in Table, d_t – testing thickness of examining material, given in Table.

2. For gamma-radiation of radionuclidic sources:

$$d = \rho_t \times d_t / \rho, \quad (3.6)$$

where d and ρ – are thickness and density of material, not given in Tables; d_t and ρ_t – are thickness and density of material, given in Tables.

In calculations, you must use as d_t the thickness of such a material which mean atomic number is the nearest to the atomic number of tested material. In the case of complete substances you must choose the atomic number of chemical element having the main fraction part in mixture. The linear absorption coefficient for compounds is estimated as the sum of partial coefficients accounting the relative mass fractions of each element of mixture.

In Europe, in accordance with EN 444-standard, the maximum tension on the X-ray tube is chosen in dependence on tested object thickness by means of the graph shown on Fig. 3.5.

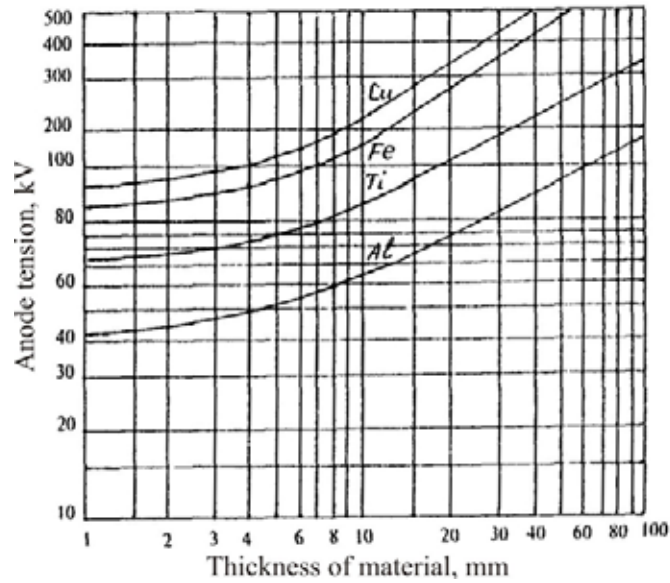


Fig. 3.5. Maximum tension on the X-ray tube in dependence on the thickness of material of the tested object

The needed source of gamma-radiation or the X-ray equipment with energy over 1 MeV (electron accelerator) are selected in dependence on thickness of testing material at applying the Table 3.7.

Table 3.7

Range of examining thickness for sources of gamma-radiation and X-ray equipment with energy over 1 MeV for steel and alloys on base of copper and nickel

Source of radiation	Examining thickness d , mm, at testing	
	In accordance with Class A	In accordance with Class B
170-Tm	$d \leq 5$	$d \leq 5$
169-Yb ¹	$1 \leq d \leq 15$	$2 \leq d \leq 12$
192-Ir	$20 \leq d \leq 100$	$20 \leq d \leq 90$
60-Co	$40 \leq d \leq 200$	$60 \leq d \leq 150$
X-ray equipment, E = 1...4 MeV E = 4...12 MeV E > 12 MeV	$30 \leq d^1 \leq 200$	$50 \leq d \leq 180$
	$d \geq 50$	$d \geq 80$
	$d \geq 80$	$d \geq 100$

¹ thickness of exam material for Al and Ti is $10 < d < 70$ for Class A and $25 < d < 55$ for Class B

If we have the tested material not listed on Graph 3.5 or in Table 3.7, we can estimate the value of thickness corresponding to the energy listed on Graph or Table with the help of so called coefficients of radiographic equivalence:

Table 3.8

Coefficients of radiographic equivalence

Material	X-radiation, kV									
	50	100	150	200	220	250	400	1 MeV	2 MeV	6-31
Carbon-ep.	0.004									
Glues	0.04									
Glassplastic.	0.35									
Magnesium	0.6	0,6	0.05	0.05	0.08					
Boron-ep.	0.75									
Aluminum	1.0	1.0	0.12	0.14	0.18	0.16				
Boron-alum.	1.0	1.0								
Titanium	3.6	5.8	0.34	0.36		0.38				
Steel	12.0	12.0	1.0	1.0	1.0	1.0	1.0	1.0	1.0	1.0
Copper		16.5	1.6	1.4	1.4	1.4	1.4			1.3
Zinc		15.0	1.4	1.3	1.3	1.3	1.3			1.2
Brass			1.4	1.3	1.3	1.3	1.3	1.2	1.2	1.2
Zirconium			2.3	2.0			1.0	1.2		
Lead	125	145	14.0	12.0	12.0	9.0	6.0	3.0	2.5	2.4
Uranium					25.0					3.9

Material	Gamma-radiation		
	¹⁹² Ir	¹³⁷ Cs	⁶⁰ Co
Carbon-ep.			
Glues			
Glassplastic.			
Magnesium			
Boron-ep.			
Aluminum	0.35	0.35	0.35
Boron-alum.			
Titanium			
Steel	1.0	1.0	1.0
Copper	1.1	1.1	1.0
Zinc	1.1	1.0	1.0
Brass	1.1	1.1	1.1
Zirconium			
Lead	4.0	3.2	2.3
Uranium	12.6	5.6	3.4

In given Table, the coefficient equal to 1.0 was given arbitrary for steel (excluding columns for 50 and 100 kV, where 1.0 was given for Al). The equivalent thickness is the product of tested object thickness and the coefficient listed in Table. For all of other materials, at definition of energy

of radiation one must use namely that material given in Table and on the Graph which radiographic density is close to the radiographic density of tested object. Standards of the USA, excluding special cases, demands that maximum voltage on X-ray tube or maximum energy of accelerated electrons in accelerator of particles were not more than values given on Fig. 3.6, 3.7, 3.8.

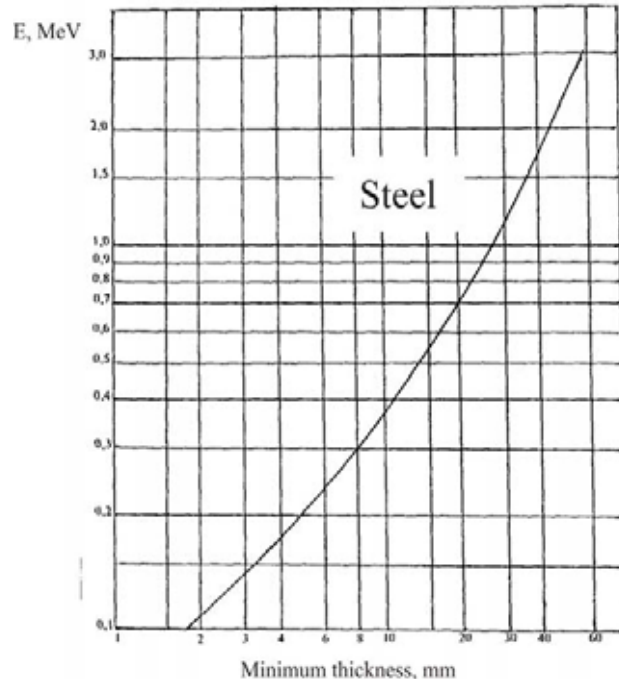


Fig. 3.6. Maximum accelerating tension at steel examining

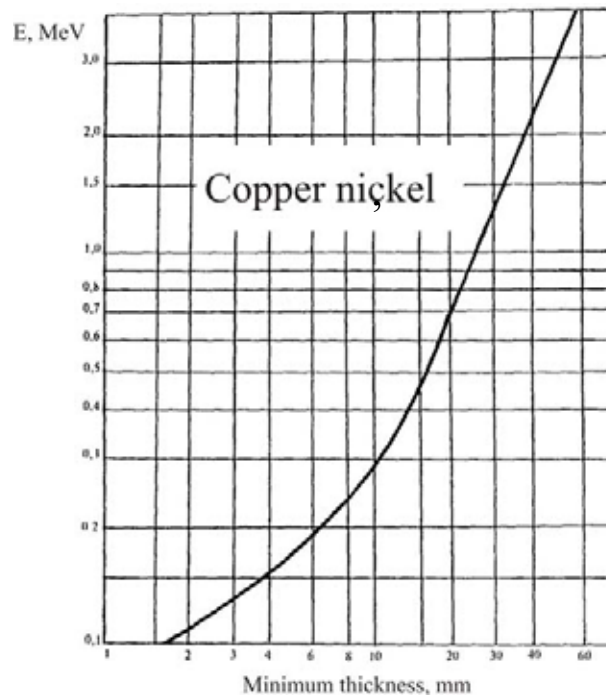


Fig. 3.7. Maximum accelerating tension at examining alloys on base of copper or nickel

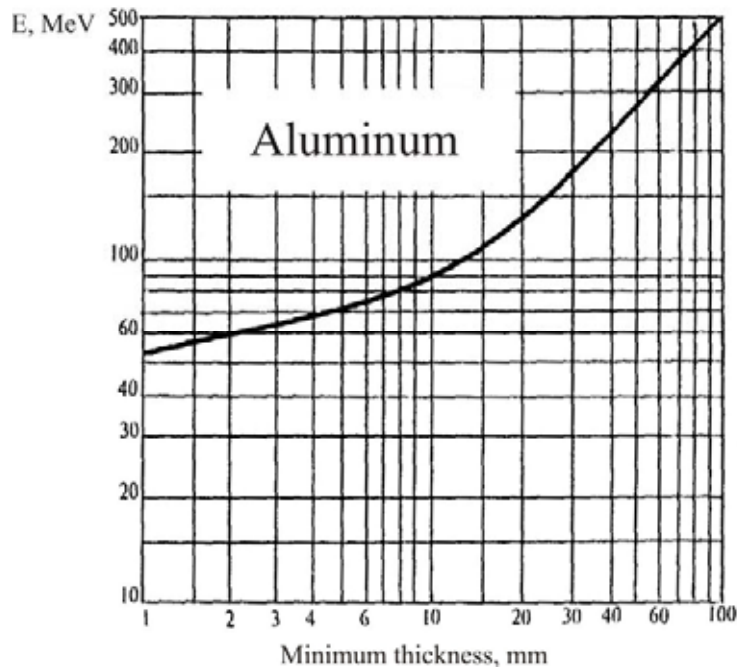


Fig. 3.8. Maximum accelerating tension at examining alloys on base of aluminum

Minimum thickness of materials recommended for testing by means of radionuclides is given in Table 3.9. At testing materials not given in Table and on figures, for choice of voltage on X-ray tube, energy of accelerated electrons or radionuclidic source one can apply the coefficient of radiographic equivalence.

Table 3.9

Minimum thickness of materials available for testing with the help of radioactive isotopes

Material	Minimum ¹ thickness, mm	
	192-Ir ²	60-Co
Steel	19	38
Copper and high – Ni – content alloys	17	33
Aluminum	64	-

¹ Maximum thickness at using radionuclides is defined mainly by exposure time, so upper limits are not given in Table.

² If another isotopes, not Ir and Co, are used, the preliminary examining of the sensitivity standard is required in order to make sure of satisfactory resolution of testing at minimum thickness of material.

3.2.3. Choice of type of radiation source (X-ray equipment, gamma-defectoscope, accelerator)

After determining the needed tension, the concrete type of X-ray apparatus is chosen taking into account the requirements for sensitivity, productivity of testing and so on. Come from testing conditions, one can choose the X-ray

equipment either stationary for working within the roentgen laboratory of given enterprise, or mobile or transportable equipment for working at field and other non-stationary conditions. At this, the main requirement produced for equipment is the range of voltages on tube exceeded the needed tension.

In Europe the concrete type of radiation source is selected with the help of Tables giving data concerning the variety of technical and exploitation parameters of different types of sources, including type, tension, maximum anode current or dose power, sizes of focal spot, design, mass, activity, etc. The same way is applied in the USA.

**3.2.4. Determining of radiation intensity
(anode current of X-ray tube, radiation yield of pulse X-ray apparatus,
radionuclidic sources and electron accelerators)**

Sizes of focus spot of irradiator

The intensity of radiation sources is:

- Maximum anode current of roentgen radiation of continuous action in mA;
- Radiation output of exposure dose power of pulsed X-ray devices in Koulomb/kg×sec or Roentgen/min (Roentgen/sec) at certain distance from anode of tube;
- Radiation outlet of gamma-defectoscopes in the same units at certain distance from radionuclidic source;
- Radiation outlet (exposure dose power) of electron accelerators (betatrons or linear accelerators) in the same units at certain distance from the target of accelerator. Values of intensities are found in Tables of parameters for concrete irradiators. Sizes of the focus spot of irradiators in mm one can also define for concrete irradiators using the same Tables.

3.2.5. Choice of X-ray films and amplifying screens

In Russia the X-ray films produced by industry, are divided by 4 classes (see Table 3.10).

Table 3.10

Classes of Russian X-ray films

Classes of films	Indices (parameters) of films		
	Sensitivity	Contrast	Graininess
1	Low	Very high	Too small
2	Average (middle)	High	Small
3	High	Average	Average
4	Very high	Low	High

At changing from the first to fourth class, the sensitivity changes its values from low to extra high, the image contrast – from extra high to low

and the graininess from extra small to high. The sensitometric parameters of Russian films are given in Table 3.11.

Table 3.11

Types and characteristics of Russian X-ray films

Class of film	Type of film	Sensitometric characteristics ¹			
		Sensitivity ² , $S_{0.85}, R^{-1}$	Contrast ³	Mean size of grain, $10^{-6}m$	Optical density of fog
1	PT – K	3	4.8	0.25	0.10
2	PT – 4M	5	3.5	0.25	0.10
	PT – CIII	10	3.0	0.55	0.15
3	PT – 1	25	3.2	0.77	0.20
4	PM – 1	400	2.8	1.16	0.20
	PT – 2	450	3.0	1.38	0.20

¹ Determined at anode voltage 80 kV;

² Sensitivity $S_{0.85}$ –value reverse to exposure dose in R needed for receiving the optical density exceeded by 0.85 unit the optical density of fog (haze);

³ Contrast of film: coefficient of contrast γ for screen films; average gradient g_s for non-screen films

At choosing the X-ray film, the following recommendation may be done:

1. Firstly, the films of fourth and third classes one must use in any cases if only the unmasking of non-permitted defects is possible at this. Using of those films are worthwhile at testing the thick-walled objects examined by the high-energy radiation; for revealing the inner geometry and its hidden damages; if one needs to compensate the time losses at exposure the object by low power sources of radiation (e.g. pulsed X-ray apparatus). If at shots received on the film of fourth class, one can't reveal the non-permitted defects, one must cross then, in consequence, to films of third class and further to films of second and first classes. Sometimes, if the customer agrees, at choosing the film you may use the recommendations of the USA standard ASTM E 94:

Note: these recommendations corresponds to commonly accepted level of the radiographic quality 2 -2T. Quality may be improved by choosing the lower number of the film type suitable by economic and technical requirements.

- Voltages which are given in the Table, corresponds to working energy of radiation.
- Standard E 94 gives also the similar recommendations for other materials: aluminum, brass, magnesium and so on.

Table 3.12

Choice of X-ray films in accordance with ASTM E 94

Thickness of material, mm	Tension on tube, radionuclidic sources, electron accelerators										
	50 – 80 kV	80 – 120 kV	120 – 150 kV	150 – 250 kV	250 – 400 kV	192-Ir	1 MV	60 – Co	2 MV	226 – Ra	6 – 31 MV
Steel											
0...6	3	3	2	1							
6...12	4	3	2	2	1						
12...25		4	3	2	2	2	1		1	2	
25...50				3	2	2	1	2	1	2	1
50...100				4	4	3	2	2	2	3	1

The amplifying coefficients of luminescent screens, applied as combine with the films, are given in Table 3.13.

Table 3.13

Amplifying coefficients of luminescent screens

Type of film	Amplifying coefficient of screen ¹					
	ЭУ – B1	ЭУ – B2	ЭУ – B3	ЭУ – B ²	БП – 1	БП – 2
Screen film (PT-2)	30	30	54	54	60	69
Non-screen film (PT-K, PT-4M, PT-1)	2	2	3,6	3,6	4	4,6

¹ Coefficient is defined at $U_a = 80$ kV and exposure time ~ 100 s,

² ЭУ – Б – Lead-Barytes screen, all another screens are Tungsten-Calcium; for all of screens the size of grain is $(6-20) \cdot 10^{-6}$ m

Table 3.14

Optimum thickness of metallic screens (Lead or Lead-Tin foils)

Source of radiation	X-ray device, V ≥ 100 kV	Radionuclidic source				
		170-Tm	75-Se	192-Ir	137-Cs	60-Co
Thickness of front/back foil, mm	0.05/0.05	0.05/0.05	0.1/0.2	0.1/0.2	0.1/0.2	0.2/0.2
Source of radiation	Electron accelerator with energy, MeV					
	6	9	18	25	30	35
Thickness of front/back foil, mm	(0.5...1.0)/ (0.5...1.5)	1/(1...1.5)	(1...1.5)/ (1.5...2)	2/(2...3)	2/(2...3)	2/(2...3)

Note: Amplifying coefficient of metallic screens at their optimal thickness given in Table, is equal to ~ 2 . At choosing of type of screen, besides the amplifying coefficient, one must take into account the clearness of the image of defects: at using the metal screens the image on the shot is more clear-cut in comparison with using of luminescent screens.

In accordance with European standards (e.g. EN 584-1) X-ray films are divided by their objective parameters, which are:

- g_2 and g_4 are gradients of characteristic curves of films at values of optical density $S_2 = S_0 + 2$ and $S_4 = S_0 + 4$, where S_0 is the optical density of fog (haze);
- σ_{s2} – mean square root deviation of optical density at $S_2 = 2 + S_0$;
- g_2 / σ_{s2} – ratio of the gradient of characteristic curve over the mean square root deviation of optical density at $S_2 = 2 + S_0$.

These parameters are estimated at voltage $V = 220$ kV on X-ray tube.

European classification has 6 classes of X-ray films, from C1 to C6. ___.

Ratio g_2 / σ_{s2} may be regarded as the ratio “signal/noise” of the image on the shot. At transfer from class C1 to C6, this ratio is decreased and corresponds to the worsening of image’s quality. The EN 584 – standard classification of X-ray films is given in Table 3.15.

Table 3.15

Limit values of gradient, gradient/noise ratio and granularity

Class of film systems	Minimum of gradient G_{\min} at		Minimum of ratio $(G/\sigma_D)_{\min}$ at $D = 2$ over D_0	Maximum of granularity $\sigma_{D\max}$ at $D = 2$ over D_0
	$D = 2$ over D_0	$D = 4$ over D_0		
C1	4.5	7.5	300	0.018
C2	4.3	7.4	270	0.018
C3	4.1	6.8	180	0.023
C4	4.1	6.8	150	0.028
C5	3.8	6.4	120	0.032
C6	3.5	5.0	100	0.039

General recommendations concerning the choice of films and metal amplifying screens in accordance with En 444 for examining the alloys on base of steel, copper and nickel are given in Table 3.16.

Brief sum of the recommendations may be expressed as following:

- At using X-ray radiation with tension more than 125 kV, the lead foil with thickness about 0.1 mm may be applied;
- At using the radionuclides, one needs to apply the front screen from lead with thickness more than 0.13 mm at 192-Ir source and more than 0.25 mm at 60-Co source;

Table 3.16

*Classes of films and types
of metal amplifying screens (by EN 444)*

Source of radiation		Exam. thickness d, mm	Classes of films ¹ at testing class		Type and thickness of metal screens for testing class	
			A	B	A	B
X-rays at voltage on tube	< 100 kV	See Fig. 3.5	C5	C3	Without screens or with front and back screen from lead, d < 0.03 mm	
	100...150 kV				Front and back screens from lead, d < 0.15 mm(max)	
	150...250 kV			C4	Front and back screens from lead, d = (0.02...0.15) mm	
169-Yb, 170-Tm		d < 5	C5	C3	Without screens or with front/back screens, d < 0.03 mm	
		d ≥ 5		C4	Front/back screens from lead, d = (0.02...0.15) mm	
X-rays at voltage from 250 to 500 kV		d ≤ 50	C5	C4	The same, d = (0.02...0.2) mm	
		d > 50		C5	Front screen from lead, d = (0.1...0.2) mm ² .	
192-Ir		20 < d ≤ 100	C5	C4	Front screen, lead, d = (0.02...0.2) mm	Front screen, lead, d = (0.1...0.2) mm ²
					Back screens, lead, d = (0.02...0.2) mm	
60-Co		d ≤ 100	C5	C4	Front and back screens, steel or copper, d = (0.25...0.7) mm ³ .	
		d > 100		C5		
Electron accelerator, E = (1...4) MeV		30 < d ≤ 200	C5	C3	Front and back screens, steel or copper, d = (0.25...0.7) mm ³	
		d > 100		C5		

Source of radiation	Exam. thickness d , mm	Classes of films ¹ at testing class		Type and thickness of metal screens for testing class	
		A	B	A	B
Electron accelerator, $E = (4...12)$ MeV	$d \leq 100$	C4	C4	Front screen, copper, steel or tantalum, $d < 1$ mm(max)	
	$100 < d \leq 300$	C5	C4	Back screen from copper or steel($d < 1$ mm) or tantalum ($d < 0.5$ mm) ⁴	
	$d > 300$		C5		
Electron accelerator, $E > 12$ MeV	$d \leq 100$	C4	–	Front screen, tantalum, $d < 1$ mm ⁵ Without back screen	
	$100 < d \leq 300$	C5	C4	Front screen, tantalum, $d < 1$ mm ⁵	
	$d > 300$ mm	C5	C5	Back screen, tantalum, $d, 0.5$ mm	

¹ Better classes of films may be applied.

² One can use the prepared packing of films with front screen less than 0.03 mm, if the additional lead screen with $d \sim 1$ mm is displaced between the testing object and the film.

³ For class A, one can use the lead screens with $d = (0.1...0.5)$ mm.

⁴ If customer and manufacturer agree, for class A one can use lead screens with $d = (0.5...1)$ mm.

⁵ If parties agree, one can use screens from tungsten.

- At using accelerators with energy more than 1 MeV, one can receive better radiographic sensitivity at copper screens instead of lead screens of equivalent thickness. Sometimes, screens from gold, tantalum and other heavy metals may be applied instead of lead screens.

3.2.6. Choice of focus distance or distance between source and object

In Russia, in accordance with the State standard 7512, one ought to choice such a distance from radiation source to object tested which meets the following requirement: the geometrical unsharpness of the defects images on shots at placing the film closely to the tested object must not be high than a half of a needed testing sensitivity at sensitivity value not more than 2 mm and not more than 1 mm at sensitivity value more than 2 mm.

Usually, the geometry unsharpness is estimated by the formula:

$$U_g = \Phi \times d / (F - d), \quad (3.7)$$

where d is object's thickness; Φ – size of focus spot of source; F – focus distance.

If the sensitivity of testing $K \leq 2$ mm, then, by GOST 7512, one can find that

$$U_g = \Phi \times d / (F - d) \leq 1/2 K.$$

So, now one can find that minimum focus distance

$$F = d (1 + 2\Phi/K), \quad (3.8)$$

or minimum distance from source to object tested must be

$$f = F - d = 2 \Phi \times d / K. \quad (3.9)$$

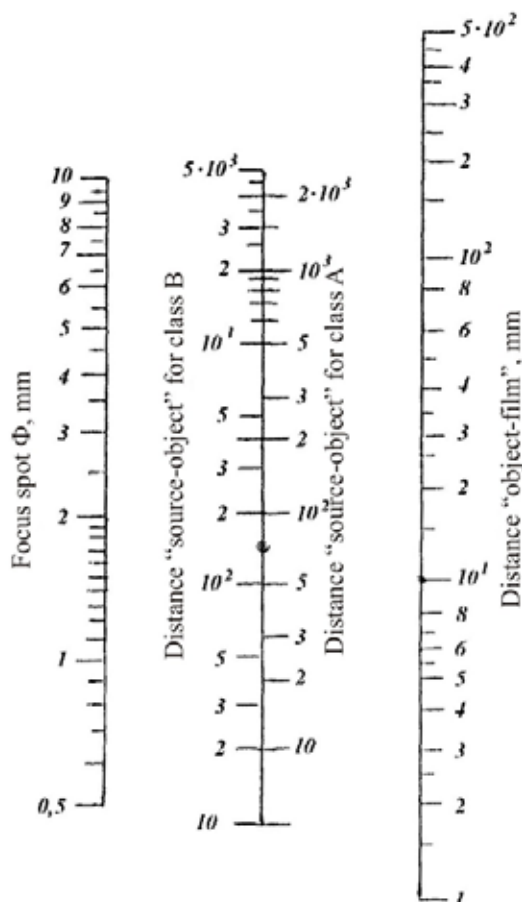
Pay attention: if, for example, the pipe with diameter D is examined through two walls with deciphering of the upper and lower sections, one ought to substitute diameter D instead of wall thickness d in above written formulae.

For testing sensitivity $K > 2$ mm, in accordance with GOST 7512, we can find: $U_g = \Phi \times d / (F - d) = 1$ mm, from which minimum focus distance (in mm) is $F = d (1 + \Phi)$, or minimum distance from radiation source to testing object (in mm) is $f = F - d = \Phi \times d$.

In accordance with European standard EN 444 the ratio of minimum distance from source to testing object – f over the size of focal spot of the irradiator – Φ is determined from the equations followed:

$$\text{For class A of testing } f / \Phi \geq 7.5 b^{2/3}, \quad (3.10)$$

$$\text{For class B of testing } f / \Phi \geq 15 b^{2/3}, \quad (3.11)$$



where b is the distance between the turned to source surface of object and the film. If the distance $b < 1.2 d$ (where d is tested object thickness), than in equations for U_g the quantity b must be substituted by object thickness d .

Given equations were applied for development the nomogram for choosing the minimum distance from source to testing object:

Fig. 3.9. Nomogram for determining the minimum distance f from source to object using distance b from object to film and size Φ of focal spot (by EN 444)

In accordance with the USA standards, the geometry unsharpness of images on X-ray film must not be more than values given in Table 3.17.

Table 3.17

Maximum values of geometry unsharpness at radiography of materials of different thickness

Thickness of material, mm	Unsharpness (max), mm
Less than 50	0.5
From 50 up to 75	0.75
From 75 up to 100	1.0
More than 100	1.8

By the USA standard ASTM E 94 U_g may be computed from the equation: $U_g = \Phi \times d / (F - d)$, or may be determined from the nomograph (see Fig. 3.10).

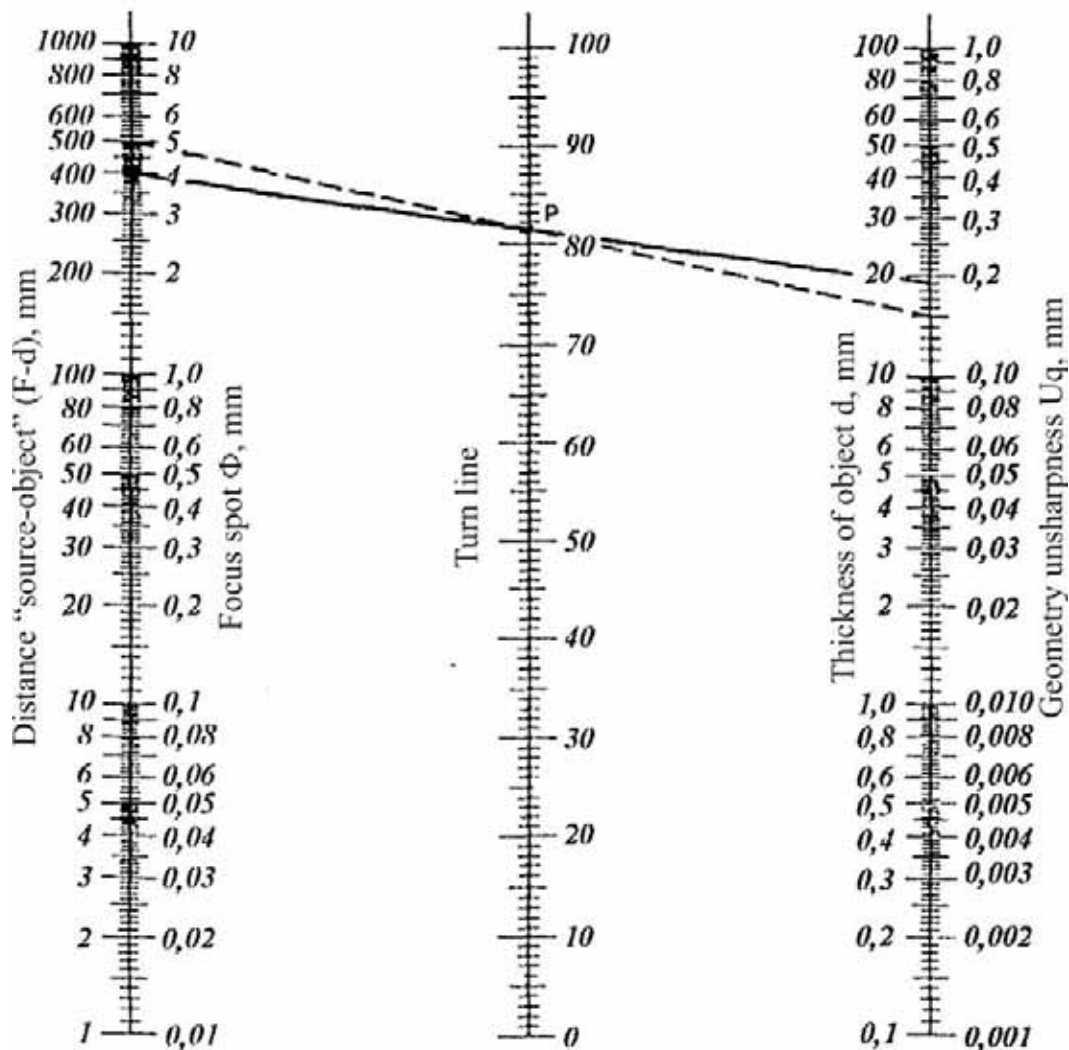


Fig. 3.10. Nomograph for determining U_g by ASTM E 94

Example of finding the value of geometry unsharpness:

Given parameters: distance “source – object” $(F - d) = 400$ mm; size of focal spot $\Phi = 5$ mm; thickness of object $d = 15$ mm.

Now, fix value 400 mm on left scale of $(F - d)$ line and fix size of focal spot 5 mm on right scale of the same line. Fix value of thickness of object 15 mm on d -scale. Then connect by straight drawing line the point of 5 mm on focal scale with 15 mm-point on thickness d -scale and fix the P point ($P = 81$) on the turn line. Then the straight line we must draw from the point 400 mm on $(F - d)$ scale through the P point on turn line toward the scale of U_g . At this, the crossing of this straight line with U_g scale gives the value of U_g in mm: $U_g = 0.19$ mm. Usually size of focal spot is defined for the concrete source of radiation, so the value of U_g may be changed for given thickness d of object by varying the focus distance F : the larger F , the smaller U_g .

3.2.7. Optical density of shots

In Russia, by GOST 7512, the optical density of images of tested section of the welded joint, the nearest zone around the joint and sensitivity indicator must not be less than 1,5 units. Maximum optical density of shots is defined by the maximum brightness of the illuminated field of the negatoscope which must not be less than 10^{S+2} , where S is the optical density of the shot.

In Europe, by requirements of EN 444 and other rules, minimum optical density of radiographs, including the optical density of the backing and haze, is determined by the data listed in Table 3.18.

Table 3.18

Minimum optical density of radiograms

Class of testing	Optical density ¹
A	≥ 2.0
B	≥ 2.3

¹ The error permitted is ± 0.1 .

Maximum permitted density is determined by the brightness of the negatoscope field in accordance with the EN 25580 rules.

By the USA standards, the optical density of the shot in the sensitivity indicator's image zone and in testing object's zone of the interest, must have the minimum value 1.8 at examining by X-rays, and value 2 at examining by gamma-radiation source.

If one looks through the clear space at once two radiographic shots placed one on other, then minimum optical density of each shot must have the value about 1.3 and the sum density must have the minimum value 2.6. Maximum optical density of single or the sum density of two radiographic shots must not be over 4.0.

3.2.8. Choice of size of tested section and evaluation of number of sections tested

In Russia, by GOST 7512, the size of section tested is determined from the point of permitted decrease of the optical density of the image of welded joint within any section of this image (including the edge of the shot) not more than 1.0 unit, in comparison with the optical density of the image of sensitivity indicator in the center of shot. The concrete length of section tested at single exposure and number of sections (exposures) of object are determined from the corresponding appendixes of standard 7512.

In Europe, they meet the rules of standard EN 444, and in this case the relation between the examining thickness at the edge of the estimated square of uniform thickness and the thickness in the centre of the beam must not be more than 1.2 for class A and not more than 1.1 for class B.

In the USA, as in Europe, the length of the tested section of the object is estimated by the relation of the uniform thickness at the edge of section over the thickness in the centre of the beam. The minimum number of sections at the exposure of circular welded joints having the external diameter D at the focus distance F and with permitted increase of the thickness on the section edge not more than 20 %, one can estimate using the nomogram given on Fig. 3.11.

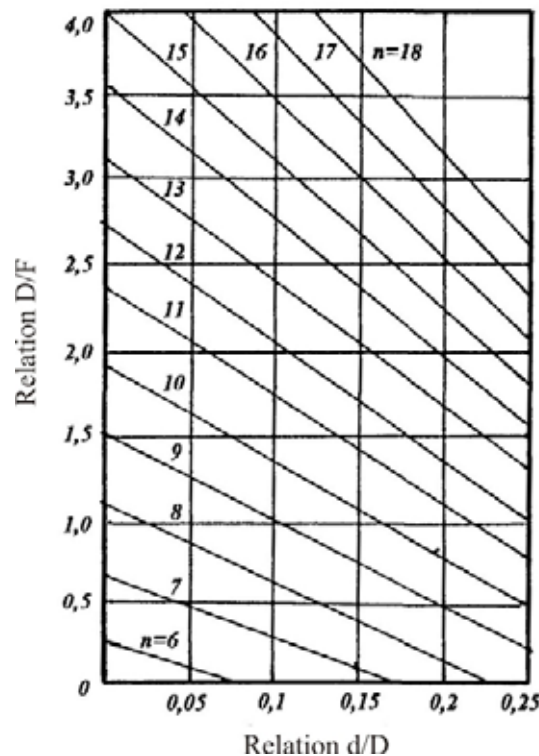


Fig. 3.11. Nomogram for estimating the minimum number of sections (exposures) n at examining of circular welded joint with diameter > 100 mm through one wall with thickness d , at focus distance F and at wall thickness increase on the edge of section not more than 20 %

Table 3.19

*Number of shots (sections) at exposure the circular articles (hollow pipes).
Film is displaced inside the pipe, front wall is under testing*

Ratio F /R	Number of shots, not less than, at d /R				
	0.5	0.4	0.3	0.2	0,1
Up to 1.2	16	14	13	12	11
1.2...1.5	15	13	12	11	10
1.5...2.0	14	12	11	10	9
2.0...4.0	13	11	10	9	8
4.0...20.0	12	10	9	8	7
20.0	11	9	8	7	6

Table 3.20

*Recommended relationships between sensitivity,
geometry unsharpness and size of defects*

Min size of defect, mm	0.1	0.2	0.3	0.4	0.5	0.6	0.7	0.8	1.0	1.2	1.5	2.0	2.5	3.0	3.5	4.0	5.0
Sensitivi ty Δd , mm of exposure	0.05	0.1	0.2	0.3	0.4	0.5	0.6	0.75	1.0	1.25	1.5	1.75	2.0	2.5			
Max U_g , mm	0.02 5	0.05	0.1	0.15	0.2	0.25	0.3	0.4	0.5	0.6	0.7	0.8	0.9	1.0			

3.2.9. Calculation of exposure time

In Russia, the exposure time at examining by X-ray devices of continuous action, is determined with the help of nomographs given in Fig. 3.12, 3.13. for joints made from Fe- and Al-alloys. Then, the correction may be done corresponding to the concrete type of X-ray device, material of object tested and exposure conditions.

The exposure time by the pulsed X-ray apparatus for alloys on the base of steel is determined with the help of nomographs given below on Fig. 3.14 up to Fig. 3.16.

The exposures at gamma-radiation examining for alloys on Fe-base may be defined from nomograms of Fig. 3.17.

Exposures (needed radiation dose at distance 1 m) at examining by bremsstrahlung radiation of betatron the Fe-based alloys, are defined with the help of nomogram of Fig. 3.18.

At applying nomograms given below, sometimes one needs to correct the exposure time found from nomograms by certain amendments.

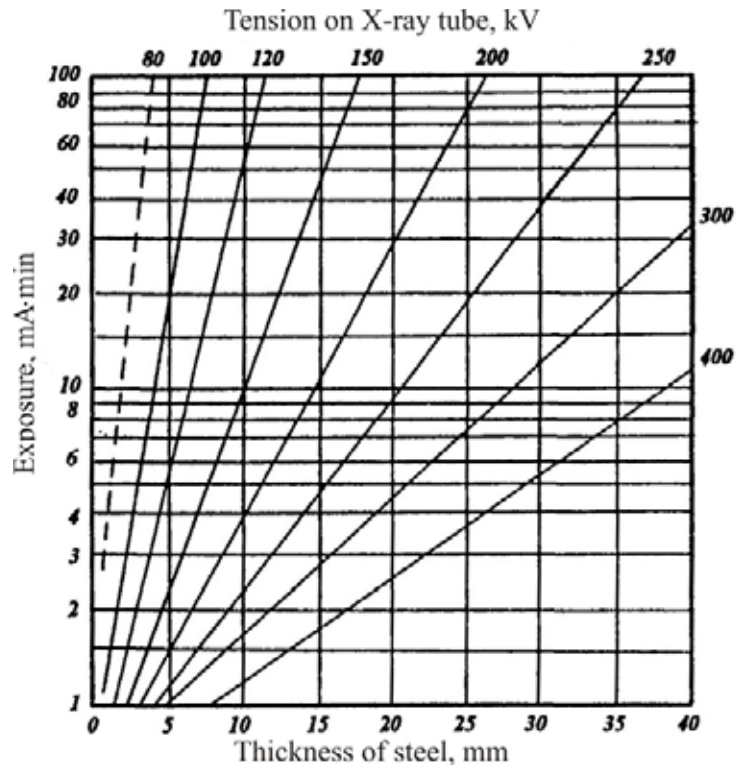


Fig. 3.12. Exposure nomogram at examining Fe- based alloys onto PT-K film at $F = 75$ cm, $S = 1.5$: drawing line – without amplifying screens, the rest –with screens from lead foil, $d = 0,05$ mm

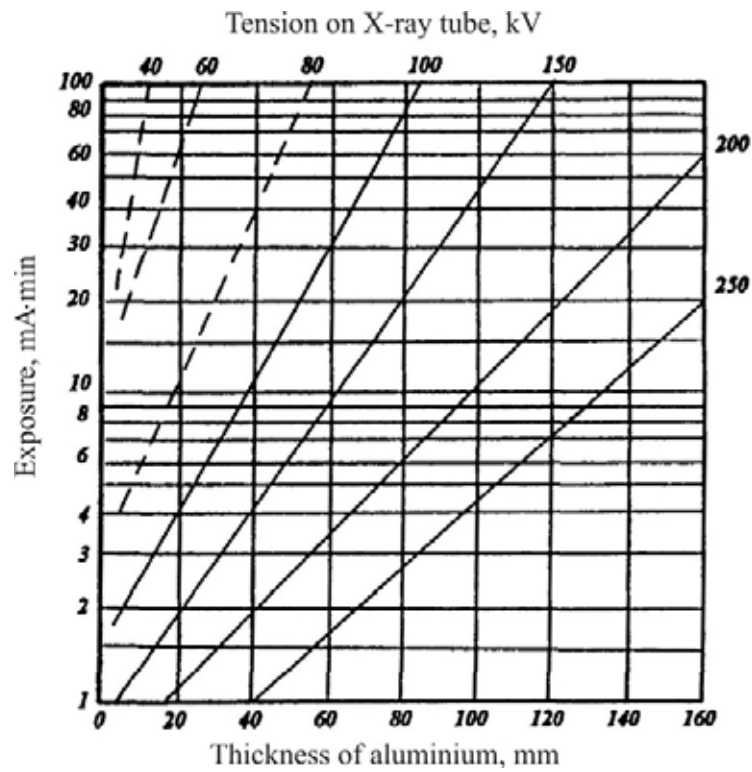


Fig. 3.13. The same for Al-based alloys

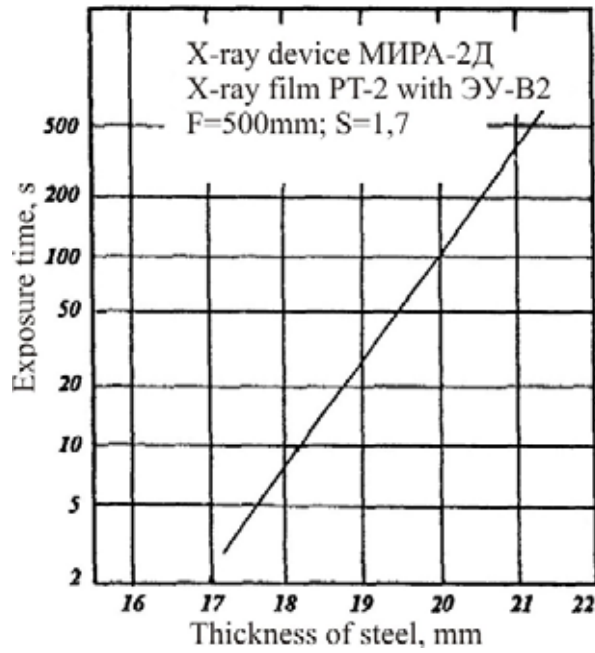


Fig. 3.14. Nomogram for Fe-based alloys at examining by pulsed X-ray device MIRA – 2D

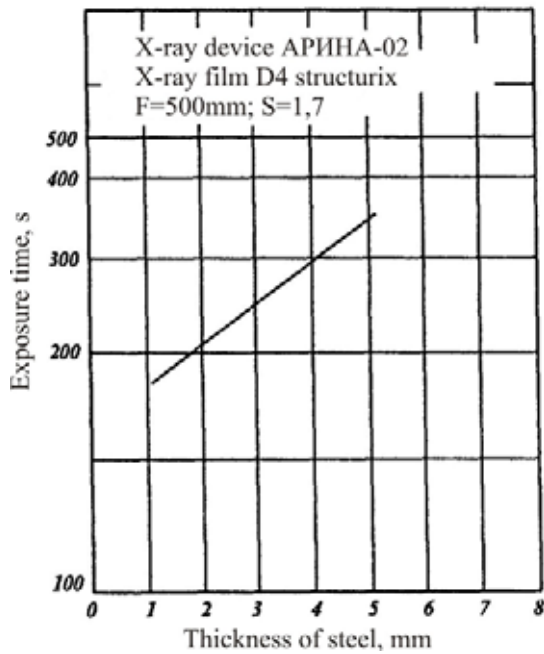


Fig. 3.15. The same at using the ARINA – 02 device

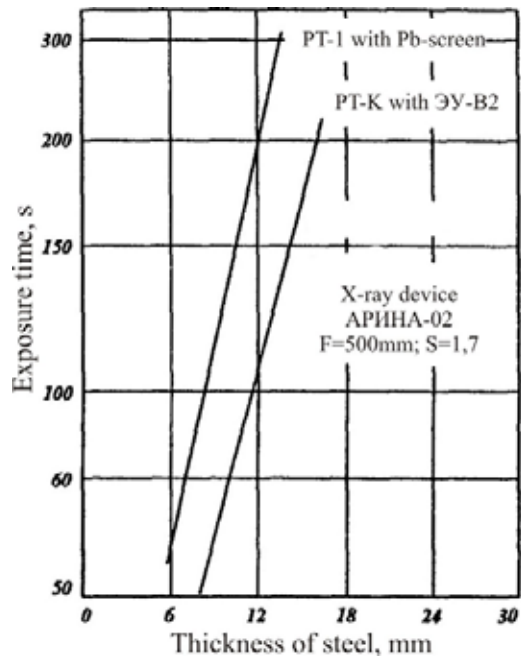


Fig. 3.16. The same, at examining Fe-based alloys by ARINA – 02

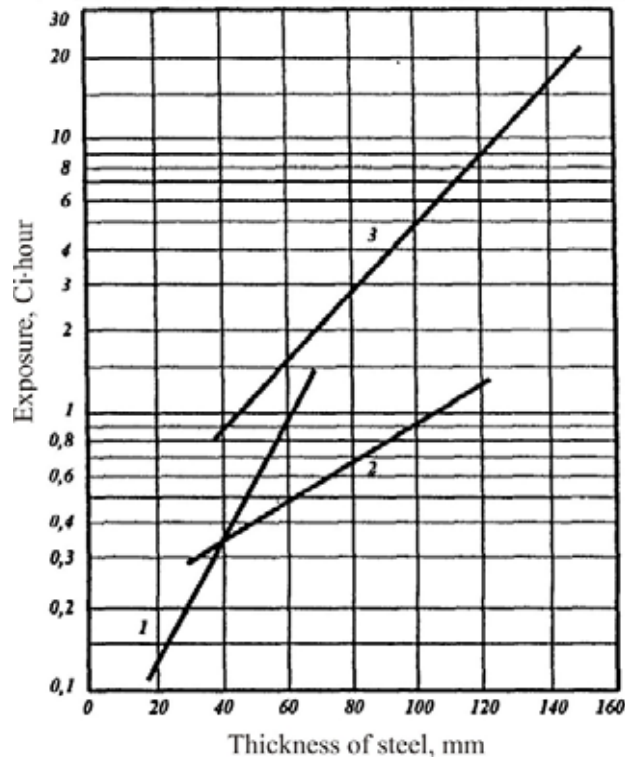


Fig. 3.17. Nomogram for finding the exposure for Fe-based alloys at using the PT-1 film ($F = 50$ cm, $S = 1.5$) at examining by gamma-radiation of radionuclides: 1 - ^{192}Ir , lead-foil with thickness 0.1 / 0.2 mm; 2 - ^{137}Cs , lead-foil with thickness 0.1 / 0.2 mm; 3 - ^{60}Co , lead-foil with thickness 0.2 / 0.2 mm

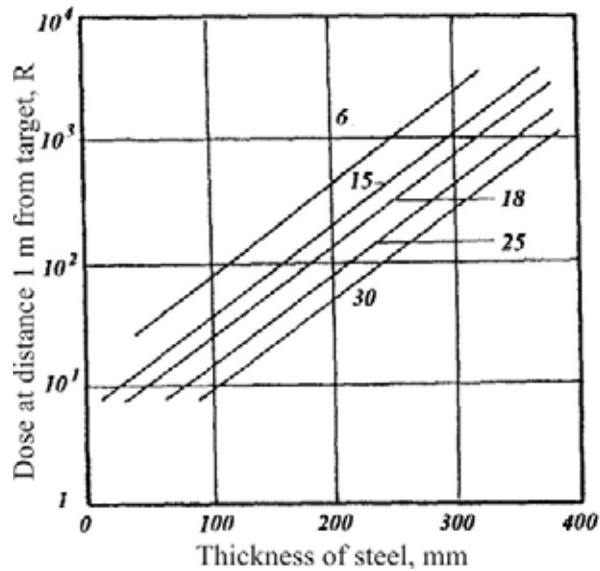


Fig. 3.18. Nomogram for finding exposures of Fe-based alloys examining at applying the bremsstrahlung radiation of betatrons with energy 6...30 MeV onto the PT-2 film with lead amplifying screens ($F = 2$ m, optical density of shots $S = 1.7$)

1. Correction for material of object.

The equivalent thickness of material under examining but not given in nomograms above, is found for the effective energy of radiation by recommendations given in section 2.4 for X-rays and bremsstrahlung radiation and for gamma-sources.

2. Correction for type of X-ray film and amplifying screens.

If we use the X-ray film differed from films listed in nomograms then we must use the transfer factors k received from Table__ and characterized the radiation sensitivity for different types of films:

$$t = t_0 (k / k_0), \quad (3.12)$$

where t_0 is exposure time taken from nomographs for given type of film and given variant of the cassette loading; k_0 is transfer factor, estimated from Table 3.21 for given type of film and variant of loading, i. e. in the same conditions as for t_0 ; k is transfer factor for film and variant of loading, for which t is estimated.

Table 3.21

Factor k of examining time transfer from PT-1 film to other ones

Variant of loading	PT -1	PT -2	PT – CIII	PT – 4M	PT -K
Without amplifying screens	1	1.7	2.5	5	8.4
With metal amplifying. screens at voltage over 100 kV	0.5	0.8	1.25	2.5	4.2
With luminescent screens at voltage 80 kV and exposure time 100 s	0.5...0.22	0.04...0.015	1.25...0.5	2.5...1.1	4.2...1.8

3. Correction of focus distance

If exposure regimes use focus distances differ from regimes listed on the nomographs given in figures mentioned above, one can find approximately the needed examining time as

$$t = t_0 (F^2 / F_0^2), \quad (3.13)$$

where t_0 is time at focus distance F_0 , found from nomogram; t is examining time at chosen focus distance F .

4. Correction on anode tension on X-ray tube

If the exposure regime differs from regimes listed in nomographs given above, the needed exposure time may be found approximately as

$$t = t_0 (V^2 / V_0^2), \quad (3.14)$$

where t is exposure time at chosen anode tension V ; t_0 is exposure time at anode tension V_0 , found in nomogram.

5. Correction on optical density of shot.

At exposure regimes with optical density differed from given in nomograms, the needed exposure time one can find approximately from relationship:

$$\lg t / t_0 = (S - S_0) / \gamma, \quad (3.15)$$

where t is time at chosen optical density S of shot; t_0 is time at optical density S_0 , found in nomogram; γ is coefficient of contrast of the X-ray film applied.

In Europe, the exposure at irradiation by X-ray devices of continuous action the objects on Fe-based alloys is determined with the help of nomograms similar to given in Fig. 3.19 for Structurix D7 film manufactured by the firm Agfa-Gevert.

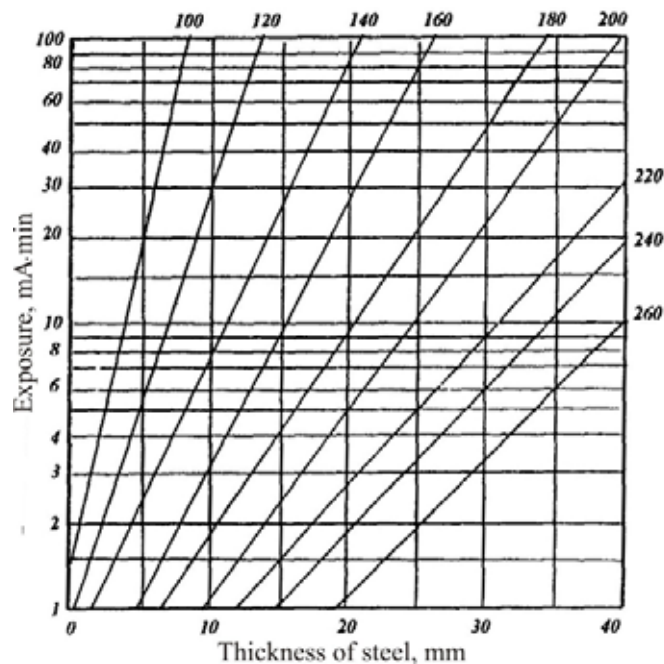


Fig. 3.19. Nomogram of exposures at examining steel-based alloys on the "Structurix D7" film with lead amplifying screens ($F=100$ cm, $s=2.0$)

If necessary, the corrections for exposure time are calculated and put into operation of checking. In particular, at transfer toward other types of films one ought to use the relative exposure factors, given in Table 3.22 below.

Table 3.22

Relative exposure factors for Structurix films

Type of film	100 kV	200 kV	192-Ir	60-Co	Linear 6-MeV accelerator
D2	10.6	8.7	9.0	10.0	10.0
D3	4.1	4.2	5.0	5.1	5.1
D4	3.1	2.6	3.0	3.1	3.1
D5	1.8	1.6	1.5	1.5	1.5
D7	1.0	1.0	1.0	1.0	1.0
D8	0.7	0.7	0.7	0.7	0.7

In the USA the approved methods of exposure time estimation are practically the same as the above described ones.

**3.2.10. Chemical – photographic development
of exposed X-ray film and its storage**

Usually the exposure time takes several minutes. After exposure the film is the subject to treatment including developing, fast washing in water, stoppage, second washing, final washing in fresh water, drying of shot... The treatment ought to be done in dark laboratory room or under red non-actinic light; at this the light source must be placed far than 50 centimeters from the film and its time of influence on film must not be over 6 minutes.

Being the determinant factor for a high quality testing, the film developing process must be kept carefully, subsequently, in different photo baths and met strictly all the rules and requirements, including those concerning the way of preparing the developer and fixing solution and their content, given in prescriptions.

The consequence of developing procedure is as follows:

1. First step. It means the developing of film in the bath with the developer of certain chemical composition in a course of certain time depended on film type and irradiation conditions.
2. Second step. Stoppage of developing process is fulfilled by bringing the film to a stop bath. Previously, the film is picked up from the first bath and washed up fast by fresh (pure) water. Then the dissolution of non-irradiated silver bromide is occurred in a fixing bath. At this, the process of silver germ formation is stopped fully.
3. Washing out of chemicals still remaining in photoemulsion is done in the bath with fresh water.
4. Finally, the X-ray film is picked out carefully from last bath and then is dried under the clear air or under fan for 1 to (3...4) hours.

The reducing of the time of automated developing is possible at using the special developers on base of Phenidone which allow to develop films in 1.5 – 2 min at increased temperature of developer. If hard water was used for preparation the developer, one ought to smooth water by boiling it or by adding in water the special smoother Trilon B with concentration in 2 gram/1 liter. One liter of developer allows to develop up to 1 m² of X-ray film. For further holding (maintenance) the action of developer, one ought to add the special restorer into solution. In order to prevent the deformation of emulsion layers, it is recommended to apply the sour fixing substance or apply the fixing matter on base of Hyposulphide, Ammoniumchlorine and Natrium metabesulphitewith adding Chromokalium alum. The just prepared developer has abnormal fog capacity, so it is permitted to use fresh developer only after passing 12 hours behind the time of preparation.

The developing is ought to do in special tank with vertical disposition of film fixed with the help of the frames. At developing, the film must be 2 – 3 times shaken sharply in order to separate the adhered air bubbles from the surface of film. The horisontal developing in a cuvette is permitted in a case when the working volume is within several tens of shots in a working shift. At this, cuvette must be rocked slightly from time to time in order to prevent the film from non-uniform developing and from sticking of films one an-other.

The developing time depends on the exhaustion and temperature of developer (see Table 3.23). The allowed range of temperatures of solutions used are given in references of development regimes.

Table 3.23

*Developing time (in rel. units) of X-ray film
in dependence on temperature and exhaustion of developer*

State of developer	Temperature of developer, °C						
	18	19	20	21	22	23	24
Fresh	1.0	0.94	0.88	0.81	0.75	0.69	0.63
Exhaust at developing of 1 m ² of film in 1 liter	1.4	1.3	1.2	1.15	1.10	1.05	1.0

In order to prevent the washing out of silver from the film before its final washing, the film must be previously washed in tank with non-running slightly sour water (2 gram of hard acetic acid (vinegar) in 1 liter of water).

At working with X-ray film, it is necessary to keep the rules of it safe storage. X-ray film evolves toxic gases at burning. X-ray films, in accordance with the “Technical conditions” of manufacturer, one ought to store on the shelves in rooms having ventilation, at certain temperature and relative humidity of air and at certain distance from heating devices and floor. X-ray

film must be prevented also from the action of direct sunlight and gases harmful for film, e.g. Hydrogen sulphide, Acetylene, Ammonia and so on. One can't store films in rooms where the presence of radioactive substances is possible or presence of light compounds of continuous action. At drying, the films ought to hang up.

At large volume of working and the necessity of reducing the treatment time of exposed film, it is recommended to dry film in special drying board having heaters, fans and filters for air cleaning. The development process in total may be automated at large volume of daily work.

Wrong operation with films and possible mistakes or errors can cause the occurring of film defects which made the interpreting of shots more difficult and, sometimes, even impossible. The most often defects occurred are haze, light and dark spots, scratches, signs of fingers, flows etc.

The interpreted shots are stored as a document of testing in a time determined by the purpose and exploitation conditions of the article tested. If the time is over, films may be utilized.

3.2.11. Interpreting of shots and rejection of joints, patterns and articles

The estimation of the quality and rejection of testing objects as results of X-ray shots analysis must be done in strong accordance with the acting technical conditions for manufacturing concrete details, units and articles.

Before interpreting one ought to estimate the quality of shots from the point of view of detection the defects caused by wrong chemical – photographic development. Then the optical density of shot is estimated which must be not less than 1.5. After this, one ought to check on shot the revelation of the sensitivity indicator's elements which guarantee the revelation of non-permitted defects, and check on shot the presence of images of marking sights (e.g. ordinal number of shot or section, pointer of examining direction, etc). If given conditions weren't performed, the shots can't be taken for interpreting. So, in this case the exposure procedure must be repeated once more time.

The conclusion is made as the result of interpreting of shots, which are interpreted in dry state with the help of negatoscope. If necessary, the fourth-multiple magnifying glass is used. At measuring the images of defects having sizes up to 1.5 mm, one ought to use the magnifying glass, and at measuring defects having sizes more than 1.5 mm one ought to use the transparent measuring ruler.

At interpreting, the shot must not contain defects of film such as scratches etc and defects occurred due to wrong development (haze, light sections caused by splashes of fixing substance on to the dry surface of film, bubbles of air stuck on the film at development, signs of fingers, dark

sections caused by lighting the non-exposed film, sights of electric discharges due to friction of film, flows etc).

The value of the optical density is estimated by means of densitometers or by visual comparison with shots having fields with measured optical densities in the range of interest.

At analysis the radiographic films, one ought to account the kinds and types of defects. All of defects which increase the path (length) of radiation in testing material (e.g. splashes of metal on surface of the article, sparks of metal etc) or represent the inclusions of materials with stronger weakening factor than the bulk material (e.g. tungsten inclusions inside steel welded joints) are revealed as a light areas which are projections of defects along the exposure direction onto the plane of X-ray film.

All of defects which reduce the path of radiation in testing media (e.g. incompleteness of any kinds such as cracks, faulty fusion (lack of fusion), gas pores etc.) or represent the inclusions with lower weakening factor than it of bulk material (e.g. inclusions from slag and so on) are revealed on shots as dark areas. So, for example, the cracks are revealed as dark thin sometimes branched winding lines. Faulty fusions are revealed as right dark lines and pores are revealed as dark spots of circular form; slag inclusions –as spots and points of irregular form and so on.

The problem of high complication is the revelation of damages caused by the tiredness, especially revelation of cracks. Best revelation is provided in a case when the plane of metal break coincides with the exposure direction within the angle not more than 5° . At this, the width of the crack must be, at any case, not less than several tens of micrometers if ever the thin thickness (less than 20 mm of steel) is exposed. The depth of crack must be about 2 ... 10 % of object thickness.

The cracks which are under the action of compressing loads can't be revealed at exposure by X-rays. In order to increase the sensitivity and revelation of cracks inside the units and elements of constructions, one needs some times to form the stretching tension providing the uncovering (opening) of cracks with the help of lifting jack, surplus pressure etc. The cracks filled with oil or other contaminations are revealed badly at X-ray exposure. The schemes of loading and loading values, in this case, must be defined by designers of the articles.

At the process of organization and assimilation of experience in the radiation defectoscopic testing, the independent industrial directions (instructions) or technological recommendations must be designed which takes into account the peculiarity of testing procedure for concrete articles, characteristics of sources applied, the optimal schemes and regimes of exposure.

3.3. Control tasks

1. Calculate the focal distance F at exposing the object with the thickness 25 mm by means of the roentgen radiation at tension 250 kV on the tube. The focus size is 5 mm, the film has fine-grained structure with $U_c=0.06$ mm. The distance from the defect to the film $b = 1$ mm.
2. The welded joint is exposed by means of the roentgen apparatus PYII-200-205 at the focal distance 75 cm. The steel article has the wall thickness 17 mm and the joint amplification 4 mm. The shooting is made on the PT-1 film with two tin-lead foils with thickness 0.05 mm. Determine the exposure time t (min).
3. For the same welded joint determine the exposure time (task 2) at the same testing conditions but on the PT-3 film with the metal amplifying screens.
4. The exposure time for testing the aluminum cast with the thickness 100 mm at the roentgen tube tension 100 kV and anode current 5 mA on the PT-1 film with the metal amplifying screens is 4 min at the focal distance 75 cm. Determine the exposure time for the same cast and the same other conditions, if only the focal distance is now 100 cm.
5. The cast from aluminum alloy with thickness 40 mm is exposed at the angle 45° . Determine the thickness of metal for which the exposure time would be calculated by means of the exposure nomogrammes.
6. It is necessary to fulfil the exposure of the assembly made from copper with thickness 10 mm by means of the apparatus PYII-200-205 on the PT-1 film at the focal distance 75 cm. Determine the exposure conditions.
7. Determine for the aluminum detail with the thickness 20 mm the exposure time for gamma-radiation of Tm^{170} at the focal distance 50 cm. The PT-1 film is disposed between two lead foils with thickness 0.05/0.05 mm. The exposure dose rate of the source is, for time of exposure, $1 \cdot 10^{-4}$ R/s at distance 1 meter.
8. Determine the exposure time if the steel article with the thickness 70 mm is exposed by the gamma-radiation of the Co^{60} at the focal distance 100 cm on the PT-1 film, disposed between two lead foils with thickness 0.2/0.2 mm. The exposure dose rate of the source is $2 \cdot 10^{-3}$ R/s at distance 1 meter.
9. Determine the exposure time t if the steel article with the thickness 70 mm is exposed by the gamma-radiation of the Co^{60} on the PT-2 film disposed between lead foils 0.2/0.2 mm. The exposure dose rate is $P = 2 \cdot 10^{-3}$ R/s at distance 1 meter, the focal distance $F = 85$ cm, and 1 year has passed from the moment for which the exposure dose rate was shown in the source passport and the moment of the exposure.

10. At the same conditions as in the task № 9, determine the article exposure time if the focal distance is 50 cm.
11. Determine the exposure time for the copper article with the thickness 70 mm and the PT-2 film disposed between lead foils with thickness 0.2/0.2 mm, if focal distance $F = 50$ cm and the radiation source is the Co^{60} .
12. Determine the exposure time t if the steel article with the thickness 45 mm and the joint amplification 5 mm is exposed by the gamma-radiation of the Cs^{137} on the PT-2 film disposed between lead foils with thickness 0.2/0.2 mm. The exposure dose rate at the moment of the passport composing was $2.2 \cdot 10^{-3}$ R/s at distance 1 meter. The focal distance is $F=50$ cm. The time passed from the moment for which the source gamma-equivalent was shown in the passport to the moment of exposure, is 5 years.
13. The radiographs of one and the same testing object are made constantly (regularly) during two years by one and the same source with radionuclide Co^{60} . How much should the exposure time be increased at the end of the above-mentioned period in comparison with the beginning if all other conditions of the radiograph receiving are conserved? It is known that Co^{60} has the half-decay period of 5.3 years.
14. The source of the base of Ir^{192} with the half-decay time of 75 days provides for the present moment the optimal exposure of the testing object during 20 min. What time of the exposure would be needed after 5 months for receiving the radiograph with the same optical density and at conserving the other testing conditions?
15. The qualitative shot of the steel housing with the thickness 8 cm is received with the exposure 10 min at the distance 100 cm between the film and the radiation source (radionuclide Co^{60}). What time would be needed for receiving the radiograph if the distance between the film and the source will decrease up to 60 cm and if the other conditions are conserved?
16. The apparatus with the accelerating tension 1 MeV and the current 3 mA and with using the lead screen of 0.25 mm thickness was taken for receiving the radiograph of the testing object from the 8 mm – thickness steel. At this, the distance between the source and the film was 120 cm, the optical density was 1.5 and the exposure time was 2 min. The similar radiograph is received at shooting under the same conditions of the steel sample with thickness 15 cm in 100 min. What time of exposure would be needed at shooting the testing object from steel with the thickness 11.5 cm if the other testing conditions are conserved?
17. The radiographic shot having the exposure 12 mA·min allows to achieve the optical density of darkening 0.8. It is desirable to increase the darkening density to the meaning 2.0. At the study the characteristic curve of the given film it was detected that the difference of the **logE** meanings

corresponding to points 0.8 and 2.0 on the axis of densities will be equal to 0.76. The antilogarithm 0.76 corresponds to the value 5.8. What would be the new exposure sufficient to achieve the needed darkening density 2.0?

3.4. SET OF TEST QUATIONS ON SECTION "RADIOGRAPHY"

1. What is a purpose of using diaphragms, collimators, filters in radiography?
 - A decrease of influence of scattering radiation;
 - B for changing the energy spectrum of radiation;
 - C for providing the better uniformity of the radiation action within total surface of X-ray film;
 - D to compensate the sharp difference of radiation thickness of different parts of the object test.
2. The low-tension X-ray tubes are provided usually with the output window made from. Explain the cause of such a choice:
 - A glass;
 - B plastic material;
 - C beryllium.
3. General principle of generation the X-rays consists in the sharp deceleration of electrons moved with high velocity in solid matter which was called:
 - A target;
 - B focusing electrode;
 - C heater;
 - D cathode.
4. If one needs to get the shot of the object made from steel and having the thickness 17 cm, which of radionuclidic sources of gamma-radiation one ought to use?
 - A Iridium-192;
 - B Thulium-170;
 - C Caesium-137;
 - D Cobalt-60.
5. The linear weakening factor and the degree of radiation absorption depend, at passing of the radiation through the layer of matter, on:
 - A atomic number, source energy and depend not on the thickness of layer;
 - B layer thickness, atomic number and value of specific activity of source's material;
 - C layer thickness and value of accumulation factor;
 - D atomic number, layer thickness and energy of radiation source;
 - E thickness, atomic number and depend not on the radiation energy.

6. The Ir-192 source with the half-decay period 75 days provides now the optimal exposure of the object at 20 min. Which exposure time will be needed 5 months later for getting the shot with the same optical density and at the constancy of other exposure conditions?

- A 20 min;
- B 40 min;
- C 60 min;
- D 1 hour 20 min;
- E 6 hours.

7. The effective focus (focal) spot of the X-ray tube:

- A is sloped at the angle about 30° related to the tube axis;
- B must be as small as possible and, at this, must not cause the reduce of the exploitation time of the tube;
- C it holds high negative potential at the tube at total time of its operation.

8. The sensitometric factor which is equal to tangent of the slope of the rectilinear part of the characteristic curve of X-ray films, is called:

- A sensitivity of the film for radiation (number of sensitivity);
- B gradient for films without screens;
- C contrast coefficient for films without screen;
- D contrast coefficient for films with screen.

9. The thin sheets of the foil from lead, disposed closely with the X-ray film at the exposure moment, increase the blackening density due to:

- A they emit the visual light due to the fluorescence;
- B at process of the exposure by photon radiation, they emit electrons which help to sensitizate the film;
- C they absorb the scattering radiation;
- D they prevent to haze the film by back scattering radiation.

10. The acceleration tension on X-ray tube influences on;

- A simultaneously on the energy and intensity of radiation;
- B it influences not either energy or intensity of radiation;
- C on energy of photon's radiation;
- D on the intensity of radiation.

11. Geometrical unsharpness of the shot:
- A** is directly proportional to the distance between the object and film and spot;
 - B** is inversely proportional to the distance between the object and film and proportional to source – object distance;
 - C** directly proportional to size of the focus spot and inversely proportional to source – object distance;
 - D** inversely proportional to the focus spot size and object – film distance.
12. X-ray films having large size of the emulsion germ (grain):
- A** give shots with better resolution than films with small-size germs;
 - B** have higher sensitivity than films with relatively small germ;
 - C** have less sensitivity than films with relatively small germ;
 - D** will need in longer exposure time for getting the qualitative shot than films with the relatively small germ.
13. Which of materials is used most often for producing the target of the X-ray tube:
- A** Copper;
 - B** Carbon;
 - C** Tungsten;
 - D** Berillium.
14. Usually, the quality of the radionuclidic image is estimated best of all with the help of:
- A** reading the density value by the densitometer;
 - B** using the standards of sensitivity;
 - C** measuring the zone of non-uniformity of the screen.
15. The main demand concerning the best geometry of the image forming is:
- A** X-ray radiation must be emitted by the focus spot of such a large size as it is allowed by the rest conditions of the exposure;
 - B** the central beam of radiation must coincide possible with the perpendicular to the film surface;
 - C** the source-object distance must be possibly small;
 - D** the film must be placed as far from the object as possible.
16. The cassette with X-ray film has usually the thin sheet of lead set from back side but not in contact with the film. What is the purpose of such a sheet?
- A** to defend the film from the back scattering;
 - B** to increase the brightness of the screen;
 - C** not “A”, not “B”;
 - D** “A” and “B”.

17. Water is the solvent in the developer. It must be:
- A** distilled;
 - B** soft;
 - C** hard;
 - D** of “drinking quality”.
18. Which from the listed lower operations are fulfilled firstly at interpreting the radiographic shots?
- A** estimation of the correctness of the testing conditions and regimes;
 - B** revelation of the articles without any defects;
 - C** rejection of the articles;
 - D** revelation of defects in accordance with technical demands, testing rules and standards.
19. The penetrating capacity of X-ray radiation is determined by:
- A** time;
 - B** current power of the tube;
 - C** source- object distance;
 - D** tension on X-ray tube or by the wave length.
20. The thickness of the half-absorption layer for Cobalt-60 radiation in steel is 2.54 cm. If the exposure dose power on the surface of the steel plate from the source side is 64 R/hour, which will be the exposure dose power on the back side of the plate having thickness 7.56 cm?
- A** 3 R/hour;
 - B** 8 R/hour;
 - C** 10 R/hour;
 - D** 13 R/hour.
21. At distance 1.22 m between the source and the film one needs in exposure time 60 s for getting the X-ray shot. Which exposure time will be needed for receiving the equivalent optical density of the shot if the source- film distance was increased up to 1.53 m?
- A** 38 s;
 - B** 48 s;
 - C** 75 s;
 - D** 94 s.

Chapter 4 RADIATION INTROSCOPY (RADIOSCOPY)

4.1. Introduction

Very often the non-destructive testing meets the problems when it is necessary to get the information about the inner structure of the object tested directly at moment of the defect appearance. Usually, the problems of such a kind are connected with the large-scale serial production (e.g. produce of rolled metal, pipe production, etc.)

The necessity of dynamic analysis of the real picture (shot) of the object is appeared also in cases when it is necessary to provide the active influence from the side of operator onto the technological process of manufacturing namely at given moment of procedure. So, the method of radiation introscopy is applied most often for these purposes.

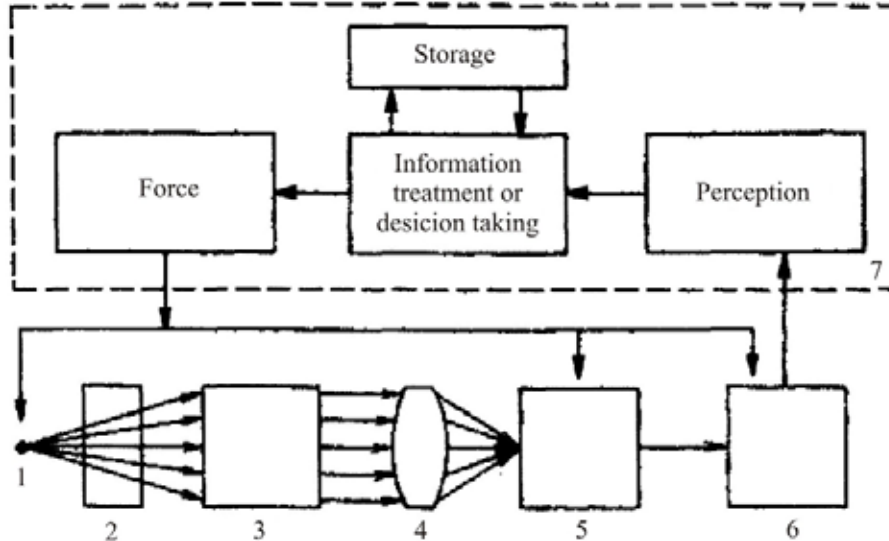


*Fig. 4.1. General block- scheme and base elements of radiation introscopy:
1 – radiation source; 2 – tested object; 3 – input screen;
4 – optical device (objective); 5 – sensitive gage (receiver); 6 – unit of treatment
and indication of signal; 7 – unit of treatment the information by operator*

For example, the insertion of the introscope into the system of welding the thick-walled steel courses allows us to detect the formation of gas pores at moment of welding and then to estimate the sizes of those pores or defects of other kind.

The radiation introscopy is based on the irradiation of the testing object by the penetrating radiation and then on the conversion (transformation) of hidden (latent) radiation image of the object into visual light-shadow or electronic image and then on transfer (transmission) of those images through distance with help of the optical facility or TV-receiver. At this, it is foreseen the active participation of an operator in procedure of analysis the light-shadow image of internal structure of the object directly during the time of checking.

Main elements of general scheme of radiation introscopy are the facility of introscope of certain design and, of course, the operator.

Functions of base elements:

1 – source irradiates the penetrating radiation with certain kind, energy and intensity; 2 – aim of testing with certain size (thickness), density, etc; 3 – input screen converts the latent radiation image into the visual light-shadow image; 4 – optical facility transmitted the information from the input screen; 5 – receiver (sensitive element) converts the light radiation into the consequence of electric signals; 6 – treats signal by amplifying, discrimination, normalization, indication and so on.

The output light signal from the converter of radiation is transferred toward the receiver through the optical device; at this the receiver makes the necessary operations with the converter's signal in order to meet signals in accordance with the type of treatment device.

Role of operator: getting of running information and its analysis; compose of general conclusion concerning the inner structure of object At this, the operator chooses and changes, if necessary, regimes of source, receiver and videomonitor operation.

The distinction between the radiography and radioscopy consists, obviously, in the fact that radiography has limitations connected with the time losses needed for roentgenographs development and interpreting (analysis). On contrary to this, radioscopy is the method of express testing because the received light-shadow image is under the analysis in the moment of testing and the operator has the possibility for executive actions (commends), changing the separate elements of procedure if needs.

In practice of radioscopy, one can distinct two different ways of conversion:

- 1) method of direct transformation of hidden (latent) radiation image into the light-shadow one:
- 2) methods of cascade transformation the latent radiation image of testing object into light-shadow one with the immediate optical transfer of visual information to operator and distant transfer with the help of TV-systems.

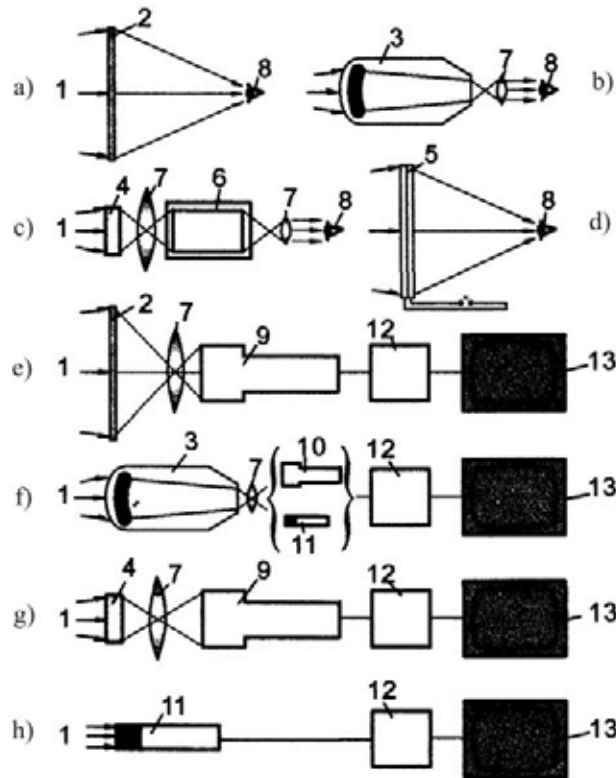


Fig. 4.2. General systems of radiation introsopes with direct watching of images (a – d) and with using the TV-systems (e – h):

- 1 – X-ray or gamma-radiation; 2 – fluoroscope screen; 3 – electron-optical converter; 4 – scintillation crystal; 5 – electro luminescent screen; 6 – electron-optical amplifier; 7 – optics; 8 – operator’s eye; 9 – superorthicon; 10 – vidicon; 11 – X-ray vidicon; 12 – TV-channel; 13 – TV-receiver

All of methods of the radioscopy apply, at their operation, four general physical phenomenons:

1. Interaction of different kinds of penetrating radiation with the matter.
2. Luminescence (fluorescence) of matter being under the action of ionizing radiation.
3. Photoeffect (internal and external) under the action of radiation or under the action of luminescence caused by radiation.
4. Secondary electron emission at conversion the photoelectron’s beams into the electric signal and at the following reproduction of visual image within the TV-systems.

The luminescence principle is the base of fluorescent screen action as well as the action of scintillation crystals and luminophors applied in the constructions of the electron-optical converters, electron-optical amplifiers and receiving TV-tubes (kinescopes).

The photoeffect phenomenon is using in the constructions of roentgenovidicones, transmitting TV-tubes (vidicones, superorticones, isocones), in electron-optical amplifiers and roentgen electron-optical converters.

The phenomenon of the secondary electron emission is used in the constructions and actions of transmitting TV-tubes and amplifiers.

The sources of radiation for radiation introscopy: most of all, the X-ray apparatus are used for the radioscopy of industrial articles and materials; different types of accelerators and gamma- and neutron sources with high activities are used within certain limits. The neutron defectoscopy has deal also with the usage of nuclear reactors having the channel of thermal neutrons withdrawal or usage of neutron generators.

The radiation introscopy maintains such the advantages of radiographs as the possibility of determination the character and shapes of the object revealed and, at this, allows getting the image of inner state of the object immediately at moment of examination. The low inertia of converting the radiation image allows to review of the object at different angles relatively the exposure direction. That leads to increase of the defect revelation probability inside object. Besides, it become possible to check the quality of articles without their disassembling and under conditions closed to exploitation ones (presence of vibration, temperature and pressure fluctuations, etc.). Another advantage of radioscopy is the possibility of wide spread of the stereoscopy principles in order to reveal the space distributions of defects inside the object. By using two sources of radiation placed at certain basic distance, one can get the stereo image of the object at moment of examining.

Disadvantages of radiation introscopy methods

1. First, but the disadvantage of most importance of introscopy in comparison with the radiography is need in application of the photographing from the screen of videomonitor if one needs in getting document, which reduces the image quality and worker the defectoscopic sensitivity of the method.
2. Secondly, radioscopy needs in higher dose of radiation absorbed by the object at time of testing, because at radioscopy in order to receive the image of the same quality as in radiography, the higher dose power is necessary. It occurs due to that fact that at film exposure the collecting of the information and formation of only the single shot (sequence, still) has place at total time of exposure. Contrary to this, in radioscopy at time of visual analysis of the shadow image, one must form the large number of sequences (shots) and all of those shots must have high enough quality, i. e. must be formed at high dose power of irradiation at surface of the converter in very short exposure time, namely – in time of single TV – sequence (shot) equal approximately 0.04 second.
3. Third disadvantage: at using the geometry of the broad beam at exposure, the quality of image is dependent, within one or another

degree, on the accumulation factor of scattering radiation which makes worse the defectoscopic sensitivity.

The method of direct transformation of the latent radiation image into the light-shadow image is called “the fluoroscopy” since here the fluoroscopic (fluorescence) screen is used as the radiation-optical converter.

Different methods of the cascade conversion are called “the radiography in real time”, “the forming of images in real time scale”. At this case, the industrial amplifiers of radiation image are applied as the radiation-optical converters, i. e. facilities inside which the radiation-optical transformation occurs due to the additional sources of energy connected not with ionizing radiation and the amplification factor of the brightness is more than 1. At this, the brightness amplification factor is the relation of the value of brightness of output screen of radiation electron-optical converter (REOC) over the value of brightness of the standard fluorescent screen at the same given conditions of irradiation the input plate of the converter and fluorescent screen.

So, the main advantage of radioscopy is that the light image on the screen becomes qualitative enough as soon as the density of the energy flow of quanta of radiation image will get the certain value. The characteristics of radiation and radiation electron-optical converters such as density of the flow of quanta’s energy, spectrum, amplification factor of radiation image amplifier of the REOC, factor of contrast transfer and so on, one can change directly at analysis process. So, it becomes possible to achieve the best quality of image even at lack of knowledge of optimal parameters of the introscope and without any calculations.

At process of the analysis of receiving image, the operator can increase the geometrical sizes of image by shifting the object toward the radiation source, or can turn the object and shift it for selection the optimal angle of the radiation fall onto the object.

If the object has non-uniform density or thickness, one can use the moving (mobile) filters for local reducing the density of the radiation energy flow interacted with the REOC. Such a way allows to analyze better the separate details of the visual picture.

The irradiation may be fulfilled at two steps: firstly, the object is irradiated by long-wave photons (i. e. low energy photons). It permits to study the areas of object with weak absorption and later, at the second step, to increase the energy of photons and search the areas with higher absorption. At present time, three different schemes of examining and organization the collection of information are mainly used: scheme with the broad beam; scheme with the beam of fan type; scheme with the beam of needle type.

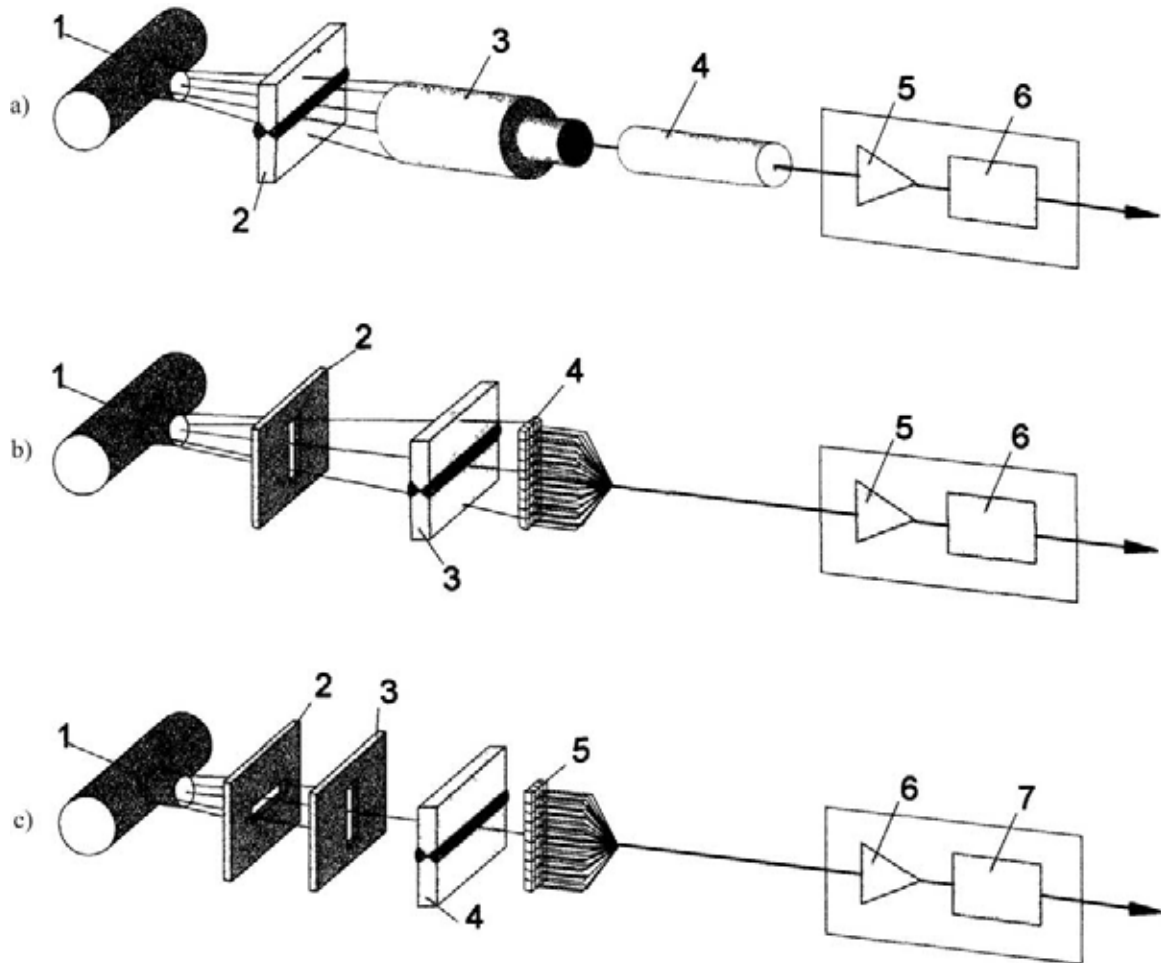


Fig. 4.3. Basic schemes of examining the testing object by means of using the different beams of penetrating radiation:

a – fan-type; b – board beam; c – needle type

1 – source of radiation; 2 – testing object; 3 – X-ray EOC;

4 – transmitting TV-tube; 5 – intensifier;

6 – analog-to-digital converter; 7 – slit-type diaphragm;

8 – linear matrix of detectors; 9 – mobile (traveling) diaphragm

Some advantages of the broad beam scheme:

- potential number of space elements which may be registered independently each from other and at once, is more than 10^6 ;
- roentgen-optical converter (fluorescent screens, REOC, roentgenovidicones) are connected visually and by the electric link with the TV-systems and produced by means of well known technologies;
- one can test the stationary (immovable) objects as well as the mobile ones.
- some advantages of schemes with fan- type beam:
- possibility of cutting off the scattering radiation;
- large dynamic range of the detector (more than 1: 1000) and high signal/noise ratio;

- linearity of detectors (“ruler” of linear discrete converters) may be improved significantly in comparison with the linearity of the TV-camera;
- rate of data transmitting is low enough and the data may be transformed into digital form and inserted into the memory of personnel computer or another calculating device.

Some advantages of schemes with beam of needle-type:

- possibility of receiving the microbeams with sizes equal to 1 micrometer and even less;
- possibility of registration the total number of effects of the radiation interactions with the object (for example, the additional information concerning the distribution of chemical elements through the volume of the object).

Different schemes of radioscopy may be compared by the relative sensitivity of the image transmitting systems:

1. Fluorescent screen has sensitivity in 5...6 %;
2. Fluorescent screen in couple with transmitting TV-tube (vidicone, plumbicone) – (2,8...4) %;
3. Fluorescent screen in couple with isocone – (1...3) %;
4. REOC (X-ray electron-optical converter) – (1...2) %;
5. Transmitting TV-tube (X-ray vidicone) – (1...2) %.

Dynamic range of the radiation-optical converter is the highest ratio between the densities of the energy flows on two different fields (areas) of the initial image at which one can detect simultaneously on the output images of every of those fields the objects of given size; more over, the contrast of initial image of given objects has the same value for every field of image.

Table 4.1

Radiation characteristics of introscope systems

Radiation system	Exposure dose power at plate of converter, R/s × 10 ⁻⁴	Density of flow of photons, photon/mm ² × s, × 10 ⁵
Fluoroscopic screen	40	8
X-ray-TV introscope with fluoroscopic screen	10	2
X-ray-TV introscope with X-ray electron-optical converter	1	0,2
Radiation introscope with X-ray vidicone	100	20
Radiation introscope with fan-type beam	100	20
Radiation introscope with needle beam	200	40

One can compare different systems of introscopy, if the sensitivity of the radiation converters is taken as the base of comparison. The sensitivity is characterized by the inverse value of the dose or flow of X-ray quanta sufficient for registration either the image with given density of the emulsion blackening or given volume of the information.

If one applied the broad beam system, the clearness of the image of inner structure of object is determined by the characteristics of the converter, when the object is placed close to converter. In such a system different converters are used, e.g. chains made from several REOC; X-ray vidicones; fluoroscopic screens combined with TV-systems having (512×512) – quantity of independent space elements (systems with 625 lines in the raster). At high projection magnification (object is placed far enough from converter), the limit of the resolution is defined by the final sizes of focal spot of the radiation source. At this, the resolution distance in the object can't be less than size of focus spot, i. e. – (0.1...5) mm.

If systems with fan-type beam are used, the resolution limit is defined by the size of active part of separate detector of linear matrix of detectors. It is considered that the detector's size may be reduced to 50 micrometers. This value is equivalent to resolution in 10 pairs of lines / mm.

For needle-type systems, the resolution limit depends on the diaphragm sizes. If X-ray tubes are used, the size of diaphragm is (0.5...2,0) mm; if the special systems of scanning microscopy are applied, then the diaphragm size may be (0.5...2) mm.

Resolution limits of different radiation systems, in pairs of lines / mm:

- X-ray film without amplifying screen – 10 pairs of lines / mm;
- X-ray film with screen – (2.5...5) pairs lines / mm;
- REOC – (2...6) pairs of lines / mm;
- Fluorescent screen – (2...3) pairs of lines / mm;
- X-ray –TV introscope with REOC – (1...3) pairs of lines / mm;
- introscope with X-ray vidicone – (10...25) pairs of lines / mm;
- introscope with fluorescent screen – (0.5...1) pairs of lines / mm;
- introscope with fan beam – (0.1...4) pairs of lines / mm.

4.2. Choice of radiation sources

The sources with low radiation yield are not used in radioscopy because low yield (small amount of particles) leads to worsening of the clearness of light image quality and the quality of testing in total. So, the choice of sources of ionizing radiation comes from:

- chemical compose and thickness of the object;
- characteristics of defects by the prognosis or of inner structure of the object;

- compatibility of the source characteristics with those of the radiation-optical converter, for its qualitative functioning.

As the rule, in radioscopy the X-ray apparatus with constant anode tension are applied. Apparatus of such a type provides the maximum energy loading related with the unit of square of the effective focus spot and, so, forms the detail radiation image with high signal/noise ratio.

Thus, the source must provide the highest intensity of radiation over the plate of converter and also the least geometrical unsharpness. Besides, the noise parameters of X-ray device in electromagnetic range of frequencies and their possible influence on the functioning of the electronics of X-ray image amplifiers must be taken into account. Very often the manufacturers of the introscopy systems recommend the concrete type of source or simply supply the system with the most appropriate source of radiation. The radionuclidic sources may be applied in digital systems of radiation introscopy because of their small sizes, portability and own radiation having high penetrating capacity. The relatively low intensity of such a source may be compensated at digital mode of the image treatment.

4.3. Choice of energy of radiation

Here, energy of radiation means the tension on the anode of X-ray tube, accelerator's energy and so on.

The necessary range of radiation energy is chosen in dependence on the thickness and density of the object examined. In reference tables of the introscopy applying one can find data connect the parameters of the object (kind of material, density, thickness) with the source energy. If needed material is not listed in reference table, the energy determination comes from the equivalent thickness of material, found similarly to that in radiography with help of the radiographic equivalency factor.

These methods are used in the same manner in Russia, Europe and the USA. The kind and energy of radiation are chosen in such a way that the radiation thickness of tested material will form approximately five thickness of the half-weakening layer:

$$d \sim 5 \times \Delta_{1/2}, \quad (4.1)$$

where $\Delta_{1/2} = \ln 2 / \mu = 0.693 / \mu$ – from the definition of the half-weakening layer.

Further, $d = 5 \times 0.693 / \mu \sim 3.5 / \mu$, and, so, $d \times \mu \sim 3.5$ – is the criteria for choosing the optimal energy. Usually, the permitted range of thickness available for testing by introscopy is

$$a \times \Delta_{1/2} \leq d \leq 10 \times \Delta_{1/2}, \text{ or } 1.7 < \mu \times d < 7.0. \quad (4.2)$$

It is practical criteria for choosing the energy of radiation.

Table 4.2

Sphere of radiation introscopy application

Thickness of examining material, mm				Converter at testing assembled units, articles and also		Tension on X-ray tube, kV		
Alloys on base of		Non-metals		Welded and riveted joints	Casts, soldered and riveted joints			
Fe	Ti	Al	Mg			Z=14, $\rho=1.4$	Z=6,2, $\rho=1.4$	Z=5,5 $\rho=0.9$
0.05...6	0.2...0.8	0.5...15	1...20	1...17	1...90	1...30	X-ray TV-syst. with vidicone, REOC, Fluor. screen	10...120
4...12	8...25	15...30	20...40	17...25	90...120	130...170	REOC, X-ray TV-syst. with scin. screen plus electron-optical converter	50...180
12...20	25...40	30...50	40...70	—	—	—	X-ray TV-syst. with REOC, fluor. screen or scin. screen	100...250
20...40	>40	>50	>70	—	—	—	Scintillatio screen or REOC	200...300
40...60	—	—	—	—	—	—	X-ray TV system with scintillation crystal and electron-optical amplifier of image brightness	220...400
>60	—	—	—	—	—	—		1000...35000 keV (accelerators)

4.4. Fluoroscopy

Up today, the fluoroscopy is wide spread method of radiology. This method consists in searching the images on the fluoroscopic screen of the so called fluoroscope in which the shielding of operator from the direct action of radiation is provided by the lead glass. Because of low levels of the luminescence brightness of fluoroscopic screens, the defect's revelation sensitivity is only within 2(5) ... 13 %. But this value may occur enough at revelation the rough (coarse) breaches of the technology of castings, welding and other processes.

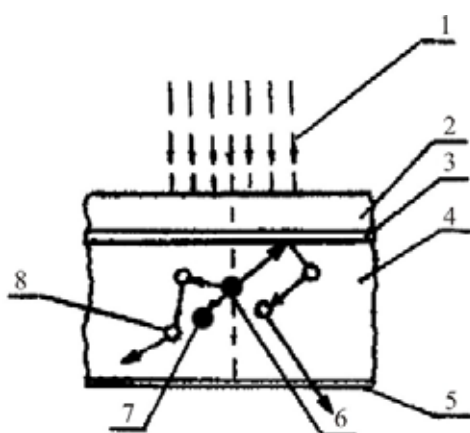


*Fig. 4.4. Scheme of luminescent screen and trajectories of light photons:
1 – X-rays; 2 – base of screens; 3 – reflecting layer; 4 – luminescent layer; 5 – protecting layer; 6 – excited crystal; 7 – absorbing crystal; 8 – light scattered crystal*

Active layer of the luminophor has usually the thickness equal to 70...280 μm ($\sim 85...120 \text{ mg/cm}^2$) and is made from particles with sizes of germs about 10 micrometers distributed in glue substance drifted onto the reflective base. Base is thin ($\sim 0.4 \text{ mm}$) plate; reflective layer is the substance such as white paint or magnesium oxide. Binding material may be transparent for the luminophor's luminescence or may have the absorbing dye for producing the light scattering. The quantity of luminophor in active layer is about 50 percent. The light yield of luminophor screen one can raise if increase its thickness or use the transparent binding layer and reflective layer but the screen resolution will be worse.

The main interaction effect at X-rays energy in about 100 keV is the photoelectric absorption of photons in material. At this, the quantitative description may be expressed through several parameters:

1. Quantum yield of screen is a fraction of X-ray photons absorbed by the screen: $Q = \text{number of photons absorbed by screen} / \text{number of photons fallen on screen}$; at this, $Q \ll 1$.
2. Quantum yield of luminescence $\eta_q = n_{\text{lum}}^\gamma / n_{\text{abs}}^\gamma$; at this, $\eta_q \gg 1$.

3. Energy yield of luminescence $\eta_{en} = W_{en} / W_{\gamma} = \eta_q \times \varepsilon_0 / E_{\gamma}$, i. e. ratio of energy effectively converted by luminophor over energy absorbed by luminophor, where ε_0 is energy of single optical photon, E_{γ} is energy of X-photon/
4. Technical yield of luminophor $\eta_{tech} = \alpha \times \eta_{en} \approx 0.5 \eta_{en}$, i. e. part of energy of optical photons which is used effectively, at this $\eta_{tech} \approx 25\%$; $\alpha \approx 0.5$ for most of screens. So, 25% is maximum value of energy yield for modern screens.

Main parameters of different types of luminophors such as density, wave length in maximum of spectral characteristics (nanometers), energy efficiency of conversion are listed in references, for example:

Name of luminophor	Density, g/cm ³	Wave length, 10 ⁻⁹ m	Energy efficiency, %
ZnS CdS – Ag	4.46	540	15...18
CaWO ₄	6.06	430	5
CsJ – Na	4.5	420	8

The spectrum of luminescence influences strongly on the functioning of introscopy systems because different receivers of light have unequal sensitivity for light with different wave length. That why the concept of “spectrum conformity” is used. Generally, the luminophor’s efficiency and screen efficiency may be presented as the produce:

$$\Pi_{lum} = \alpha \times Q \times \eta_{en} \times \kappa. \quad (4.3)$$

The contrast coefficient of the luminescent screen is the relative increment of brightness of light image of the screen over the relative increment of intensity of radiation image:

$$\gamma = (\Delta B/B) / (\Delta \varphi/\varphi). \quad (4.4)$$

For most of screens $\gamma = 1$ at E_{γ} used in radiology. If the radiation scattered by the object is not in account, the contrast of the radiation image $\Delta \varphi/\varphi = \mu \times \Delta x$, where Δx is size of defect. The threshold value of the relative increment of brightness perceptible by human eye, for screen’s brightness in $(3 \cdot 10^{-3} - 3) \text{ cd/m}^2$ is expressed as

$$100 \cdot \Delta B/B = 1.6 \cdot B^{-0.38}.$$

So, the relative sensitivity at the fluoroscopy can’t be better than

$$\kappa (\%) \geq 100 \cdot \Delta x/x = 1.6 \times (\mu \cdot x \cdot B^{0.38}). \quad (4.5)$$

The influence of scattered radiation is strong at close disposition of object and screen and the influence reduces at increase of geometrical magnification at raising the distance between the object and screen. The optimal geometrical magnification:

$$M_{\text{opt}} = 1 + (U_{\text{screen}} / \Phi_{\text{source}}),$$

where U_{screen} is geometrical unsharpness of screen's conversion, Φ_{source} is focal spot size.

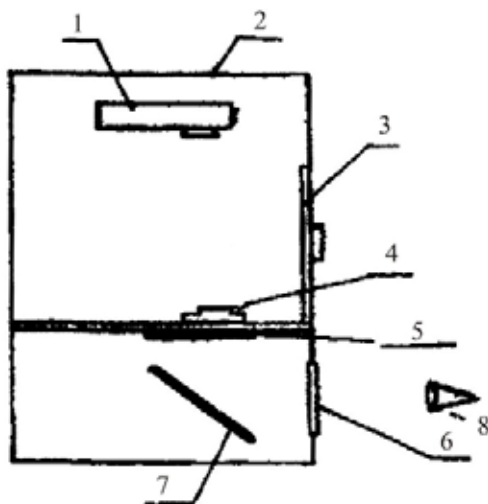


Fig. 4.5. Type scheme of fluoroscope:

1 – radiation source; 2 – protecting frame (shielding); 3 – door; 4 – testing object; 5 – fluoroscopic screen; 6 – window from lead glass; 7 – mirror; 8 – eye of operator

The object is placed directly onto the surface of the screen or between the irradiator and the screen and may be shifted or turned. The typical focus distance is 400 – 500 mm. The plate mirror is applied for reducing the radiation loading within the window square. The mirror is produced with the front reflecting surface having reflection factor about 90 % for visual light. That is important for preventing from observing false images. The usage of such a mirror leads toward the losses of brightness and, so, reduces the fluoroscopic sensitivity of facility. That why the best results one achieves at applying the shielding windows purposed for direct observing the images from the screen. The shielding windows must meet satisfactorily the following requirements:

- must have high enough weakening factor for ionizing radiation (with value about 10^6);
- must have high transparency;
- must have small enough radiation scattering factor.

So, within mentioned requirements, the most appropriate material is glass containing heavy elements in its composition such as lead, barium or silicon. Shielding glass has high density equal to 6.2 g/cm^3 and safety factor equal to ~ 0.55 in comparison with pure lead. At this, the light let passing factor must be high enough and be constant at time of fluoroscope exploitation.

So far as radiation safety norms and rules strongly limit the permitted exposure dose on external surface of shielding box (not more than 0.3 mR/ hour),

then fluoroscopes operates usually at the anode tension $U_a \leq 200$ kV. That why in the radioscopy with fluoroscopes one can examine steel-made objects with thickness up to 3 mm and aluminum articles with thickness up to 60 mm.

4.5. Brightness of screen luminescence

The fluoroscopic sensitivity depends on the screen luminescence brightness and the sensitivity increases at brightness increasing. In its turn, the screen brightness depends on the characteristics of the screen, in particular on the luminophor's sensitivity for radiation and sizes of luminophor's crystals. The more crystals size and ionizing radiation intensity fallen onto the screen surface, the higher luminescence brightness. Maximum brightness of fluoroscopic screens is got at the effective anode tension 60 kV which corresponds to maximum tension 120 kV.

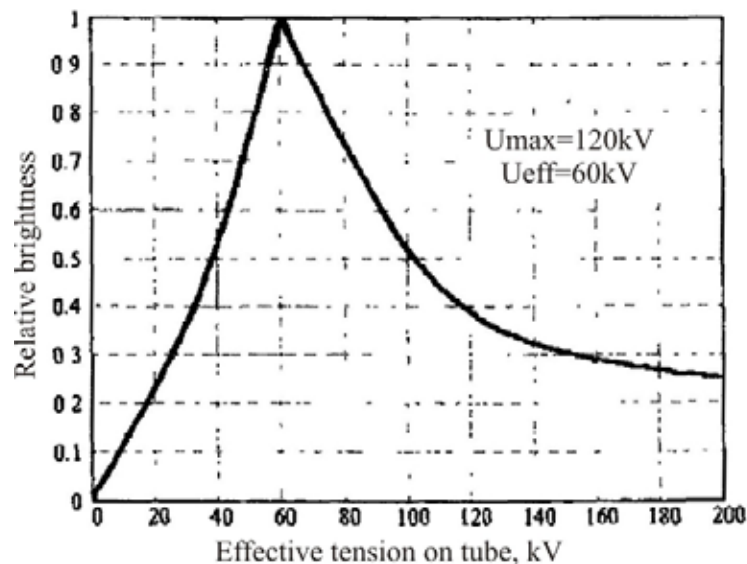


Fig. 4.6. Dependence of brightness of fluoroscopic screen luminescence upon the effective tension on surface of X-ray film

4.6. Screen's unsharpness

Screen unsharpness is defined as the boundary width between two adjacent sections of the screen with different screen brightness and is measured by help of microphotometer. Generally, the unsharpness of fluoroscopic screens depends on the size of the luminophor crystal and usually is about 0.5...1,0 mm.

4.7. Spectral structure of luminescence

The choice of phosphorus for the screen at given energy brightness of luminescence is defined by its spectrum. The luminescence spectrum occupies the visual, blue-violet, ultra-violet and infrared parts of total spectrum

of electromagnetic waves. At this, the wave length of luminescence maximum is, in average, 530 nanometers; the short wave boundary is 493 nanometers and long wave boundary is 578 nanometers. These values correspond to one-half of the intensity maximum. The optimal mass content of luminophor from CdSO_4 in screen mixture, from the view of light intensity and spectral conformity for human eye and for the Sb-Cs photocathode, is (45...50) %. The density of luminophor in fluoroscopic screens is, in average, about 4.5 g/cm^3 at the layer thickness about 85 mg/cm^2 . For screens used at visual analysis, it is necessary to provide well perception of luminescence by human eye so the spectrum must lie in visual area of the electromagnetic wave's spectrum. Human eye has different sensitivity for visual rays of different color, namely small sensitivity in infrared and ultra-violet areas and high sensitivity for visual light in the certain range of wave's length, as shown in figure below.

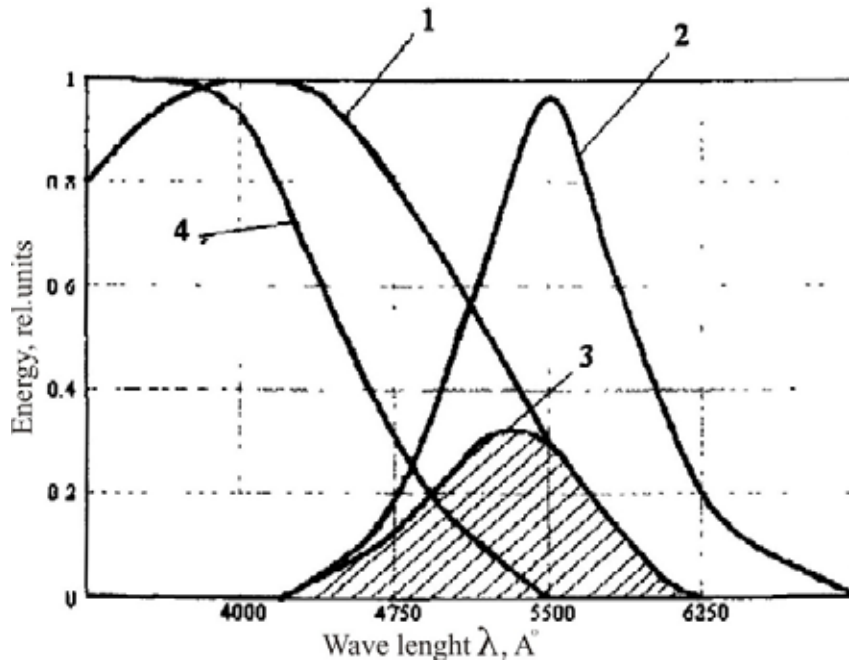


Fig. 4.7. Spectral distribution of relative sensitivity:
 1 – relative brightness of luminescence for CaWO_4 screen; 2 – human eye sensitivity for visual light; 3 – relative value of light flow of CaWO_4 screen perceptible by eye; 4 – relative sensitivity of BrAg – salt of X-ray film

Usually, the brightness levels of fluoroscopic screens are in the range of $3 \cdot 10^{-4}$ (night)...0.06...3 (day) cd/m^2 , that are low enough. So, the optimal perception of information from images of such a low brightness is connected with the application of principles of physiological optics. The human eye has so-called day and night mechanisms of vision and the transfer from day to night vision has place at the brightness level about 0.06 cd/m^2 . The brightness of fluoroscopes at action is often less than 0.06 cd/m^2 . The vision sharpness (clearness) and the contrast threshold of brightness depend significantly

on the background brightness of the image analyzed. The measure of the vision sharpness is the inverse value of minimum angular distance between two points at which the eye can see this gap. Value of the angle equal to 1' corresponds with the unit of the vision sharpness. The vision sharpness increases at raise of image brightness and can achieve the visible level at transfer from night to day vision. At brightness level $B = 0.3 \text{ cd/m}^2$, two separate points are visible at angle equal to $1.80'$. If the distance between screen and eye is 250 mm which is usually recommended distance at visual testing, this value corresponds to the resolution equal to 0.13 mm.

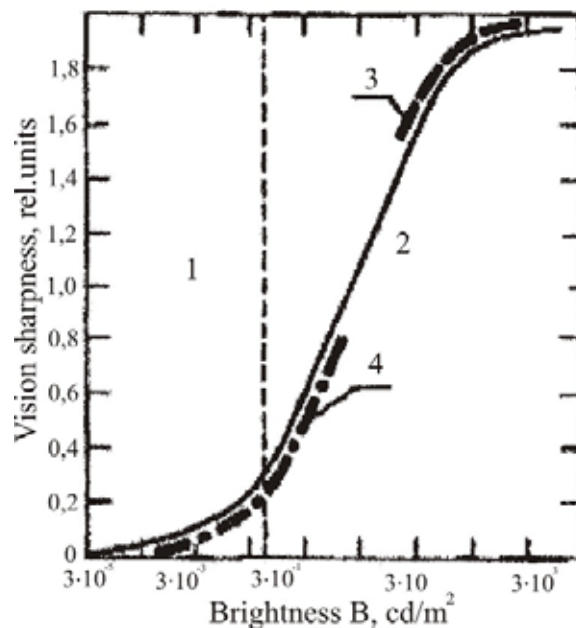


Fig. 4.8. Dependence of vision sharpness of human eye on the brightness of image under analysis:

1 – night vision, 2 – day vision, 3,4 – sections, characterized values of sharpness at image analysis from X-ray film and from fluoroscopic screen

The sharpness of vision depends also on the wave length of visual light. Usually, the vision sharpness is determined for so-called “white” light, at this for yellow and yellow-green light the sharpness is slightly more. The least threshold contrast of the brightness $\Delta B/B = (0.01 \dots 0.02)$ is achieved within wide range of brightness of the image background equal to $(\sim 1 - 1 \cdot 10^3 \text{ cd/m}^2)$. If the brightness fluctuates at its very low values, then the threshold contrast gets worse (for example, $\Delta B/B \approx 0.04$ at $B \sim 0.06 \text{ cd/m}^2$).

So, the dark adaptation of eye is needed if the screen brightness is less than 0.3 cd/m^2 . Under these conditions, one needs in 1 minute of dark adaptation to detect the image contrast equal to 1 percent. The dark adaptation leads to widening (expansion) of pupil of eye and increase of its light sensitivity. The night vision (sight) begins its functioning after passing about

10 minutes of adaptation and still improves next 30 minutes of adaptation. In practice, 20 minutes of adaptation is well enough. In order to hold the working state of the eye, one needs to use red light in the searching room and use glasses with red light filters in areas placed out of testing zone.

Thus, the common sensitivity of introscopy at using fluoroscopes is within (2...5) %, but one can receive the sensitivity in ~ 1.5 % at testing aluminum objects and using the powerful X-ray apparatus. That why the common sphere of fluoroscopes application is the testing of casts from lightly-melted alloys, the inspection of the quality of assemblies and monitoring the passenger's luggage.

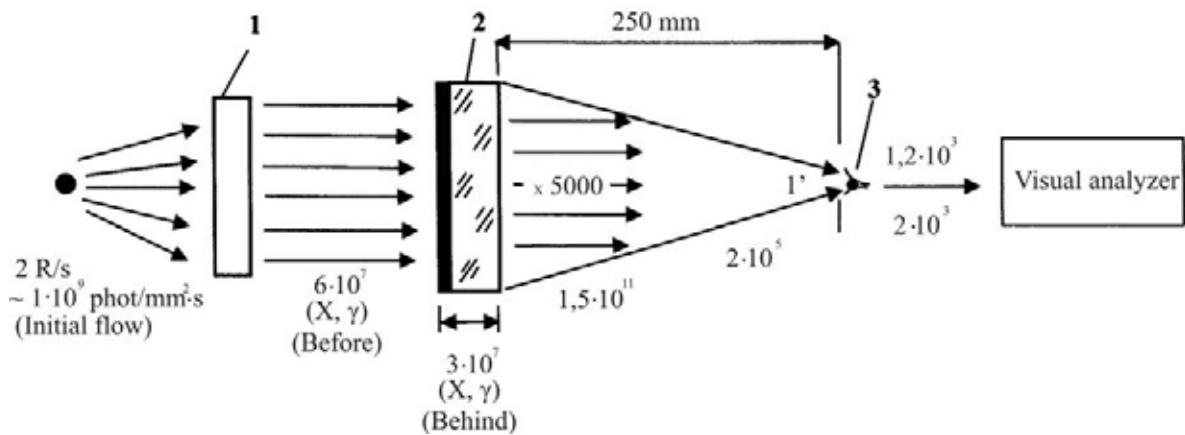


Fig. 4.9. General sequence of receiving and analysis of light-shadow image at using fluoroscopes

The general sequence of receiving and analysis of light-shadow image at using fluoroscopes is as follows:

1. Exposure dose power on the input plate of the object is $\sim 2 \text{ R/s}$ at flow density of X-ray photons $\sim 1 \cdot 10^9 \text{ photons/mm}^2 \cdot \text{s}$ (typical values for common used apparatus);
2. Behind the object and on the input plate of the fluorescent screen, only ~ 6 % of initial intensity of the particles flow has passed through the object thickness. So, the number of photons remained is about $6 \cdot 10^7 \text{ photons/mm}^2 \cdot \text{s}$;
3. Conversion inside the screen: quantum yield of the screen is about 0,5 or ~ 50 %, so the number of absorbed photons is $3 \cdot 10^7 \text{ photons/mm}^2 \cdot \text{s}$;
4. Quantum yield of the luminescence of the screen is 5000, so the total number of photons of luminescence is $3 \cdot 10^7 \times 500 = 1.5 \cdot 10^{11} \text{ light photons/mm}^2 \cdot \text{s}$;
5. Number of light photons reached the human eye from the screen's square equal to 1 mm^2 in 1 second and at the object – eye distance equal to 250 mm is $2 \cdot 10^5 \text{ photons/mm}^2 \cdot \text{s}$;
6. Number of photons, absorbed by the retina of eye, at the quantum yield of the retina ~ 3 %, is only $6 \cdot 10^3 \text{ photons/mm}^2 \cdot \text{s}$;

7. At last, the final number of photons absorbed by the eye in ~ 0.2 second which is the eye integration time, only $N_\lambda \sim 1.2 \cdot 10^3$ photons/ $\text{mm}^2 \cdot \text{s}$.
8. Additionally to these, the contrast of fluctuations of the signal, transmitted into the human brain is $K = 100 / \sqrt{N_\lambda} \sim 3.5 \%$. This value is about 100 times more than the contrast of the fluctuations of the radiation image.

As far as the available number of the initial X-ray photons is limited, from one hand, by low efficiency of its generation in irradiators and, from other hand – by requirements of radiation safety, the scheme of fluoroscope needs in introduction the facility with which the eye will be allowed to collect the enough amount of the signal photons. This facility must have higher quantum efficiency in comparison with the human eye and also larger sensitive surface than the human eye and higher brightness of the light-shadow image on the plate of the output screen in order to use in total the high resolution capacity of the eye at high levels of brightness.

Such a facility is called “radiation image amplifier”.

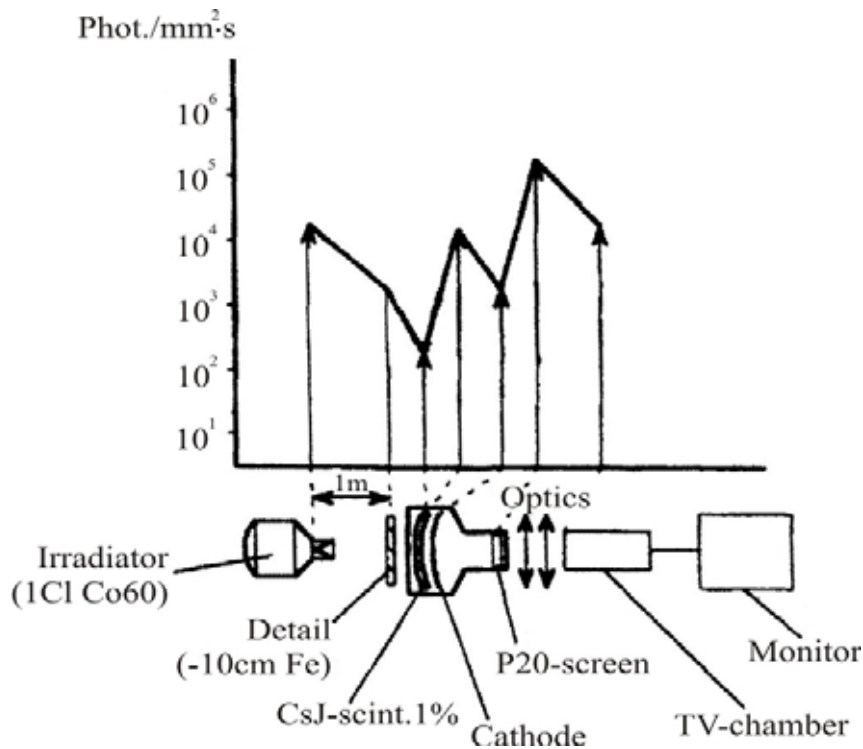


Fig. 4.10. Diagram of amount of particles corresponding to every step of transformation at 1 mm^2 square and at time 1 s

4.8. Interpreting of fluoroscopic images

The interpreting in fluoroscopy differs from interpreting of radiograms. At this, main difference consists in the fact that the fluoroscopic image is the positive image when the radiograph is the transparent negative. Generally, the defect's revelation by fluoroscopy is not difficult. Defects occurred often

such as cracks, pores, inclusions, blowholes etc are recognized easily due to its characteristic (typical) images:

1. Gas shells – they are recognized on the fluoroscopic screen as light, equally outlined areas. When shells are filled by inclusion from slag or other material, then their image becomes darker and the contour of image takes the irregular, incorrect shape (form). One can detect the gas shells in aluminum casts, if the diameter of the defect is about 8 % of the thickness of cast in defect location, but not less than 1.5 mm.
2. Blowholes – they are observed on the screen in the form of light areas having non-equally contours. The value (size) and the real place of those blowholes one can determine at rotating the casts. The most successful detection has place at recognizing blowholes having diameters not less than 2 mm or having not less than 10 % of thickness of that part of the cast in which blowholes are appeared.
3. Inclusions – they are revealed on the screen in form of dark or light areas or points. Being inclusions heavier or denser than the bulk metal, the inclusion's image on the screen is darker than the surrounding background; and, vice versa, is lighter if inclusion's density and mass are lesser in comparison with bulk matter. It is necessary for successful revelation of inclusions that dense inclusions were about 20 % heavier, and light inclusions were about 30 % lighter than bulk material.
4. Non-fusions – At moving metal within thin sections of casting forms from both sides, the case of untimely cooling of metal is possible. Non-fusions are the result of such untimely, non-uniform cooling of different parts of the casts. At interpreting, the non-fusions have a view of light stripes or ovals on the screen of facility.
5. Cracks – the image of cracks on the screen has a view of light longitudinal sections. The cracks are revealed successfully if have minimum width equal to the linear dimensions of the mentioned above defects. Many of cracks haven't such a minimum width and have also the irregular contours. That why their detection by the method of fluoroscopy is more difficult task in comparison with the radiography.

4.9. Determination of defect's sizes

The determination of sizes of defects revealed by the fluoroscopy is performed at comparison of those defects with the known ones. The special fluoroscopic standards of sensitivity with the artificial defects (usually with the holes of different diameters and depths) are used or the standard articles with known defects. In order to estimate the quality of the image, the miras are used now in the radioscopy as well as in radiography and now the CERL-standard with double wires takes more important.

4.10. Fluorography

The fluoroscopic image from the screen may be photographed onto the ordinal photo-film. At photographing of the image, the slight increment of image's contrast has place, that why the slight increase of sensitivity becomes also possible. The application of the films with small-size germs of emulsion and strong light optics allows to fulfill shots on the films with compact formats. The fluorography of materials and articles is available at higher tensions on X-ray tubes (up to 250 kV and more) which widen significantly the permitted range of examining thickness in comparison with the fluoroscopy.

4.11. Amplifiers of radiation images

The improvement of the fluoroscope's scheme had place in long time period by using the magnifying facilities between the screen and the human vision apparatus. There were two different directions of the development: the usage of the electron-optical converters (EOC) and roentgen electron-optical converters (REOC) from one side, and the usage of the TV-facilities (roentgen-TV-apparatus, TV-systems with roentgen vidicone), from other side.

Radiation-optical converters (EOC, REOC). The main parameters of X-ray image amplifiers are:

1. Dimensions of the working (operating) field. That is the section of the input plate surface of converter which may be applied for receiving the output image at given testing conditions. The working field is defined mainly by the size of the input screen of the converter.
2. Scale of the radiation image conversion. That is the ratio of the linear dimension of the conversion element of the output image over the analogue linear size of the element of the initial radiation image. The conversion scale is determined by the sizes of input and output screens of the radiation transformers. At this the output screen is the screen where the image perceptible by human eye is formed. The conversion scale one can change by means of focusing systems of the REOC or TV-systems.
3. Brightness magnification factor of the REOC. That is the ratio of the brightness value of the output screen of the converter over the value of standard fluoroscopic screen at the equal given conditions of irradiation both input plates of the converter and fluoroscopic screen. The advanced REOC have the conversion scale 1: 10 and may achieve the value of factor of magnification of the brightness equal to $\sim 10^4$.
4. Resolution limit of the REOC. That is the most number of stripes in each 1 mm of the initial image developed by the stripe radiation mira which may be recognized separately at the analysis the output image

under the optimal conditions of the converter operating. At this, the stripe and the gap on the mira are considered as two lines of the mira. The resolution limit, at analysis by eye, depends significantly on the observer properties. More over, it depends on the image contrast of the mira and parameters of ionizing radiation in such a manner that the lower the photon's energy, the better the details of the mira are visible. So, the radiation energy within 30 – 50 keV is better than 60 – 80 keV. The resolution limit is influenced also by the random character of the quantum fluctuations of ionizing radiation. So, the resolution limit is reduced at low values of the exposure dose power.

5. Limit of energy flow density at the input of the converter. That is the most value of the energy flow density of ionizing radiation which leads not toward the serious (irreversible) breaches of the converter operating.
6. Brightness of dark background of the REOC. That is the average value of the brightness of output screen at absence of the input screen irradiation.
7. Geometrical distortion of the radiation image. That is the deviation of forms of the image conversion relatively the form of the image on the input screen.
8. Degree index of the vision field. That is the additional number of artifacts and its sizes on the output screen. The artifacts are false elements of the output image which are absent on the input image and appeared at the conversion process.
9. Zone characteristics of the conversion. Parameters of the conversion differ almost always for different sections of the conversion field. For example, the difference in the brightness from centre toward the edge due to the distortion; those changes increase strongly with the raise of the input screen diameter from 10 % (at $\varnothing = 16$ cm) up to 30 % (at $\varnothing = 32$ cm).
10. Contrast transfer factor. That is the ratio of the value of contrast of the element of the output converted image over the value of the contrast of the element of the input image. At this, contrast $\gamma = \Delta\varphi/\varphi = \Delta B/B \sim 1.0$. The transfer factor for radiation TV-system with the REOC: $\gamma_{\text{syst}} = \gamma_1 \times \gamma_2 \times \gamma_3 \times \gamma_4$, where γ_1 is the transfer factor of the REOC (~ 0.8); γ_2 is transfer factor of transmitting TV-tube (~ 0.9); γ_3 is factor of the amplifying loop of the TV-system (~ 1.0); γ_4 is the transfer factor of kinescope (~ 3.0). Thus, the sum value of the transfer factor is ≈ 2.16 . Transfer factor of human eye is about 0.3.
11. Time resolution. That means the REOC response relatively the change of the radiation image in time. It depends on the velocity of physical processes passing in separate elements of the REOC.

So, general parameters of the systems with external and inner input screens:

1. Radiation TV-settings with the external fluoroscopic screen: size of the working field is 240×320 mm; resolution limit is 0.8 pairs of lines /mm;
2. Radiation TV-sets with the REOC: size of working field is Ø (150...300) mm, resolution limit is about (1.5 – 3.0) pairs of lines/mm.

4.12. Radiation image amplifiers

There are the special roentgen- visual devices with the operating principle based on the conversion of the X-ray image of the examining object into the visual one at once with the brightness magnification. Being amplified by brightness, the image is observed further by the operator from the output screen of the REOC or from the video-monitoring facility of the closed TV-system included into the amplifier structure. The most wide-spread amplifiers are the devices of so called single-cascade type or electron-optical converters (EOC).

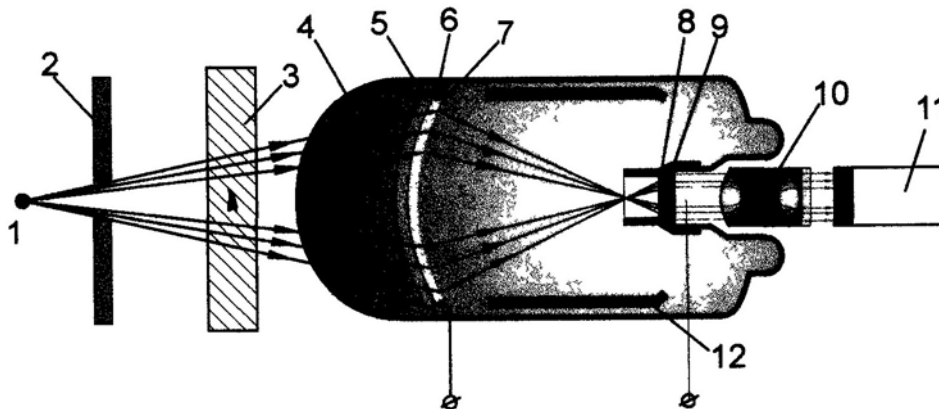


Fig. 4.11. Scheme of the EOC:

- 1 – source of radiation, 2 – lead slit diaphragm, 3 – testing object,
4 – glass vacuum tube, 5 – aluminum backing, 6 – luminescence screen,
7 – photocathode, 8, 9 – output screen, 10 – optical lens, 11 – objective, photoapparatus,
12 – transmitting TV-tube, 13 – metallized cover (shielding screen)*

The vacuumed, with the pressure about 10^{-7} mm of Hg column (torr), glass tube 4 has two screens inside: the input and output screens. The input screen consists from aluminum backing of spherical form 5 with the layer of the luminescent matter 6 covered onto it. The surface of this layer is provided with the semi-transparent Sb-Cs photocathode 7, chosen by its sensitivity and conformity with light radiation of the luminescent screen. The output screen of EOC represents the glass plate 9, covered by the fluoroscopic composition 8 and displaced in the cone-type aluminum anode 12 with the hole. The side walls of glass tube are covered by electroconductive layer 13. Working tension about 25 kV is added between the input screen and anode. The tension + 300 B relatively to the cathode is added onto the conductive

covering functioning as the focusing electrode. X-rays or gamma radiation, being fallen onto the luminescent screen 6, caused further its luminescence. Under the luminescence action, the photocathode 7 emits photoelectrons. At this, the electrons emitting from any point of the photocathode are focused then by the electrostatic field within the corresponding point of the output screen 8 – 9, being the reason of its luminescence.

As the result, we have the visual image on the output screen which corresponds strongly to the roentgen image on the input screen of the EOC. Sizes of the output screen are about 10 times less than the sizes of input screen. Due to the acceleration of electrons and to reducing of the image size, the total magnification of the brightness is about 1000. Recently, the EOC were designed and applied which have the brightness magnification about 3000 and even more. The image on the output screen is observed with the help of monocular or binocular optics 10 and then is transmitted through the TV-system.

The image quality of the EOC is defined by the own properties of the luminescent screen applied. The resolution capacity of the screen is about 3 pairs of lines/mm, but due to the distortions at transfer the image through elements of the system, its resolution capacity reduces up to 2.5 pairs of lines/mm. The image contrast creating by the luminescent screen of the EOC reduces due the thermoelectronic current from photocathode, lightings due to inner reflections in converter and so on. At this, the total losses of the contrast are not more than 15 %. The brightness of the output screen of EOC is about 1000 times higher than that of the fluoroscopic screen, so the usage of the EOC allows to exam objects at lower tension on X-ray tube in comparison with the fluoroscopic screen. Being combined with high brightness of the image, EOC improves the revelation of defects.

So, if other testing conditions are the same, the defect' revelation at examining with X-rays and the application the EOC is approximately two times better than for fluoroscopic screens and (2 – 4) times worse in general than for application of the radiography.

The sensitivity and revelation capacity of the radioscopy at using the sealed radionuclidic sources coupled with the EOC is about (1.5 – 2.0) times worse in comparison with the usage of X-ray tubes. For example, sensitivity of testing of duraluminum with thickness (20...30) mm by Tm-170 with the EOC, is approximately (1.5 – 2) times less than sensitivity at X-rays examine.

4.13. TV – arrangements

The usage of the TV devices for distant transmitting the fluoroscopic image allows to automatize the testing procedure and reduce significantly the danger of irradiation of service personnel by ionizing radiation. Scheme of the fluoroscopic testing with TV-system is shown in Fig. 4.12.

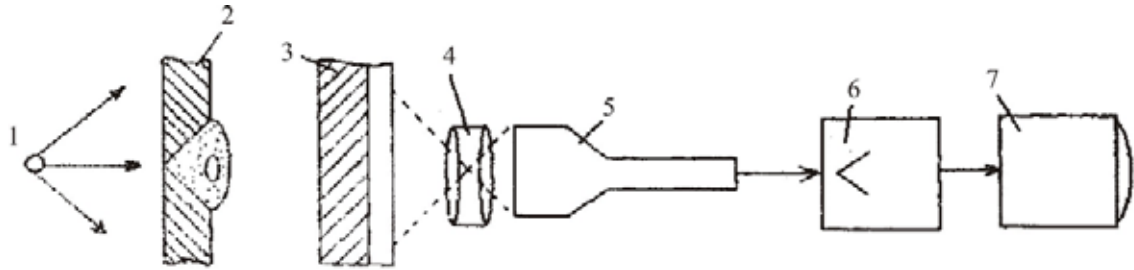


Fig. 4.12. Scheme of visual method with usage of TV device:

1 – source of radiation, 2 – testing object, 3 – fluoroscopic screen (or EOC is possible), 4 – optical system, 5 – transmitting TV-antennae, 6 – amplifier, 7 – TV-receiver

At the TV transfer of fluoroscopic image the simultaneous amplifying of the brightness has place. The clearness of the transmitted image depends on the number of lines of the TV equipment. The native industry produces the TV devices of different types, e.g. ПТТ-24 (industrial TV-set), ПТТ-102 etc. In the radioscopy mainly the industrial equipment of closed type is applied. Here, the video-signal is transmitted by means of coaxial cable. The length of coaxial cable may form hundreds of meters, which provides the convenience of the usage of the TV-device in shop and sometimes field conditions.

The industrial radiation arrangement consists from three main elements: transmitting TV-tube, TV channel of communication, containing video-amplifier, generators of evolvant, elements of the synchronization, providing the development of the image, correction and control elements, coaxial cable and other elements. In dependence on the purpose of industrial TV device, it applies several transmitted TV-tubes, several TV-receivers and communication channel adds with units of communication and control and so on.

Besides the design, industrial TV sets differ by the kind of the applied transmitting tubes, for example devices with tubes of the superorticone type, aimed for operation at conditions of low illumination of objects and devices with transmitting tubes of the vidicone type aimed for transfer of high brightness images. In this case, the TV-sets are significantly simpler from the point of design and exploitation.

4.14. Usage of fluoroscopy

In industry, the fluoroscopic methods are applied mainly for inter-processing testing the quality of materials and procurements of detail, for testing mechanisms, separate units and so far. Method can be used successfully for testing the completed articles produced in great amounts at condition of been met the testing requirements. In the Table below the areas of usage the fluoroscopic testing providing the highest sensitivity are given.

It is difficult to overestimate the importance of introscopy, its spheres of applying are wide. In machine-making it is necessary for

searching the quality of metals and, in first turn for materials designed on the base of polymers, glass-plastics, ceramics and so on, for improving the methods of defectoscopy and determining of sizes, types and orientation of defects; for studying the reliability index of aggregates' work, tired strength, inner tensions etc. In metallurgy, means of introscopy serves for studying and monitoring of the kinetics of high-temperature processes at the boundary (front) of metal –slag; for automatize checking of the quality of hot and cool metal at rolling process on bloomings and slabbings, in cutting and sheet metal produce. In blast-furnace works, the introscopy is used for testing the state of the inner brick-lining. In ferrous metal industry, the input checking of row materials, fuel, the analysis of materials through the technological process, the analysis for checking of contaminations in the environment are needed. At this the absence of the automated means of the articles testing reduces sharply the labor productivity and the subjectivity of testing may lead to the delivery of materials and articles having the dangerous hidden defects.

Table 4.3

Spheres of fluoroscopy application

Methods of fluoroscopy	Range of voltage on X-ray tube, kV	Thickness of examining material, mm		
		Alloys on base of		
		magnesium	aluminum	steel
Fluoroscopy	30...150	10...90	6...60	–
EOC	30...250	110...200	75...150	6...25
TV-devices	30...200	110...200	75...150	25...100

In chemistry, methods of introscopy are need for active checking of several technological processes. The building of the aggregates for chemical synthesis with high temperature and pressure and aggressive substances caused inter-crystallite and other kinds of corrosion, requires the development of the high sensitivity methods and means for revelation the microdefects in the construction's materials at manufacturing and exploitation of chemical equipment; also, the revelation of changes in micro-structure of metals and the definition of the initial stage of its destruction are needed as well as the testing of the quality of protective coverings of metals of pipes and other elements of the aggregates. Chemical machine-making requires the development of the automated means for looking for the state of the construction materials and elements of the equipments of radiation chemistry working at conditions of irradiation by beta-particles, flows of neutrons and gamma-rays. In building industry, means of the introscopy

are wide spread for studying the strength characteristics of building materials and constructions. In the sphere of semi-conductive materials and quantum radioelectronic the introscopy serves for studying the quality of materials, quality of the optical perfection and the structural uniformity of monocrystals non-transparent (opaque) for visual light etc.

Besides, the introscopy is needed in the practice of scientific experience, in radioastronomy, in medicine for biochemical and encelographic investigations, pathological changes inside the vital organism.

The most significant effect is achieved at the inculcation of radiation introscopy methods for testing the casts from aluminum and magnesium alloys. The modern technique of casting can't provide the all-where density of cast metal because of appearance of pores inside metal due to gas outlet and shrinkage. The inner tensions in casts are caused by non-equal cooling of metal or mechanical breaking of shrinkage. Thus, the examining of casts by X- or gamma-rays is the method for detection the inner defects of metal without its destruction.

Testing of ingots. In Germany, the testing of the steel ingot with cross-section 200×200 mm at the process of rolling is made with usage of the fluoroscopic equipment having EOC with diameter about 230 mm. The betatron on energy 31 MeV was used as radiation source. The image on the output screen of the EOC is observed with help of closed TV-set with the super-orticone transmitting tube. At this, the shells and slag inclusions are revealed in the studied ingots. Betatrons and linear accelerators are applied for testing steel ingots with thickness up to 300 mm. It was shown by practice that usage of accelerators is very expensive, so it was recommended to apply the fluoroscopic arrangement with the EOC sensitive to gamma radiation of radionuclide Co-60 which allows to define exactly the displacement of the defect giving at this large economical effect at checking of edges of burning hot ingots, because of defining the exact boundaries of scraps at presence of shells and slag inclusions.

Testing of casts. Radioscopy is wide spread in Russia and abroad (USA, France and other) for cast quality testing. Method allows to reveal well big porosity, gas and shrinking shells, flux and slag inclusions and also the cracks having sufficient width and depth corresponding the sensitivity of the method. The revelation of cracks makes easier by the fact that introscopy provides the searching of cast under different angles relatively the beam of radiation. Practice of several years of testing the cast details from light alloys had shown that defects represented gas pores and shrinking shells with sizes about 0.5...5 mm are revealed distinctly by the image on the TV-screen. At this, the examining time for detail moving in front of the converter screen with the velocity about 1 m/min, is reduced up to minimum. But the time for the set of auxiliary operations is still comparatively big. The advanced equipments are devices with totally automatized and mechanized testing

operations beginning from settling and picking up of details and ending by marking and shooting of defect's section. All together, it allows to increase the productivity and economical efficiency of the introscopy methods.

Testing of welding and soldering quality. Main method of testing of welded and soldered joints at present is the radiography, having low productivity compared with the automated technological processes of welding or soldering. As the result, the large time gap occurs between the welding (soldering) process and the process of non-destructive testing. Introscopy allows to raise productivity of NDT several times. That why methods and means of introscopy got recently wide usage in this branch of testing. At this, testing velocity may achieve 1 – 3 m/min. In Russia, the testing of thin-walled welded joints from steel is performed, for example, by X-ray TV introscope with ЛИ-417, ЛИ-423 X-ray vidicones, having the TV-amplification up to 30 times and high resolution capacity. As the result, at radioscopy of welded joints from 1.5 mm-steel made by Ar-arc welding at stationary regime, one can reveal practically the same defects as at the radiography with X-ray film PT-1 (gas pores with diameter over 0,2 mm and cross-cut cracks with the exposure about 0.1 mm etc). The testing of welded joints from steel and titanium alloys with thickness 1.5...2 mm had shown the distinctive revelation on the TV screen of shells, porosity and faulty fusions. For thicker joints from steel up to 20 mm and aluminum alloys up to 50 mm, more effective is the usage OF the TV introsopes on base of scintillation crystals CsJ (Tl). Here, the sensitivity of method, measured with the help of the ditch standard, achieves 1...3 % for steel with thickness 3...18 mm and from 3 to 0.8 % for aluminum alloys with thickness 3...50 mm. Such a sensitivity is only 1.3 – 2 times worse of the sensitivity of radiography. At testing the longitudinal and circular welding joints of steel pipes with 5 mm walls, the X-ray TV introscope of ПИ-10Т type is used successfully for detection of pores, cracks, tungsten and slag inclusions. Here, the TV amplification of image, the possibility of the change of its polarity, displacement of articles with the velocity about 1 m/min relatively the scintillation crystal assist all together in good detection of defects.

Testing of electronic components. The fluoroscopic method is under usage in aviation instrument-making and radio-electronics for the NDT-testing of transistors, silicon diodes, melted fuses and other hermetical electronic units and details. In the USA, they made the testing in comparison of radiographic and fluoroscopic checking of details and electro-schemes from thin foils from aluminum and nichrome with thickness 200...400 Å covered onto glass backing with thickness 1.5 mm, modules and other details. Fluoroscopic testing was performed with closed TV-system with X-ray-sensitivity vidicone. Comparative checking had proved that image on TV-

screen amplified up to 30 times, has better resolution comparatively with the image on the high-granularity X-ray film. More over, the probability of the defect's detection in electronic assemblies, particular in modules, is risen due the possibility of searching the image under different angles. At the same time, the detection of defects inside electronic schemes of foil-type covered onto glass backing as well as the detection of aluminum wire with diameter 1 mm inside the steel housing of transistor are still very difficult and even impossible by neither fluoroscopy nor by radiography.

Testing of solid fuel. Solid fuel for rockets is tested usually by radiography on its packaging uniformity with help of accelerators or Co-60. The fluoroscopic testing of fuel of the rocket jets with diameter about 760 mm and with length about 177 mm is fulfilled using equipment with the Van-de- Graaf accelerator on energy 2 MeV and device of "Lumicone" type with the EOC and TV system. The jet with fuel is irradiated by the bremsstrahlung radiation which falls onto the input screen after passing through fuel; every turn of jet follows by the vertical shift and by turn again. At this, the substitution of the Co-60 radiography by the fluoroscopy allows to achieve high economic efficiency for each of jets.

4.14. Type methods of selection of regimes of radioscopy

1. Material and thickness of the object tested are the initial parameters defined the choice of regimes of the introscopy.
2. Norms of defects. (requirements relatively the quality of object). In Russia, the permitted sizes of defects in objects tested are given in technical documentation of object, technical conditions, rules of testing and taking, State and branch standards, instructions etc.
3. The permitted defects of welded joints may be defined by class of joint by GOST 23055, or by class of the sensitivity by GOST 7512, or with accounting of the worse of revelation of defects at the radiographic testing of moving objects.
4. Definition of testing sensitivity and choice of sensitivity indicators (penetrometers). The sensitivity of radioscopy one ought to define at beginning and end of every party of details tested and also at beginning and end of working shift with help of the corresponding sensitivity models settling on moving with working velocity or on the stationary settled object. At last case, one ought to account the worsening of sensitivity of testing followed by the shift of testing object. In Russia, in radioscopy as well as in radiography they use the wire, ditch or plate (lamellate) models by GOST 7512. At this, the sensitivity of testing in mm and the ordinal number of the corresponding sensitivity model is chosen in accordance with norms of defects and with account of testing velocity.

5. Choice of radiation energy (tension on X-ray tube or accelerator's energy). In Russia the needed range of radiation energy is chosen in dependence on the thickness and density of examining material with help of the reference tables determining the sphere of application of the radioscopy by GOST 20426. If not listed, energy for concrete materials are defined by the concept of the equivalent thickness and radiographic equivalency factor.
6. Choice of type of radiation source (X-ray apparatus, electron accelerator). In radioscopy one ought to choose such a source of radiation, that provides the most intensity of radiation over the surface of the radiation converter and the least geometrical unsharpness. You can do it with help of reference tables given in the corresponding section of item "Radiography" for X-ray devices and accelerators.
7. Definition of the radiation intensity (i. e. anode current of X-ray tube, radiation yield of accelerators) and sizes of focal spot of the irradiator. Maximum anode current in mA for X-ray devices, radiation yield (exposure dose power) of accelerators (betatron or linear accelerator) in Koulomb/ kg·s or in R/ min (R/s) at certain distance from the target of accelerator we can determine for concrete irradiators using the reference tables for corresponding sections of item "Radiography".
8. Choice of the radiation converter. In the radioscopy the following image converters or radiosopic systems may be used for receiving information:
 - fluoroscopic screen;
 - X-ray EOC (REOC) or scintillation monocrystal with electron-optical amplifier EOA) of the image brightness;
 - X-ray TV-arrangement with X-ray sensitive vidicone;
 - X-ray TV-device with fluoroscopic screen;
 - X-ray TV-device with REOC;
 - X-ray TV-device with scintillation monocrystal;
 - X-ray TV-device with scintillation monocrystal and EOA.

In Russia, the image converter or radiosopic system is selected in accordance with GOST 20426 in dependence on thickness and density of tested details and patterns. The concrete type of arrangement you ought to choose from reference table come from the best sensitivity relatively defects, the highest resolution capacity and highest productivity of testing.
9. Selection of mechanical manipulator. In Russia, the company which performs the radiosopic testing of articles, must provide the projecting and produce of the specialized mechanical manipulator with distant control made the following operations:

- testing of small-size details:
 - mechanized feed of details (patterns) toward the image converter; necessary scanning shifts of detail relatively the image converter; distant marking of the defect sections or detail (pattern); transportation of details passed testing from the image converters.
 - testing of large-size articles: hard coaxial fitting of the source and radiation converter; necessary shifts of the source and radiation converter linked between each other, relatively the tested articles (or vice versa); distant marking of the defect sections of the article.
10. Choice of testing regimes. Main regimes of defectoscopic testing in the radioscopy are tension on X-ray tube; anode current of X-ray tube; current of the focusing coil of the X-ray tube with sharp focus; focus distance F ; distance from testing detail to input screen of the radiation converter; velocity of testing. In Russia, regimes of radioscopy are selected by the following way:
- Tension on X-ray tube is settled in dependence on thickness and density of testing material using data for maximum permitted tensions at testing steel and aluminum by the radioscopy;
- Anode current is chosen equal to maximum possible for given type of tube;
- Current of the focusing coil of the tube with sharp focus is defined beforehand by the best of clearness of the image of examining wire model at all of tensions on the tube;
- Focus distance from the anode of the tube up to input window of the image converter one ought to settle equal to minimum possible in range of 5 – 50 cm, come from the condition of manipulating by the testing detail during testing process and from demands relatively the sensitivity;
- Distance from testing object to converter's screen ought to be settled equal to minimum possible and not more than one third of the focus distance at working with ordinary tubes and not over a half of focus distance at using tubes with sharp focus;
- Velocity of the tested object displacement in front of the converter screen ought to be settled in accordance with the needed sensitivity relatively defects and productivity of testing. For facilities with the fluoroscopic screens, scintillation monocrystals and the REOC the velocity of shift must not be more than 1...1.5 m/min, not more than 0.1...0.5 m/min for devices with X-ray vidicones.
11. Technique of testing and rejecting of examined objects.
- Before testing, it ought to observe carefully details and articles taking special notice of extracting of surface defects and sort out details by groups taking in account the purpose of fulfilling testing with minimum number of the changes of testing regimes.

Before testing of first detail, the sensitivity of testing ought to be defined by the sensitivity model settled.

The testing is ought to make using the mechanical manipulator controlled distantly which provides the fitting and necessary shifts of the testing object and marking on it the defect sites.

At the radioscopy, the quality of testing object one can estimate directly at time of the examination. At the rejection of the testing joints and details one ought to follow the permitted norms of defects on concrete object as it is noticed above in the point 2.

Registration of the testing result is ought to make by means of the video-reading of the images of the defect sections at laser disks or by other way agreed with the customer.

4.15. Control tasks

1. Explain the idea of the signal/noise ratio of the ideal TV-introscop at the monoenergetic radiation (in the ideal introscop the total quality of radiation, fallen into the converter, is absorbed inside it and the TV-system does not contribute any distortions).
2. Explain the influence of the real converter on the signal/noise ratio for the simplest case of assumption that the radiation absorption in converter occurs due to the photoeffect.
3. Depict the typical dependence of the relative sensitivity of the introscop on the testing article thickness. Explain how the sensitivity is determined experimentally? Due to what the sensitivity is decreased in thick and thin articles?
4. Substantiate how the dependence of the sensitivity on the testing article thickness will change at the increase of the roentgen tube current?
5. Substantiate how the dependence of the sensitivity on the testing article thickness will change at the increase of the roentgen tube tension if the tube current is not changed?
6. Explain the influence of the focal spot of the radiation source on the geometrical distortions. Does the image contrast decrease at the focal spot increase?
7. Explain the concept of the effective and mean (average) absorption factors of the roentgen radiation. How is the image contrast computed for the roentgen radiation?
8. How much is the value of the mean time for human eye shady adaptation?
9. Which minimum of the object's illumination can be revealed by human eye?

10. Explain how the value of the image threshold contrast, revealed by the human eye, depends on the brightness of the background?
11. Fulfil the comparison of the bremsstrahlung radiation (4 MeV) absorbed energy values for monocrystal screens NaI(Tl), KI(Tl), CsI(Tl), using the data of the Table 4.3 (p. 69 of the [1]). Note: make the computing at the condition of equality of the thickness and the radiation absorption mass factors by monocrystals. Take the monocrystals thickness equal to 2 cm.
12. Explain the difference of the “narrow”(pencil) and broad (extended) beams of the radiation. In what cases these kinds of the geometry of the radiation – raying of objects are used?
13. By which values the geometrical conditions of the radioscopy are determined?
14. What is the build-up (accumulation) factor and how it influences the roentgen image quality?

4.16. SET OF TEST QUATIONS ON SECTION “RADIOSCOPY”

1. In the practice of radiation testing, the radioscopy uses to test objects with thickness of about ____ layers of half-weakening of the examining radiation:
 - A** 2 layer;
 - B** 3;
 - C** 5;
 - D** 8.

2. The aim of including the amplifiers of image’s brightness in the composition of the radiation introscopy systems is:
 - A** increase of brightness of the light –shadow images of objects tested;
 - B** increase of the detection efficiency of ionizing radiation passed through the object;
 - C** increase of signal/noise ratio inside the light-shadow image;
 - D** D – A and C.

3. Main types of X-ray TV-arrangements used in the advanced radiation testing are given below in the consecutive order. The resolution capacity of arrangements is increased in consequence:
 - A** arrangements with –REOC-fluoroscopic external screen – X-ray vidicone;
 - B** with – X-ray vidicone –REOC –fluoroscopic external screen;
 - C** with – fluoroscopic external screen – REOC – X-ray vidicone;
 - D** with – REOC –X-ray vidicone – fluoroscopic external screen.

4. The main distinction between the radiography and radioscopy is:
- A** fluoroscopic image is more bright;
 - B** fluoroscopy gives the image in the “real time” mode;
 - C** fluoroscopy possesses more sensitivity;
 - D** fluoroscopy gives positive and radiography gives negative image of the object tested.
5. Sensitivity of aluminum object’s testing for the common used fluoroscopic systems using powerful tubes with tension 100...150 kV, focus spot size 2...5 mm, ordinary fluoroscopic screen and distance about 400 mm between target of the source and screen, and at the screen placed as close to object as possible, is equal approximately:
- A** 1 %;
 - B** 1.5 %;
 - C** 2.0 %;
 - D** 2.5 %.
6. Which of kinds of glasses listed below one ought to use as the shielding window material in the fluoroscopy equipment:
- A** optical glass;
 - B** organic glass;
 - C** glass containing oxides of barium;
 - D** glass containing lead and silicon.
7. One from disadvantages of the fluoroscopic testing consists in low brightness of the image received. At this, one of the brightness increase methods in which the energy of light of the initial luminescent surface converts into electrons accelerated and focused onto the fluorescent screen of smaller size, is performed in the special arrangement called:
- A** betatron;
 - B** image amplifier;
 - C** electronic amplifier;
 - D** electrostatic generator
8. Two serious barriers on practical realization of high-sensitive fluoroscopy are:
- A** necessity in periodic changing of screens applied;
 - B** expensive cost and low productivity of the screen;
 - C** necessity of using the long-wave part of X-rays and their low intensity;
 - D** limited brightness and coarse-granularity of the fluoroscopic screen.

9. The phenomenon of luminescence consists in:
- A** emitting of ionizing radiation from the surface of the luminescent screen due to the interaction of visual light with the matter of luminophor;
 - B** emitting of the electric current at the conversion of ionizing radiation inside the matter of luminophor;
 - C** emitting of flashes of visual light from germs of luminophor at the interaction of ionizing radiation with the matter of luminophor.
10. The hidden (latent) radiation image of testing object is:
- A** distribution of intensities of ionizing radiation outlet the object after interactions with the object's matter and absorption and weakening in it;
 - B** the part of the intensity of ionizing radiation that can't be detected by converters (detectors);
 - C** non-visible part of the spectrum of electromagnetic waves.
11. Main distinctions between the radiography and radioscopy consist in:
- A** radiography as well as radioscopy have not any limitations connected with time losses at shot development and analysis, but the operator can't change any stage of testing process at time of examining;
 - B** radiography has limitations connected with time losses at shot development and analysis but has, in return, the sensitivity 2–10 times better than in radioscopy;
 - C** radioscopy is the express method of testing and the operator has possibility to change any parameters of examining procedure at moment of testing.
12. X-ray vidicone is the device purposed for:
- A** emitting the X-ray radiation with ultra-low energy of photons;
 - B** the particular kind of the X-ray-electron-optical converter;
 - C** the kind of the transmitting TV-tube sensitive for X-rays and combining the properties of the REOC and transmitting tube.
13. Operator's functions in the radioscopy are:
- A** perception visual information, – treatment of it, – executive actions directed at the process's elements;
 - B** analysis of the visual image, – rejection of spoilage, – documentation of defects occurred

14. Sources of radiation for radioscopy:

- A** X-ray apparatus of continuous action and the highest possible intensity of low-energy X-ray photons;
- B** only pulsed X-ray apparatus and different kinds of accelerators;
- C** gamma- and neutron sources with high activities (within certain limits)

15. Radioscopy needs in higher dose of radiation absorbed by the object at the time of testing:

- A** due to necessity to form large number of shots in time of testing with high enough quality of every shot;
- B** requirement comes from the point of view of providing the radiation safety at radioscopy;
- C** all of luminophors applied in radioscopy have low sensitivity for low doses of irradiation.

Chapter 5

WORK SAFETY IN THE RADIATION DEFECTOSCOPY

5.1. Dosimetric values in the radiation safety

The purpose of the radiation safety is the exclusion of the radiation injury and the limitation of the risks of unfavourable consequences for human health down to the acceptable level without preventing from the development of new progressive technologies and their realisation in practice. In accordance with the modern notion, the quantitative measure of health damage from the ionizing radiations action is the dose. Therefore, a system of the dosimetric values composes the basis of the radiation safety.

5.1.1. Ionizing radiations

The ionizing radiation is such radiation (the corpuscular as well as the electromagnetic) which realizes the ionization of the medium at passing through it and interacting with it. The ionization process consists in the formation of the positively – and negatively – charged particles which are formed at the derangement of the electron from the atomic electron shell. As a result of the single ionization act the electron carrying the negative charge and the positively charged ion is formed. The carriers of any kind of the ionizing radiation must have the energy allowing to tear the link between the electron and atom and transfer to the deranged electron the kinetic energy sufficient for the next ionization acts.

Depending on the features in the ionization process realization, the ionizing radiations are divided into the directly ionizing radiations and the indirectly ionizing radiations.

The indirectly ionizing radiations are the flows of the uncharged particles (namely photons and neutrons), which do not ionize directly the media but at the interaction with the media they generate the flows of the charged particles which are the directly ionizing radiation. These charged particles are called the secondary particles.

The direct interaction of the protons of the roentgen – and gamma – radiation includes three different processes: (1) the photoelectric absorption (photoeffect); (2) the Compton scattering; (3) the pair formation. Which of the processes will be dominating at one or other conditions, depends on the

photon energy and on the media element composition. Given processes are considered in detail in section 1.

The photoeffect is the dominating process at the comparatively low photons energies (up to hundreds keV). At the increase of the photon energy, beginning from the $h\nu = 100$ keV the photoeffect cross-section is fast decreased as $(h\nu)^{-3}$ at $h\nu \leq 0,5$ MeV and as $(h\nu)^{-3}$ at $h\nu > 0,5$ MeV. At the increase of the charge Z of the media elements, the photoeffect cross – sections are increasing fast as Z^m , where $m \cong 4$. The ionization of the media is realized by the electrons torn from the atomic electron shell as the photoeffect result.

The Compton scattering process is prevalent in comparison with the other processes of the photon interactions with the matter at the widest interval of the photons energy:

from 0.5 to 5 MeV – in lead; from 0,1 to 10 MeV – in iron; from 0,05 to 15 MeV – in aluminum; from 0,02 to 23 MeV – in air. At photons energy not less than 1,02 MeV, to the above-mentioned processes of the photon interactions with the matter, the pair formation process is added.

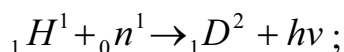
All three processes of the photons interactions with the matter are more intensive in the media with the high effective atomic number. Therefore, lead screens or the concrete reinforced with the iron ore or with the barium minerals are applied for the weakening of the roentgen – and the gamma-radiation.

The directly ionizing radiations are the flows of the charged particles (beta-particles, alpha-particles, protons) having the kinetic energy enough for realization of the media atoms ionization acts. For the directly ionizing radiation the ionization process consists in the electric interaction of the charged particle (beta, alpha-particle, proton, heavy ion) with the electron on the material atomic electron shell through which the particle flies. The electric interaction of the flying charged particle with the electron of the atomic shell leads to the break of link between the electron and atom. The atom loses the electron. As a result, the atom or the molecule which has this atom becomes a positively charged ion.

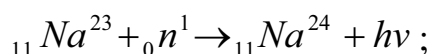
The mechanism of the ionization by neutrons depends considerably on their energy. For the fast neutrons with the energy 1 MeV and more the process of the neutron collision with the hydrogen nuclei is more important for the ionisation. At the interaction, neutron transfers a part of kinetic energy to the hydrogen nucleus. As the result the kinetic energy is got by the positively charged particle (the hydrogen nucleus, i. e. the proton), which is in this case the directly ionizing particle. In the biological tissue, at the collision with the fast neutrons, besides the recoil proton the recoil nuclei of carbon, oxygen and nitrogen which realize the ionization of the media can also appear. However, the possibility of the appearance of the recoil nuclei, which are heavier than the proton, is comparably little but it is increased

with the rise of the neutrons energy. After a number of interactions the neutron loses its kinetic energy and transfers in the category of the moderate or thermal neutrons. The moderate and the thermal neutrons are also the ionizing radiation but the ionization mechanism of such neutrons is different. The moderate and the thermal neutrons enter in the nuclear reactions with the media nuclei. The directly ionizing or the undirectly ionizing radiations appear as a result of these reactions. The main reaction at the thermal neutrons absorption is the reaction of the radiation capture. It is such a reaction at which the neutron capture is taking place with the emission of the gamma – radiation photon. The example of the radiation capture reaction:

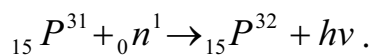
1) the capture of the neutron by the nucleus of the light hydrogen (protium) with the formation of the attenuation kernel of the heavy hydrogen (deuterium) and with the photon emission:



2) the capture of the neutron by the nucleus of sodium – 23 with the formation of the radioactive nucleus of sodium – 24 and with the photon emission:



3) the capture of the neutron by the nucleus of phosphorus – 31 with the formation of the radioactive nucleus of phosphorus – 32 and with the photon emission:



The ionization of the media is stipulated by the absorption processes and the processes of scattering of photons which are emitted at the reactions of the neutron radiation capture. In the case of the radionuclide formation at the radiation capture reaction, the additional source of the media ionization may be the beta – particles and the photons emitted at the radionuclide decay.

5.1.2. Parameters of the ionizing radiation field

The space – time distribution of the ionizing radiation in the media forms the field of the ionizing radiation. The spreading of the ionizing radiation in the media is described with the help of the field parameters which are the functions $f(x, y, z, t)$ of the space coordinates x, y, z and the time t . The main (basis) parameters of the ionizing radiation field are: (1) the particles flow; (2) the particles fluency and; (3) the power of the particles fluency.

The flow of particles $F(\vec{r}, t)$ is equal to the particles number crossing the given surface in time unit, where r is the radius – vector determining the coordinates x, y, z of the point in space. Formally the particles flow is determined by the relationship:

$$F(\vec{r}, t) = \lim_{\Delta t \rightarrow 0} \frac{\Delta N}{\Delta t} = \frac{dN}{dt}, \quad (5.1)$$

where $N(\vec{r}, t)$ is the number of particles passing across the given surface (in the time interval Δt).

The dimensionality of the particles flow in the terms of SI has the form of S^{-1} (1/second).

The fluency of particles $\Phi(\vec{r}, t)$ in the point \vec{r} of the space is equal to the ratio of the number of particles of all directions in space, which have crossed the small sphere with the centre in the point \vec{r} , to the square of the large cross-section of this sphere. The sphere must be so small in order to be able to envelop only such dimension of space within which the fluency has the same value. The value of the fluency of particles gives the quantitative information about the number of particles crossing the space in environs of the point \vec{r} . The particles fluency is determined formally by means of the relationship:

$$\Phi(\vec{r}, t) = \lim_{\Delta S \rightarrow 0} \frac{\Delta N(\vec{r}, t)}{\Delta S} = \frac{\Delta N}{\Delta S}, \quad (5.2)$$

where $\Delta N(\vec{r}, t)$ is the number of particles of all directions in space which have crossed the surface of the small sphere with the centre in the point \vec{r} ; ΔS is the square of the large cross – section of this small sphere.

The power of the particles fluency $\Phi^1(\vec{r}, t)$ is determined as the value of the fluency in time unit. Formally, the power of the particles fluency is determined with the help of the relationship:

$$\Phi^1(\vec{r}, t) = \lim_{\Delta t \rightarrow 0} \frac{\Phi(\vec{r}, t)}{\Delta t} = \frac{d\Phi}{dt}, \quad (5.3)$$

where $\Phi(\vec{r}, t)$ is the fluency value during the time interval Δt in environs of the point \vec{r} .

In the partial case of the parallel particles flow the power of the particles fluency is equal to the number of particles crossing in unit of time the surface of the single square disposed perpendicularly to the direction of the particles motion.

Dimensionalities of the particles fluency and the power of the particles fluency in the SI have the form of m^{-2} and $m^{-2}s^{-1}$ correspondingly.

5.1.3. Coefficients of the ionizing radiation interaction with the material

The weakening of the gamma-radiation in the material is determined with the help of the linear weakening coefficient. The linear coefficient μ of the gamma-radiation weakening is equal to the ratio of the part dN/N of photons interacting with the material at the passing of the distance dl , to this distance, i. e.

$$\mu = \frac{1}{N} \cdot \frac{dN}{dl}, \quad (5.4)$$

where N is the number of photons.

The linear weakening factor is added from the linear weakening factors stipulated by the photoelectric absorption τ , the Compton scattering σ_c and the pair formation K :

$$\mu = \tau + \sigma_c + K. \quad (5.5)$$

The energy transfer from photons to the secondary charged particles is described with the help of the energy transfer coefficient.

The energy transfer coefficient μ_{tr} is equal to part of the falling photons energy converted into the kinetic energy of the charged particles in the material layer of the single thickness. The energy transfer coefficient is determined formally by the formula:

$$\mu_{tr} = \frac{1}{W} \cdot \frac{dW_k}{dl}, \quad (5.6)$$

where W is the sum energy of photons fallen onto the layer of the material with the thickness dl ; dW_k is the sum of the initial kinetic energies of all charged particles realized by the gamma-radiation in the material layer with the thickness dl .

A part of the kinetic energy of the secondary charged particles, realized by the gamma-radiation, is spent for the bremsstrahlung radiation which is not absorbed in the place of its formation. In order to account for only that part of the secondary particles kinetic energy which is absorbed in the material, one uses the coefficient of the energy absorption.

The energy absorption factor is calculated by the formula:

$$\mu_{en} = \mu_{tr} \cdot (1 - g), \quad (5.7)$$

where g is the part of the secondary particles kinetic energy, which is spent for the bremsstrahlung radiation.

One can see from the designations of the introduced coefficients of the weakening, energy transfer and energy absorption that they all have the dimensionality reverse to the length. This dimensionality in the terms of SI is m^{-1} .

In some calculations, for example, for complex materials it is convenient to apply the mass coefficients. The value of the mass coefficients of the weakening, energy transfer and energy absorption is determined by the formula:

$$\mu_m = \frac{\mu}{\rho}, \quad (5.8)$$

where ρ is the material density.

In the terms of SI the dimensionality of the mass coefficients has the form m^2kg^{-1} .

For the description of the charged particles energy loss at their passing through the matter, the value of the total linear bremsstrahlung capacity is used. The total linear bremsstrahlung capacity S is equal to the energy lost by the charged particle on the unit of the length. The bremsstrahlung capacity is determined formally by the formula:

$$S=dW/dl, \quad (5.9)$$

where dW is the energy lost by the particle on the path dl .

The total linear bremsstrahlung capacity is added from the linear bremsstrahlung capacity stipulated by the collisions, and the linear bremsstrahlung capacity stipulated by the bremsstrahlung radiation (radiation losses of the charged particles).

The dimensionality of the linear bremsstrahlung capacity in terms of SI has the form of $\text{J}\cdot\text{m}^{-1}$. Besides the bremsstrahlung capacity the mass bremsstrahlung capacity S_m is also used and it is equal

$$S_m = S/\rho. \quad (5.10)$$

The dimensionality of the mass bremsstrahlung capacity in terms of SI has the form of $\text{J}\cdot\text{m}^2\cdot\text{kg}^{-1}$.

5.1.4. Penetrating capacity of the ionizing radiation and the linear energy transfer

The most important parameters of the ionizing radiation for the radiation safety purposes are the penetrating capacity and the linear bremsstrahlung capacity stipulated by collisions. The energy transferred to the material at the collisions is the locally transferred energy as distinct to the losses for the bremsstrahlung radiation, which passes far away from the particle track. In order to underline this distinction, the linear bremsstrahlung capacity stipulated by the collisions got a special name: the linear energy transfer (LET). For the quantitative description of the penetrating capacity of the ionizing radiation the values of the particles path in the media, the layers of the one-half weakening, the linear and mass coefficients of the weakening are applied. The penetrating capacity indicates the potential possibilities of the protection from the external flow of the ionizing radiation.

The linear energy transfer L is determined formally by the relationship:

$$L = dE/dl, \quad (5.11)$$

where dE is the energy transferred to the material by the particle at the collisions on the path length dl .

The value of LET is the measure of the density of the energy transferred locally along the ionizing particle path. The value of LET characterizes the biological efficiency of the ionizing radiation.

5.1.4.1. Alpha-radiation

The alpha-radiation is the flow of the alpha-particles which are the helium nuclei. The alpha-particles are concerned with the heavy charged particles. The mass of the alpha-particles is approximately 7300 times larger than the electron mass. The alpha-particles, passing in the media, transfer their energy on the excitation and the ionization of the media atoms. The main are the losses on the ionization. The paths of the alpha-particles with different kinetic energy in different materials are given in Table 5.1.

Table 5.1

Paths of alpha-particles in different media

Energy of Alpha-particle, MeV	Path of alpha-particle		
	in air, cm	in biol. tissue, micrometer	in aluminum, micrometer
1	2	3	4
4	2.37	26.2	16.5
5	3.29	36.7	22.2
6	4.37	48.8	28.8
7	5.58	62.4	36.2
8	7.19	78	43.4
9	8.66	94.4	52.2
10	10.2	112	61.6

As one can see from Table 5.1, the paths of alpha-particles in the media are short, and it means that the penetrating capacity of the alpha-radiation is very low. The air layer with the thickness of several centimeters can fully protect from the external flow of alpha-radiation. For the protection from the alpha-particles by means of aluminum the layer with the thickness only in several tens of micrometers is needed. Therefore, the protection from the external flow of the alpha-radiation is essentially fully provided by the air layer and by clothes. So any special measures are not required.

Since the path of the alpha-particles in the media is short, then, on the contrary, the LET of the alpha-particles is high and makes up about 100 keV at 1 micrometer of the biological tissue. The high value of the LET indicates the high biological efficiency of the alpha-radiation. The influence of the alpha-radiation upon the people can be realized at the penetration of the alpha-radiation sources inside organism. The main way of preventing of the alpha-radiation influence on human organism consists in the exclusion and limitation of the entrance of the alpha – radiation sources into organism.

5.1.4.2. Beta-radiation

Beta-radiation is the flow of the beta-particles (i. e. electrons). Beta-particles, which move in the media, transfer their energy on the excitation and ionization of the media atoms.

For the beta-particles with high energy the radiation losses also occur. However, in the area of the beta-particles energy which is in practice of the radiation safety, the radiation losses are small. The paths of the beta-particles with the different kinetic energy and in different media are given in Table 5.2.

Table 5.2

Paths of the monoenergetic beta-particles in different media

Energy of beta-particle, MeV	Path of beta-particle		
	in air, cm	in water, mm	in aluminum, mm
0,5	154,7	1,74	0,83
1	835,3	4,29	2,03
1,5	835,3	6,96	3,27
2	835,3	9,59	4,48
3	1276	14,8	6,85

As one can see from Table 5.2, the path of the beta-particles in the materials are considerably (hundreds of times) longer than the paths of alpha-particles, therefore the penetrating capacity of the beta-radiation is greater than that of alpha-radiation. However, the protection from the external flow of the beta-radiation as well as from the external flow of alpha-radiation causes no sufficient difficulties.

The beta-radiation is fully absorbed by the air layer of a few meters and the thickness of a few millimeters is enough for the protection by the aluminum. The penetrating capacity of the beta-radiation in the material is higher than that of the alpha-radiation.

The LET of the beta-radiation is correspondingly lower. The LET for the beta-radiation constitutes only units keV on 1 micrometer of the biological tissue. The lower LET stipulates the lower biological efficiency of beta-radiation in comparison with alpha-radiation. For the quantitative estimation of the penetrating capacity of beta-radiation, side by side with the path value the meaning of half – value weakening layer is also used. The half – value weakening layer is equal to such thickness of the material at passing through which the intensity of the parallel flow of beta-particles is reduced two times.

5.1.4.3. Gamma-radiation

The linear coefficient of the weakening may be used as a measure of the penetrating capacity of gamma-radiation. But more obvious parameter

characterizing the penetrating capacity of the gamma – radiation is the layer of half – value weakening.

The half – value weakening layer is taken to be equal to such thickness of the material at passing through which the intensity of the parallel narrow beam of photons is decreased two times. Coming from the absorption relationship for gamma – radiation, one can write:

$$I(\Delta_{1/2}) = \frac{I_0}{2} = I_0 \cdot \exp(-\mu \cdot \Delta_{1/2}). \quad (5.12)$$

The solution of the equation (5.12) relatively to the layer $\Delta_{1/2}$ of the half – value weakening gives:

$$\Delta_{1/2} = \frac{\ln 2}{\mu} = \frac{0.693}{\mu}. \quad (5.13)$$

As it is expected, the simple connection is present between the parameters μ and $\Delta_{1/2}$ which characterize the penetrating capacity of gamma – radiation (see the formula 5.13). Meanings of the half – value weakening layer for the narrow parallel beam of photons of the different energy and in the different materials are given in Table 5.3.

As one can see from Table 5.3, for weakening the photons flows only two times, the air layer of several tens of meters or the water layer with thickness up to 10 cm or the aluminum layer with thickness of several cm are needed. It means that all kinds of gamma – radiations have a high penetrating capacity. In connection with this the realization of the protection from the external sources of gamma – radiation is a complex engineering problem and it calls for significant material costs. Naturally, at a high penetrating capacity the value of the LET for gamma – radiation is small.

Table 5.3

The half – value weakening layers for gamma – radiation in different materials

Energy of photons, MeV	Half – value weakening layer, cm		
	in air	in water	in aluminum
1	2	3	4
0.2	4331	5.33	2.17
0.3	4950	5.78	2.48
0.4	5775	6.93	2.77
0.5	6300	6.93	3.15
1	8663	9.9	4.33
2	11550	13.86	5.78
3	17325	17.33	7.7

For example, for the cobalt – 60 gamma-radiation (with the energy of gamma-quantums 1,1 and 1,3 MeV) the value of the LET is 0,3 keV on 1 micrometer of the biological tissue.

5.1.5. Dosimetric values

The effects caused by the ionizing radiation in the material, depend on the quantitative characteristics of the radiation field and on the degree of the radiation interaction with the matter which is characterized by the interactions coefficients considered in points 1.2 and 1.3. Dosimetric values are the physical measures of real and potential effects stipulated by the ionizing radiation.

5.1.5.1. Kerma

The energy transfer by the indirectly ionizing radiation is determined quantitatively by the value of the kerma \underline{K} . Kerma is the ratio of the sum of initial kinetic energies of all charged particles which are let out by the indirectly ionizing radiation in the elemental volume of the matter, to the mass of the matter in this elemental volume. The value of the kerma is calculated by the formula:

$$K = dW_k / dm, \quad (5.14)$$

where dW_k is the sum of the initial kinetic energies of all charged particles let out by the indirectly ionizing radiation in the elemental volume of the material; dm is the mass of then material. The dimensionality of the kerma in terms of SI has the form: Joule/kg. The value of the kerma 1 Joule/kg has a special name “One Gray (Gy)”. The using of the out-system term 1 rad (radiation absorption dose) = 0.01 Gy is admitted temporarily.

5.1.5.2. The exposure dose

The air ionization at the gamma-radiation passing is applied for the design of the devices allowing to detect the presence of the gamma-radiation and to measure its intensity. The ionization of the air under the gamma-radiation action has allowed to introduce the idea of the exposure dose of the gamma-radiation. The exposure dose X is equal to the ratio of the sum of the electric charges of the same pole generated in the air at full deceleration of all secondary electrons, which have been formed by the gamma-quantums in the elemental volume of the air, to the air mass in this volume. The exposure dose X is calculated by the formula:

$$X = dq / dm, \quad (5.15)$$

where dq is the sum of the electric charges of the same pole; dm is the air mass in the elemental volume.

The dimensionality of the exposure dose in terms of SI is coulomb/kg (Cu/kg). The using of the out – system term of the exposure dose roentgen, is admitted temporarily. $1R = 2.58 \cdot 10^{-4} \text{ Cu/Kg}$ and $1 \text{ Cu/Kg} = 3876 \text{ R}$.

5.1.5.3. The absorbed dose

The fundamental dosimetric value used in the radiation safety is the absorbed dose D . The absorbed dose D is determined by the relationship

$$D = d\vec{W} / dm , \quad (5.16)$$

where $d\vec{W}$ is the mean energy transferred by the ionizing radiation to the material in the elemental volume; dm is the material mass in this elemental volume.

So, the absorbed dose is determined by the energy absorbed in the unit of the material mass. The dimensionality of the absorbed dose in terms of SI has the form Joule/kg. The value of the absorbed dose 1 Joule/kg has a special name 1 gray (Gy). The using of the out – system term $1 \text{ rad} = 0.01 \text{ Gy}$ is admitted temporarily.

At the solution of some practical problems of the radiation safety it is useful to apply the concept of the absorbed dose D_{tis} which is the mean dose for the human organ or the organism tissue. This dose is determined in accordance with the relationship:

$$\bar{D}_{tis} = W_{tis} / m_{tis} , \quad (5.17)$$

where W_{tis} is the total energy absorbed in the organ or the tissue; m_{tis} is the mass of this organ or the tissue of standard human. At the condition when the sum of the kinetic energies of all charged particles coming into the volume element is equal to the sum of the kinetic energies of all charged particles going out this volume element, the secondary particles equilibrium takes place. The secondary particles equilibrium is realized if in the area from which the secondary charged particles can come into the considered volume element there is observed the space constancy of the following parameters: (1) the fluency, energy spectrum and the direction distribution of the primary particles; and (2) the radiation – material interaction coefficients (the mass factor of the energy absorption and the mass bremsstrahlung capacity) for the primary particles as well as for the secondary ones.

The first condition of the secondary particles equilibrium is fully realized only at the uniform distribution of the radioactive material in the infinitely extended media. With some approach the equilibrium of the secondary particles may be realized if the radiation field changes slightly inside the area whose sizes are comparable with the maximum path of the secondary particles.

For gamma – radiation sets free the electrons by means of the photoeffect, the Compton effect and the effect of the electron–positron pair formation, the equilibrium of the secondary particles is realized in the air, in the water, in the biological tissue and in the materials with the effective ordinal numbers near the above-mentioned, if the energy of photons is not higher than 3 MeV.

In the presence of the secondary particles equilibrium, the absorbed dose in the material is equal to

$$D = K - B, \quad (5.18)$$

where B is the energy loss of the secondary charged particles on the bremsstrahlung radiation. In many cases one can neglect the loss of energy on the bremsstrahlung radiation and then

$$D \cong K, \quad (5.19)$$

i. e. the absorbed dose is approximately equal to the kerma. If the exposure dose in the air is equal to 1 roentgen, then the corresponding absorbed dose in the air is 0.87 rad. If the case of the secondary particles equilibrium and the small value of losses on the bremsstrahlung radiation is assumed, the value of the absorbed dose in the air is equal to the air kerma (see the expression 5.19). In this approach at the exposure dose in 1 Roentgen the air kerma is 0.87 rad (radiation absorbed dose).

5.1.5.4. The equivalent dose

It is known that the biological efficiency of the ionizing radiation depends not only on the absorbed dose (i. e. the energy absorbed in unit of mass of the biological tissue) but also on the type and energy of radiation stipulating the dose. The influence of this dependence is strong enough so it must be taken into account. This accounting is provided by means of using the weighting factor for the absorbed dose. This dimensionless weighting factor named the quality factor depends on the radiation characteristics and it is a rough estimation of the biological efficiency of this radiation as related to the biological efficiency of the radiation for which the quality coefficient is equal to 1. At present it is considered that the value of the radiation quality factor is determined by the linear energy transfer L. The International Commission on Radiological Protection (ICRP) recommends the following dependence of the quality factor on the linear energy transfer (LET):

$$Q(L) = \begin{cases} 1 & \text{at } L = 3.5 \text{ KeV} / \mu\text{m} \\ 0.3 \cdot L & \text{at } 3.5 \text{ KeV} / \mu\text{m} \leq L \leq 100 \text{ KeV} / \mu\text{m}. \end{cases} \quad (5.20)$$

The product of the absorbed dose on the radiation quality factor

$$H = D \cdot Q \quad (5.21)$$

is named “the equivalent dose”.

Since the quality factor is dimensionless, then the dimensionality of the equivalent dose coincides with the dimensionality of the absorbed dose and in terms of SI has the form of Joule/kg. In order to avoid a misunderstanding, the equivalent dose has received a special name “zivert” (Zv) as distinct from the gray (Gy) used for the absorbed dose.

Formula (5.21) determines the meaning of the equivalent dose in the point where there is a certain value of the linear energy transfer L and therefore the value of quality factor Q. For the determination of the biological effect of the organ irradiation the mean value of the linear energy transfer is calculated most adequately. However, there are situations when the distribution of the linear energy transfer L and the quality factor Q in all the mass of the irradiated organ is unknown. In this situation the ICRP recommends to use the approximate values of the quality factor depending on the kind of the ionizing radiation. In order to distinguish the approximate value of the quality factor from the accurate value, the approximate value was named: “the radiation weighting factor W_R ”. It is considered that the value of the radiation weighting factor depends only on the kind of the ionizing radiation irradiating the organ or the tissue and it is independent on the considered organ or tissue. The values of the radiation weighting factor chosen for the different kinds of the ionizing radiation are given in Table 5.4.

The mean absorbed dose in the organ, multiplied by the radiation weighting factor of the corresponding radiation, is considered as an acceptable approach for the mean equivalent dose in the organ:

$$H \cong W_R \cdot \bar{D}, \quad (5.22)$$

where \bar{D} is the mean for the organ absorbed dose.

Table 5.4

Values of the radiation weighting factor

Kind of radiation and energy range	Value
Roentgen and gamma – radiation of all energies	1
Electrons and mesons of all energies	1
Neutrons with the energy	
Less than 10 KeV	5
From 10 KeV to 100 KeV	10
More than 100 KeV and up to 2 MeV	20
More than 2 MeV	10
Alpha – particles, fission fragments, heavy nuclei	20

The field of the ionizing radiation acting on the organ may consist from several types of radiation having different values of the radiation

weighting factor. In this case, the equivalent dose in the organ must be calculated separately for every type of the radiation. The total equivalent dose is received by means of the ionizing radiation, i. e.

$$H_{tot} = \sum_R W_R \cdot \bar{D}_{ris(R)} , \quad (5.23)$$

where $\bar{D}_{ris(R)}$ is the mean absorbed dose in tissue τ from the ionizing radiation of R type; W_R is the radiation weighting factor for the ionizing radiation of R type.

The value of the equivalent dose for the organ received by described way may be slightly different from the value calculated with the accounting of the detail distribution of the quality factor in all organ mass. However, such difference is considered unessential for the purpose of the radiation safety.

5.1.5.5. Effective dose

The unfavourable biological effects appearing as a result of the radiation action are divided into deterministic and stochastic. It is considered that the deterministic effects appear in the irradiated organism only after the exceeding of the certain threshold by the dose and they do not appear if this threshold is not exceeded. For the deterministic effects, an increase of the organ injury seriousness with the dose increase is characteristic. The stochastic effects have a probable character. These effects appear in the dose range which is lower than the dose range stipulating the deterministic effects. For the dose range of the stochastic effects the function of the dose is not the injury seriousness but the value of probability or the frequency of appearance of the injurious effects. Today it is considered that for the stochastic effects there is no threshold by the dose and that the value of the probability of the stochastic effects appearance is proportional to the value of the dose, i. e. the so-called linear non-threshold conception is applied.

In the dose range stipulating the deterministic effects in the irradiated organs the absorbed doses are used. As for the stochastic effects, the frequency of their appearance depends not only on the magnitude of the equivalent dose in the organ but also on what organ (or organs) has been irradiated. Therefore, the idea of weighting equivalent dose (i. e. twice weighting absorbed dose) has been introduced and it correlates well enough with the level of the stochastic effects. This dose is named “the effective dose” (ED) or the effectance.

The factor with the help of which the equivalent dose in tissue T is weighted is named “the tissue weighting factor W_T ”. This factor determines the part of the stochastic risk stipulated by the tissue irradiation T, from the total risk appearing at the uniform irradiation of all the human body.

If several organs (tissues) have been irradiated, then the effective dose is calculated by the formula:

$$E = \sum_T W_T \cdot H_T, \quad (5.24)$$

where W_T is the tissue weighting factor for the organ (tissue) T and H_T is the mean equivalent dose in the organ T.

The summing in formula 5.24 is spread on all irradiated organs and tissues. The equivalent dose in the organ T is determined through the absorbed doses from the different radiation types by the formula 5.23. Taking into account this formula, the effective dose may be determined through the absorbed doses in organs with the help of the formula:

$$E = \sum_T W_T \cdot \sum_R W_R \cdot \bar{D}_{T(R)}. \quad (5.25)$$

The values of the tissue weighting factors are chosen so, that at the uniform irradiation of all the body the value of the effective dose E will be received numerically equal to the equivalent dose of all the body irradiation, the equivalent dose in every organ is the same and coincides with the equivalent dose for all the body, i. e. $H_T = H_0$ for all T where H_0 is the equivalent dose in any organ (including all the body) at the uniform irradiation. In this case formula 5.24. for the effective dose may be written in the following form:

$$E = H_0 \cdot \sum_T W_T. \quad (5.26)$$

One can see from formula 5.26 that $E = H_0$ at the condition that $\sum_T W_T = 1$, i. e. the values of the tissue weighting factors must be chosen so, that their sum by all organs will be equal to 1. The values of the tissue weighting factors taken at present are given in Table 5.5.

Table 5.5

Values of tissue weighting factors

Number	Tissue or organ	Value	Number	Tissue or organ	Value
1	Gonads	0.2	7	Milk gland	0.05
2	Red marrow	0.12	8	Liver	0.05
3	Large intestine	0.12	9	Gullet	0.05
4	Lungs	0.12	10	Thyroid gland	0.05
5	Stomach	0.12	11	Skin	0.01
6	Urinary bladder	0.05	12	Bone surfaces	0.01
			13	Rest	0.05

The values W_T given in Table 5.5, are concerned with the population with the same number of men and women and within a wide age range. The list of twelve organs for which the value of W_T is determined is called “the main list”. The “Rest” or the additional list consists of the following organs (tissues), everyone of which can be irradiated separately: adrenals (glands); brain; small intestine; upper large intestine; kidneys; muscles; pancreas; spleen; forked gland and uterus.

Organs of the main as well as the additional list are receptive to the appearance of cancer. If other organs are detected which have a significant risk of the cancer appearance, then they will be included in the main list (every organ with its weighting factor W_T) or in the additional list constituting the “Rest”. In such an exceptional case when any organ from the additional list gets the equivalent dose which is higher than the maximum dose for the main list organs, the tissue weighting factor 0.025 must be applied for this organ, and to the mean equivalent dose for the totality of organs remaining in the additional list, the tissue weighting factor 0.025 must be applied too. The equivalent dose for the “Rest” is calculated as the mean equivalent dose in all the body excluding the organs and tissues of the main list. The unit of the measuring of the effective dose in SI as well as the equivalent dose is zivert (Zv). The values of the weighting factors W_R and W_T depend on the level of knowledge in radiobiology and can be made more precise from time to time. The equivalent and the effective doses are intended for the using in the radiation safety and are suitable for the radiobiological applications. These doses provide a base for the estimation of the probability of the stochastic effects for the absorbed dose which are significantly less than thresholds for the deterministic effects.

For all considered doses (absorbed, equivalent and effective) the idea of the “dose rate” is also present. The dose rate characterizes the velocity of the dose build-up (accumulation) and is determined formally as the derivative of the dose function by the time, i. e., for example, the dose rate of the absorbed dose D is equal to dD/dt .

5.1.5.6. The additional dosimetric values

The prolonged irradiation of organs with the dose rate changing in time occurs after the radionuclide entering the organism. The integral by the time from the equivalent dose rate was named “the expected equivalent dose at the given time interval”:

$$H(t) = \int_{t_0}^{t_0+t} H(\sigma) d\sigma, \quad (5.27)$$

where t_0 is the moment of the single activity entering; t is the time interval in which the equivalent dose is determined; $H(\tau)$ is the dependence of the equivalent dose rate on the time in the organ.

In many cases the interval in which the expected dose is determined is considered to be equal to 50 years. In these cases the expected dose is called “the half – century”. The expected effective dose is determined in the same way.

The considered doses are connected with the individual irradiation. Side by side with it, a practical interest is presented also by the values concerned with the irradiation of groups and populations.

These values take into account the numbers of the irradiated population by means of the multiplication of the mean dose in a group by the number of persons in the group. By this way the received values were called “the collective doses”. At this, the equivalent dose as well as the collective effective dose may be calculated.

The collective effective dose from the radionuclide in external media may be accumulated during a prolonged time overlapping the life duration of several generations. This dose must be distinctive from the half – century expected dose. It was called by a special name “the collective dose in the limit”. This dose is applied for the estimation of a single rejection of the radionuclide in the external media or for estimation of any kind of activity accompanied by continuous rejection of the radionuclides in the external media. If the integration is fulfilled with certain limits, the corresponding collective effective dose is limited by the certain time.

5.1.6. Radioactivity parameters

Stable nuclei are in a steady state, so the probability of their decay is equal to zero. The probability of the radionuclide decay is not equal to zero because the radionuclide is a quantum-mechanical system which is in the energy excited and therefore, in an unsteady state. Radionuclides are unsteady in different measure: some are steady less and others are more unsteady. The excited state of the radionuclide is taken away as a result of the radioactive decay. After a single radioactive transformation, or the chain of ones, in the final stage the stable nucleus is formed.

In the process of radioactive transformation the nucleus of one element is transformed into the nucleus of another element. For example, at the decay of tritium the stable helium is formed and at the decay of carbon – 14 the stable nitrogen is formed. The less steady a nucleus, the more probable is its decay and with higher frequency the decay acts occur in the given totality of the radionuclide nuclei. As a quantitative measure of the radionuclide unsteadiness in the nuclear physics the decay constant λ is used and it is equal to the part of total nuclei number having the decay at the unit of time.

This determination allows to write the following differential equation of the radioactive decay:

$$dN/dt = -\lambda N, \quad (5.28)$$

where $N(t)$ is the number of radioactive nuclei being the function of time; t is the time. With the accounting of the initial condition $N(0)=N_0$ the law of the radioactive decay has the following form:

$$N(t) = N_0 \cdot \exp(-\lambda t), \quad (5.29)$$

where N_0 is the number of the radioactive nuclei at zero moment of time.

Another more obvious and used often parameter characterising the velocity of the radioactive nuclei decay, is the half-decay period $T_{1/2}$. The half-decay period is equal to the time interval during which the number of radioactive nuclei is decreased two times owing to the decay. The formula which connects the half-decay period with the decay constant can be received by means of the relationship 5.29. If to assume that $t=T_{1/2}$, in the accordance with the determination of the half-decay period, $N(T_{1/2})$ must be equal to $N_0/2$, i. e. one can write:

$$N(T_{1/2}) = N_0/2 = N_0 \cdot \exp^{-\lambda T_{1/2}}. \quad (5.30)$$

From the equation 5.30 may be determined that

$$T_{1/2} = \ln 2 / \lambda = 0.693 / X. \quad (5.31)$$

Therefore, the less half-decay period, the faster the number of radioactive nuclei is decreased in the course of time. And, therefore, the higher is the probability of their decay. A very wide range of half-decay periods is observed. There are radionuclides with very short half-decay periods in several parts of a second and, on the other hand, there are radionuclides with very long half-decay periods of several billion years. The activity A measure of a radioactive preparation is the number of decays of radioactive nuclei occurring in a unit of time. Hence, the activity of the preparation may be calculated by the formula:

$$A = \lambda \cdot N, \quad (5.32)$$

where N is the number of radioactive nuclei in preparation. In the SI the unit of the activity is the Becquerel (Bq). The activity 1 Bq has such a radioactive preparation in which 1 decay occurs in 1 second. Side by side with the main term, becquerel, the derivative units are used: mBq (milli becquerel- 10^{-3} Bq), kBq (kilo becquerel – 10^3 Bq), MBq (Mega becquerel – 10^6 Bq) and others. The out-system unit of the activity – curie (Ci) is also used. 1 curie = $3.7 \cdot 10^{10}$ Bq, or 1Bq = $2.7 \cdot 10^{-11}$ curie. The derivative units are also used: pCi (pico curie = 10^{-12} Ci); nCi (nano curie = 10^{-9} Ci), mCi (micro curie = 10^{-6} Ci), mCi (milli curie = 10^{-3} Ci), kCi (kilo curie = 10^3 Ci); MCi (Mega curie = 10^6 Ci) and others. The dimensionality of the activity in the SI has view S^{-1} .

For radioactive sources distributed in space, depending on the character of the distribution of radioactive nuclei in the source the following values are used: the specific activity, the volumetric activity, the surface activity and the linear activity.

For practice of the radiation safety it is important to have the dosimetric characteristic of the radionuclide side by side with the radionuclide energy spectrum. This characteristic is the gamma-constant. The gamma-constant is widely applied in the solution of the dosimetry problems and in protection from the ionizing radiations.

For the out-system units of the exposure dose rate the gamma-constant of the radionuclide is equal to the exposure dose rate in roentgens in one hour, generated by the nonfiltered gamma-radiation of the point isotope source with activity 1 mCi at the distance 1 cm. The calculation of gamma-constant is fulfilled in accordance with the formula:

$$\Gamma = 3.7 \cdot 10^7 \left(\frac{\text{decay}}{\text{s} \cdot \text{mCi}} \right) \cdot \sum E_i \left(\frac{\text{MeV}}{\text{quantum}} \right) \cdot n_i \left(\frac{\text{quantum}}{\text{decay}} \right) \cdot \mu_i \cdot n_i \cdot m_i \left(\frac{\text{cm}^2}{\text{g}} \right) \cdot \frac{1.6 \cdot 10^{-6} \left(\frac{\text{erg}}{\text{MeV}} \right) \cdot 3600 \left(\frac{\text{S}}{\text{hour}} \right)}{4 \cdot \pi \cdot 87.3 \left(\frac{\text{erg}}{\text{g} \cdot \text{roentgen}} \right)} \left[\frac{\text{roentgen} \cdot \text{cm}^2}{\text{hour} \cdot \text{mCi}} \right], \quad (5.33)$$

where E_i is the energy of gamma-quantums of i-line with the output n_i (quantums/decay), MeV; $\mu_i \cdot n_i \cdot m_i$ is the mass absorption factor of the energy in air for the gamma-quantums with energy E_i (cm^2/gram); 87.3 (erg/gram·roentgen) is the absorbed dose in air at the exposure dose 1 roentgen; $1.6 \cdot 10^{-6}$ (erg/MeV) is the energy equivalent of 1 MeV; 3600 seconds are in 1 hour.

In SI the gamma-constant of the radionuclide is equal to the absorbed dose rate in air in AttoGrays at 1 S, generated by the nonfiltered gamma-radiation of the point isotope source with activity 1 Bq at the distance of 1 meter. The gamma-constant of the single radionuclide in SI is calculated by the formula:

$$\Gamma = \frac{1 \left(\frac{\text{decay}}{\text{s} \cdot \text{Bq}} \right) \cdot \sum_{i=1}^K E_i \left(\frac{\text{MeV}}{\text{quantum}} \right) \cdot n_i \left(\frac{\text{quantum}}{\text{decay}} \right) \cdot \mu_i \cdot n_i \cdot m_i \left(\frac{\text{m}^2}{\text{kg}} \right) \cdot 1.6 \cdot 10^{-13} \left(\frac{\text{J}}{\text{MeV}} \right) \cdot 10^{18} \left(\frac{\text{aGy}}{\text{Gy}} \right)}{4 \cdot \pi \cdot 1 \left(\frac{\text{J}}{\text{kg} \cdot \text{Gy}} \right)} \left[\text{aGy} \cdot \text{m}^2 / \text{s} \cdot \text{Bq} \right]. \quad (5.34)$$

Besides the gamma-constant, in the SI the kerma-constant of the radionuclide is also used. The kerma-constant of the radionuclide is calculated by the same formula as the gamma-constant in the SI with a difference: instead of the mass energy absorption factor $\mu_e \cdot n_i \cdot m_i$ the mass energy transfer factor $\mu_e \cdot n_i \cdot m_i$ is used.

The gamma-equivalent of the source is applied for sources comparison by the ionizing action of their gamma-radiations. Sources of gamma-radiation, generated at the same conditions with the same exposure dose rate, have the same gamma-equivalent. The unit of the gamma-equivalent is 1 milligram – equivalent of radium. (1 mgr – eqv). Such a point radioactive source whose gamma-radiation generates the same exposure dose rate at the same other conditions as the gamma-radiation of 1 milligram of radium – 226 at the platinum filter 0.5 mm has the gamma-equivalent equal to 1 milligram-equivalent of radium.

The point source in 1 milligram-equivalent of radium – 226, being in the equilibrium with the daughter decay products, at the platinum filter 0.5 mm generates the exposure dose rate 8.4R/hour at the distance of 1 cm. The activity of 1 milligram of radium – 226 is equal to 1 millicurie. Since the gamma-constant of the radionuclide is equal to exposure dose rate in 8.4 r/hour at the distance of 1 cm from the point source with activity 1 millicurie, the gamma-constant of radium – 226 at platinum filter 0.5 mm is equal to 8.4 [R·cm²/hour·mCi].

5.2. Complex of technical means and measures for the labour safety provision in radiation defectoscopy

5.2.1. Danger factors and the safety system structure in radiation defectoscopy

There are radiation and nonradiation danger factors in radiation defectoscopy. At the radioisotopic defectoscopy the main radiation danger factor is the external irradiation of the personnel by gamma-, beta-radiation and by neutron flow from radionuclide sources. Besides, the essential contribution in the irradiation dose may be got by the bremsstrahlung radiation generated at beta-sources using and also the gamma-radiation from materials activated by the flow of neutrons. The external irradiation, depending on the used defectoscopy method, may be the common (total) (the irradiation of all body of defectoscopist) or the local (the irradiation of separate organs of the body). The uniformity degree of the defectoscopist body irradiation is influenced by the defectoscope type and by the examination technology features for the tested articles. At the examination of the massive articles by the directed radiation beam and at the panoramic examination in most cases the comparatively uniform irradiation of all body of defectoscopist takes place; but at the examination of details in almost inaccessible locations the biggest irradiation has place for hands, head area and the pelvis. The roentgen defectoscopy of articles may be accompanied by the action of direct and scattered (reflected) roentgen radiation on the personnel. The level of its action

is determined by the tension and current added to apparatus roentgen tube, by the operating regime, properties of examining material and by the exploitation conditions. One must note that at this kind of defectoscopy the assembly-adjusting operations with the roentgen defectoscope are taken to the radiation – dangerous works. When using the electron accelerators (betatrons) for the radiation defectoscopy aims, the main factors of the radiation danger are the beams of accelerated electrons rejected from the accelerator; the bremsstrahlung radiation appearing at the interaction of accelerated electrons with the target and the objects in the environment; the unused roentgen radiation from the high-voltage electronic apparatus of the accelerator.

Defectoscopes with the electron accelerator as well as the roentgen apparatus are different from the radioisotopic defectoscopes by the fact that if necessary (for example, at the labour conditions worsening), the generation of the ionizing radiation may be momentarily stopped. The main dangerous and harmful industrial factors of nonradiation nature appearing at the radiation defectoscopy are systematized in Table 5.6. They prevail in the defectoscopy of the articles when the electron accelerators are used, and a minimum of their number is applied at the exploitation of the radioisotopic defectoscopes.

Table 5.6

Main dangerous factors

Defectoscope type	High tension	Heat release	nitrogen oxides and ozone	High frequency and super-high frequency	Noise	Direct electric and magnetic fields
Radioisotopic: in the location in plant;	±*	–	+	–	–	–
on the open ground	±*	–	–	–	–	–
Roentgen: in the location in plant;	+	–	+	–	–	–
on the open ground	+	–	–	–	–	–
Electron accelerator: in the location in plant;	+	+	+	+	+	+
on the open ground	+	+	–	+	+	+

*Depending on the design and purpose of radioisotopic defectoscope.

The complex of technical means, organizational and sanitary – hygienic measures directed on the safety provision in the radiation defectoscopy fulfillment, is the system, all structural parts of which are connected with each other.

The organization of the measures concerned with the guarantee of the defectoscopist's labour safety depends on the type of the used radiation sources, on articles examination technology features, on defectoscopes disposition and planning decisions, on radiation protection system and other factors.

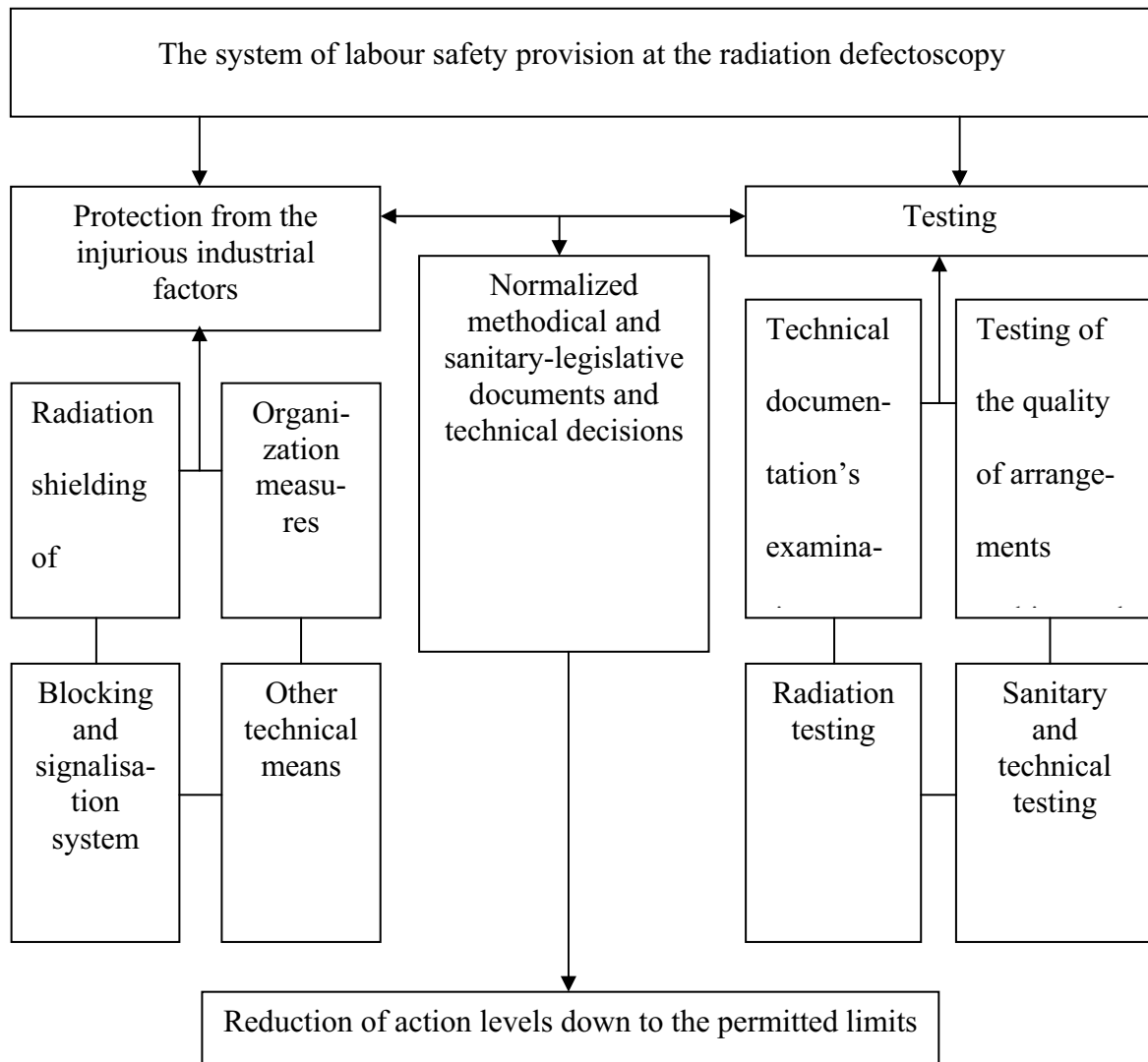


Fig. 5.1. The structure of the safe working conditions provision in the radiation defectoscopy

The monitoring of the safety standards maintenance is fulfilled on the projection stage (the examination of technical documents of the defectoscopes and the defectoscopic laboratories, etc.) as well as on the stage of technical arrangements manufacture and their exploitation (e.g. the testing of the shielding constructions quality, defectoscopes, etc.). The scheme of the radiation safety system at the defectoscopy conducting is shown in general form in Fig. 5.1.

This system consists of two sub-systems including the protection from the damage factors and the monitoring at all stages of design and

manufacture of arrangements and at their exploitation. The protection from the harmful industrial factors includes the radiation shielding, organizational measures, the blocking and signalization systems and also other technical means providing the labour safety.

In the monitoring sub-system the main attention is given to fulfilment of the radiation monitoring of the safety at the defectoscopes exploitation, to sanitary-hygienic monitoring, to examination of the technical documentation, to the shielding constructions quality testing and to the efficiency of the radiation caps of the defectoscopic arrangements.

5.2.2. Protection from the ionizing radiations

The shielding of the radiation defectoscopes must provide a reduction of the exposure dose rate and the fast neutrons flow density (at the disposition of the radiation source in the storage position) down to permissible levels.

The radiation protection of the stationary, mobile and portable defectoscopes is provided from the materials with a high atomic number Z , (e.g. uranium, lead, tungsten alloys, etc.) for the protection from bremsstrahlung radiation and from the hydrogen-containing materials for protection from neutrons. In the case of using depleted uranium as the shielding material, it is covered by the nonactive matter providing the absorption of the beta-radiation of uranium. For protection from the beta-radiation the combined shielding (aluminium, lead and so on) is used. The most optimal form of shielding is spherical or cylindrical.

During the design of the defectoscopes construction one must take into account their purpose, so the requirements to the stationary defectoscopes shielding differ from demands put forward to the protection of mobile and especially portable defectoscopes. The construction of the latter must provide a possibility of their transport and their technological manoeuvrability in the various industry conditions.

Pressured lead blocks in the hermetic housings from a high-melting material (in order to prevent the lead smelting in case of the fire), different tungsten alloys and uranium blocks in hermetic housings from the stainless steel are used in gamma-defectoscopes. The use of tungsten alloys and, especially, the use of uranium reduces significantly the mass of the defectoscope radiation cap shielding.

In containers purposed for the transportation and storage of the gamma-radiation sources, the iron cast, lead, tungsten alloys, uranium and the combination of shielding materials (lead-iron cast; lead-tungsten; lead-uranium and so on) are used as shielding materials.

For the protection from the unused radiation the roentgen tubes are inserted into the special shielding frames having windows for the working

beam output. Shielding frames are purposed also for the protection of workers from the high tension. As the insulating medium in the frames the transformer oil is applied and also the bakelite, plastics, gas SF-6 and others and as the shielding material the sheet lead with steel as the constructive material.

The massive design of the betatron magnet containing a large number of ferrum weakens significantly the unused bremsstrahlung radiation which is generated as a result of the interaction of the scattered electrons with the walls of the accelerating chamber and spread in all directions. The intensity and the angular distribution of this radiation depend considerably on the betatron design. The detailed data about the unused bremsstrahlung radiation output give a possibility to calculate the shielding housing of betatron more accurately. For protection from the unused bremsstrahlung radiation of betatron the sheet lead connected constructively with the magnet is applied. Mainly the instalments of betatron irradiator which are not protected by the magnet design are shielded by lead. The shielding construction of betatron includes also a collimator for the formation of the radiation beam of the given shape.

The calculation and the projection of the shielding facilities of the radiation defectoscopes and the shielding constructions consist in determination of the shielding thickness of radiation cap, walls, floor and roof of working chamber providing the reduction of the protection level up to the regulated meaning.

Protection from ionizing radiations must be projected with the accounting of the irradiated person category and the duration of the irradiation. For persons attributed to the category A (defectoscopists, dosimetrists and, etc.) the project dose rate on the shielding surface must not be over $1,4 \cdot 10^{-2}$ millizivert / hour (1.4 milliber/hour) in the 36-hour working week and $1,2 \cdot 10^{-2}$ millizivert / hour (1.2 milliber/hour) in 41-hour working week. In separate cases an increase of the dose rate under condition of limitation of time of the personnel presence in the radiation – dangerous zone is allowed. At the protection calculation it is assumed that the annual limitedly permissible dose of 50 millizivert (5 ber) at the uniform irradiation corresponds to the dose equal to 1 millizivert (100 milliber) during the 36-hour working week or with 0.17 millizivert (17 milliber) during the 6-hour working day. Let's consider the methods of the protection calculation mainly applied in practice.

Calculation of the protection by means of the weakening multiplicity. The weakening multiplicity K of radiation is the value that indicates by how many times it is needed to reduce the exposure dose rate of radiation – \dot{X} , the intensity, the flow density or the absorbed dose rate of radiation \dot{D} in order to receive the given readings of \dot{X}_0 or \dot{D}_0 :

$$K = \dot{X}/\dot{X}_0 \text{ or } K = \dot{D}/\dot{D}_0. \quad (5.35)$$

For the given energy of gamma-radiation and chosen shielding material the value K depends only on the shielding thickness. There are the universal tables in which the dependence of thickness of shielding from different materials (water, concrete, iron, lead, tungsten, uranium) on the energy for the point isotropic mono-energy sources of photon radiation is given as well as the weakening multiplicities by the dose for the infinite geometry. In practice the shielding facilities have the barrier geometry. For the determination of the shielding thickness by means of the universal tables for such geometry, it is necessary to multiply the required for the barrier geometry weakening multiplicity K_b by the correction δ_g and then for the received weakening multiplicity $K = K_b \cdot \delta_g$ it is necessary to determine the shielding thickness by means of the universal tables. The values of δ_g are also given in the universal tables. The accounting of the barrier geometry is essential at a low radiation energy. In the radiation defectoscopy sources with the nonmonoenergy radiation are applied most often. Therefore, it is expedient to determine the shielding thickness by means of nomograms and graphs received on the basis of experimental and theoretical data concerned with the weakening of the divergent beam of the gamma-radiation of sources applied in the defectoscopy.

For the estimation of the shielding thickness one can apply the approximate method of calculation of the shielding thickness by the weakening layers. The weakening layer $\Delta 1/k$ shows the shielding thickness which weakens the radiation dose (energy flow density, particles density and so on) by K times. At the shielding calculations the layers of half-value ($\Delta 1/2$) and tenth-value ($\Delta 1/10$) weakening are applied most often. The shielding thickness $\Delta 1/2$ corresponds to the radiation weakening multiplicity equal to 2 and the shielding thickness $\Delta 1/10$ – to 10. For the multiplicity K of radiation weakening by the shielding the needed number of half-value weakening layers n is equal to:

$$K = 2^n. \quad (5.36)$$

The value $K > 10^3$ is convenient to present as a product of two co-factors, one of which is $K = 10^3$. For example, $16000 = 16 \cdot 10^3 \approx 2^4 \cdot 2^{10}$. Then, $n = 4 + 10 = 14$ layers of half-value weakening. If the values of K and $\Delta_{1/2}$ for the given energy of gamma-radiation and chosen material are known, the shielding thickness d is determined by means of the following relationship:

$$d \approx \Delta_{1/2} \cdot n. \quad (5.37)$$

The method of the shielding calculation with the help of half-value weakening layers is approximate because the value of $\Delta_{1/2}$ for wide beams is changed for the given radiation energy and shielding material depending

on its thickness which is proportional to the weakening multiplicity. The accounting of the change of weakening layer value with the change of thickness at $K \leq 10^3$ can be conducted by using the values of weakening layers $\Delta_{1/10}$, $\Delta_{1/100}$, $\Delta_{1/1000}$. Leading off with the shielding thickness corresponding the weakening multiplicity $K > 10^3$ the value of the layer of tenth-value weakening does not change practically with the increase of shielding thickness and may be taken constant and equal to the asymptotic value $\Delta_{1/10}^{QS}$. There is a method of the shielding thickness calculation with the use of the values of $\Delta_{1/10}$, $\Delta_{1/100}$, $\Delta_{1/1000}$, $\Delta_{1/10}^{QS}$ for the weakening multiplicity $K=I \cdot 10^m$, where $1 \leq I \leq 10$; m is the integral positive number. Then the shielding thickness may be calculated with good accuracy by formulas:

at $m = 0$,

$$d = \Delta_{1/10} \cdot \xi; \quad (5.38)$$

at $m = 1$,

$$d = \Delta_{1/10} + \Delta_{1/10} \cdot \xi; \quad (5.39)$$

at $m = 2$,

$$d = \Delta_{1/100} + (\Delta_{1/100} - \Delta_{1/10}) \cdot \xi; \quad (5.40)$$

at $m \geq 3$,

$$d = \Delta_{1/1000} + \Delta_{1/10}^{QS} (m-3) + \Delta_{1/10}^{QS} \cdot \xi, \quad (5.41)$$

where ξ is the factor connecting the layer $\Delta_{1/10}$ with the layer $\Delta_{1/I}$, weakened the radiation by I times; $\Delta_{1/I} = \Delta_{1/10} \cdot \xi$; the value of ξ are

$$\xi = \ln(I/2.3).$$

There are tables of values $\Delta_{1/2}$, $\Delta_{1/10}$, $\Delta_{1/100}$, $\Delta_{1/1000}$, and $\Delta_{1/10}^{QS}$ for different materials (concrete, lead, iron and tungsten) needed for conducting the calculation of shielding.

Method of competitive lines. For the nonmonoenergy sources the shielding calculation is fulfilled with the help of the competitive lines method which comes to the calculation of shielding from the monoenergy sources by using the universal tables or by half-value weakening layers. This method consists in the following: the needed weakening multiplicity of source radiation K is determined, the partial weakening multiplicity of photons of i -energy group with the relative contribution P_i is calculated:

$$K_i = K \cdot P_i, \quad (5.42)$$

then for every K_i and E_{oi} the needed shielding thickness d_i is determined by means of universal tables or half-value weakening layers. The energy of

photons which needs the highest values of thickness of shielding d_m is named the main line of the spectrum. The energy of photons which needs the next value of shielding thickness d_c behind the main line, is named the competitive line; the finite thickness d of the shielding is determined by relationships:

$$d = d_m + \Delta_{1/2}, \text{ if } (d_m - d_c) = 0; \quad (5.43)$$

$$d = d_c + \Delta_{1/2}, \text{ if } 0 < (d_m - d_c) < \Delta_{1/2}; \quad (5.44)$$

$$d = d_m, \text{ if } (d_m - d_c) > \Delta_{1/2}. \quad (5.45)$$

In these relationships $\Delta_{1/2}$ is the highest value from the layers of half-value weakening for the main and competitive lines. The role of main and competitive lines changes depending on the weakening multiplicity.

The protection from the direct X-radiation. The X-radiation has a continuous energy spectrum with maximum energy corresponding to the nominal tension on the X-ray tube U_0 . At the calculation of the shielding from the X-radiation one must take into account the change of its spectral composition appearing owing to the stronger absorption of the low-energy components of the spectrum with the rise of the thickness of shielding layer.

The different nomograms received on the base of the experimental data are applied for the determination of the protection thickness from the direct X-radiation with the maximum energy less than 300 keV. With the help of the nomogram given in Fig. 5.2, the thickness of the needed lead protection d is found for the given values of K_1 which are determined in accordance with the formula:

$$K_1 = t \cdot I / 3R^2, \quad (5.46)$$

where t is time (duration) of irradiation in a day; I is the current in the tube, mA; R is the distance between the X-ray tube and the working location, meters. The found value of the thickness of lead protection provides a reduction of the exposure dose of radiation on the working place up to 1 millizvert (100mR) in a week.

The protection from the scattered X-radiation. The intensity and the energy of the scattered X-radiation depend on the tension, the value of the tube anodic current, the square of the irradiation in the examining object, the angle of scattering and on the material of the examined object. The determination of dependence of the intensity of the scattered X-radiation on all the above-mentioned factors is very difficult, therefore in most cases the data are used received on the base of the experimental studies. In Table 5.7 the values of

$\alpha = \dot{X}_{sc} / \dot{X}_{dir}$, received on the base of experiments, are given, where \dot{X}_{sc} is the exposure dose rate of the scattered at angle 90° X-radiation measured on

the distance 1 meter from the scatterer; \dot{X}_{dir} is the exposure dose rate of the direct beam of the X-radiation. Using the data from Table one can determine the needed thickness of the shielding from the scattered radiation.

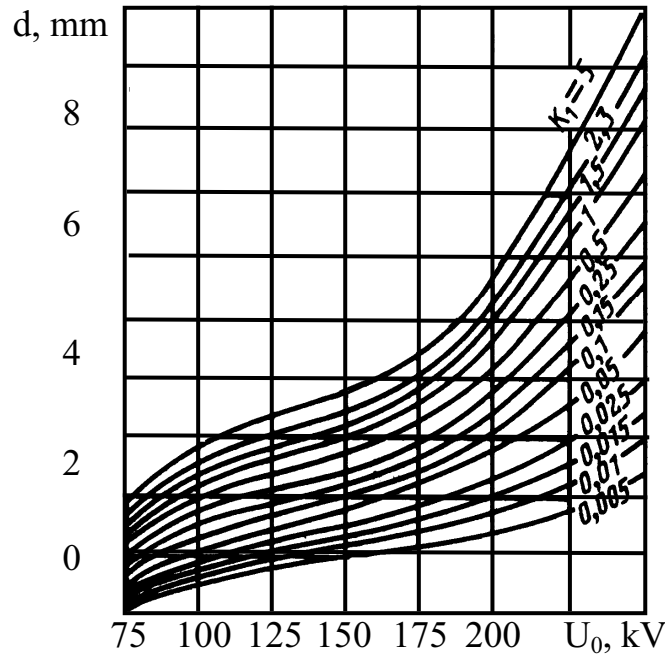


Fig. 5.2. The nomogramme for the calculation of the lead shielding thickness from the direct roentgen radiation

The protection from beta-radiation. For protection from electrons (beta-particles) it is necessary that the screen thickness should be not less than the maximum path of beta-particles in this material. The maximum path R_{al} (gram/cm²) of electrons with energy E_0 (MeV) in aluminum may be determined with the help of the following empiric formulas:

for $0.15 \text{ MeV} < E_0 < 0.8 \text{ MeV}$

$$R_{ac} = 0.407E_0^{1.38} \quad (5.47)$$

for $0.8 \text{ MeV} < E_0 < 3 \text{ MeV}$

$$R_{ac} = (0.542E_0 - 0.133). \quad (5.48)$$

Table 5.7

Values of α for different U_0 and irradiation fields

U_0 , kV	Size of irradiation field, cm	α , %
75	18×25	0.1
80	10×15	0.05
100	10×15	0.05
200	6×8	0.034
1000	20×20	0.076

For beta-particles with the continuous spectrum and the maximum energy E_0 the path R_{ac} (gram/cm²) in aluminum is determined from the following empiric relationships:

for $0.01 \text{ MeV} \leq E_0 \leq 2.5 \text{ MeV}$

$$R_{ac} = 0.412E_0^{1.265-0.218\lg E_0}; \quad (5.49)$$

for $E_0 > 2.5 \text{ MeV}$;

$$R_{ac} = 0.530E_0 - 0.706. \quad (5.50)$$

The maximum path of electrons R_X (gram/cm²) in any material can be estimated by using the formula:

$$R_X = R_{AC} \frac{(Z/A)_{AC}}{(Z/A)_X}, \quad (5.51)$$

where Z_{ac} , Z_X are the atomic numbers of aluminum and material in which the path of beta-particles is determined; A_{al} , A_X are the atomic masses of aluminum and this material.

At the calculation of protection from beta-radiation it is needed to foresee the shielding not only from beta-particles but also from the bremsstrahlung radiation appearing at the deceleration of electrons in the source or in the shielding material.

At the deceleration of mono-energy electrons with energy E_1 higher than 5 MeV in a thick target (the thickness of the thick target is equal to the maximum path of electrons) the output (yield) of bremsstrahlung radiation (MeV/decay) P is determined by the formula:

$$P = 5.77 \cdot 10^{-4} \cdot \bar{Z} \sum_{i=1}^m n_{li} E_{li}^Z. \quad (5.52)$$

The yield of bremsstrahlung radiation at the deceleration of beta-particles having a continuous spectrum, in case of the thick target it is calculated by the formula:

$$P = 1.23 \cdot 10^{-4} (\bar{Z} + 3) \sum_{i=i}^m n_{Bi} \cdot E_{Bi}^Z. \quad (5.53)$$

Here \bar{Z} is the effective atomic number of the matter in which the deceleration of beta-particles is taking place; n_{Bi} and n_{li} are yields of beta-particles and mono-energy electrons at a single decay of the nucleus, correspondingly; E_{bi} is the maximum energy of beta-spectrum, MeV; m is the number of lines of beta-particles or electrons in the radionuclide spectrum.

Formulas (5.52) and (5.53) are received under the condition that electrons (beta-particles) are fully absorbed in the source and the self-absorption of the bremsstrahlung radiation in it is absent.

At the deceleration of the accelerated electrons with maximum energy E_{\max} in the thick target, the yield of the bremsstrahlung radiation P is calculated by the formula:

$$P = 5.77 \cdot 10^{-4} \cdot \bar{Z} \cdot E_{\max}^2 . \quad (5.54)$$

The angular distribution of the bremsstrahlung radiation is calculated theoretically or determined experimentally. For the calculation one can assume that the effective energy of the bremsstrahlung radiation spectrum $E_{\text{eff}} = 1/2 E_{\max}$, if $E_{\max} \leq 10$ MeV, and that $E_{\text{eff}} = 1/3 E_{\max}$, if $10 \text{ MeV} < E_{\max} < 30 \text{ MeV}$.

At the calculation of the protection from the bremsstrahlung radiation it is useful to apply the dependences of half-value weakening layer thickness $\Delta_{1/2}$ of this radiation in different materials on the maximum energy of radiation.

Methods of calculation of shielding from the neutron radiation.

The main propositions at the neutron radiation protection calculation, based on the processes of the neutron interaction with the matter, are:

1) the protection from the neutron radiation is based on the absorption of the thermal and moderate neutrons. Fast neutrons must be first moderated;

2) neutrons with $E > 0.5$ MeV, being scattered on the nuclei of absorbing medium, experience inelastic collisions. At this nuclei transfer in excited state and then return into initial state with emission of gamma-quantums and beta-particles. At $E_n < 0.5$ MeV neutrons experience mainly the elastic scattering;

3) as a result of inelastic and elastic scatterings, neutrons are moderated up to thermal energies and at further diffusion may be absorbed in the shielding or may be left out from shielding limits; at the absorption in the shielding the capture gamma-radiation appears;

4) under the action of neutron-radiation many materials are activated (i. e. become the sources of beta-and gamma-radiation). This fact must be taken into account at the protection calculation.

For a narrow-beam of fast neutrons the weakening occurs in accordance with the formula:

$$Y_X = J \cdot e - \sum_t \cdot X , \quad (5.55)$$

where Σ_t is the total macroscopic cross-section of the shielding material:

$$\Sigma_t = \sigma_t \cdot N, \quad (5.56)$$

where $N = 6.023 \cdot 10^{23} (\rho/A)$ is the number of nuclei in 1 cm^3 of matter; σ_t is the microscopic cross-section of the shielding material; ρ is the density and A is the atomic mass of the shielding material:

$$\sum_t = \sum_s + \sum_a = \rho \cdot \frac{6.023 \cdot 10^{23}}{A} (\sigma_s + \sigma_a) , \quad (5.57)$$

where Σ_s, Σ_a are macroscopic cross-sections of scattering and absorption; σ_s, σ_a are microscopic cross-sections correspondingly.

$$J_x = J \cdot l - \frac{X}{L}, \quad (5.58)$$

where L is the relaxation length depending on E_n , shielding material, thickness of shielding and shielding geometry. There are tables in the reference books for values of L in different materials.

For a calculation of water shielding from the laboratory (α, n) – sources of neutrons one can use nomograms plotted for the limitedly permissible dose of the professional irradiation (for the personnel). Several parameters are interconnected in nomograms: the source power W (n^0/S) and distances (thicknesses) R (cm) and X (cm) or the dependence of K on X for different sources: (Po-Be); (Ra-Be); (Pu-Be) and so on.

Calculation of protection from fast neutrons with the use of the removal cross-section. For the simplified calculation of multi-layer shielding consisting of hydrogen-containing and heavy materials the theory of the fast neutron removal was suggested. In the H-containing medium the density of the neutron flow will decrease owing to the elastic scattering. In the combined medium the inelastic scattering will occur on the heavy nuclei with the subsequent effective moderation (elastic scattering) on nuclei of hydrogen so the cross-section will be significantly increased with the energy decrease.

At the isotropic scattering $\Sigma_{tot} \rightarrow \Sigma_a$, and it can be seen as the removal cross-section. But at energy of 5–10 MeV the scattering on the middle and on heavy nuclei is non-isotropic, mainly forward, therefore the Σ_{rem} is less:

$$\Sigma_{rem} = \Sigma_t - \Sigma_s \cdot \cos, \quad (5.59)$$

for $E_n = 8$ MeV the experimental value of $\Sigma_{rem} \approx (0.6-0.7)\Sigma_t$. The Σ_{rem} is determined experimentally.

The law of weakening for heterogeneous materials is

$$D(y,t) = D_n(y-t) \cdot e^{-\Sigma_{rem} \cdot t}, \quad (5.60)$$

where $D(y,t)$ is the dose of neutrons emitted in some point B at the distance y from the source S in the presence of the plate from the heavy material with the thickness t ;

$D_n(y-t)$ is the radiation dose in the H-containing material without the plate from heavy material with the thickness t

$$\Sigma_{rem} = \frac{1}{t} \ln \frac{D_n(y-t)}{D(y,t)}. \quad (5.61)$$

The removal cross-section is determined by the experimental way. The law of neutrons weakening in homogeneous materials (the uniform mix of hydrogen with heavy components) has the following form:

$$D(y, A)_M = D_n(y) \cdot e^{-\sum_{i=1}^m \sigma_{rem_i} \cdot \frac{L_0}{A_i} \cdot \rho_i \cdot y}, \quad (5.62)$$

where $D(y, A)_M$ is the neutron radiation dose at the distance y from the source in the homogeneous medium; $D_n(y)$ is the neutron radiation dose at the distance y from the source in pure hydrogen with the equivalent volumetric density; σ_{rem_i} is the microscopic cross-section of removed i -component.

The calculation of radiation weakening in the mazes. Testing of the articles quality at industrial plants is conducted often in the working chambers. The lay-out of the working chamber usually has the form of the maze (Fig. 5.3).

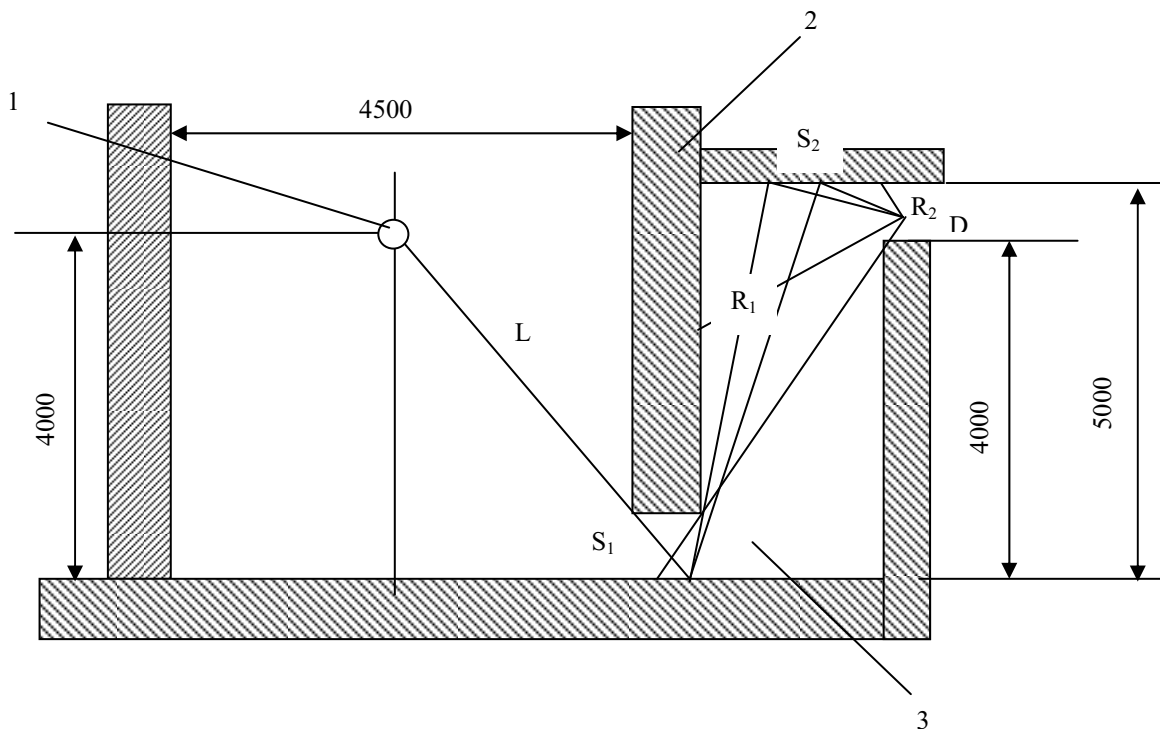


Fig. 5.3. The scheme of the working chamber maze calculation for the gamma-defectoscopy of large-sized articles:
 1 – radiation source ^{192}Ir with activity $3,7 \cdot 10^{12}$ Bq (100 Ci);
 2 – shielding (concrete); 3 – maze

Labyrinths with two turns, at passing through which the radiation undergoes at least twofold reflection, provide a reduction of the radiation dose rate on the maze output down to the permissible level at the exploitation of the X-ray – and gamma-defectoscopes of all types applied for the conducting of the radiation defectoscopy.

A calculation of the maze shielding from concrete may be fulfilled also by means of the empiric formula:

$$X^{\circ} = \frac{\bar{m}_i \cdot A \cdot K_{\gamma}}{L^2 \cdot \prod_{i=1}^2 R_i^2}, \quad (5.63)$$

where m_i is the empiric factors equal to $6.0 \cdot 10^2$ and $2.8 \cdot 10^5$ for the first and the second turn of the maze; L is the distance from the source to the centre of the square S_1 , cm; R_1 is the distance from the centre of square S_1 to the calculated point (the distance between the scattered squares S_1 and S_2 for the two-elbow maze), cm; R_2 is the distance from the centre of square S_2 to the calculated point for the two-elbow maze, cm.

The proposed calculation of mazes in the locations for the examination is suitable in the case of the exploitation of the radioisotopic gamma-defectoscopes. At the application of other sources of ionizing radiations (X-ray defectoscopes, betatrons) the order of the reflected radiation calculation is preserved. However, in the formulas given above one must use the value of the radiation yield of radiation (radiation dose rate at the distance 1 meter from the source) and the value of dose albedo must be calculated for the effective energy of radiation which is determined on the basis of data about the spectral structure of the ionizing radiation.

5.2.3. Providing of the safety at the conducting of the radiation defectoscopy

Depending on the testing article geometry the scheme of the radiation defectoscope disposition as related to the article is chosen. So, for articles of the cylindrical form the source of ionizing radiation or defectoscope can be positioned on its axis line for the directed or panoramic examining or for examining from the external side. At the examining of planes, details of machines, angles or angular constructions and also at the examining of the facilities frames the defectoscope or the source of the radiation must be disposed in such a way that the direction of the radiation beam will be normal to the examining article (Fig. 5.4).

Naturally, that in articles of different forms the weakening of the ionizing radiation occurs in a different way and the radiation field behind the testing articles is formed in a different way too. As one can see from (Fig. 5.4), the direct radiation in types 2,4–7 articles passes a longer path in material (at one and the same thickness) and, correspondingly, is absorbed more effectively than in the plane articles. Therefore, the intensity of the direct radiation behind the article of the plane form is always higher than in the rest of the cases, i. e. $d_1 < d_2 < d_3 \dots$.

The theoretical relationships for the determination of X_A (dose rate in some given point A) are needed in bulky calculations, which in the practice

of the radiation defectoscopy is not always acceptable. Besides, at the fulfillment of such calculations it is needed to draw the additional reference literature for the detection of the value of radiation albedo α_i and also the dose build-up factors B . Therefore in the industrial conditions the value of \dot{X} is determined experimentally in the given point with the help of the dosimetric devices, the safety distances are maintained for the case of the defectoscopy in the plant, field conditions and on the open grounds.

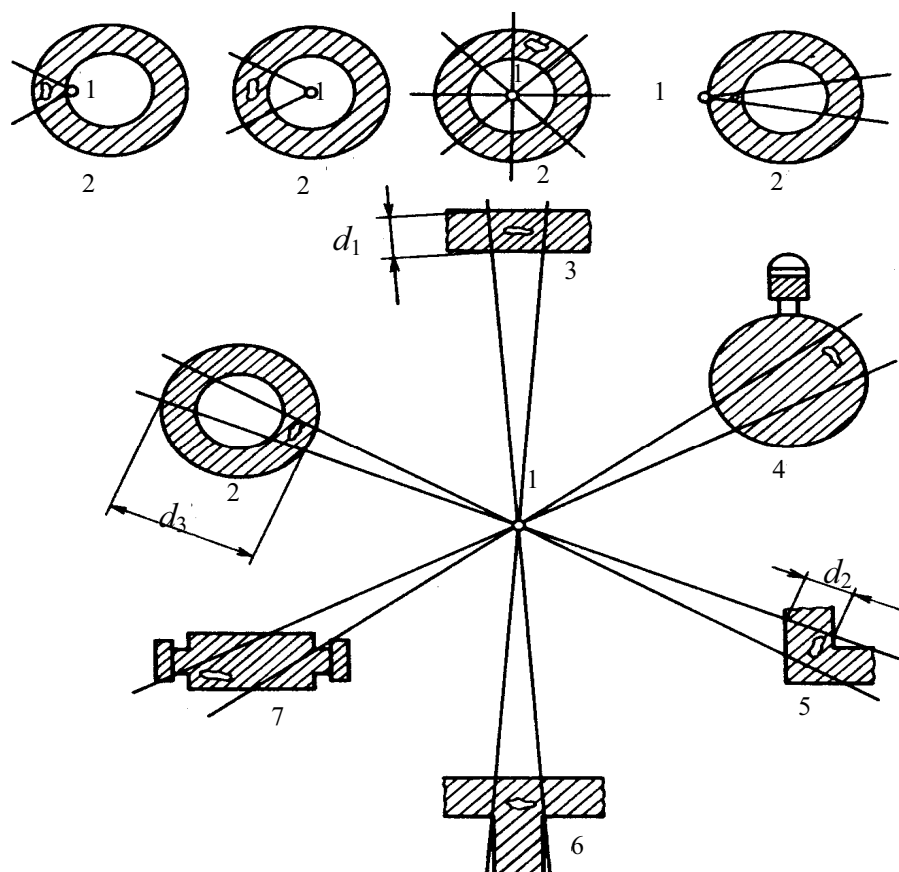


Fig. 5.4. The examining scheme for articles with the different geometry:
 1 – radiation source (defectoscope); 2 – tanks, pipes, vessels; 3 – plane;
 4 – details of machines; 5 – angle; 6 – angular constructions; 7 – housing of equipment

For providing the safety conditions for the operation of defectoscopists and persons working near the place of the examination, the articles must be examined at the minimal possible angle of the radiation working beam divergence by using for this aim collimators (diaphragms) and tubes; if necessary one must mount behind the examining article the shielding screen overlapping the radiation beam and direct it toward another side from the nearest working places; limit the articles examining time by means of using of high-sensitive films, intensifying screens, etc.; the control panel of the mobile and portable apparatus must be disposed at such a distance from the place of

examining which provides the safety conditions of the personnel labour or must be disposed behind the shielding screen. After the assembling of the shielding screens the sizes of the radiation-harmful zone and the efficiency of the shielding facilities action must be tested by means of the direct measuring of the exposure dose rate of the X-radiation with the help of dosimeters. The radiation-harmful zone must be guarded. Before the start of examining and at the time of the examining it is desirable to give the light and sonic signals.

During the design of the typical laboratory plan for gamma-and X-ray defectoscopy one must take into account the following points: the combination of gamma-and X-ray-methods of defectoscopy; the mechanization of the articles delivery to the examining location; the automation of the examination process; the optimal set of the auxiliary rooms; the building of the shielding walls and apertures with sizes needed for the reduction of the ionizing radiation level on the external surface of the shielding down to the permissible values.

The composition, number and sizes of the laboratory rooms are determined by the technical project. The sizes of rooms for the radiation defectoscopy depend on the overall dimensions of testing articles and the applied defectoscopic apparatus. In the determination of the locations sizes it is necessary to take into account the requirements of the working sanitary rules and norms of the industrial plants projection.

As a rule, the structure of a gamma-and X-ray laboratory has the following locations: working chamber (usually with the square not less than 20 m²); room for control panel with the square not less than 10–12 m²; the photolaboratory with the area not less than 10 m²; locations for the personnel, for processing of the testing results and films storage and also the sanitary-domestic rooms. The similar locations must be provided also when using the electron accelerators but in this case the working chamber square must be not less than 40 m².

The design of the defectoscopic laboratories projects and their building are fulfilled in accordance with the standards of working sanitary rules. In the technical task of the project the following parameters are indicated: the calculated data about the radiation shielding thickness of the working chamber; the applied protection materials; the requirements imposed on the disposition of locations of the defectoscopic laboratory; the requirement for the ventilation, water-supply and sewerage, heating, illumination, energetic arrangements and to the rooms finishing. It is recommended to dispose the laboratories for the radiation defectoscopy in a one-storeyed building or in one-storeyed extension because in this case the protection of the working chamber floor is not needed and lower standards are set to the protection of the roof.

The stationary radiation defectoscopes must be switched in a circuit of the doors blocking control switching off the high tension (or transferring the source in the storage position) at the opening of the door into the working chamber.

The repeated switching of the high tension (or the transfer of the source to the working position) must be fulfilled only from the control panel of the apparatus after closing the door into the working chamber. The light signalisation notifying about the necessity to leave the working chamber at once before the apparatus switching must be maintained in the working chamber, too. The floor in the working chamber and in the room for control panel must be made from the electroinsulating materials or must be covered with the dielectric rugs near the personnel working places. The light tableau is mounted on the control panel of the defectoscope and over the entrance into the working chamber having the warning inscriptions "X-ray examination" and others, illuminated during the defectoscope switching on (at the high tension switching or at the source transfer into the working position) and switched off after the examining end.

The laboratory plan and its technical task must be submitted to the departments of the capital construction and the safety techniques to the local organs of the state sanitary supervision and then are approved by the chief engineer and the director of the plant where the radiation defectoscopy is conducted.

At the finish with the construction or the laboratory repair a representative of the local organs of the sanitary supervision is asked to carry out a dosimetric testing of the laboratory rooms. The admittance of the laboratory to the exploitation is made by a commission consisting of the representatives of the interested plant, local organs of the state sanitary supervision, labour inspection, organs of the home affairs. The commission must state the accordance of the accepted object to its project and standards of the working norms and rules; the presence of the conditions of the radiation safety for the personnel and the population; the provision of the conditions for defectoscopes and radiation sources storage; the commission solves the problem of the laboratory exploitation possibility and of receiving the sources of the ionizing radiations by the plant. The commission draws up a statement of acception in which are shown the purpose of the laboratory rooms, the kind and the power of the radiation source (the nominal tension and the current of the X-ray tube, the activity of the radiation source for the radioisotopic defectoscopes, the maximum energy of the radiation and the current in the case of the using of the electrophysical type defectoscopes).

On the basis of the acception statement the local organs of the sanitary supervision mount the sanitary passport which gives the right for the radiation defectoscopy conducting. The sanitary passport is given for a period of not more than three years. The copy of the plant sanitary passport is directed to the organs of the home affairs for the registration.

The problem of the radiation safety provision at the radiation introscopy conducting may be solved much more succesfully in the case of

the television technique application in the combination with the X-ray electron-optical converter. Arrangements worked in the accordance with the scheme: X-ray electron-optical converter – the television system have the widest application in industry. Radiation introsopes with the application of the television technique not only transfer the light – shade image of the testing article onto the safety place but, at the same time, they allow to gain brightness and to increase the defects image.

Radiation introsopes, in which the television arrangements are used, are usually composed from the radiation source; electron-optical system transforming the information contained in the radiation beam passed through the examining article into the visual image; mechanical system for the fixing and the shift of the testing object. These introsopes allow to observe the image without the preliminary vision adaptation to the darkness; increase the amount of information about the testing object owing to the higher contrast sensitivity and the resolution capacity; provide the safety of defectoscopists work at the examination; give a possibility to fulfil the testing simultaneously by several defectoscopists with the help of separate television screens and to tape the television images of the examined articles. As radiation sources, in the radiation introscopy are used the same X-ray apparatus, betatrons and electrons linear accelerators as in the radiography.

5.3. Control tasks to the section “Work safety in the radiation defectoscopy”

1. Determine the value of the radiation intensity and the gamma-radiation fluency rate for two monoenergetic beams of gamma-radiation with photons energies 0.05 and 2.0 MeV, if the exposure dose rate in every beam is equal to 3 mR/s ($7.74 \cdot 10^{-7}$ Coulomb/kg).
2. Show that the following values are equivalents of the 1 Roentgen ($2.58 \cdot 10^{-4}$ Coulomb/kg): $2.08 \cdot 10^9$ of ions pairs in 1 cm^3 of air; $7.1 \cdot 10^4$ MeV on 1 cm^3 of air; $1.61 \cdot 10^{12}$ of ions pairs on a gram of air; $5.46 \cdot 10^7$ MeV on every 1 gram of air.
3. In vacuum there is some spherical surface covered uniformly by a thin nonabsorbed layer of the radioactive nuclide emitting gamma-radiation with the total (full) energy $2 \cdot 10^7$ MeV/second. Calculate the intensity of the radiation at the distance 1 meter from the sphere centre if the radius of the sphere is equal to 0.5 meters.
4. At normal conditions in 10 cm^3 of the air the number of $8.3 \cdot 10^{10}$ of ions pairs was formed under the action of gamma-radiation. What is the value of the dose calculated for 1 kg of air if the uniform irradiation is taking place in the infinitely large space?

5. What is the absorbed dose of the mixed gamma-neutron radiation in the tissue-equivalent by the atomic composite material if the exposure dose of the gamma-radiation is 0.15 R and neutron fluency is $3 \cdot 10^5$ (neutron·cm²)⁻¹? The energy of gamma-quanta is 300 keV and the neutron energy is 8 MeV.
6. The rate of gamma-quanta fluency changes in the course of time in accordance with the law: $\Phi_\gamma = \Phi_0 \cdot \exp(-t/\tau)$. The time of the irradiation is 2.4 hours; $\tau = 1.5$ hours; $\Phi_0 = 4.5 \cdot 10^9$ 1/cm²·s; the energy of gamma-quanta is 1 MeV. Find the radiation dose in units of Gray at $t = 0$, if the electron equilibrium is provided.
7. What is the fluency rate of particles of the directed monoenergetic radiation with the energy 2.5 MeV through some square when the normal to it is disposed under the angle 30° relative to the direction of the radiation spreading, if the intensity of the radiation is equal to 1.2 Watt/m²?
8. The radioactive source of gamma-radiation with the sum activity 5100 Curie of the Cobalt-60 nuclide creates in the irradiated volume the maximum exposure dose rate of 650 R/min. Determine the radiation intensity in the irradiated volume in terms of Watt/m².
9. The number of atoms in the radioactive nuclide with the activity 1.8 Curie is equal to $8.9 \cdot 10^{13}$. What is the half-life period of the given nuclide.
10. The gamma-equivalent of the radioactive preparation is 0.5 gamma-equiv of Radium. Determine the number of decays in the preparation in 1 hour.
11. Determine gamma-equivalents of radioactive preparations of ²⁴Na, ⁶⁰Co, ¹³⁷Cs and ¹⁹²Jr with the activity 10, 50, 100 and 250 milliCurie correspondingly.
12. There are five point gamma-irradiating preparations in the laboratory: Co-60, Zn-65, Ar-110, Eu-155 with the activity 10.6, 67.5, 9.8 and 103 milliCurie correspondingly, and the 10.5 milliCurie of Radium in the equilibrium with the daughter products of the decay. What kind of the source must one apply for the experiment in order to receive the maximum dose rate at the constant geometry of the experiment?
13. Find the fluency rate of electrons appearing in water the isotropic field of the photon radiation with the energy 400 keV under the electron equilibrium conditions if the dose rate is equal to 0.15 Gray/second.
14. Find the medium value of the linear energy transfer (LET) of electron in water, appearing under the action of the photon radiation if at the dose rate of 20 microGray per hour the density of electrons flow is 8.7 cm⁻²·s⁻¹.
15. Calculate the quality coefficient of neutrons with the energy 5 MeV, taking into account only the elastic scattering on the nuclei of elements composing the tissue formula, and considering that photons path in the

tissue is 250 micrometers and that the quality factor of recoil nuclei of the Carbon and Oxygen is each equal to 15.

16. Calculate the medium linear energy transfer (LET) of protons appearing in the biological tissue as the result of the elastic scattering of neutrons with the energy 8 MeV, considering that the medium protons path in the tissue is 34 milligram/cm².
17. Find the quality factor of the primary radiation, taking into account that the dose in the tissue is stipulated by the charged particles of four kinds giving the contributions 30, 40, 20 and 10 % (per cent) and having quality factors equal to 7; 1; 20; and 10 correspondingly.
18. Find the quality factor of the mixed gamma-neutron radiation, if the neutron energy is equal to 5 MeV, the density of the neutron flow is $3 \cdot 10^8 \text{ cm}^{-2} \cdot \text{s}^{-1}$ and the dose rate of gamma-radiation in the biological tissue is 0.01 Gray/second. The quality factor of neutrons is equal to 7.
19. Find the effective dose received by a human if the equivalent dose of the irradiation of lungs is 1 Zivert. The tissue weighting factor for lungs is 0.12.

REFERENCES

1. Nondestructive testing and diagnostics: Reference book/Under edition-in-chief of prof. Kluev V.V. – M.: “Mashinostrojenie” Publ. House, 1995. – 321 p.
2. Devices for the nondestructive testing of material and articles: Reference book in 2 volumes. Volume 1/ Under edition-in-chief of prof. Kluev V.V. – M.: “Mashinostrojenie” Publ. House, 1986. – 488 p.
3. Nondestructive testing: Practical text-book in 5 books. Book 4. Testing by means of radiation’s/ Under edition-in-chief of Sukhorukov V.V. – M.: “Vysshaja shkola” Publ. House, 1992. – 321 p.
4. Abramov A.I., Kazansky Ju.A. Bases of the experimental methods of the nuclear physics. – M.: “Energoatomizdat” Publ. House, 1985. – 488 p.
5. Kluev V.V., Leonov B.I., Gusev E.A. Industrial radiation introscopy. – M.: “Energoatomizdat” Publ. House, 1985. – 136 p.
6. Gurvitch A.M. Physical principles of the radiation testing and diagnostics. – M.: “Energoatomizdat” Publ. House, 1989. – 168 p.
7. Kluev V.V., Gusev E.A. Nondestructive testing by high-energy courses. – M.: “Energoatomizdat” Publ. House, 1989. – 176 p.
8. Labour safety in radiation defectoscopy: Reference book/ Under edition-in-chief of prof. Margulis U.Ya. – M.: “Energoatomizdat” Publ. House, 1986. – 208 p.
9. Obodoevsky P.M. Collection of tasks on the experimental physics: Educational text-book for the high educational institution. – M.: “Energoatomizdat” Publ. House, 1987. – 280 p.
10. Mashkovitch V.P. Shielding from the ionizing radiations: Reference book. – M.: “Energoatomizdat” Publ. House, 1982. – 296 p.
11. GOST 7512. Nondestructive testing. Welded joints. Radiographic method.
12. GOST 20426. Nondestructive testing. Radiation defectoscopic methods. Sphere of application.
13. GOST 23055. Classification of welded joints by the results of radiographic testing (inspection).
14. Norms of radiation safety HPБ-96 (NRS). Hygienic standards. – M.: Inform. – Publ. Center of Goscomsanepidnadzor (inspectors) of Russia, 1996. – 127 p.

15. Norms of radiation safety HPБ-76/87 and General sanitary Rules at working with radioactive substances and other sources of ionizing radiation OЦП-72/87. – M.: “Energoatomizdat” Publ. House, 1988. – 160 p.
16. Sanitary Rules at radiosopic defectoscopy № 1174-74. – M.: Ministry of health services of USSR, 1974. – 27 p.
17. Sanitary Rules at execution of X-ray defectoscopy № 2191-80. – M.: Ministry of health services of USSR, 1980. – 36 p.
18. Rules of safety at transportation of radioactive substances ПБТРБ-73. – M.: “Atomizdat”, 1974. – 22 p.
19. EN 444. Non-destructive testing – General principles for radiographic examination of metallic materials by X- and gamma-rays.
20. EN 473. Qualifications and certification of non-destructive testing personnel – General principles.
21. EN 584 – 1. Non-destructive testing – Industrial radiographic film – Classification of film systems for industrial radiography.
22. DIN-54109. Bildgute von Röntgen und Gamma-Filmaufnahmen an metallischen Werkstoffen.
23. ASTM E 94. Standard Practice for Radiographic Testing.
24. Rumiantsev S.V. Radiation defectoscopy. – M.: “Atomizdat” Publ. House, 1974. – 512 p.
25. Dobromyslov V.A., Rumiantsev S.V. Radiation introscopy. – M.: “Atomizdat” Publ. House, 1972. – 352 p.
26. Rumiantsev S.V., Shtanj A.S., Goltsev V.A. Reference book on radiation methods of non-destructive testing. – M.: “Energoizdat” Publ. House, 1982. – 240 p.
27. Klyiev V.V., Sosnin F.R. Theory and practice of radiation testing. – M.: “Mashinostrojenie” Publ. House, 1998. – 170 p.
28. Rumiantsev S.V., Dobromyslov V.A., Borisov O.I., Azarov N.T. Non-destructive methods of welded joints testing. – M.: “Mashinostrojenie” Publ. House, 1976. – 335 p.
29. Rumiantsev S.V., Dobromyslov V.A., Borisov O.I. Type methods of radiation defectoscopy and safety. – M.: “Atomizdat” Publ. House, 1979. – 200 p.
30. Roentgenotechnique: Reference book. In 2 books./ Under edition-in-chief of V.V. Klyiev. – M.: “Mashinostrojenie” Publ. House, Book 1. – 1992. – 480 p.; Book 2. – 1992. – 368 p.
31. Gorbunov V.I., Pokrovsky A.V. Radiometric systems of radiation testing. – M.: “Atomizdat” Publ. House, 1979. – 120 p.
32. Aleshin N.P., Shcherbinsky V.G. Testing of quality of welding works. – M.: “Vysshaja shkola” Publ. House, 1986. – 207 p.

APPENDIX 1

ANSWERS TO THE CONTROL TASKS FOR THE SECTION “PRINCIPLES OF THE RADIATION TESTING”

1. 1250.
2. “a” – at the two times increase of the anode tension; “b” – the intensity of the anode current can be increased by means of the heat current increase; “c” – at the increase of the intensity of the anode current, the number of the accelerated electrons hitting onto the target of the roentgen tube anode in time unit, increases too, and at the anode tension increase the energy of electrons is increased.
3. $6.9 \cdot 10^{12} \text{ s}^{-1}$
4. $l_{\text{tot}} = 1.9 \text{ cm}$; $l_{\text{comp}} = 2.5 \text{ cm}$; $l_{\text{ph}} = 1.5 \text{ cm}$; $l_{\text{pair}} = 1.8 \text{ cm}$; $l_{\text{tot}}^{-1} = l_{\text{ph}}^{-1} + l_{\text{comp}}^{-1} + l_{\text{pair}}^{-1}$
5. $w_{\text{ph}} = 0.013$
6. $\mu_{\text{comp m1}} = 0.039 \text{ cm}^2/\text{gr}$; $\mu_{\text{comp m2}} = 0.012 \text{ cm}^2/\text{gr}$
7. $\sigma_{\text{tot}}(1-2\varepsilon)$ and $\sigma_{\text{tot}} \cdot 3/8\varepsilon (\ln 2\varepsilon + 1/2)$
8. $w_{\text{pair}} = 0.28$.
9. 3.5 mm.
10. It is necessary for the pair formation that the gamma-quantum energy was more than $2 mc^2$, where m is the particle mass. Obviously, one can always cross into such reading system in which the gamma-quantum energy is less than $2 mc^2$ and so the pair formation is impossible. But if the given process is impossible within any single (one) system, it is impossible in any other one too.
11. 2.
12. 0.8.
13. 0.8.
14. 1 meter.
15. $M(v) = \pi/4[M_n(v) + M_n(3)/3 - M_n(5)/5 + M_n(7)/7]$;
 $M(0.5) = \pi/4[M_n(0.5) + 1/3 \cdot M_n(1.5) - 1/5 \cdot M_n(2.5) + 1/7 \cdot M_n(3.5)]$;
 $M(1) = \pi/4[M_n(1) + 1/3 \cdot M_n(3) - 1/5 \cdot M_n(5)]$;
 $M(2) = \pi/4[M_n(2)]$;
 $M(3) = \pi/4[M_n(3)]$;
 $M(4) = \pi/4[M_n(4)]$;

$$M(5) = \pi/4[M_n(5)].$$

16. $\mu \cdot x = 2.$
17. 0.01.
18. 0.08.

**ANSWERS TO THE CONTROL TASKS FOR THE SECTION
“RECEIVING AND REGISTRATION OF ROENTGEN
AND GAMMA-RADIATION”**

1. $i(t) = q(t) \cdot v(t) \cdot E/v.$
2. $\Delta t = 26$ microseconds.
3. The negative impulse. For receiving the positive impulse, one must take off the signal from the other electrode of this scheme.
4. $Q = 6 \cdot 10^{-15}$ Coulomb; Amplitude $A = 3 \cdot 10^{-4}$ V.
5. $J = j_+ + j_- = e \cdot (n_+ v_+ + n_- v_-)$; $n_+(x) = n_0 \cdot x/v$; $n_-(x) = n_0 \cdot (d-x)/v.$
6. $n \approx 10.$
7. $v_{\text{threshold}} \approx 488$ V.
8. Amplitude $A = 1$ millivolt.
9. $d = 220$ micrometers.
10. $W_p = 37$ electronVolt.
11. $n_{\text{ph}} \approx 2.2 \cdot 10^4.$
12. $L(\epsilon) = L_0 ch/\epsilon^2 \cdot \exp[-hc(1/\epsilon - 1/\epsilon_0)^2 / 2\sigma^2].$
13. The gas scintillators have advantages. Their light going out (exit) is proportional to the energy of fragments. They allow to work at considerable intensities of the background from the alpha and gamma-radiation and also have a short time of the excitation.
14. $n_{\text{ph}} = 5.1 \cdot 10^4.$
15. 1 microAmper/Lumen = 0.2 %.
16. The long-wave boundary of the spectral sensitivity of the photo multiplier is determined by the red boundary of the photo effect for the cathode material, i. e. by the photoelectric work of exit. The short-wave boundary is determined by the transparency of the backing (base layer) onto which the photocathode is placed.
17. The negative signal takes off from the anode, because the electrons are collected onto the anode.
18. $dM/M = 1.2$ %.

**LIST OF TRUE ANSWERS TO THE TEST
“RECEIVING AND REGISTRATION OF ROENTGEN
AND GAMMA-RADIATION”**

№	A	B	C	D
1				+
2		+		
3	+			
4			+	
5			+	
6			+	
7	+			
8				+
9				+
10		+		
11		+		
12			+	
13		+		
14				+
15	+			
16			+	
17		+		
18	+		+	
19				+
20		+		
21		+		
22		+		
23	+			
24			+	
25			+	
26	+			
27	+			

**ANSWERS TO TESTING QUESTIONS
FOR SECTION “RADIOGRAPHY”**

1. Solution: $l_{nT} = \frac{\Phi \cdot b}{F - b}$. Let's assume that $l_{nT} = U_2 = U_c$. Then

$$\frac{\Phi \cdot b}{F - b} = \frac{5 \cdot 1}{F - 1} = 0.06; \Phi \cdot b / l_{nT} = F - 1; F = 840(\text{mm});$$

$$U_{t,t} = \sqrt{U_2^2 + U_c^2} = 0.085(\text{mm})$$

2. Solution: use the nomograph II 5.1 (steel, apparatus PYII-200-205; tension $V = 80 \dots 200$ kV; for the PT-1 film with the tin-lead foils $d = 0.05$ mm; $F = 75$ cm; optical density $D_{opt} = 1.3 \dots 1.5$). Steel with thickness 21 mm (17 mm+4 mm) may be exposed at the tension 120...200 kV. For those tensions correspond the exposures from 90 to 3 mA·min. At the roentgen tube current 10 mA the exposure time is changed correspondingly from 9 to 0.3 min. For the better detection of defects at the relatively short exposure (time) it is expedient to conduct the exposing at the lower tension, for example, at 140 kV and exposure 20 mA·min. Therefore, $t = 2$ min at $I_a = 10$ mA.
3. Solution: the time of the exposure on the PT-1 film $t_0 = 2$ min which was found in the previous task must be multiplied by the transfer factor taking into account the difference in the films sensitivity: $t = t_0 \cdot K = 2 \cdot 1.8 = 3.6$ min.
4. Solution: $t = t_0 \cdot \frac{F^2}{F_0^2} = 4 \cdot \frac{100^2}{75^2} \approx 7$ min.
5. Solution: $l_u \approx \frac{1}{\cos \varphi} = \frac{40}{\cos 45^\circ} = \frac{40}{0.707} \approx 57$ (mm).
6. Solution: in order to use the nomograph 5.1a, it is necessary firstly to determine the equivalent thickness of steel:

$$d_{eq.Fe} = d_{Cu} \cdot \frac{(\mu/\rho)_{Cu} \cdot \rho_{Cu}}{(\mu/\rho)_{Fe} \cdot \rho_{Fe}} = 10 \cdot \frac{0.57 \cdot 8.94}{0.424 \cdot 7.89} \approx 15$$
(mm). $(\mu/\rho)_{Cu}$ and $(\mu/\rho)_{Fe}$ are the mass weakening factors of the copper and steel. Let us assume that the testing will be conducted at $V_a = 140 \dots 150$ kV. One can find in Tables that mass weakening factors in copper and steel are correspondingly 0.57 cm²/gr and 0.424 cm²/gr at $V_a = 144$ kV and $\rho_{Cu} = 8.94$ gr/cm³, $\rho_{Fe} = 7.89$ gr/cm³. These meanings are substituted into the formula for $d_{eq.Fe}$. It is seen from the nomograph 5.1a that the exposure for steel with the thickness 15 mm at $V_a = 140$ kV is 7 mA·min, i. e. at the current 5 mA the time of the exposure is 1.4 min.
7. Solution: the exposing time is determined by means of the nomograph 5.33. From the point of the intersection of exposure dose ratio value lines and the given thickness of aluminum for the Tm^{170} -source we lead a straight line in parallel to the diagonal n toward the intersection with the focal distance line. The received intersection point determines the exposure time $t \approx 0.09$ hour.
8. Solution: from the point of the intersection of the exposure dose rate values of the source by nomograph 5.34 and thickness of the steel for Co^{60} , we lead a straight line in parallel to the diagonal n toward the

intersection with the line of the focal distance F . The point of the intersection determines the line of the exposure time t . $t = 0.17$ hour.

9. Solution: according to nomograph in Fig. 4.21 (relative change of the exposure dose rate in time $P_t/P_0 \cdot 100\%$), the exposure dose rate of the source at the distance 1 meter up to the moment of the exposure is 84 % from the passport value, i. e.

$$P = 2 \cdot 10^{-3} \text{ R/s} \cdot 0.84 \approx 1.7 \cdot 10^{-3} \text{ R/s.}$$

According to nomograph in Fig. II.6.8,b we find, for the steel with the thickness 70 mm and PT-2 foil, the exposure dose $D = 5R$ at the distance

1 meter. The exposure time: $t = \frac{D}{P} = \frac{5R}{1.7 \cdot 10^{-3} (\text{R/s}) \cdot 60 (\text{s/min})} \approx 49 \text{ min.}$

10. Solution: at the focal distance change the exposure time is changed by $(F/F_0)^2$ times, where F_0 is the focal distance for which the nomograph was made (85 cm); F is the given focal distance (50 cm).

$$\text{Therefore } t = \frac{D}{P} \cdot \left(\frac{F}{F_0} \right)^2 = \frac{5}{1.7 \cdot 10^{-3} \cdot 60} \cdot \frac{2500}{7225} \approx 17 \text{ min.}$$

11. Solution: the equivalent thickness of steel $l_{\text{eq}} = l_{\text{Cu}} \cdot \frac{\rho_{\text{Cu}}}{\rho_{\text{Fe}}}$, so

$l_{\text{eq,Fe}} = 70 \cdot \frac{8.9}{7.85} = 79.4 \text{ mm.}$ Using the nomograph in Fig. II.6.8,b we find for the thickness 79.5 mm and for PT-2 film the exposure dose 6.9R at the distance 1 meter. The exposure time $t = \frac{D}{P} = \frac{6.9}{1.7 \cdot 10^{-3} \cdot 60} \approx 69 \text{ min.}$

12. Solution: using the graph in Fig. 4.21, we find the exposure dose rate of the source at the moment of exposing. It is equal to 87.5 % of the initial value, i. e. $P = 2.2 \cdot 10^{-3} \cdot 0.875 = 1.93 \cdot 10^{-3} (\text{R/s})$. The total thickness of the exposing material is $d = 45 + 5 = 50 (\text{mm})$. Using the nomograph in Fig. 6.7, a, we find for the steel with the thickness 50 mm and for PT-2 film the exposure dose $D = 0.45R$ at the distance 1 meter.

$$\text{Therefore: } t = \frac{D}{P} = \frac{0.45}{1.93 \cdot 10^{-3} \cdot 60} \approx 4 \text{ min.}$$

13. The exposure time must be increased 1.25 times.
 14. Behind 5 month, two half-decay periods have passed and the source activity is 4 times less. Therefore, the exposure time must be 4 times longer, i. e. 80 minutes.
 15. The exposure time must be 30 minutes.
 16. It is necessary to increase the exposure time to 36 minutes.

17. The exposure must be 70 mA·min, if the needed blackening density must be 2.0.

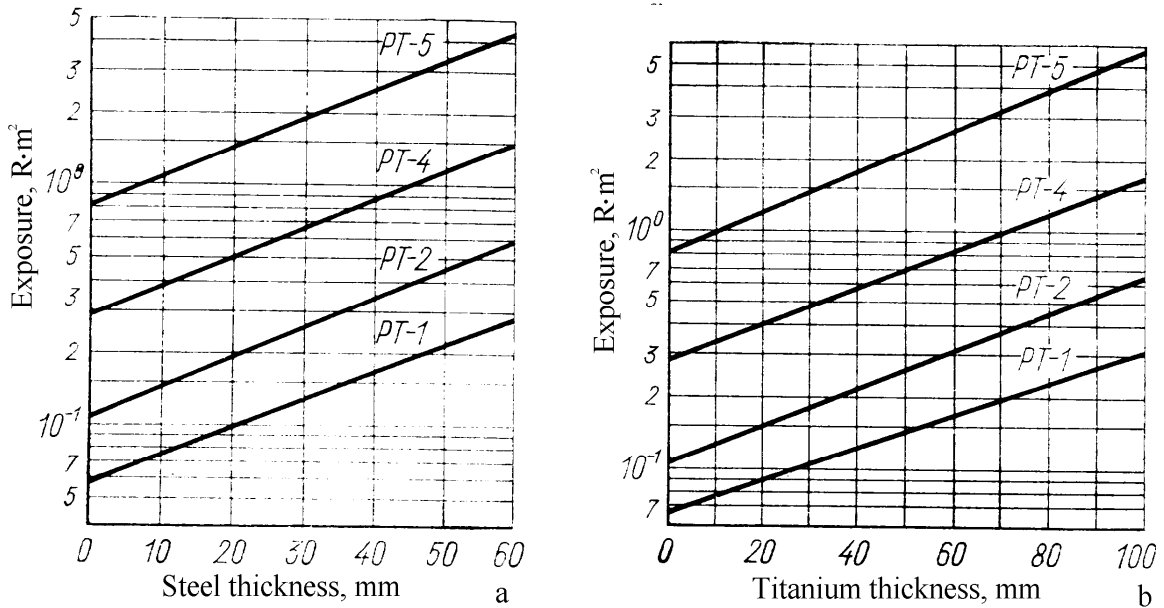


Fig. 1. Nomograms for determination of the radioscopy exposure of the steel-base (a) and titanium-base (b) alloys by gamma-radiation of Cs^{137} at the lead foils 0.1/0.2 mm thickness; $F = 50$ cm; $D_{opt} = 1.5$

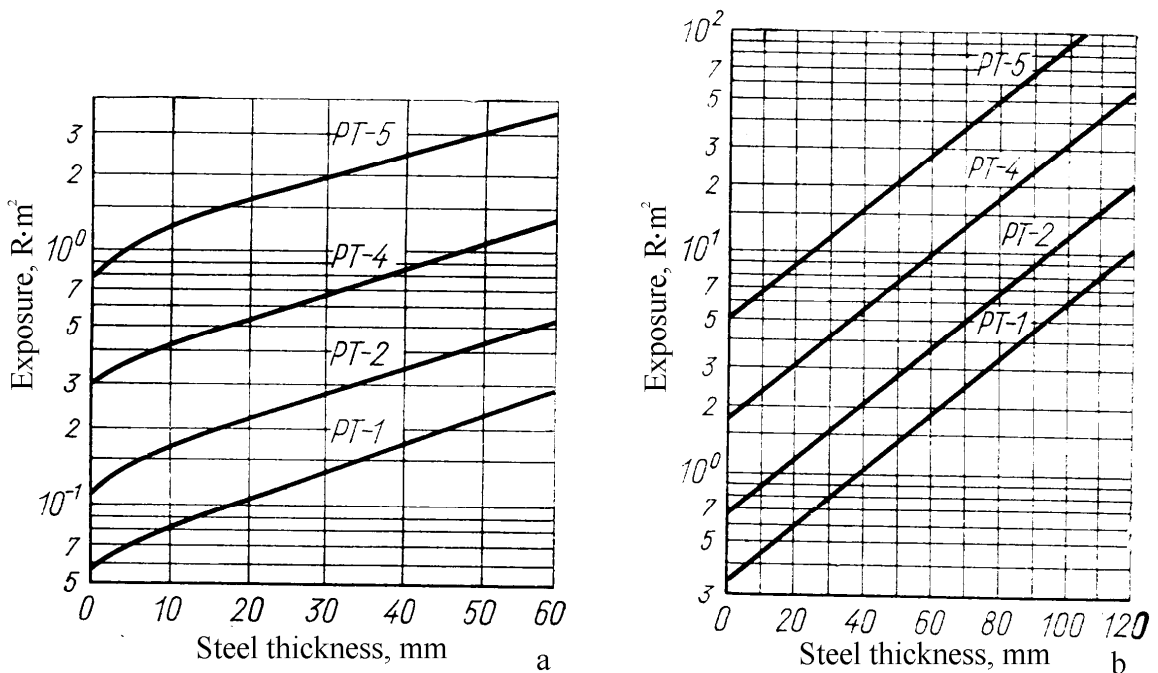


Fig. 2. Nomograms for determination of the radioscopy exposure of the steel-base alloys by gamma-radiation of Eu^{152} (a) and Co^{60} (b) on the PT-type films with lead foils having the thickness, correspondingly, 0.1/0.2 and 0.2/0.2 mm; $D_{opt} = 1.5$. For Co^{60} $F = 85$ cm, for Eu^{152} $F = 50$ cm

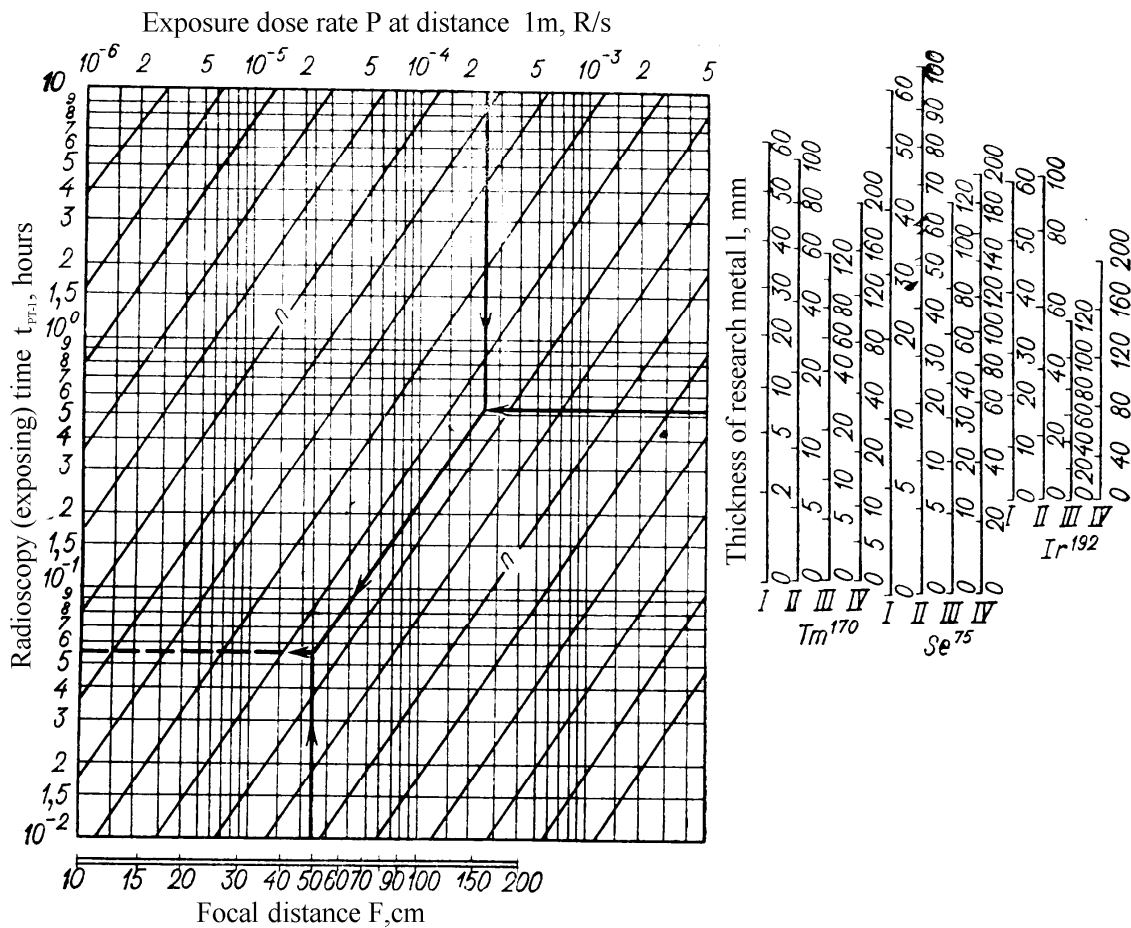


Fig. 3. Universal nomogram for determination of the radioscapy exposure of the steel-base (I), titanium-base (II), aluminum (III) and magnium (IV) on the PT-1 film (at $D_{opt} = 1.5$) by gamma-radiation from sources: Tm^{170} ($\delta_{Pb} = 0.05/0.05$ mm); Se^{75} ($\delta_{Pb} = 0.1/0.2$ mm); Ir^{192} ($\delta_{Pb} = 0.1/0.2$ mm), using the given exposure dose-rate P of the source radiation and the given thickness of the exposed material. The nomogram key: Pln, nFt

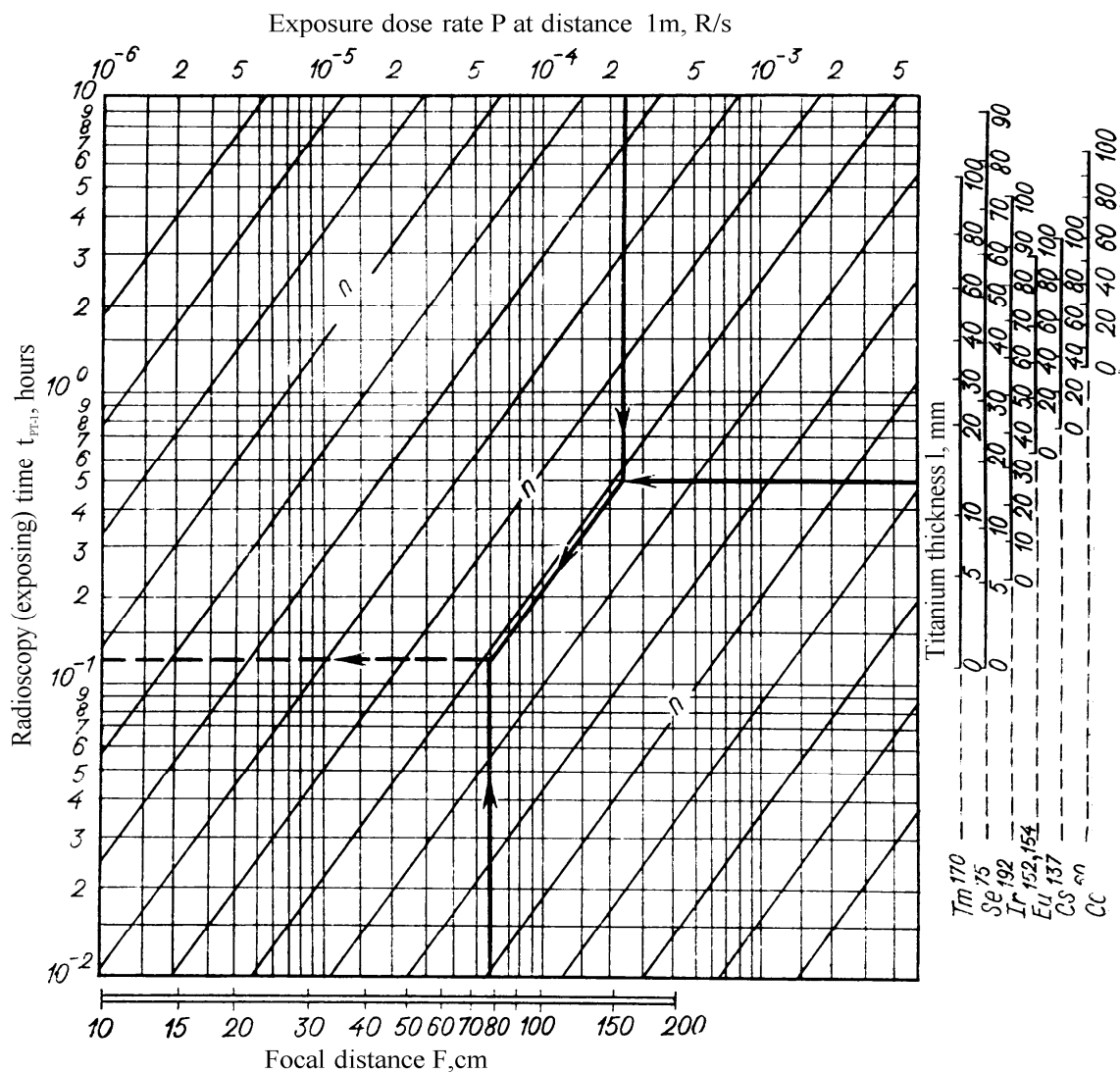


Fig. 4. Universal nomogram for determination of the radioscopy exposure of the steel-base alloys on the PT-1 film (at $D_{opt} = 1.5$) by from sources: Tm^{170} ($\delta_{pb} = 0.05/0.05$ mm); Se^{75} ($\delta_{pb} = 0.1/0.2$ mm); Ir^{192} ($\delta_{pb} = 0.1/0.2$ mm); $Eu^{152,154}$ ($\delta_{pb} = 0.1/0.2$ mm); Cs^{137} ($\delta_{pb} = 0.1/0.2$ mm); Co^{60} ($\delta_{pb} = 0.2/0.2$ mm). The nomogram key: Pln, nFt

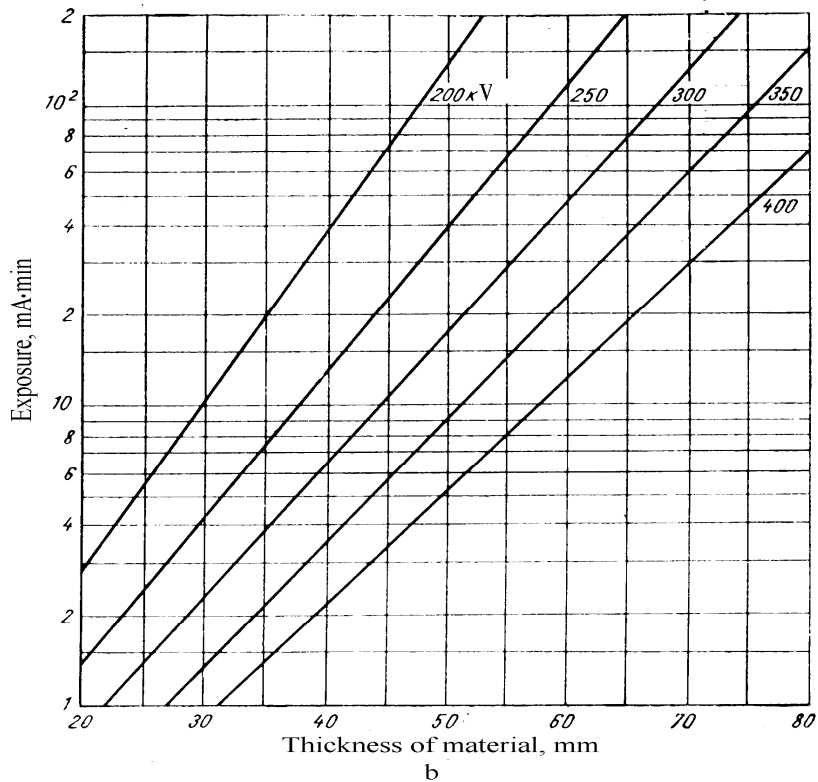
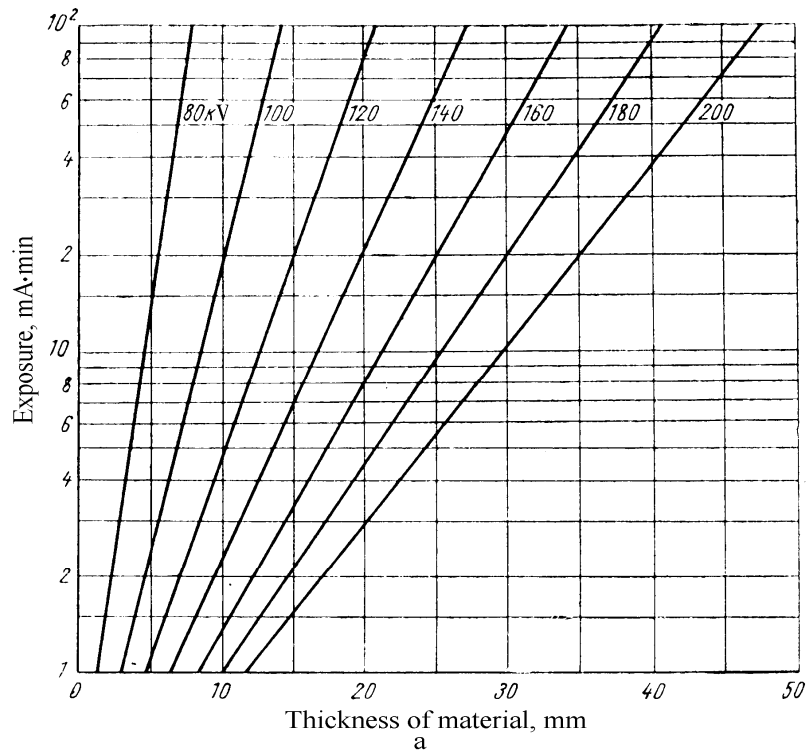


Fig. 5. The radioscopy (exposing) of the steel-based alloys by the PYII-200-20-5 apparatus; $V = 80 \dots 200$ kV (a) and by the PYII-400-5-1; $V = 200 \dots 400$ kV (b) on the PT-1 film with the tin-lead foils with thickness 0.05 mm ($F = 75$ cm; $D_{opt} = 1.3 \dots 1.5$). The roentgen tube tension is shown by figures near the corresponding straight lines

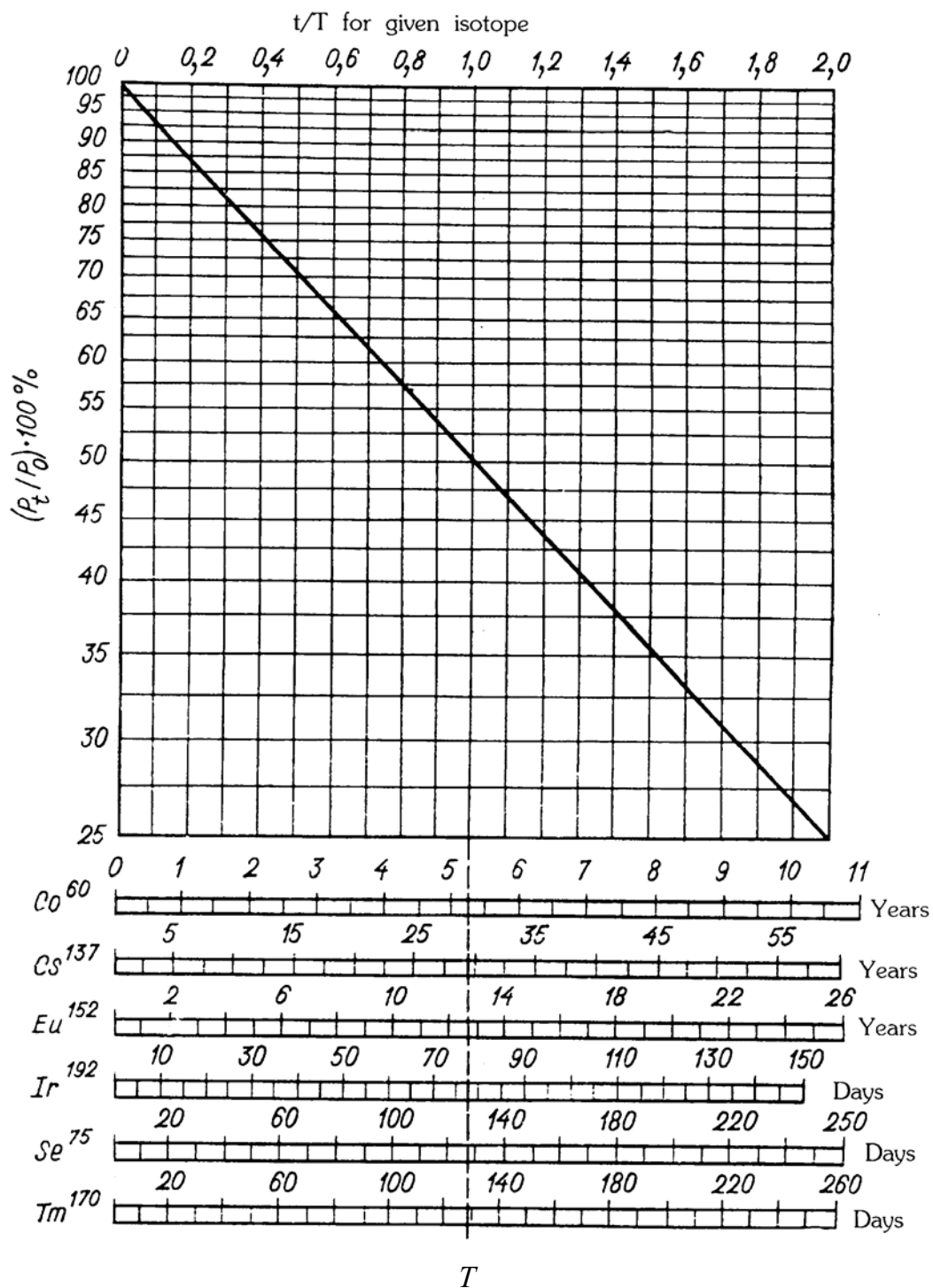


Fig. 6. Relative change in time for the exposure dose rate $P_t/P_0 \cdot 100\%$ of the radioactive sources of radiation

LIST OF TRUE ANSWERS TO THE TEST “RADIOGRAPHY”

№	A	B	C	D
1	+			
2			+	
3	+			
4				+
5				+
6				+
7		+		
8			+	
9		+		
10	+			
11			+	
12		+		
13			+	
14		+		
15		+		
16	+	+		
17				+
18	+			
19				+
20		+		
21				+

ANSWERS TO TESTING QUESTIONS FOR SECTION “RADIOSCOPY”

- Let's assume that at the absence of the defect, the testing article is the plane plate with the thickness X , onto which the uniform flow of the radiation with density $N_0 \left(\frac{\text{quanta}}{\text{m}^2 \cdot 2} \right)$ and energy E is falling. In this case, the $n_f = N_0 \cdot s \cdot t \cdot e^{-\mu x}$ quanta fall on average during the same time onto the elementary square of the converter disposed behind the plate, where μ is the linear factor of the quanta weakening. If the plate has a cavity with the depth Δx , then the elementary square of the converter is hit by the $n_d = N_0 \cdot s \cdot t \cdot e^{-\mu(x-\Delta x)}$ quanta. Therefore, the signal from the defect will be $n_0 = n_d - n_f \approx N_0 \cdot s \cdot t \cdot e^{-\mu x} \cdot \mu \cdot \Delta x$.

Since the number of quanta is the fortuity value distributed in accordance with the Poisson law, then the roof-mean-square deviation of the quanta number so, the $\delta = \sqrt{n_f} = n_{\text{noise}} = \sqrt{N_0 \cdot s \cdot t \cdot e^{-\mu x}}$ signal/noise ratio $\Psi = \frac{n_s}{n_{\text{noise}}} = (N_0 \cdot s \cdot t \cdot e^{-\mu x})^{\frac{1}{2}} \mu \Delta x$.

(10 marks)

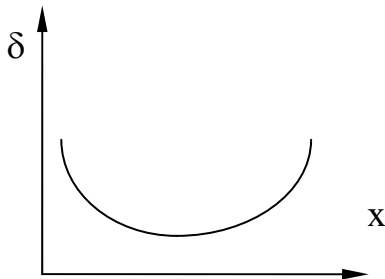
2. In the simplest case the influence of the converter is that the converter does not absorb the total quantity of radiation fallen onto it. Let's assume that the transformer has the thickness h and the linear radiation weakening factor μ_n . If one assumes that the radiation interaction occurs due to the photoeffect, i. e. the quantum, being interacted, has lost all its energy inside the converter (this event really has place at low energies for converters with high atomic number), then from n_c quanta fallen onto the converter, the number of absorbed quanta is: $n_{cn} = n_c (1 - e^{-\mu_n h})$, and from n_ϕ quanta number of absorbed is: $n_{\phi n} = n_\phi (1 - e^{-\mu_n h})$. In accordance with these, the signal/noise ratio after the interaction with the converter will be:

$$\psi = \frac{n_{cn}}{\sqrt{n_{\phi n}}} = \frac{n_c}{\sqrt{n_\phi}} (1 - e^{-\mu_n h})^{\frac{1}{2}} = \psi (1 - e^{-\mu_n h})^{\frac{1}{2}}.$$

One can see that the ratio will decrease $(1 - e^{-\mu_n h})^{\frac{1}{2}}$ times.

(5 marks).

3. The typical dependence of the relative sensitivity of the introscop on the testing article thickness expressed with the help of the relative size of the minimum detected defect, is shown in Fig. 1 where $\delta = \Delta x/x$. It is clear from Fig. 1



that the sensitivity has maximum value at mean values of x and becomes worse at increase and decrease of the thickness. The value δ is determined experimentally by means of the sensitivity standards. In accordance with state standard 7512 – 82, the wire and ditched standards are used. At using the ditched standard, $\delta = \frac{l_{\min}}{x + h_{st}}$, where l_{\min} is the depth of the minimum detected ditch, h_{st} is the standard's thickness, x is the thickness of the tested article.

Depending on the testing article's thickness, the standards of different thickness N 1, 2, 3 are used. At using the wire standard, $\delta = \frac{d_{\min}}{x}$, where d_{\min} is the diameter of the minimum detected wire. The worsening of the sensitivity at the decrease of the testing article's thickness is stipulated by the fact that the contrast sensitivity of the transmitting TV-tubes is limited and at the thickness decrease, at the constant radiation energy and constant δ , the contrast is decreased continuously, since $\delta = \mu \Delta x = \mu \delta_x$.

The worsening of the sensitivity at testing article thickness increase is stipulated, at low energies, by the increase of the built-up factor of scattered radiation and by decrease of the illumination of the photolayer of the transmitting tube, and as the consequence, by the decrease of its contrast sensitivity.

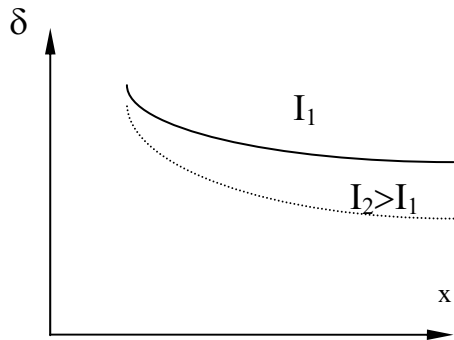
At high energies, the decrease of the signal/noise ratio occurs also simultaneously on the transmitting tube input, since

$$\psi = \left(N_0 \cdot S \cdot t \cdot e^{-\mu x} \right)^{\frac{1}{2}} \mu \Delta x .$$

(10 marks)

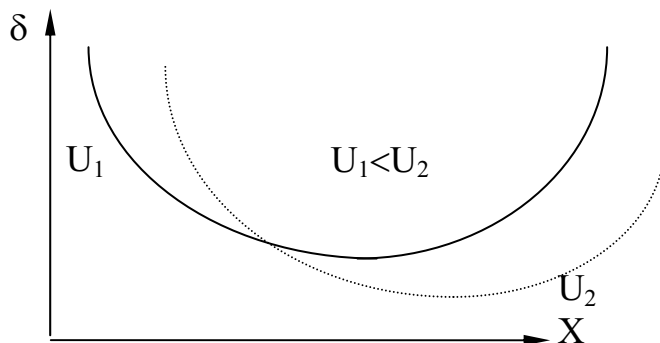
4. At the increase of the roentgen tube current and at the constant anode tension, the radiation intensity increases proportionally to the current, leading to the converter brightness increase and to the illumination increase of the photolayer. As the result, the contrast sensitivity of the transmitting TV-tube is risen in those cases where it was limited by the insufficient illumination, i. e. at the mean and large thickness of the tested article. At those values of thickness also the relative sensitivity of the introscope is increased correspondingly.

At small thickness, where the illumination was already enough for providing the nominal contrast sensitivity, the relative sensitivity of the introscope is not practically changed.



(10 marks)

5. At the increase of the roentgen tube tension, the radiation intensity increases approximately proportionally U^2 and the maximum spectral energy of quanta, leading to the decrease of μ_c – the differential factor of the radiation weakening and to the decrease of the roentgen image contrast. The influence of the scattered radiation is simultaneously decreased. Therefore the sensitivity is decreased in the area of the small thickness (δ is increased) and the sensitivity is increased in the area of large values of thickness.

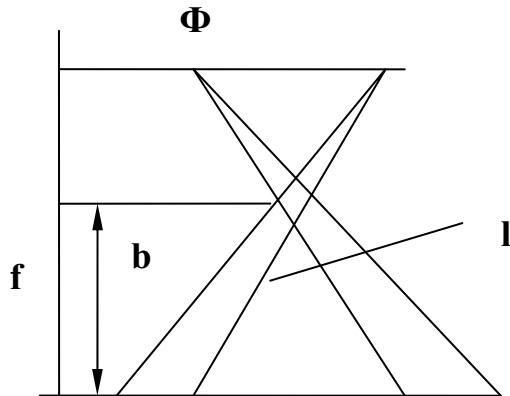


(10 marks)

6. The decrease of the focal spot size leads to the rise of the geometrical distortions. The half shade is also risen and the total shade is decreased. At the focal spot square less than the defect square, the value of the contrast is not changed. Hence, due to that the eye can detect better the image with the sharp borders then the exposure of defects becomes worse. If the focal spot is larger than the defect, then the image contrast is decreased. For the square focal spot with the size Φ and for square defect with the size l , at $l_f < b\Phi$:

$$K = \mu \Delta x \left(\frac{l \cdot f}{b \cdot \Phi} \right)^2, \text{ where } f \text{ is the focus – converter distance and } b \text{ is the}$$

defect-converter distance. So, at the same current and tension the better exposure will be provided at using the tube with a small focal spot.



(5 marks)

7. It is useful in engineering computing to change the real spectrum of the roentgen tube radiation by any equivalent monoenergetic radiation. At this, two cases are possible:

a) The initial end the and radiation in intensities are taken equal to each other (are equalised), at this one can insert the monoenergetic radiation having the linear weakening factor:

$$\mu_{\ominus} = \frac{1}{x} \ln \frac{\int_0^{E_N} S_0(E) dE}{\int_0^{E_N} S_0(E) e^{-\mu(E)x} dE}, \text{ where } S_0(E) \text{ is the energetic spectrum.}$$

b) The contrasts at the small changes of thickness are equalised, then one can insert the monoenergetic radiation having the another linear weakening factor μ_c

$$\mu_c = \frac{\int_0^{E_N} S_0(E) e^{-\mu(E)x} \mu(E) dE}{\int_0^{E_N} S_0(E) e^{-\mu(E)x} dE}.$$

There is the following relationship between μ_{\ominus} and μ_c :

$$\mu_{\ominus} - \mu_c = x \left(\frac{d\mu_{\ominus}}{dx} \right).$$

Then the roentgen image contrast is $\mathbf{K} = \mu_c \Delta x$

(10 marks)

8. The time, in which the human eye in the dark can get the 80 – percentage level of its maximum sensitivity, is 15...20 minutes.

(3 marks)

9. The minimum illumination level revealed by the human eye is 10^{-9} lux (for comparison: the threshold sensitivity of the most sensitive TV – transmitting tubes is $\sim 10^{-4} : 10^{-5}$ lux).

(3 marks)

10. The dependence of the threshold contrast on the background brightness is shown in the Table. The least threshold contrast is achieved within the range of the background brightness from 1 to 10^3 candela/m². The increase of the threshold contrast at the small brightness is explained by the brightness fluctuations but the very high brightness – by its blinding action. (4 marks)
11. If the initial intensity of the bremsstrahlung radiation is I_0 , then the absorption bremsstrahlung radiation will occur in the monocrystal and it will be equal to:

$$1. I_0 \left[1 - e^{-\left(\frac{\mu_1}{\rho_1}\right) d_1 \rho_1} \right] - \text{for NaI (Tl);}$$

$$2. I_0 \left[1 - e^{-\left(\frac{\mu_2}{\rho_2}\right) d_2 \rho_2} \right] - \text{for KI(Tl);}$$

$$3. I_0 \left[1 - e^{-\left(\frac{\mu_3}{\rho_3}\right) d_3 \rho_3} \right] - \text{for CsI(Tl).}$$

Taking into account that for $E = 4$ MeV $\left(\frac{\mu}{\rho}\right) \ll 1$ and the values $\rho_1, \rho_2, \rho_3 < 5$ gr/cm³, then, at $d = 2$ cm:

$$\left(\frac{\mu_i}{\rho_i}\right) d_i \cdot \rho_i \ll 1, \text{ therefore}$$

$$I_0 \left[1 - e^{-\left(\frac{\mu_i}{\rho_i}\right) d_i \rho_i} \right] \cong 1 - 1 + \left(\frac{\mu_i}{\rho_i}\right) d_i \rho_i = \frac{\mu_i}{\rho_i} d_i \rho_i.$$

Since the mass absorbing factors of monocrystals are approximately equal to each other, and also the thicknesses of the considered monocrystals are

the same (i. e. $\frac{\mu_1}{\rho_1} = \frac{\mu_2}{\rho_2} = \frac{\mu_3}{\rho_3}$ and $d_1 = d_2 = d_3$), then the ratio of the

absorbed energies of fallen energy 4 MeV in monocrystals **NaI(Tl)**, **KI(Tl)**, **CsI(Tl)** will be equal to the ratio of their densities ρ_1, ρ_2, ρ_3 .

(10 marks)

12. The “narrow” (pencil) beam of the ionising radiation consists, before the interaction with the matter, of the directed initial radiation and, after the interaction with it, – of the certain part of the initial radiation having interacted with the medium.

The “broad” (extended) beam of the ionising radiation consists, before the interaction with the medium, of the directed initial radiation and, after the interaction with it, – of the certain part of the initial radiation having not interacted with the medium and of the certain part of the scattered radiation.

The “pencil” beam geometry is used mainly in the radiation defectoscopy where the beam collimation on the path to the exposing object and behind it (on the defector input) allows to exclude the influence of the build-up factor on the detector signal and to obtain a high signal/noise ratio and the defectoscopic sensitivity. The “broad” beam geometry is used in radiography and radioscopy. Those methods allow to reveal the form (shape) and the character of the defects. It is characteristic for them that the image is formed at once on the total square of the exposure field and the lower signal/noise ratio due to the build-up factor influence.

(10 marks)

13. The geometrical conditions of the radioscopy are determined by the set of values: the focal spot (it is the projection of the radiation source onto the image plane); the focal distance (the distance from the radiation source to the “radiation-light” or the “radiation-signal” converter; the distance from the exposing object to the converter and by the size of the radiation field (the value of the exposed section of the object).

(5 marks)

14. The build-up factor is the value which is determined by the ratio of the broad beam intensity of the roentgen radiation behind the barrier-absorber to the intensity of narrow beam.

The scattered radiation decreases the contrast of the defect’s radiation image and, so, the probability of the defect detection decreases at build-up factor increase. The numeral values of the absolute and relative sensitivities of the defect’s testing for the most widespread in the radiation introscopy converters – the fluoroscopic screens and scintillation crystals may be determined, with taking into account the build-up factor, by means of formulas, given in [3]: $\delta = K_{th} \cdot \frac{B}{\mu}$, where K_{th} is the threshold contrast of

the eye; δ is the testing absolute sensitivity; B is the build-up factor; μ is the linear factor of the roentgen radiation weakening.

$\delta_{rel} = K_{th} \cdot \frac{B}{\mu \cdot d}$, where d is the testing object thickness in the exposed area; δ_{rel} is the relative sensitivity of the testing.

(5 marks)

LIST OF TRUE ANSWERS TO THE TEST “RADIOSCOPY”

№	A	B	C	D
1			+	
2				+
3			+	
4		+		+
5		+		
6				+
7		+		
8	+		+	
9			+	
10	+			
11		+	+	
12			+	
13	+			
14				+
15	+			

ANSWERS TO THE CONTROL TASKS FOR THE SECTION “WORK SAFETY IN THE RADIATION DEFECTOSCOPY”

1. $7 \cdot 10^{-3}$ and $11 \cdot 10^{-3}$ Joule/m²·second;
2. $9 \cdot 10^{11}$ and $3.5 \cdot 10^8$ 1/m²·second;
3. $1.05 \cdot 10^{-7}$ Joule/m²·second;
4. $3.5 \cdot 10^3$ Joule/ kg (Gray), Gy
5. $0.13 \cdot 10^{-2}$ Gy;
6. $9.5 \cdot 10^5$ Gy;
7. $2.6 \cdot 10^{12}$ 1/m²·second;
8. $3.4 \cdot 10^5$ Joule/m²·second;
9. 2.6 hours;
10. $3 \cdot 10^3$ (decays);
11. 235 for every preparation;
12. $2.6 \cdot 10^{12}$ 1/m²·second;
13. 2.1 keV/micrometer;
14. 7.4;
15. 12 keV/micrometer;
16. 3.5;
17. 6;
18. 0.12 Sivert (Sv);

APPENDIX 2

RUSSIAN – ENGLISH VOCABULARY OF STANDARDIZED TERMS AND ATTRIBUTES ON RADIATION TESTING AND DIAGNOSTICS

Term/Термин	Definition (attribute) /Определение
Радиационная техника Radiation engineering	Область техники, создающая радиационные устройства и методы их построения
Радиационное аппаратостроение Radiation apparatus engineering	Направление радиационной техники, создающее радиационные облучательные устройства и методы их построения
Радиационное приборостроение Radiation instrumentation engineering	Направление радиационной техники, создающее радиационные информационные устройства и методы их построения
Радиационное устройство Radiation device	Устройство, использующееионизирующие излучения для измерения характеристик веществ или преобразования энергии нецепных ядерных реакций в другие виды энергий или получения информации, кроме информации о характеристиках ионизирующих излучений и (или) их полей, параметрах взаимодействия ионизирующих излучений со средой, характеристиках источников ионизирующих излучений
Радиоизотопное устройство Radioisotope device	Радиационное устройство, в котором ионизирующее излучение создается радионуклидом, входящим в состав самого устройства
Радиационно-информационные устройство Information radiation device	Радиационное устройство, предназначенное для получения информации

<p>Радиационный измеритель</p> <p>Radiation meter</p>	<p>Радиационно-информационное устройство, предназначенное для получения измерительной информации</p> <p>Примечание. В зависимости от признаков, установленных ГОСТ 16263–70, радиационный измеритель может быть измерительным преобразователем, измерительным прибором, измерительной установкой, измерительной системой, в которых в качестве первичных сигналов используются радиационные сигналы</p>
<p>ИСТОЧНИКИ РАДИАЦИОННОГО ИЗЛУЧЕНИЯ</p> <p>РАДИОНУКЛИДНЫЕ ЗАКРЫТЫЕ</p> <p>SEALED RADIONUCLIDIC SOURCES OF RADIATION</p>	
<p>Рабочая поверхность закрытого радионуклидного источника ионизирующего излучения</p> <p>Рабочая поверхность источника</p> <p>Emitting area of source</p>	<p>Поверхность или часть поверхности закрытого радионуклидного источника ионизирующего излучения, предназначенная для выхода ионизирующего излучения, используемого при эксплуатации источника</p>
<p>Герметичность закрытого радионуклидного источника ионизирующего излучения</p> <p>Герметичность источника</p> <p>Containment of source</p>	<p>Свойство конструкции радионуклидного источника ионизирующего излучения препятствовать взаимным контактам радиоактивного материала и окружающей среды, исключая как загрязнения среды радиоактивным веществом, так и проникновение среды в источник выше допустимых действующими нормами уровней в условиях, предусмотренных для использования и испытания источника</p>
<p>Целостность закрытого радионуклидного источника ионизирующего излучения</p> <p>Целостность источника</p> <p>Integrity of source</p>	<p>Свойство когерентного закрытого радионуклидного источника ионизирующего излучения соответствовать техническим требованиям и по герметичности, и по внешнему виду</p>

<p>Утечка радиоактивного вещества из закрытого радионуклидного источника ионизирующего излучения</p> <p>Утечка радиоактивного вещества</p> <p>Leakage of radioactive substance</p>	<p>Перенос радиоактивного вещества из закрытого радионуклидного источника ионизирующего излучения в окружающую среду</p>
<p>Герметизирующая система закрытого радионуклидного источника ионизирующего излучения</p> <p>Герметизирующая система источника</p> <p>Containing system of source</p>	<p>Совокупность элементов конструкции закрытого радионуклидного источника ионизирующего излучения, предназначенная для обеспечения его герметичности</p>
<p>Капсула закрытого радионуклидного источника ионизирующего излучения</p> <p>Капсула</p> <p>Sealed radiation source envelope</p>	<p>Элемент конструкции закрытого радионуклидного источника ионизирующего излучения, выполненный в виде оболочки, которая обеспечивает самостоятельно или совместно с другими элементами конструкции источника его герметичность в условиях, предусмотренных для его использования</p>
<p>Тип закрытого радионуклидного источника ионизирующего излучения</p> <p>Тип источника</p> <p>Type of source</p>	<p>Разновидность закрытых радионуклидных источников ионизирующего излучения, обладающих определенной, только им присущей совокупностью конструктивных признаков и радиационно-физических характеристик</p>
<p>Подложка закрытого радионуклидного источника ионизирующего излучения</p> <p>Подложка источника</p> <p>Source backing</p>	<p>Элемент конструкции закрытого радионуклидного источника ионизирующего излучения, предназначенный для нанесения и (или) закрепления на нем радиоактивного материала</p>

<p>Активный сердечник закрытого радионуклидного источника ионизирующего излучения</p> <p>Активный сердечник источника</p> <p>Active core of source</p>	<p>Элемент конструкции закрытого радионуклидного источника ионизирующего излучения, включающий активную часть</p>
<p>Активная часть закрытого радионуклидного источника ионизирующего излучения</p> <p>Активная часть</p> <p>Active volume of source</p>	<p>Радионуклидный источник ионизирующего излучения, конструкция которого препятствует взаимным контактам радиоактивного материала и окружающей среды и исключает ее загрязнение радиоактивным веществом выше допустимого действующими нормами уровня в условиях, предусмотренных для использования источника</p>
<p>Закрытый радионуклидный источник ионизирующего излучения</p> <p>Закрытый радионуклидный источник излучения</p> <p>Закрытый источник</p> <p>Sealed radiation source</p>	<p>Область в закрытом радионуклидном источнике ионизирующего излучения, в которой распределен радиоактивный материал или радиоактивное вещество</p>
<p>Ионизирующее излучение</p> <p>Ндп. Радиоактивное излучение</p> <p>Ionizing radiation</p>	<p>Излучение, взаимодействие которого со средой приводит к образованию ионов разных знаков.</p> <p>Примечание. Общепринято видимый свет и ультрафиолетовое излучение не включать в понятие “ионизирующее излучение”</p>
<p>Непосредственно ионизирующее излучение</p> <p>Directly Ionizing radiation</p>	<p>Ионизирующее излучение, состоящее из заряженных частиц, имеющих кинетическую энергию, достаточную для ионизации при столкновении.</p> <p>Примечание. Непосредственно ионизирующее излучение может состоять из электронов, протонов, альфа-частиц и др.</p>

Косвенноионизирующее излучение Indirectly Ionizing radiation	Ионизирующее излучение, состоящее из незаряженных частиц, которые могут создавать непосредственно ионизирующее излучение и (или) вызывать ядерные превращения. Примечание. Косвенноионизирующее излучение может состоять из нейтронов, фотонов и др.
Первичноеионизирующее излучение Primary radiation	Ионизирующее излучение, которое в рассматриваемом процессе взаимодействия со средой является или принимается исходным
Вторичноеионизирующее излучение Secondary radiation	Ионизирующее излучение, возникающее в результате взаимодействия первичного ионизирующего излучения с рассматриваемой средой
Измерение ионизирующего излучения Ionizing radiation measurement	Измерение физической величины, характеризующей источник или поле ионизирующего излучения, радиоактивные образцы или взаимодействие ионизирующих излучений с веществом
Нуклид Nuclide	Вид атома с данными числами протонов и нейтронов в ядре
Радионуклид Radionuclide	Нуклид, обладающий радиоактивностью
Изотоп Isotope	Нуклид с числом протонов в ядре, свойственным данному элементу
Радиоизотоп Radioisotope	Изотоп, обладающий радиоактивностью
Фотонное ионизирующее излучение Фотонное излучение Photon radiation	Электромагнитное косвенное ионизирующее излучение
Гамма-излучение Ндп. Гамма-лучи Gamma-radiation	Фотонное излучение, возникающее при изменении энергетического состояния атомных ядер или аннигиляции частиц

Тормозное излучение Brake (bremsstrahlung) radiation	Фотонное излучение с непрерывным энергетическим спектром, возникающее при уменьшении кинетической энергии заряженных частиц
Характеристическое излучение Characteristic radiation	Фотонное излучение с дискретным энергетическим спектром, возникающее при изменении энергетического состояния электронов атома
Рентгеновское излучение Ндп. Рентгеновские лучи Рентгеновы лучи Лучи Рентгена X-radiation	Фотонное излучение, состоящее из тормозного и (или) характеристического излучений
Корпускулярное излучение Corpuscular radiation	Ионизирующее излучение, состоящее из частиц с массой, отличной от нуля. Примечание. Нейтринное излучение также относится к корпускулярному излучению
Альфа-излучение Ндп. Альфа-лучи Alpha-radiation	Корпускулярное излучение, состоящее из α -частиц, испускаемых при ядерных превращениях
Электронное излучение Electron radiation	Корпускулярное излучение, состоящее из электронов и (или) позитронов
Бета-излучение Ндп. бета-лучи Beta-radiation	Электронное излучение, возникающее при бета-распаде ядер или нестабильных частиц
Фотоэлектроны Photoelectrons	Электронное излучение, возникающее при фотоэлектрическом взаимодействии фотонного излучения с веществом
Комптоновские электроны Compton-electrons	Электронное излучение, возникающее при комптоновском (некогерентном) рассеянии фотонного излучения
Протонное излучение Proton radiation	Корпускулярное излучение, состоящее из ядер ^1H

Нейтронное излучение Neutron radiation	Корпускулярное излучение, состоящее из нейтронов. Примечания: 1. Нейтроны, испускаемые при делении атомных ядер, называются нейтронами деления. 2. Нейтроны, испускаемые при взаимодействии фотонного излучения с атомными ядрами, называются фотонейтронами
Тепловые нейтроны Thermal neutrons	Нейтронное излучение, находящееся в термодинамическом равновесии с рассеивающими атомами среды
Быстрые нейтроны Fast neutrons	Нейтронное излучение с энергией нейтронов в интервале от 200 до 20 МэВ
Космическое излучение Ндп. Космические лучи Cosmic radiation	Ионизирующее излучение, состоящее из первичного ионизирующего излучения, поступающего из космического пространства, и вторичного излучения, возникающего в результате взаимодействия первичного ионизирующего излучения со средой
Моноэнергетическое ионизирующее излучение Ндп. Монохроматическое излучение Monoenergetic radiation	Ионизирующее излучение, состоящее из фотонов одинаковой энергии или частиц одного вида с одинаковой кинетической энергией
Смешанное ионизирующее излучение Ндп. Немонохроматическое излучение Polyenergetic radiation	Ионизирующее излучение, состоящее из частиц различного вида или из частиц и фотонов
Направленное ионизирующее излучение Directional radiation	Ионизирующее излучение с выделенным направлением распространения

ХАРАКТЕРИСТИКИ ИОНИЗИРУЮЩИХ ИЗЛУЧЕНИЙ И ИХ ПОЛЕЙ CHARACTERISTICS OF IONIZING RADIATIONS AND FIELDS OF RADIATION	
<p>Естественный фон ионизирующего излучения</p> <p>Естественный фон</p> <p>Natural background radiation</p>	<p>Ионизирующее излучение, состоящее из космического излучения и ионизирующего излучения естественно распределенных природных радиоактивных веществ</p>
<p>Фон ионизирующего излучения</p> <p>Фон</p> <p>Background radiation</p>	<p>Ионизирующее излучение, состоящее из естественного фона и ионизирующих излучений посторонних источников</p>
<p>Поток ионизирующих частиц</p> <p>Particles flux</p>	<p>Отношение числа ионизирующих частиц dN, падающих на данную поверхность за интервал времени dt к этому интервалу</p> $\Phi_n = \frac{dN}{dt}$
<p>Плотность потока ионизирующих частиц</p> <p>Particles flux density</p>	<p>Отношение потока ионизирующих частиц $d\Phi_n$, проникающих в объем элементарной сферы, к площади поперечного сечения dS этой сферы</p> $\varphi = \frac{d\Phi_n}{dS}$
<p>Поток энергии ионизирующих частиц</p> <p>Particle energy flux</p>	<p>Отношение суммарной энергии (исключая энергию покоя) dE всех ионизирующих частиц, падающих на данную поверхность за интервал времени dt, к этому интервалу $\Phi = \frac{dE}{dt}$</p> <p>Примечание. Суммарная энергия всех ионизирующих частиц не включает энергию покоя</p>
<p>Плотность потока энергии ионизирующих частиц</p> <p>Particle energy flux density</p>	<p>Отношение потока энергии ионизирующих частиц $d\Phi$, проникающих в объем элементарной сферы, к площади поперечного сечения dS этой сферы</p> $\varphi = \frac{d\Phi}{dS}$

Перенос ионизирующих частиц Particle fluence	Отношение числа ионизирующих частиц dN , проникающих в объем элементарной сферы, к площади поперечного сечения dS этой сферы $F_N = \frac{dN}{dS}$
Перенос энергии ионизирующих частиц Particle energy fluence	Отношение суммарной энергии (исключая энергию покоя) dE всех ионизирующих частиц, проникающих в объем элементарной сферы, к площади поперечного сечения dS , этой сферы, $F = \frac{dE}{dS}$
ПАРАМЕТРЫ ВЗАИМОДЕЙСТВИЯ ИОНИЗИРУЮЩИХ ИЗЛУЧЕНИЙ СО СРЕДОЙ PARAMETERS OF IONIZING RADIATION INTERACTIONS WITH MATTER	
Энергетический спектр ионизирующих частиц Energy radiation spectrum	Распределение ионизирующих частиц по энергии. Примечание. Аналогичным образом строят определения временного и пространственного спектров ионизирующих частиц
Эффективная энергия фотонного излучения Effective photon radiation energy	Энергия фотонов такого моноэнергетического фотонного излучения, относительное ослабление которого в поглотителе определенного состава и определенной толщины такое же, как у рассматриваемого немонаэнергетического фотонного излучения
Граничная энергия спектра бета-излучения Maximum energy of beta-radiation	Наибольшая энергия бета-частиц в непрерывном энергетическом спектре бета-излучения данного радионуклида
Средняя энергия спектра бета-излучения Beta-particles mean energy	Средняя энергия бета-частиц, определяемая по энергетическому спектру бета-излучения данного радионуклида
Поглощенная доза излучения Доза излучения Absorbed dose	Отношение средней энергии dE , переданной ионизирующим излучением веществу в элементарном объеме, к массе dm вещества в этом объеме, $D = \frac{dE}{dm}$

<p>Мощность поглощенной дозы излучения</p> <p>Мощность дозы излучения</p> <p>Absorbed dose rate</p>	<p>Отношение приращения поглощенной дозы излучения dD за интервал времени dt к этому интервалу</p> $P = \frac{dD}{dt}$
<p>Керма</p> <p>Kerma</p>	<p>Отношение суммы первоначальных кинетических энергий dE_N всех заряженных частиц, появившихся под действием косвенно ионизирующего излучения в элементарном объеме специального вещества, к массе dm вещества в этом объеме</p> $K = \frac{dE_N}{dm}$ <p>Примечание. В качестве специального вещества применяют: воздух—для фотонного излучения, биологическую ткань—для косвенно ионизирующих излучений, используемых в медицине и в биологии, и любой подходящий материал—при излучении радиационных эффектов</p>
<p>Мощность кермы</p> <p>Kerma rate</p>	<p>Отношение приращений кермы dK за интервал времени dt к этому интервалу</p> $K = \frac{dK}{dt}$
<p>Экспозиционная доза фотонного излучения</p> <p>Экспозиционная доза</p> <p>Exposure dose</p>	<p>Отношение суммарного заряда dQ всех ионов одного знака, созданных в воздухе, когда все электроны и позитроны, освобожденные фотонами в элементарном объеме воздуха с массой dm, полностью остановились в воздухе, к массе воздуха в указанном объеме</p> $D_0 = \frac{dQ}{dm}$
<p>Массовый коэффициент ослабления</p> <p>Mass attenuation factor</p>	<p>Отношение линейного коэффициента ослабления к плотности δ среды, через которую проходит косвенно ионизирующее излучение</p> $\mu / \delta = -\frac{1}{\rho N} \cdot \frac{dN}{dl}$ <p>Примечание. Для нейтронного излучения массовый коэффициент ослабления равен отношению произведений постоянной Авогадро на микроскопическое сечение взаимодействия нейтронов данной энергии с веществом к молярной массе вещества</p>

<p>Линейный коэффициент ослабления</p> <p>Linear attenuation factor</p>	<p>Отношение доли $\frac{dN}{N}$ косвенно ионизирующихся частиц данной энергии, претерпевших взаимодействие при прохождении элементарного пути dl в среде, к длине этого пути</p> $\mu = -\frac{1}{N} \cdot \frac{dN}{dl}$ <p>Примечание: под воздействием здесь подразумеваются процессы, в которых изменяется энергия и (или) направление движения косвенно ионизирующих частиц. Для фотонного излучения линейный коэффициент ослабления равен сумме линейных коэффициентов ослабления, обусловленных фотоэффектом, комптоновским (некогерентным) рассеянием и образованием электронно-позитронных пар</p>
<p>Средний линейный пробег ионизирующей частицы</p> <p>Mean linear range</p>	<p>Средняя глубина проникновения ионизирующей частицы в данном веществе в заданных условиях</p>
<p>ИСТОЧНИКИ ИОНИЗИРУЮЩИХ ИЗЛУЧЕНИЙ</p> <p>SOURCES OF IONIZING RADIATION</p>	
<p>Источник ионизирующего излучения</p> <p>Ionizing radiation source</p>	<p>Объект, содержащий радиоактивный материал или техническое устройство, испускающее или способное испускать ионизирующее излучение</p>
<p>Радиоактивный материал</p> <p>Вещество</p> <p>Radioactive materials</p>	<p>Материал (вещество), в состав которого входит радионуклид или радионуклиды</p>
<p>Радионуклидный источник излучения</p> <p>Radioactive source</p>	<p>Источник ионизирующего излучения, содержащий радиоактивный материал</p>
<p>Контрольный источник ионизирующего излучения</p> <p>Контрольный источник</p> <p>Monitoring source</p>	<p>Радионуклидный источник ионизирующего излучения, предназначенный для проверки средств измерений ионизирующих излучений</p>

Образцовый источник ионизирующего излучения Образцовый источник Reference source	Радионуклидный источник ионизирующего излучения, предназначенный для проверки по нему других средств измерений ионизирующих излучений и утвержденный в установленном порядке в качестве образцовой меры радиационного параметра или радиационных параметров
ХАРАКТЕРИСТИКИ РАДИОАКТИВНЫХ ОБРАЗЦОВ И ИСТОЧНИКОВ ИОНИЗИРУЮЩИХ ИЗЛУЧЕНИЙ CHARACTERISTICS OF RADIOACTIVE MODELS AND SOURCES OF IONIZING RADIATION	
Активность радионуклида в источнике (образце) Активность радионуклида Activity	Отношение числа dN спонтанных ядерных переходов из определенного ядерно-энергетического состояния радионуклида, происходящих в данном его количестве за интервал времени dt , к этому интервалу $A = \frac{dN}{dt}$ Примечание. Под “определенным ядерно-энергетическим состоянием” радионуклида подразумевается его основное состояние, если не указано какое-либо другое состояние
Удельная активность радионуклида Specific activity	Отношение активности радионуклида в радиоактивном образце к массе образца
Объемная активность радионуклида Volumetric activity	Отношение активности радионуклида в радиоактивном образце к объему образца
ОБЩИЕ МЕТОДЫ ИЗМЕРЕНИЙ ИОНИЗИРУЮЩИХ ИЗЛУЧЕНИЙ GENERAL METHODS OF IONIZING RADIATION’S MEASUREMENT	
Ионизационный метод измерений ионизирующих излучений Ионизационный метод Ionizing method	Метод измерений ионизирующих излучений, основанный на измерении ионизационного эффекта, возникающего в веществе чувствительного объема ионизационного детектора под воздействием ионизирующего излучения

Сцинтилляционный метод измерения ионизирующих излучений Сцинтилляционный метод Scintillation method	Метод измерений ионизирующих излучений, основанный на регистрации и анализе сцинтилляций, возникающих в веществе чувствительного объема сцинтилляционного детектора под воздействием ионизирующего излучения
Фотолюминесцентный метод измерений ионизирующих излучений Фотолюминесцентный метод Photoluminiscent method	Метод измерений ионизирующих излучений, основанный на измерении люминесценции вещества чувствительного объема радиолюминесцентного детектора при фотостимулированном освобождении энергии, запасенной в этом веществе под воздействием ионизирующего излучения
Термолюминесцентный метод измерений ионизирующих излучений Термолюминесцентный метод Thermoluminiscent method	Метод измерений ионизирующих излучений, основанный на измерении люминесценции вещества чувствительного объема термолюминесцентного детектора при термостимулированном освобождении энергии, запасенной в этом веществе под воздействием ионизирующего излучения
Калориметрический метод измерений ионизирующих излучений Калориметрический метод Calorimetrique method	Метод измерений ионизирующих излучений, основанный на измерении тепловой энергии, получаемой калориметрическим детектором в результате преобразования переданной энергии ионизирующего излучения в тепловую
Эмиссионный метод измерений ионизирующих излучений Эмиссионный метод Emission method	Метод измерений ионизирующих излучений, основанный на измерении числа заряженных частиц, испускаемых веществом чувствительного объема эмиссионного детектора под воздействием ионизирующего излучения
Фотографический метод измерений ионизирующих излучений Фотографический метод Photographic method	Оптический метод измерения ионизирующих излучений, осуществляемый посредством измерения изменения под воздействием ионизирующего излучения оптической плотности светочувствительного материала после его проявления

Химический метод измерений ионизирующих излучений Химический метод Chemical method	Метод измерений ионизирующего вещества, основанный на измерении концентрации продуктов радиационно-химических реакций в веществе химического детектора под воздействием ионизирующего излучения
Спектрометрический метод измерений ионизирующих излучений Спектрометрический метод Spectrometric method	Метод измерений ионизирующих излучений, основанный на измерении распределения измеряемой характеристики ионизирующего излучения по заданному параметру
Активационный метод измерений ионизирующих излучений Активационный метод Activation method	Метод ядерных реакций, осуществляемый посредством измерения активности радионуклидов, образующихся в веществе активационного детектора под воздействием ионизирующего излучения
Метод счета ионизирующих частиц Counting method	Метод измерения ионизирующих излучений, основанный на измерении числа отдельных актов взаимодействия ионизирующих частиц с веществом чувствительного объема
МЕТОДЫ ИЗМЕРЕНИЯ КОЭФФИЦИЕНТА КАЧЕСТВА ИОНИЗИРУЮЩИХ ИЗЛУЧЕНИЙ METHODS OF MEASURING OF QUALITY FACTOR OF IONIZING RADIATION	
Метод линейной передачи энергии Метод ЛПЭ Linear energy transfer method	Спектрометрический метод измерения коэффициента качества ионизирующих излучений, осуществляемый с помощью спектрометра линейной передачи энергии
Метод колонной рекомбинации Column recombination method	Ионизационный метод измерения коэффициента качества ионизирующих излучений, осуществляемый с помощью ионизационной камеры, работающей в режиме колонной рекомбинации

Радиоактивность Radioactivity	Самопроизвольное превращение неустойчивого нуклида в другой нуклид, сопровождающееся испусканием ионизирующего излучения
Ионизирующая частица Ionizing particle	Частица корпускулярного ионизирующего излучения или фотон
Сопутствующая частица Accompanying particle	Ионизирующая частица, возникающая в ядерной реакции одновременно с другой частицей, принимаемой за основную
Сопутствующее излучение Accompanying radiation	Излучение, сопровождающее измеряемое ионизирующее излучение, но не являющееся объектом измерения должно быть по возможности исключено или уменьшено
ДЕТЕКТОРЫ ИОНИЗИРУЮЩИХ ИЗЛУЧЕНИЙ, СЦИНТИЛЛЯЦИОННЫЕ SCINTILLATION DETECTORS OF IONIZING RADIATION	
Сцинтилляционный детектор ионизирующего излучения Детектор Scintillation detector	Радиолуминесцентный детектор, в котором используется сцинтиллирующее вещество, испускающее кванты света под воздействием ионизирующего излучения и конструкция которого обеспечивает оптическую связь непосредственно или через световод с фоточувствительным устройством
Гетерогенный сцинтилляционный детектор ионизирующего излучения Гетерогенный детектор Geterogeneous detector	Сцинтилляционный детектор ионизирующего излучения, состоящий из одного или нескольких сцинтилляторов и светопроводящей среды
Дисперсный сцинтилляционный детектор ионизирующего излучения Дисперсный детектор Dispersion detector	Гетерогенный сцинтилляционный детектор ионизирующего излучения, в котором сцинтиллирующее вещество диспергировано в прозрачной среде

<p>Воздухоэквивалентный сцинтилляционный детектор ионизирующего излучения</p> <p>Воздухоэквивалентный детектор</p> <p>Air equivalent scintillation detector</p>	<p>Сцинтилляционный детектор ионизирующего излучения, эффективный атомный номер материалов которого равен или близок к эффективному атомному номеру воздуха</p> $Z_{эфф} \cong 7.7$
<p>Тканеэквивалентный сцинтилляционный детектор ионизирующего излучения</p> <p>Тканеэквивалентный детектор</p> <p>Tissue equivalent scintillation detector</p>	<p>Сцинтилляционный детектор ионизирующего излучения, эффективный атомный номер которого близок атомному номеру биологической ткани.</p> $(Z_{эфф} = 6 - 13)$
<p>Сцинтилляционный экран</p> <p>Scintillation screen</p>	<p>Сцинтилляционный детектор ионизирующего излучения, предназначенный для получения видимого изображения при рентгено-, гамма-дефектоскопии</p>
<p>ОСНОВНЫЕ КОНСТРУКТИВНО-ТЕХНОЛОГИЧЕСКИЕ ХАРАКТЕРИСТИКИ</p> <p>MAIN DESIGN AND TECHNOLOGICAL CHARACTERISTICS</p>	
<p>Сцинтиллятор</p> <p>Scintillator</p>	<p>Определенное количество сцинтиллирующего вещества, содержащегося в сцинтилляционном детекторе в качестве элемента, чувствительного к ионизирующему излучению</p>
<p>Основное вещество сцинтиллятора</p> <p>General matter of scintillator</p>	<p>Вещество, прозрачное для фотонов сцинтилляции, весовое содержание которого в сцинтилляторе преобладает</p>
<p>Активатор сцинтиллятора</p> <p>Активатор</p> <p>Activator</p>	<p>Примесь в основном веществе сцинтиллятора, придающая ему или усиливающая его сцинтилляционные свойства в определенной области температур.</p> <p>Примечание: термин применяется для неорганических сцинтилляторов</p>

<p>Сцинтилляционная добавка</p> <p>Primary scintillation solute</p>	<p>Примесь в основном веществе сцинтиллятора, способная испускать оптические фотоны под воздействием возбуждения, полученного от молекул основного вещества.</p> <p>Примечание. Термин применяется для органических сцинтилляторов</p>
<p>Контейнер сцинтилляционного детектора ионизирующего излучения</p> <p>Контейнер</p> <p>Container</p>	<p>Контейнер, предназначенный для изоляции сцинтиллятора от воздействия внешней среды и светового излучения</p>
<p>Входное окно сцинтилляционного детектора ионизирующего излучения</p> <p>Входное окно</p> <p>Entrance window</p>	<p>Часть поверхности сцинтилляционного детектора ионизирующего излучения, через которую в сцинтиллятор попадает ионизирующее излучение</p>
<p>Выходное окно сцинтилляционного детектора ионизирующего излучения</p> <p>Выходное окно</p> <p>Optical window</p>	<p>Часть поверхности сцинтилляционного детектора ионизирующего излучения, прозрачная для фотонов сцинтилляции</p>
<p>Отражатель сцинтилляционного детектора ионизирующего излучения</p> <p>Отражатель</p> <p>Reflector</p>	<p>Часть сцинтилляционного детектора ионизирующего излучения, предназначенная для улучшения условий светособирания</p>

**ОСНОВНЫЕ РАДИОМЕТРИЧЕСКИЕ
И СПЕКТРОМЕТРИЧЕСКИЕ ХАРАКТЕРИСТИКИ
GENERAL RADIOMETRIC
AND SPECTROMETRIC CHARACTERISTICS**

<p>Сцинтилляционная эффективность</p> <p>Ндп. Косвенная эффективность</p> <p>Scintillation efficiency</p>	<p>Отношение суммарной энергии (E_ϕ) фотонов сцинтилляции к энергии (E), выделенной ионизирующей частицей в сцинтилляторе, $\eta = \frac{E_\phi}{E}$.</p> <p>Примечание. Для данного сцинтиллятора значение η зависит от вида ионизирующей частицы и ее энергии</p>
<p>Технический энергетический выход сцинтилляционного детектора ионизирующего излучения</p> <p>Technical outlet of scintillation detector</p>	<p>Отношение суммарной энергии (L_ϕ) фотонов сцинтилляции, прошедших через выходное окно сцинтилляционного детектора ионизирующего излучения, к энергии (E), выделенной ионизирующей частицей в сцинтилляторе,</p> $T = \frac{L_\phi}{E}$
<p>Коэффициент светособирания сцинтилляционного детектора ионизирующего излучения</p> <p>Коэффициент светособирания</p> <p>Light collection efficiency</p>	<p>Отношение суммарной энергии (L_ϕ) фотонов сцинтилляции, прошедших через выходное окно сцинтилляционного детектора ионизирующего излучения, к суммарной (E_ϕ) фотонов этой сцинтилляции</p> $\tau = \frac{L_\phi}{E_\phi} = \frac{T}{\eta}$
<p>Эффективность регистрации сцинтилляционного детектора ионизирующего излучения</p> <p>Эффективность регистрации</p> <p>Detection efficiency</p>	<p>Отношение числа зарегистрированных ионизирующих частиц или фотонов к числу частиц или фотонов данной энергии, попавших на входное окносцинтилляционного детектора ионизирующего излучения</p>

**ДЕТЕКТОРЫ ИОНИЗИРУЮЩИХ ИЗЛУЧЕНИЙ,
ГАЗОВЫЕ, ИОНИЗАЦИОННЫЕ
GAS IONIZATION DETECTORS OF IONIZING RADIATION**

Газовый ионизационный детектор Gas ionization detector	Ионизационный детектор, принцип действия которого основан на использовании электрического разряда в газе под действием ионизирующего излучения
Общее давление газа-наполнителя газового ионизационного детектора Общее давление газ-наполнителя Filling gas total pressure of gas ionization detector	Сумма парциальных давлений газов внутри газового ионизационного детектора
Импульс газового ионизационного детектора Импульс Gas ionization detector pulse	Кратковременное изменение электрического сигнала, возникающее в результате прохождения через газовый ионизационный детектор ионизирующей частицы или одновременно несколько частиц
Ложный выходной сигнал газового ионизационного детектора Ложный выходной сигнал Spurious output signal of gas ionization detector	Выходной сигнал, вызванный любой причиной, кроме прохождения через газовый ионизационный детектор ионизирующего излучения, для регистрации которого он предназначен
Чувствительный объем газового ионизационного детектора Чувствительный объем Sensitive volume	Объем газового ионизационного детектора, в котором акты ионизации могут вызывать разряды, приводящие к появлению выходных импульсов

Рабочая поверхность газового ионизационного детектора Рабочая поверхность Working surface	Часть поверхности газового ионизационного детектора, после прохождения через которую или в результате взаимодействия с которой частица (фотон) может произвести ионизацию в чувствительном объеме и вызвать выходной сигнал
Первичная ионизации в газовом ионизационном детекторе Первичная ионизация Primary ionization of gas ionization detector	Ионизации, вызываемая регистрируемым излучением в чувствительном объеме газового ионизационного детектора
Гашение разряда в газовом ионизационном детекторе Гашение разряда Gas discharge quenching	Процесс окончания разряда в газовом ионизационном детекторе
Газовое усиление газового ионизационного детектора Газовое усиление Gas amplification of gas ionization detector	Процесс увеличения ионизации в газе -наполнителе газового ионизационного детектора за счет энергии электрического поля
Порог Гейгера Geiger threshold	Наименьшее напряжение, при котором в счетчике Гейгера-Мюллера заряд в импульсе не зависит от первичной ионизации. Разность между рабочим напряжением и порогом Гейгера

**ВИДЫ ГАЗОРАЗРЯДНЫХ СЧЕТЧИКОВ
И ИОНИЗАЦИОННЫХ КАМЕР
KINDS (TYPES) OF GAS DISCHARGE COUNTERS
AND IONIZATION CHAMBERS**

<p>Газоразрядный счетчик Счетчик Gas discharge counter</p>	<p>Газовый ионизационный детектор, имеющий коэффициент газового усиления больше единицы, в котором отдельные акты ионизации вызывают появление на выходе электрических импульсов. Примечание. В зависимости от вида регистрируемого излучения наименование газоразрядных счетчиков строят с добавлением терминологического элемента, называющего вид регистрируемого излучения. Например: счетчик альфа-частиц (краткая форма “α-счетчик”), счетчик бета-частиц (краткая форма “β-счетчик”), счетчик нейтронов (краткая форма “n-счетчик”), счетчик рентгеновского излучения (краткая форма “x-счетчик”) и т. д.</p>
<p>Пропорциональный счетчик Proportional counter</p>	<p>Газоразрядный счетчик, работающий в режиме несамостоятельного газового разряда, в котором разряд в импульсе пропорционален первичной ионизации, а коэффициент газового усиления больше единицы и не зависит от первичной ионизации</p>
<p>Счетчик с ограниченной пропорциональностью Limited proportionality counter</p>	<p>Газоразрядный счетчик, работающий в режиме несамостоятельного газового разряда, в котором коэффициент газового усиления зависит от первичной ионизации</p>
<p>Счетчик Гейгера-Мюллера Geiger-Muller counter</p>	<p>Газоразрядный счетчик, работающий в режиме нестабильного самостоятельного разряда, в котором заряд в импульсе не зависит от первичной ионизации</p>
<p>Коронный счетчик Corona counter</p>	<p>Газоразрядный счетчик, работающий в режиме коронного разряда, у которого импульс тока при прохождении ионизирующей частицы превышает шум короны</p>

Искровой счетчик Spark counter	Газоразрядный счетчик, работающий в режиме искрового разряда
Самогасящийся счетчик Self quenched counter	Счетчик Гейгера-Мюллера, в котором гашение разряда происходит за счет использования внешней гасящей цепи
Счетчик с гашением органическим паром Organic vapour quenched counter	Самогасящийся счетчик, в котором гасящим агентом является пар органического вещества
Счетчик с гашением галогеном Галогенный счетчик Halogen quenched counter	Счетчик Гейгера-Мюллера, в котором гасящим агентом является галоген
Борный счетчик Boron counter	Счетчик тепловых и надтепловых нейтронов, содержащих в качестве радиатора бор и его соединения. Примечание. Для счетчика, содержащего BF_3 , допустим термин “ BF_3 -счетчик”
Гелий-3 счетчик He^3 -счетчик Helium-3 counter	Счетчик нейтронов, содержащий в качестве радиатора газ гелий-3
Газоразрядный счетчик с окном Счетчик с окном Window counter	Газоразрядный счетчик, в котором часть баллона обладает слабым поглощением регистрируемого излучения
Торцевой газоразрядный счетчик Торцевой счетчик End window counter	Счетчик с окном, которое расположено перпендикулярно к его оси

Газовая ионизационная камера Ионизационная камера Gas ionization chamber	Газовый ионизационный детектор, в котором электрическое поле используется для собирания без газового усиления зарядов, возникающих в чувствительном объеме под воздействием ионизирующего излучения. Примечание. В зависимости от вида регистрируемого излучения наименование ионизационных камер строят с добавлением терминологического элемента, называющего вид измеряемого излучения. Например: ионизационная камера альфа-частиц (краткая форма “ α -камера”), ионизационная камера бета-частиц (краткая форма “ β -камера”), ионизационная камера нейтронного излучения (краткая форма “n-камера”), ионизационная камера рентгеновского излучения (краткая форма “x-камера”) и т. д.
Интегральная ионизационная камера Интегральная камера Intergrading ionization chamber	Ионизационная камера, в которой заряд, накопленный в течение некоторого интервала времени под воздействием ионизирующего излучения, приводит к изменению разности потенциалов между электродами камеры
Токовая ионизационная камера Токовая камера Current ionization chamber	Ионизационная камера, предназначенная для регистрации излучения по среднему току, возникающему в ней под воздействием ионизирующего излучения
Импульсная ионизационная камера Импульсная камера Pulse ionization chamber	Ионизационная камера, предназначенная для регистрации излучения по импульсному току, возникающему при прохождении через нее отдельных ионизирующих частиц
Ионизационная камера с сеткой Grid ionization chamber	Ионизационная камера с дополнительным электродом в виде сетки, предназначенная для измерения энергии альфа-частиц или осколков деления

**ПАРАМЕТРЫ И ХАРАКТЕРИСТИКИ
ГАЗОВЫХ ИОНИЗАЦИОННЫХ ДЕТЕКТОРОВ
PARAMETERS AND CHARACTERISTICS
OF GAS IONIZATION DETECTORS**

Заряд в импульсе газового ионизационного детектора Заряд в импульсе Charge in a pulse	Полный заряд одного знака, собирающийся на электродах газового ионизационного детектора в процессе формирования электрического импульса
Коэффициент газового усиления газового ионизационного детектора Gas amplification factor of gas ionization detector	Отношение заряда в импульсе газового ионизационного детектора к заряду первичной ионизации
Амплитуда импульса напряжения газового ионизационного детектора Voltage pulse amplitude of gas ionization detector	Наибольшее значение импульса напряжения на выходе газового ионизационного детектора, измеряемое в определенных условиях действия излучения и для определенной измерительной установки
Ход с жесткостью газового ионизационного детектора Ход с жесткостью Registration efficiency dependence on radiation energy	Зависимость эффективности регистрации газового ионизационного детектора от энергии излучения
Напряжение начала счета газового ионизационного детектора Напряжение начала счета Threshold voltage of gas ionization detector	Наименьшее значение напряжения, приложенного к газовому ионизационному детектору, при котором импульсы могут быть зарегистрированы системой с заданными характеристиками
Напряжение насыщения ионизационной камеры Saturation voltage of ionization chamber	Наименьшее значение напряжения между электродами ионизационной камеры, при котором основные параметры камеры (чувствительность, собственный фон) не превышают допустимых пределов

<p>Счетная характеристика газового ионизационного детектора</p> <p>Счетная характеристика</p> <p>Counting rate versus of voltage characteristic of gas ionization detector</p>	<p>Зависимость скорости счета от напряжения питания газового ионизационного детектора, измеряемая при постоянном потоке или мощности дозы излучения и определенных параметрах измерительного устройства</p>
<p>Плато счетной характеристики газового ионизационного детектора</p> <p>Плато</p> <p>Plateau of counting-rate-versus-voltage characteristic of gas ionization detector</p>	<p>Пологая часть счетной характеристики газового ионизационного детектора с наклоном, не превышающим заданного значения</p>
<p>Наклон плато счетной характеристики газового ионизационного детектора</p> <p>Наклон плато</p> <p>Plateau slope of gas ionization detector</p>	<p>Изменение скорости счета газового ионизационного детектора на 1 В изменения напряжения, выраженное в процентах</p>
<p>Протяженность плато счетной характеристики газового ионизационного детектора</p> <p>Plateau length of gas ionization detector</p>	<p>Разность между напряжениями конца и начала плато счетной характеристики газового ионизационного детектора</p>
<p>Мертвое время газового ионизационного детектора</p> <p>Мертвое время</p> <p>Dead time of ionization detector</p>	<p>Интервал времени после возникновения заряда, в течение которого газовый ионизационный детектор не способен регистрировать частицы (фотоны)</p>
<p>Время восстановления газового ионизационного детектора</p> <p>Время восстановления</p> <p>Recovery time of gas ionization detector</p>	<p>Наименьший интервал времени между двумя попаданиями ионизирующих частиц в газовый ионизационный детектор, при котором эти частицы регистрируются отдельно</p>

Ток насыщения токовой камеры Saturation current of current chamber	Ток в цепи собирающего электрода токовой камеры, соответствующий напряжению насыщения
ОСНОВНЫЕ ФУНКЦИОНАЛЬНЫЕ УЗЛЫ, ПРИНАДЛЕЖНОСТИ И ВСПОМОГАТЕЛЬНЫЕ УСТРОЙСТВА ГАММА-АППАРАТОВ MAIN FUNCTIONAL UNITS, FITTINGS AND AUXILIARY ARRANGEMENTS OF GAMMA – APPARATUS	
Радиационная головка гамма-аппарата Радиационная головка Radiation cap of gamma – apparatus	Функциональный узел гамма-аппарата, предназначенный для выпуска и перекрытия пучка измерения, а также для хранения источника излучения в перерывах между рабочими циклами
Держатель источника гамма-излучателя Держатель источника Source’s holder	Часть гамма-аппарата с одним или несколькими гнездами для размещения и крепления источников гамма-излучения
Транспортер источника гамма-излучения Транспортер Carrier of gamma radiation source	Функциональный узел гамма-аппарата, обеспечивающий перемещение источника гамма-излучения в рабочее положение и возврат в положение хранения
Ампулопровод источника гамма-излучения Ампулопровод Source guide	Часть транспортера, предназначенная для направления источника гамма-излучения при его перемещении
Коллимирующая головка гамма-аппарата Collimation cap of gamma apparatus	Радиационный наконечник гамма-аппарата, снабженный устройством для формирования пучка гамма-излучения

Контейнер гамма-аппарата Контейнер Container	Вспомогательное устройство гамма-аппарата, предназначенное для хранения источника гамма-излучения в нерабочем положении
Перезарядный контейнер гамма-аппарата Charging container	Контейнер гамма-аппарата, предназначенный для зарядки и перезарядки гамма-аппарата в условиях эксплуатации
Транспортно-перезарядный контейнер гамма-аппарата Transportation and charging container	Перезарядный контейнер гамма-аппарата, обеспечивающий транспортирование источника гамма-излучения
СРЕДСТВА ИЗМЕРЕНИЙ ИОНИЗИРУЮЩИХ ИЗЛУЧЕНИЙ MEANS OF IONIZING RADIATION MEASUREMENT	
Прибор (установка) для измерения ионизирующих излучений Radiation meter Radiation measuring assembly	Измерительный прибор (установка), предназначенный для получения измерительной информации о физических величинах, их поля, источники ионизирующих излучений и результаты взаимодействия ионизирующих излучений с веществом
Дозиметр Dosimeter	Прибор или установка для измерения ионизирующих излучений, предназначенные для получения измерительной информации об экспозиционной дозе и мощности экспозиционной дозы фотонного излучения и (или) об энергии, переносимой ионизирующим излучением или переданной им объекту, находящемуся в поле действия излучения
Индивидуальный дозиметр Ндп. Интенсиметр E. Energy fluence ratemeter	Дозиметр, габаритные размеры и масса которого позволяют, не затрудняя выполнения производственных операций, применять его для ношения человеком с целью определения экспозиционной, поглощенной и эквивалентной доз, полученных за время нахождения его в полях ионизирующего излучения

<p>Радиометр</p> <p>Radiation meter (radiometer)</p>	<p>Прибор или установка для измерений ионизирующих излучений, предназначенный для получения измерительной информации об активности радионуклида в источнике или образце, производных от нее величин, о плотности потока и (или) потоке и флюенсе (переносе) ионизирующих частиц</p>
<p>Спектрометр</p> <p>Radiation spectrometer</p>	<p>Прибор или установка для измерений ионизирующих излучений, предназначенный для получения измерительной информации о распределении ионизирующего излучения по одному или более параметрам, характеризующем источники и поля ионизирующих излучений</p>
<p>Энергетическая зависимость прибора (установки) для измерения ионизирующих излучений</p> <p>Энергетическая зависимость</p> <p>Ндп. Ход с жесткостью</p> <p>E. Energy dependence of a radiation meter (radiation measuring assembly)</p>	<p>Зависимость чувствительности прибора (установки) для измерения ионизирующих излучений от энергии измеряемого излучения</p>
<p>Энергетическое разрешение спектрометра</p> <p>Энергетическое разрешение</p> <p>Energy resolution (of a radiation spectrometer)</p>	<p>Параметр, характеризующий способность спектрометра различать близкие по энергии ионизирующие частицы</p>

**ДЕТЕКТОРЫ ИОНИЗИРУЮЩИХ ИЗЛУЧЕНИЙ/
DETECTORS OF IONIZING RADIATION. ОБЩИЕ ПОНЯТИЯ /
GENERAL CONCEPTS**

<p>Детектор ионизирующего излучения</p> <p>Ндп. Датчик</p> <p>Radiation detector</p>	<p>Чувствительный элемент средства измерений, предназначенный для преобразования энергии ионизирующего излучения в другой вид энергии, пригодной для регистрации и (или) дальнейшего преобразования одной или нескольких величин, характеризующих воздействующее на детектор излучение.</p> <p>Примечание. При необходимости подчеркнуть вид регистрируемого ионизирующего излучения, наименование детекторов ионизирующего излучения строят с добавлением терминологического элемента, называющего вид излучения. Например: детектор альфа-частиц (краткая форма α-детектор), детектор бета-частиц (краткая форма β-детектор), детектор нейтронов (краткая форма n-детектор), детектор рентгеновского излучения (краткая форма x-детектор), детектор гамма-излучения (краткая форма γ-детектор) и т. д.</p>
<p>Аналоговый детектор ионизирующего излучения</p> <p>Аналоговый детектор</p> <p>Analogue detector</p>	<p>Детектор ионизирующего излучения, позволяющий получать измерительную информацию в аналоговой форме</p>
<p>Дискретный детектор ионизирующего излучения</p> <p>Дискретный детектор</p> <p>Pulse detector</p>	<p>Детектор ионизирующего излучения, позволяющий получать измерительную информацию в дискретной форме.</p> <p>Примечание. Дискретный детектор, у которого выходные сигналы представляют электрические импульсы, называется импульсным детектором</p>
<p>Пропорциональный детектор ионизирующего излучения</p> <p>Пропорциональный детектор</p> <p>Linear detector</p>	<p>Детектор ионизирующего излучения, у которого выходной сигнал прямо пропорционален некоторой физической величине, характеризующей излучение.</p> <p>Примечание. Обычно такой физической величиной является энергия, потерянная излучением в чувствительном объеме детектора</p>

<p>Непропорциональный детектор ионизирующего излучения</p> <p>Непропорциональный детектор</p> <p>Non linear detector</p>	<p>Детектор ионизирующего излучения, у которого выходной сигнал не является прямо пропорциональным некоторой физической величине, характеризующей излучение</p>
<p>Твердотельный детектор ионизирующего излучения</p> <p>Твердотельный детектор</p> <p>Solid-state detector</p>	<p>Детектор ионизирующего излучения, у которого вещество чувствительного объема находится в твердом состоянии</p>
<p>Жидкостный детектор ионизирующего излучения</p> <p>Жидкостный детектор</p> <p>Liquid detector</p>	<p>Детектор ионизирующего излучения, у которого вещество чувствительного объема находится в жидком состоянии</p>
<p>Газовый детектор ионизирующего излучения</p> <p>Газовый детектор</p> <p>Gas detector</p>	<p>Детектор ионизирующего излучения, у которого вещество чувствительного объема находится в газовом состоянии</p>
<p>ОСНОВНЫЕ ВИДЫ ДЕТЕКТОРОВ ИОНИЗИРУЮЩИХ ИЗЛУЧЕНИЙ GENERAL KINDS OF DETECTORS OF IONIZING RADIATION</p>	
<p>Ионизационный детектор</p> <p>Ionization detector</p>	<p>Детектор ионизирующего излучения, принцип действия которого основан на использовании ионизации в веществе чувствительного объема детектора</p>
<p>Полупроводниковый детектор ионизирующего излучения</p> <p>Полупроводниковый детектор (ППД)</p> <p>Semiconductor detector</p>	<p>Ионизационный детектор, в котором используется электрическое поле для собирания неравновесных носителей зарядов, образованный ионизирующим излучением в полупроводниковом материале чувствительного объема детектора</p>

Кристаллический детектор ионизирующего излучения Кристаллический детектор Crystal conduction detector	Ионизационный детектор, у которого вещество чувствительного объема имеет однородную кристаллическую структуру
Искровой детектор ионизирующего излучения Искровой детектор Spark detector	Ионизационный детектор, в котором при прохождении ионизирующей частицы в чувствительном объеме образуется искровой разряд
Радиолюминесцентный детектор ионизирующего излучения Radioluminescence detector	Детектор ионизирующего излучения, принцип действия которого основан на использовании люминесценции вещества чувствительного объема детектора под воздействием ионизирующего излучения
Термолюминесцентный детектор ионизирующего излучения Termoluminescence detector	Радиолюминесцентный детектор, в котором используется термолюминесцентное вещество, испускающее при термостимулировании кванты света, интенсивность которых зависит от энергии, накопленной в детекторе в процессе облучения ионизирующим излучением. Примечание. Радиолюминесцентное вещество – активизированное серебром фосфатное стекло, которое стимулируется ультрафиолетовым излучением
Детектор Черенкова Cerenkov detector	Детектор ионизирующего излучения, принцип действия которого основан на использовании эффекта Вавилова-Черенкова, возникающего в среде, оптически связанной непосредственно или через световод с фоточувствительным устройством.
Химический детектор ионизирующего излучения Chemical detector	Детектор ионизирующего излучения, принцип действия которого основан на использовании выхода химических реакций в веществе, происходящих под воздействием ионизирующего излучения
Зарядовый детектор ионизирующего излучения Зарядовый детектор Charge detector	Детектор ионизирующего излучения, принцип действия которого основан на использовании электрического поля, возникающего при воздействии ионизирующего излучения на вещество чувствительного объема детектора

Калориметрический детектор ионизирующего излучения Калориметр Calorimetric detector	Детектор ионизирующего излучения, принцип действия которого основан на тепловой энергии, создаваемым ионизирующим излучением в веществе чувствительного объема детектора за счет переданной энергии
Радиодефекционный детектор ионизирующего излучения Ionizing radiation detector based on using of radiation-induced defect	Детектор ионизирующего излучения, принцип действия которого основан на использовании дефектов в веществе чувствительного объема детектора возникающих под воздействием ионизирующего излучения
Трековый детектор ионизирующего излучения Track detector	Детектор ионизирующего излучения, принцип действия которого основан на получении видимых или становящихся видимыми после соответствующей обработки траектории ионизирующих частиц, проходящих через детектор или образующихся в нем
ПРИБОРЫ РАДИОИЗОТОПНЫЕ RADIOISOTOPE DEVICES	
Радиоизотопный прибор Ндп. Радиоактивный пробор Radioisotope instrument	Техническое средство, принцип действия которого основан на регистрации результатов взаимодействия ионизирующего излучения с материалом или средой, имеющее в своем составе закрытый радиоизотопный источник излучения
Измерительный радиоизотопный прибор Ндп. Радиоактивный измеритель Radioisotope measuring apparatus	Радиоизотопный прибор, имеющий нормированные метрологические свойства, предназначенный для выработки сигнала измерительной информации в форме, доступной для непосредственного восприятия
Релейный радиоизотопный прибор Ндп. Радиоактивное реле Бета-реле, Гамма-реле Radiosotope relay apparatus	Радиоизотопный прибор, регистрирующий изменение плотности потока частиц и (или) плотности потока энергии ионизирующего излучения по отношению к заданному пороговому значению путем перехода из одного выходного состояния в другое

<p>Радиоизотопный толщиномер</p> <p>Ндп. Радиоактивные весы</p> <p>Бета-толщиномер, отражательный радиоактивный измеритель толщины</p> <p>Radioisotope thickness gauge</p>	<p>Измерительный радиоизотопный прибор, предназначенный для измерения и (или) контроля толщины или среднего значения поверхностной плотности контролируемого материала</p>
<p>Радиоизотопный уровнемер</p> <p>Ндп. Радиоактивный уровнемер</p> <p>Радиоактивный измеритель уровня</p> <p>Radioisotope level gauge</p>	<p>Измерительный радиоизотопный прибор, предназначенный для измерения и (или) контроля положения границы раздела двух сред</p>
<p>Радиоизотопный плотномер</p> <p>Ндп. Радиоактивный плотномер</p> <p>Radioisotope density gauge</p>	<p>Измерительный радиоизотопный прибор для измерения среднего значения плотности твердых, жидких и газовых сред или их смесей</p>
<p>Радиоизотопный влагомер</p> <p>Ндп. Радиоактивный влагомер</p> <p>Radioisotope moisture meter</p>	<p>Измерительный радиоизотопный прибор, предназначенный для измерения относительной влажности материалов</p>
<p>Радиоизотопный концентратомер</p> <p>Ндп. Радиоизотопный анализатор содержания</p> <p>Radioisotope concentration meter</p>	<p>Измерительный радиоизотопный прибор, предназначенный для измерения и (или) контроля количественного состава заданных (заданного) компонентов в жидких и твердых средах или газовых смесях</p>

ALBUM
GENERAL CONCEPTS AND DEPENDENCES
OF RADIATION TESTING AND DIAGNOSTICS

Group	I	II	III	IV	V	VI	VII	VIII	IX	X	XI	XII	III	IV	V	VI	VII	VIII	IX	X	XI	XII	III	IV	V	VI	VII	VIII	IX	X	XI	XII																																																																							
1	1 H Hydrogen 1.00794 -250.14 -252.87 0.071	2 He Helium 4.002602	3 Li Lithium 6.941 180.54 1349 -350.91 1.274	4 Be Beryllium 9.012 1450 -276.9	5 B Boron 10.811 2000 -254.9	6 C Carbon 12.011 3500 -3000	7 N Nitrogen 14.007 -195.8	8 O Oxygen 15.999 -183	9 F Fluorine 18.998 -188	10 Ne Neon 20.180 -248.6	11 Na Sodium 22.990 97.8	12 Mg Magnesium 24.305 1200	13 Al Aluminum 26.982 933	14 Si Silicon 28.086 1410	15 P Phosphorus 30.974 -112	16 S Sulfur 32.06 280	17 Cl Chlorine 35.453 -34	18 Ar Argon 39.948 -186	19 K Potassium 39.098 2000	20 Ca Calcium 40.078 1480	21 Sc Scandium 44.956 1530	22 Ti Titanium 47.88 1660	23 V Vanadium 50.942 1910	24 Cr Chromium 51.996 2130	25 Mn Manganese 54.938 1510	26 Fe Iron 55.845 2730	27 Co Cobalt 58.933 1490	28 Ni Nickel 58.69 1450	29 Cu Copper 63.546 1280	30 Zn Zinc 65.38 920	31 Ga Gallium 69.723 29.8	32 Ge Germanium 72.61 2310	33 As Arsenic 74.922 360	34 Se Selenium 78.96 220	35 Br Bromine 79.904 -7.6	36 Kr Krypton 83.80 -153	37 Rb Rubidium 85.468 390	38 Sr Strontium 87.62 2800	39 Y Yttrium 88.906 1530	40 Zr Zirconium 91.224 2030	41 Nb Niobium 92.906 2470	42 Mo Molybdenum 95.94 2620	43 Tc Technetium 98.906 2910	44 Ru Ruthenium 101.07 2630	45 Rh Rhodium 102.905 2200	46 Pd Palladium 106.42 1550	47 Ag Silver 107.868 2160	48 Cd Cadmium 112.411 420	49 In Indium 114.818 327	50 Sn Tin 118.710 232	51 Sb Antimony 121.760 477	52 Te Tellurium 127.60 449	53 I Iodine 126.905 184	54 Xe Xenon 131.29 -108	55 Cs Cesium 132.905 28.5	56 Ba Barium 137.327 2730	57 La Lanthanum 138.905 912	58 Ce Cerium 140.12 2790	59 Pr Praseodymium 140.908 3270	60 Nd Neodymium 144.24 1020	61 Pm Promethium 144.913 1000	62 Sm Samarium 150.36 1360	63 Eu Europium 151.96 820	64 Gd Gadolinium 157.25 1310	65 Tb Terbium 158.925 1340	66 Dy Dysprosium 162.50 1410	67 Ho Holmium 164.930 1340	68 Er Erbium 167.26 1360	69 Tm Thulium 168.934 1340	70 Yb Ytterbium 173.05 1360	71 Lu Lutetium 174.967 1360	72 Hf Hafnium 178.49 2370	73 Ta Tantalum 180.948 2990	74 W Tungsten 183.84 3410	75 Re Rhenium 186.207 3180	76 Os Osmium 190.23 2630	77 Ir Iridium 192.222 2410	78 Pt Platinum 195.084 2010	79 Au Gold 196.967 1490	80 Hg Mercury 200.59 2340	81 Tl Thallium 204.387 2320	82 Pb Lead 207.2 2710	83 Bi Bismuth 208.980 2710	84 Po Polonium 209 2090	85 At Astatine 210 2100	86 Rn Radon 222 -71	87 Fr Francium 223 -200	88 Ra Radium 226 700	89 Ac Actinium 227 1000	90 Th Thorium 232.038 1780	91 Pa Protactinium 231.036 1500	92 U Uranium 238.029 1170	93 Np Neptunium 237.048 900	94 Pu Plutonium 244.064 900	95 Am Americium 243.061 1610	96 Cm Curium 247.070 1610	97 Bk Berkelium 247.070 1610	98 Cf Californium 251.083 1610	99 Es Einsteinium 252.083 1610	100 Fm Fermium 257.103 1610	101 Md Mendelevium 258.103 1610	102 No Nobelium 259.103 1610	103 Lr Lawrencium 260.103 1610

Modern version of Mendeleev's Periodic Table of the Elements
Современная периодическая система элементов Д.И.Менделеева

Atomic mass, relative
Атомная масса, относительная

Atomic №, symbol
Атомный номер, обозначение

Melting point (°C)
Температура плавления (°C)

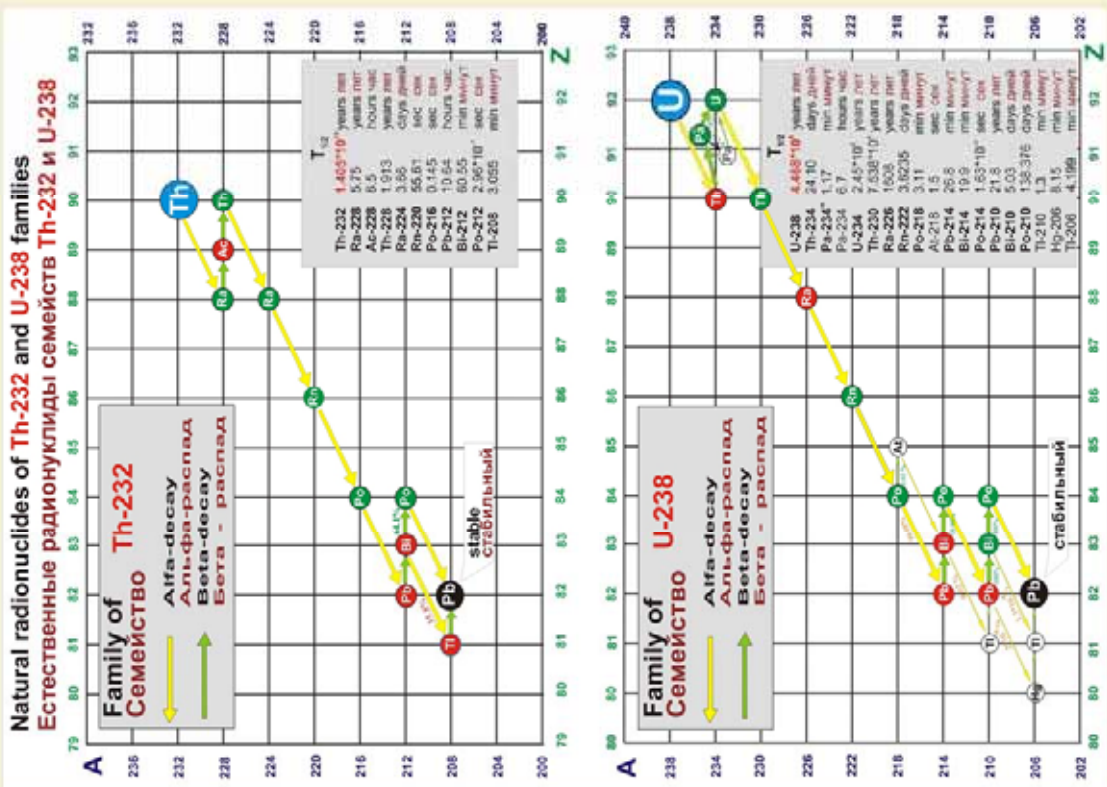
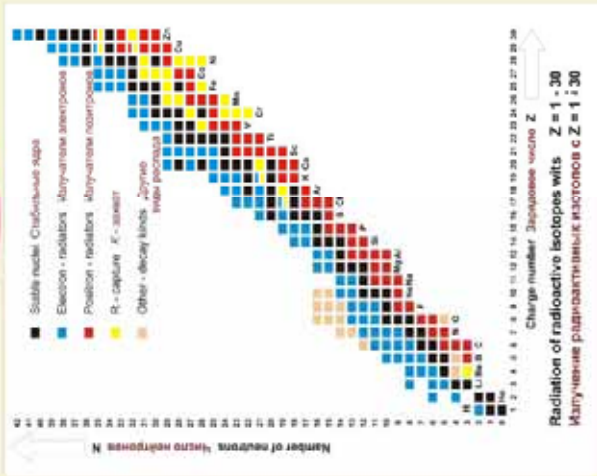
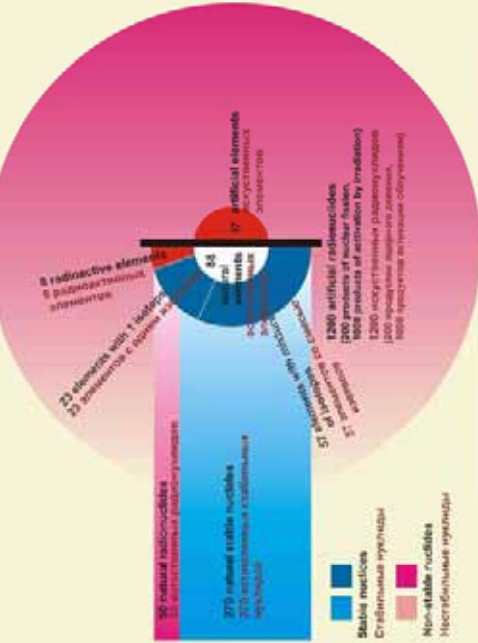
Boiling point (°C)
Температура кипения (°C)

Density, g/cm³
Плотность, г/см³

Name
Название

* Element has no stable nuclides.
For radioactive elements, the value in parentheses refers to the number of nuclides (mass number) of the most stable isotope.
Элемент не имеет устойчивых нуклидов. Для радиоактивных элементов значение в скобках относится к числу нуклидов (массовое число) наиболее долгоживущего нуклида.

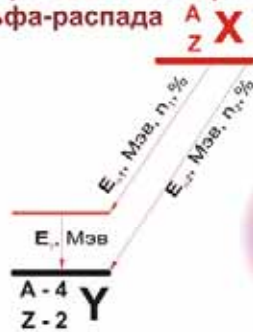
Isotopes Изотопы



SOURCES OF ALPHA-RADIATION ИСТОЧНИКИ АЛЬФА - ИЗЛУЧЕНИЯ

Drawing of alpha-decay

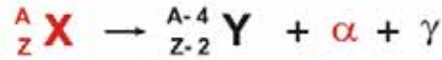
Графическое изображение альфа-распада



Radioactive nucleus
Радиоактивное ядро

Formula of alpha-decay

Формула альфа-распада



Daughter nucleus
Дочернее ядро



Alpha-particles (Helium nuclei) are thrown out from radioactive nuclei. The ordinal number Z of daughter nucleus reduces by 2 and mass number A reduces by 4.
Из радиоактивных ядер выбрасываются альфа-частицы (ядра гелия). Порядковый номер Z дочернего ядра уменьшается на 2, массовое число A уменьшается на 4.

General characteristics of isotopes

Основные характеристики изотопов, используемых в альфа-источниках

Isotopes Изотопы	Half-decay period Период полураспада	Kind and average energy of radiation, Mev Вид и средняя энергия излучения, Мэв	
		α	γ
Np -237	2,2 * 10 ⁶ years года	4,73	-
Po -210	138,4 days дни	4,45 - 5,24	0,823
Pu -238	2,85 years года	5,69	0,49 - 0,63
Pu -242	375 * 10 ³ years года	4,84	0,16
Am -241	432,3 years года	5,42	0,26 - 0,95

Codification of sources

Кодировка источников

АИП - metallic backing +
Pu preparation fused into an enamel
- металлическая подложка +
препарат Pu, впеченный в эмаль.
АДИ - ceramic backing +
Pu preparation on outside surface +
case made from aluminum
- керамическая подложка +
препарат Pu на внешней поверхности
+ корпус из алюминия.

АКЛ, АИП-Н, АРИА - alpha-source based on Am preparation
- альфа-источники на основе Am.

ФАКТ-1(Po), САДТРИН-Н-10 - activation detectors based on Po and Np

- активационные детекторы на основе Po и Np.

Design of sources Конструкция источников

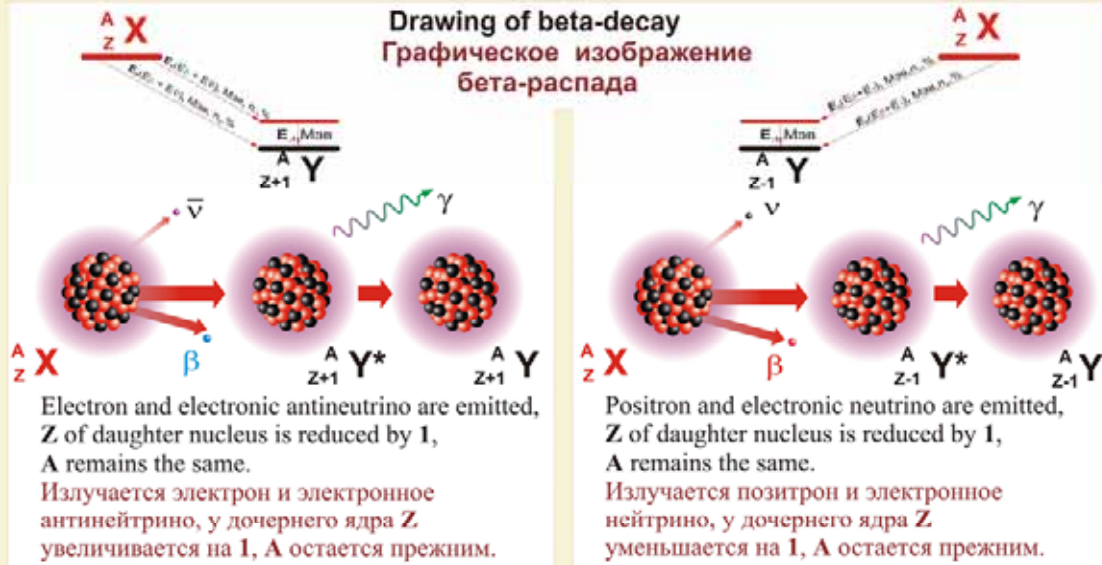


Usage: acquisition of demonstrative device, taking down the charges of static electricity, roentgenometric analysis, activation analysis, bench-mark sources in checking and measuring apparatus, gauges of fire alarm (signalling), base for receiving the sources of neutrons.

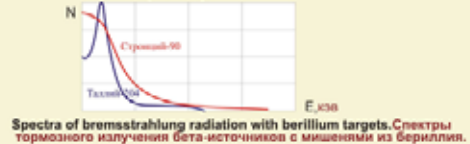
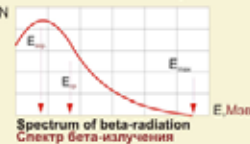
Применение: комплектация демонстрационных приборов, снятие зарядов статического электричества, рентгенометрический анализ, активационный анализ, реперные источники в контрольно-измерительных приборах, датчики пожарной сигнализации, являются основой для получения источников нейтронов.

SOURCES OF BETA-RADIATION ИСТОЧНИКИ БЕТА - ИЗЛУЧЕНИЯ

Formula of beta-decay Формула бета-распада



Spectra of beta-preparations radiation Спектры излучения бета-препаратов.



General characteristics of isotopes Основные характеристики изотопов, используемых в бета-источниках

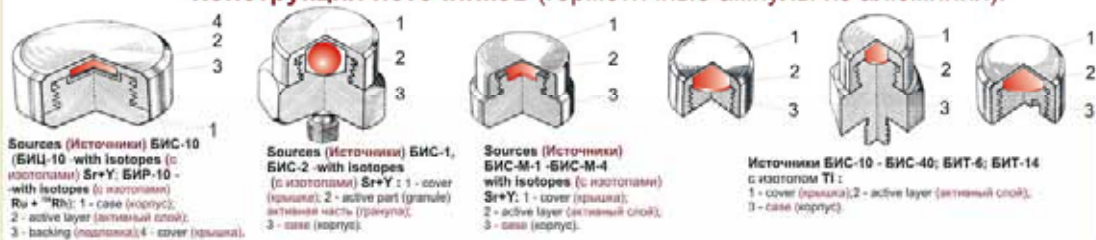
Isotopes Изотопы	Half-decay period Период полураспада	Kind and average energy of radiation, pДж Вид и средняя энергия излучения, пДж		
		α	β	γ
Sr-90 Y-90	28,7 years года	-	0,031	-
	64,26 years года	-	0,150	roentg рентг. 0,0026
Ru-106	367 days дней	-	0,0018	-
Rh-106	29,9 sec секунд	-	0,227	-
Ce-139	140 days дней	-	-	-

Codification of sources Кодировка источников

БИС - beta-source from Sr+Y
бета-источник Sr+Y
БИЦ - beta-source from Ce
бета-источник из Ce
БИР - beta-source from Ru+Rh
бета-источник Ru+Rh

Design of sources (hermetic ampoules made from aluminum).

Конструкция источников (герметичные ампулы из алюминия).

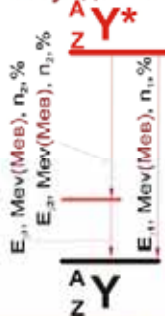


Usage: devices for measuring and testing the parametrs of articles and technological processes: - micrometers, - thicknessmeters, - measuring instruments for surface density, - as the base of sources of bremsstrahlung photon radiation, in medicine and biology.

Применение: в приборах для измерения и контроля параметров изделий технологических процессов, (β - микрометры, β - толщиномеры поверхностной плотности), в качестве основы источников тормозного фотонного излучения, в медицине, в биологии.

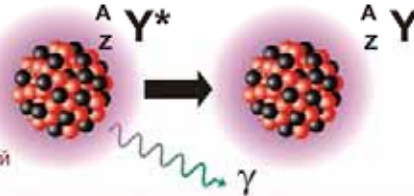
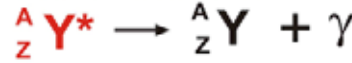
SOURCES OF GAMMA-RADIATION ИСТОЧНИКИ ГАММА - ИЗЛУЧЕНИЯ

Drawing of daughter nucleus transfer from excited into stable (base) state **Графическое изображение перехода дочернего ядра из возбужденного состояния в основное**

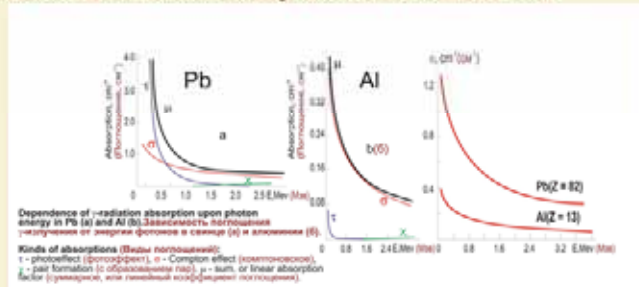
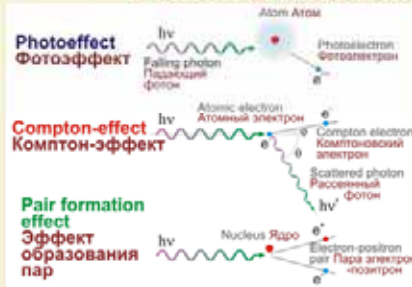


Daughter nuclei at **alpha-, beta-**decays, at nuclear reactions, at spontaneous fission of nuclei are presented firstly in excited state electromagnet radiation (gamma-quanta) with wave length $\lambda = (10^{-3} - 10^{-4})$ nm. Дочерние ядра при **альфа-, бета-**распадах, в ядерных реакциях, при спонтанном делении ядер вначале находятся в возбужденном состоянии и далее переходят в основное состояние, излучая короткое электромагнитное излучение (гамма-кванты) с длиной волны $\lambda = (10^{-3} - 10^{-4})$ нм

Formula of daughter nucleus transfer from excited into stable (base) state **Формула перехода дочернего ядра из возбужденного состояния в основное**



Main types of gamma-radiation interaction with substance Основные виды взаимодействия гамма-излучения с веществом



General characteristics of isotopes Основные характеристики изотопов

Isotopes Изотопы	Half-decay period Период полураспада	Kind and average energy of radiation, pJ Вид и средняя энергия излучения, пДж		
		α	β	γ
Co - 60	5,272 years годы	-	0,156	$(0.94-1.05) \cdot 10$
Cs - 137	30,16 years годы	-	0,030	0.106
Tm - 170	128,6 days дни	-	0,051	0.0125-0.0135
Se - 75	120,4 days дни	-	0,013-0.108	0.0106-0.0916
Ir - 192	74,08 days дни	-	-	0.047-0.098

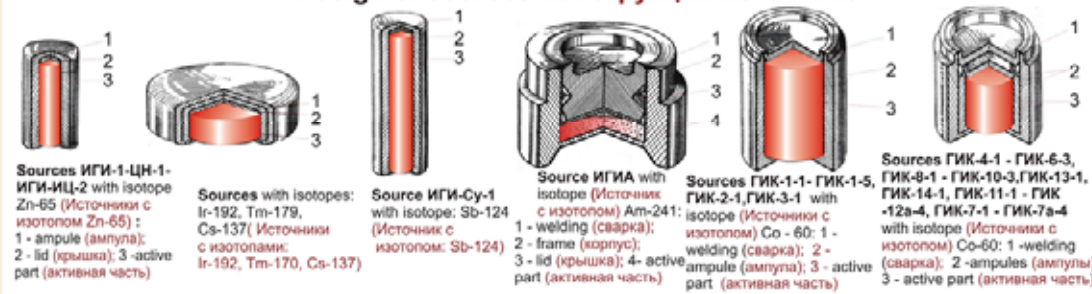
ИГИА - hermetic ampoules from stainless steel, filled with gamma-preparation (герметичные ампулы из нержавеющей стали, заполненные препаратом).

Codification of sources Кодировка источников

ИГИ - sources made as single or double hermetic ampoules from aluminum alloy, filled with one or another preparation and irradiated by neutrons (источники в виде одинарных или двойных герметичных ампул из алюминия, сплавов алюминия, заполненных тем или иным препаратом и облученных нейтронами).

ГИК - preforms made as rods, disks, fractions or chaffs, irradiated by neutrons and inserted into hermetic single or double ampoules made from stainless steel (заготовки в виде стержней, дисков, дробы или сечки, облученных нейтронами и помещенных в герметичные одинарные или двойные ампулы из нержавеющей стали).

Design of sources Конструкция источников

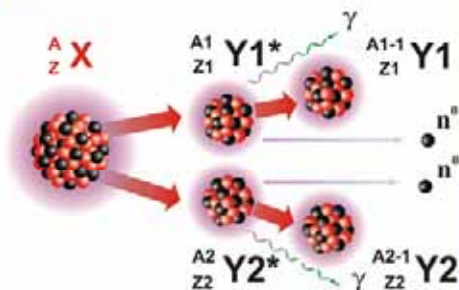
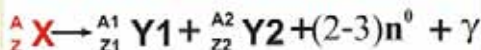


Usage: for radiography, densitometry, thicknessmetry, at X-ray fluorescent analysis, in radioisotope devices.

Применение: для радиографии, плотнометрии, толщинометрии, при рентгенофлуоресцентном анализе; в радиоизотопных приборах.

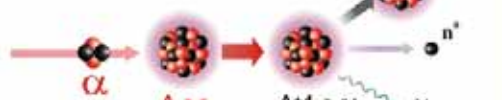
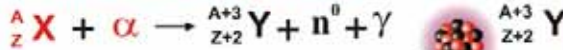
SOURCES OF NEUTRON RADIATION ИСТОЧНИКИ НЕЙТРОННОГО ИЗЛУЧЕНИЯ

On base of spontaneous fission
На основе спонтанного деления

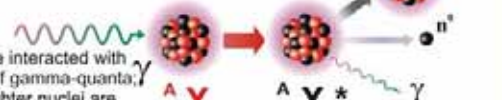
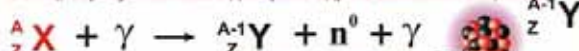


Spontaneous fission of nucleus, and 2-3 neutrons are irradiated at this event. Спонтанное деление ядра, при этом излучаются 2-3 нейтрона.

On base of nuclear reactions (α, n^0) and (γ, n^0)
На основе ядерных реакций (α, n^0) и (γ, n^0)

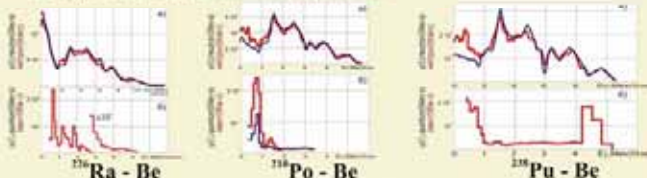


Nuclei are interacted with the flow of alpha-particles; new daughter nuclei are formed at once with the emission of neutrons. Ядра взаимодействуют с потоком альфа-частиц; образуются новые дочерние ядра с вылетом нейтронов.

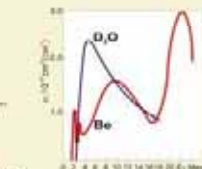


Nuclei are interacted with the flow of gamma-quanta; new daughter nuclei are formed at once with the emission of neutrons. Ядра взаимодействуют с потоком гамма-квантов; образуются новые дочерние ядра с вылетом нейтронов.

Spectra of neutrons from (α, n) -sources and from attendant gamma-radiation. Спектры нейтронов (α, n) -источников и сопутствующего гамма-излучения.

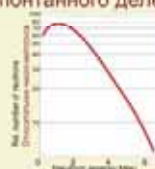


(γ, n) source
источник



Cross-section of neutrons formation on D_2O and Be nuclei. Сечение образования фотонейтронов на ядрах дейтерия и бериллия.

Source of spontaneous fission
Источники спонтанного деления



Spectrum of Cf-252
Энергетический спектр Cf-252

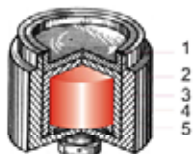
General characteristics of isotopes
Основные характеристики изотопов

Isotopes Изотопы	Half-decay period Период полураспада	Kind and average energy of radiation, pJ Вид и средняя энергия излучения, пДж		
		α	β	γ
Pu-238	87,7 years годы	0,875	-	0,0026
Cf-252	2,64(n) 85,3(o) years годы	0,980	-	0,007
Po-210	138,4 days дней	0,7209	-	0,1334
Pu-240	6540 years годы	0,826	0,033	0,0026
Pu-242	375 * 10 ³ years годы	0,784	0,033	0,0026

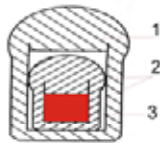
Codification of sources
Кодировка источников

ИНК - hermetic double ampules from stainless steel, filled by Cf-252 oxides (- герметичные двойные ампулы из нержавеющей стали, заполненные окислами Cf-252).
ИБН - hermetic double ampules from stainless steel, filled by Pu-Be combination (- герметичные двойные ампулы из нержавеющей стали, заполненные соединением Pu-Be)
ИНКМ - hard needles of different length or flexible assemblings consisting from 3-6 diminutive sources, inserted flexible frame (- жесткие иглы различной длины или гибкие сборки из 3-6 миниатюрных источников, помещенных в гибкую оболочку)

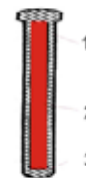
Design of sources Конструкция источников



Sources ИБН-1 with Pu isotopes
(Источники с изотопами Pu):
1 - welding (сварка); 2 - frame (станок);
3 - capsule (капсула);
4 - active part (активная часть);
5 - inset (вкладыш).



Sources ИНК-1 - ИНК-10 with radionuclide Cf-252
(Источники с радионуклидом Cf-252):
1 - outward plug (наружная пробка);
2 - capsule (капсула);
3 - active part (активная часть).

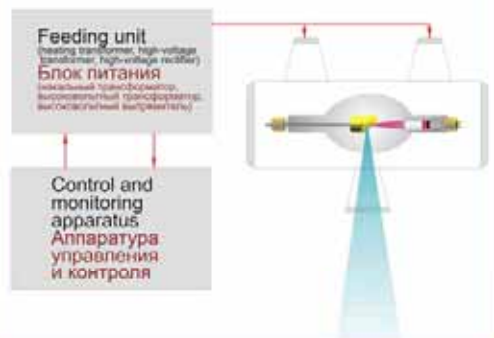


Sources ИНКМ-Ш with radionuclide Cf-252
(Источники с радионуклидом калифорния-252): 1 - capsule (капсула); 2 - active part (активная часть); 3 - welding (сварка).

Usage: moisture determining in soil and grounds; search of useful minerals; determination of element composition of materials by neutron-activation method and spectrometry; in devices of special application.

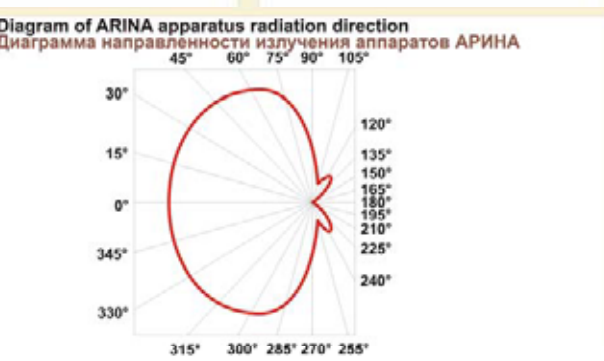
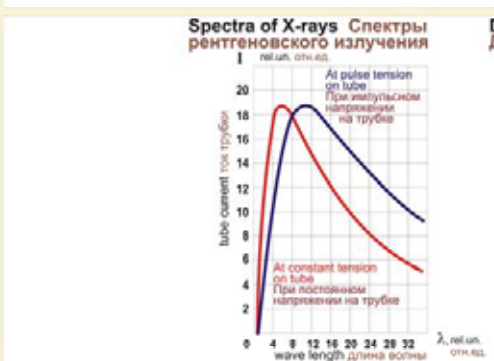
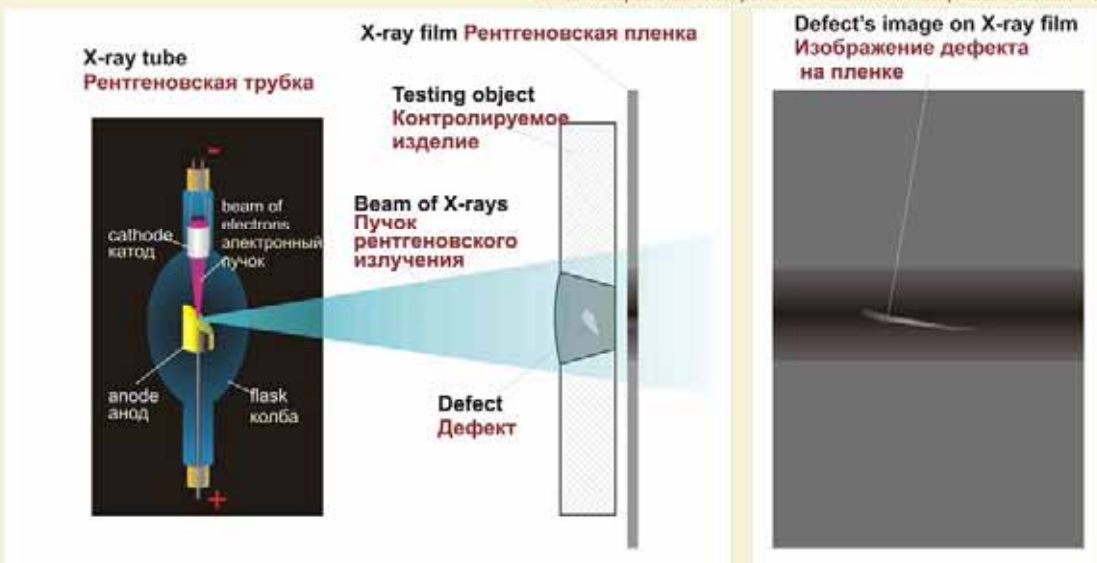
Применение: определение влажности грунтов, разведка полезных ископаемых, определение элементного состава материалов методами нейтронно-активационного анализа и спектрометрии, для изделий спецтехники.

X-RAY APPARATUS IN DEFECTOSCOPY РЕНТГЕНОВСКИЕ АППАРАТЫ В ДЕФЕКТОСКОПИИ

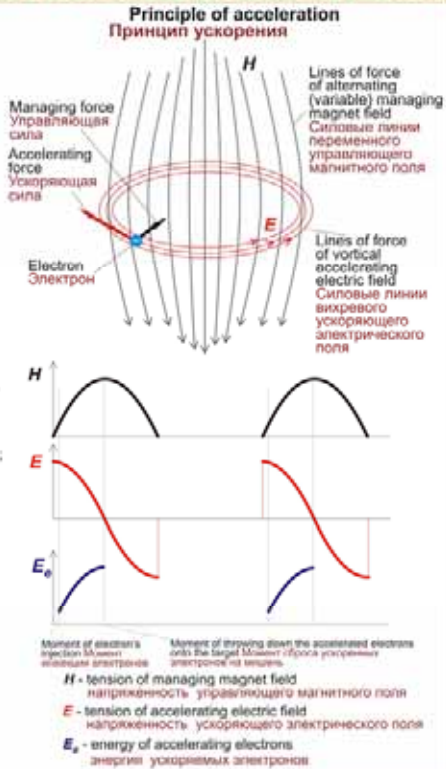
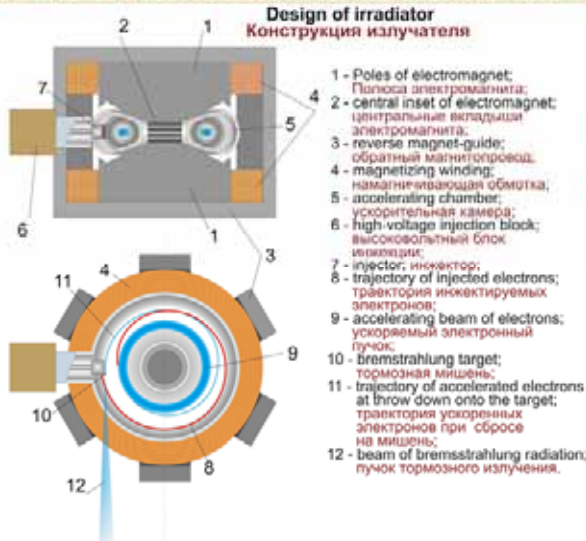


X-ray defectoscopy is based on the weakening of X-rays, which is depended upon the density and atomic number of elements forming the substance's material. The presence of such the defects as cracks, blisters or inclusions of the alien material will bring the different weakening (absorption) of X-rays after their passage through the material. One can detect the presence and disposition of different non-uniformities of the checking material by registering the distribution of intensity of the X-rays passed the substance. X-radiation is generated inside the X-ray tubes due to the bremsstrahlung of the high-speed electrons on the targets made from the materials having high Z number (e.g. tungsten).

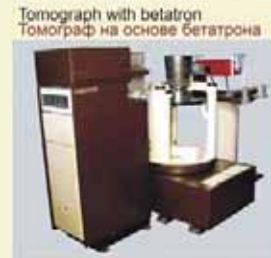
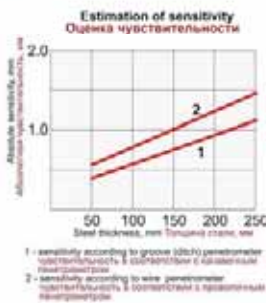
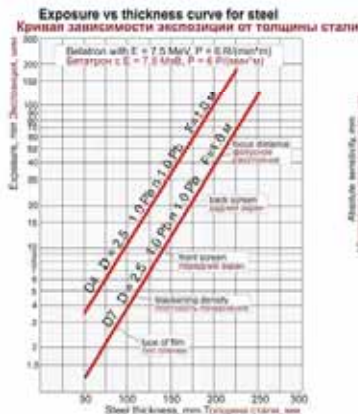
Рентгенодефектоскопия основана на поглощении рентгеновских лучей, которое зависит от плотности среды и атомного номера элементов, образующих материал среды. Наличие таких дефектов, как трещины, раковины или включения инородного материала, приводит к тому, что проходящие через материал лучи ослабляются в различной степени. Регистрируя распределение интенсивности проходящих лучей, можно определить наличие и расположение различных неоднородностей материала. Рентгеновское излучение генерируется в рентгеновских трубках за счет торможения высокоскоростных электронов в мишенях из материала с большим Z.



BETATRON - THE CYCLIC INDUCTIVE ACCELERATOR OF ELECTRONS БЕТАТРОН - ЦИКЛИЧЕСКИЙ ИНДУКЦИОННЫЙ УСКОРИТЕЛЬ ЭЛЕКТРОНОВ



Parameters / Параметры	МИБ-2,5 РХБ-2,5	МИБ-3	МИБ-4 РХБ-4	МИБ-6 РХБ-6	МИБ-7,5 РХБ-7,5	МИБ-10
Maximum energy of bremsstrahlung radiation, MeV / Максимальная энергия тормозного излучения, МэВ	2,5	3	4	6	7,5	10
Disc rate (mm) of distance L on base target, (mm) / Частота вращения диска на расстоянии L от основания, (об/мин)	0,1	2	1	3	5	16
Pulse frequency of radiation, Hz / Частота пульсов излучения, Гц	50	400	200	200	200	100
Power consumption, kVA / Потребляемая мощность, кВт	0,7	2,5	2,0	3,0	3,0	3,6
Mass of radiation, kg / Масса излучения, кг	27	50	56	100	110	275
Total mass of betatron, kg / Общая масса бетатрона, кг	45	120	120	180	220	405
Foot print size, mm / Размеры footprint в мм	0,2 x 3	0,2 x 3	0,25 x 3	0,25 x 3	0,25 x 3	0,3 x 3
Maximum testing thickness inverts, mm / Максимальная контролируемая толщина изделий, мм	-	130	150	250	300	350



The reactor under testing
Контролируемый реактор



Images of tested articles
Изображения контролируемых изделий

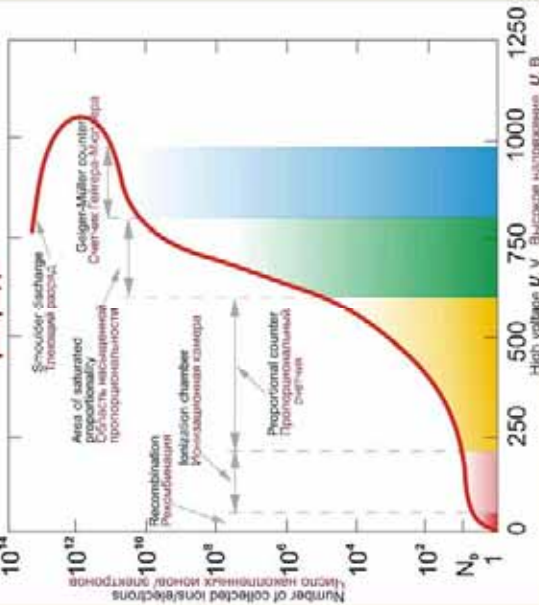


Bridge inspection
Инспекция моста



GAS-FILLED IONIZATION DETECTOR

Volt-ampere characteristic of gas discharge Вольт-амперная характеристика газового разряда



**UDRG-50 Detector (without housing)
Детектор УДРГ-50 (без кожуха)**

Dead time of gas ionization - time period after discharge arrears so within which the detector is incapable of registration the particles (photons).
Мертвое время - интервал времени после возникновения разряда, в течение которого газовый ионизационный детектор не способен регистрировать частицы (фотоны).

Resolution time - the least time period between two hits of ionizing particles into gas ionization detector at which those particles are capable of registration separately.
Время разрешения - наименьший интервал между двумя последовательными ионизирующими частицами в газовой ионизационной детекторе, при котором эти частицы регистрируются раздельно.

Recovery time - time period from the discharge beginning to the moment at which the amplitude of plateau pulse of gas voltage is established.
Время восстановления - интервал времени от начала разряда до момента, когда амплитуда бьешающего газового ионизационного детектора достигнет 0,5 максимального значения, возможного в данных условиях.



CTC-22 - γ -rays counter (счетчик γ -излучения)



S-IM-16 - neutron counter (счетчик нейтронов)



**End-window α and β -ray counter
СБМ-13**
Трещиновая α, β -ионизационная камера для тепловых нейтронов счетчик СБМ-13



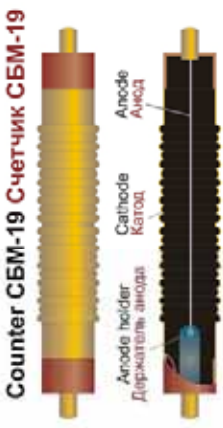
S-IM-56 - neutron counter (счетчик нейтронов)



Internal structure of S-IM-9 counter (Внутренняя структура счетчика СИМ-9)

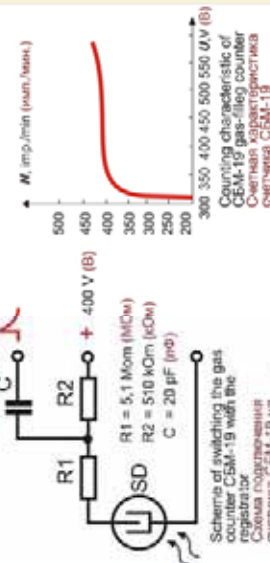


Internal structure of SBT-10 and β -ray counter (Внутренняя структура α, β -счетчика СБТ-10)



Counter SBM-19 Счетчик СБМ-19

Design of SBM-19 type counter Конструкция счетчика СБМ-19



General characteristics of SBM-19 counter
Основные характеристики счетчика СБМ-19

- registration range (for γ -radiation) $1 \cdot 10^3 \dots 3 \cdot 10^4$ μ R/s (мкР/с) - диапазон регистрации γ -излучения
- working voltage range 350 ... 475 V (В) - диапазон рабочего напряжения
- plateau length voltage of counter ... не менее 100 V (В) - протяженность плато счетной характеристики
- threshold voltage 280 ... 320 V (В) - напряжение начала счета



Ionization chamber for registration the beam of accelerated electrons
Ионизационная камера для регистрации пучка ускоренных электронов



Ionization chambers for registration the beam of radiation of neutron
Ионизационные камеры для регистрации тормозного излучения бетатрона

SCINTILLATION DETECTOR СЦИНТИЛЯЦИОННЫЙ ДЕТЕКТОР

Scintillators Сцинтилляторы

Organic Органические

- organic crystals органические кристаллы
- liquid and solid solutions of scintillating substances жидкие и твердые растворы сцинтиллирующих веществ
- organic gases органические газы

Inorganic Неорганические

- alkaline-halide щелочногалогенидные
- zinc-sulphide цинксульфидные
- oxide оксидные
- scintillators on the base of noble gases (liquid, solid and gas ones) сцинтилляторы на основе благородных газов (жидкие, твердые, газообразные)

General characteristics of scintillators

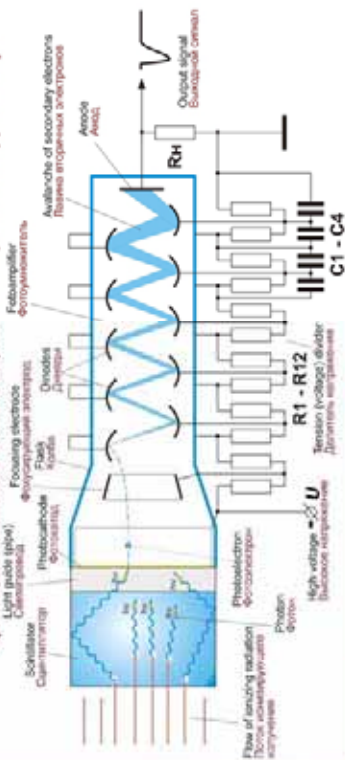
Основные характеристики некоторых сцинтилляторов

Scintillator Сцинтиллятор	Density, g/cm ³ Плотность, г/см ³	Atomic number Атомный номер	Luminescence decay time, ns Время высвечивания, нс	Scintillation efficiency (rel. eff.) Сцинтилляционная эффективность	Energy for formation of single photoelectron Энергия, необходимая для образования фотоэлектрона, эВ	Average energy of single photoelectron, eV Средняя энергия одного фотоэлектрона, эВ	Ratio of scintillation for α - and β -radiation, rel. Средняя относительная сцинтилляционная эффективность для α - и β -излучения, rel.
Inorganic Неорганические							
NaI(Tl)	3.67	32	250	0.153	19.6	3	0.5
CsI(Tl)	4.51	54	700	0.06	36.6	2.2	0.5
ZnS(Ag)	4.09	23	1000	0.1	27	2.7	1
Bi ₂ Ge ₂ O ₇	7.13	28	300	0.02	163.5	2.6	0.2
Organic Органические							
Антрацен (C ₁₄ H ₁₀)	1.25	6	25 - 30	0.034	81.4	2.77	0.1
Нафталин (C ₁₀ H ₈)	1.45	6	70 - 80	0.017	176.4	3.6	0.1
Стильбен (C ₁₄ H ₁₂)	1.16	6	4 - 8	0.03	116.6	3.5	0.1
Толуол (C ₇ H ₈)	1.18	6	4 - 7	0.032	96	3.16	0.1
Plastics Пластмассовые							
Terphenyle in polystyrene Терфенил в полистироле	1	6	5	0.015	210	3.1	0.1

Content of scintilblock (without housing) Состав сцинтиблока (без кожуха)



Principle scheme of scintillation detector Принципиальная схема сцинтилляционного детектора



General view of scintillators Общий вид сцинтилляторов



Usage of scintillation detectors: spectrometry of ionizing radiation; temporal measuring; measurement of spatial coordinates; registration of rare events. **Применение сцинтилляторов:** спектрометрия радиоактивного излучения; временная регистрация; измерение пространственных координат; регистрация редких событий.

Conversion (scintillation) efficiency: ratio of energy of light flash over the energy of charged particle absorbed with scintillator volume. **Конверсионная эффективность:** отношение энергии световой вспышки к поглощенной в объеме сцинтиллятора энергии заряженной частицы.

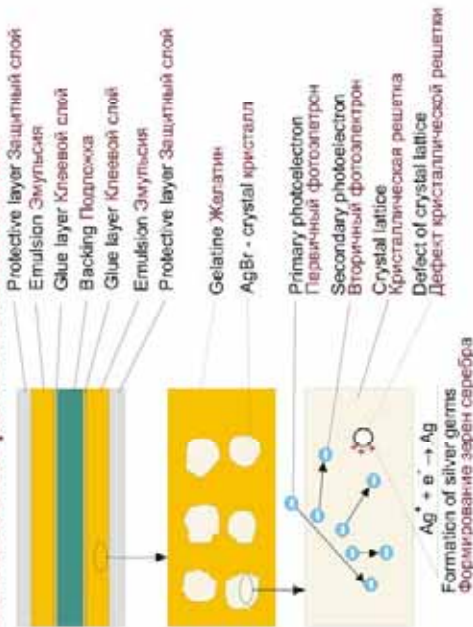
Technical efficiency: ratio of light energy withdrawn from scintillator over the energy of charged particle inside the scintillator. **Техническая эффективность:** отношение световой энергии, выходящей из сцинтиллятора, к энергии, поглощенной в нем частицей.

Фотоумножители Фотоэлектронные умножители

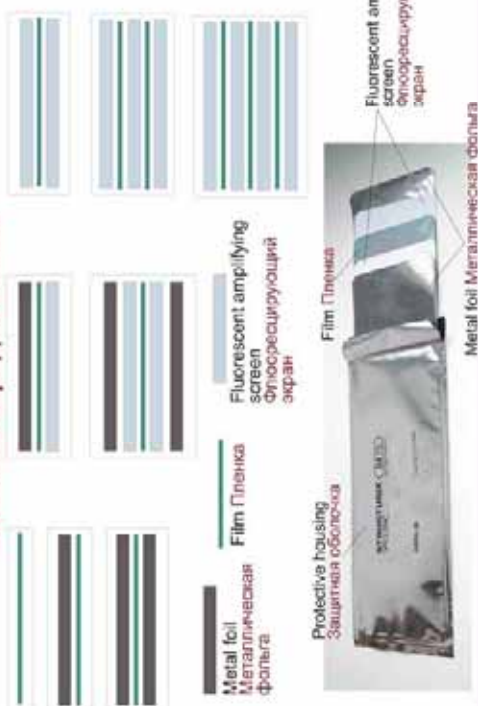


X-RAY FILM РЕНТГЕНОГРАФИЧЕСКАЯ ПЛЕНКА

Structure of layers of X-ray film Строение слоев рентгеновской пленки



Different ways of cassette loading Способы зарядки кассеты



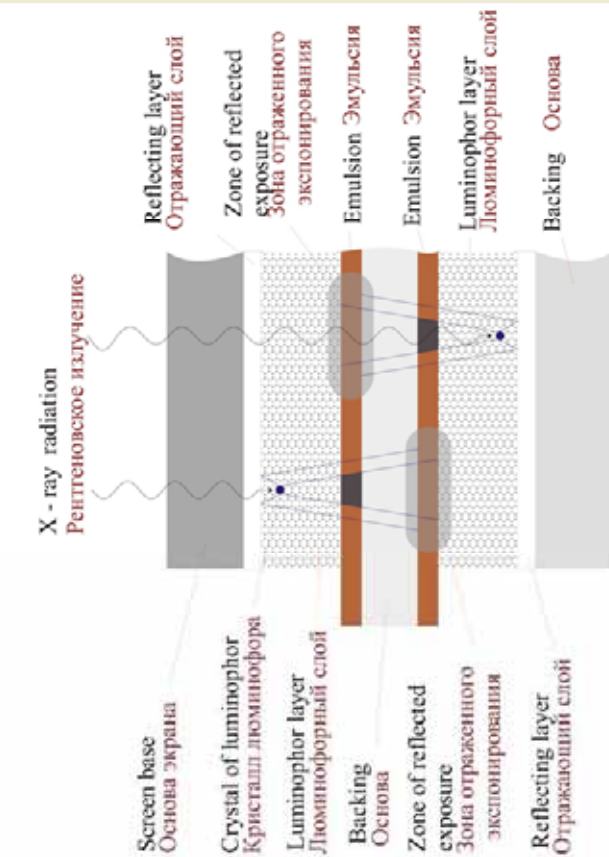
Classes of X-ray films and kinds of metal amplifying screens at radiography of steel and Cu-and Ni-based alloys. Классы пленок и типы металлических усиливающих экранов при радиографии стали и сплавов на основе Cu и Ni.

Source of ionizing radiation Источник ионизирующего излучения	Exposing thickness, mm Толщина, мм	Class of film Класс пленки	Kind and thickness of metal screen, mm Тип и толщина экрана, мм
Co ⁶⁰ Кобальт-60 ионизирующее излучение	U = 100 kV x 45	C3 (PT-4M)	White screen for with front and back screens 0.300-1.5 (Pt) Back screen 0.300-1.5 (Pt) Back screen 0.300-1.5 (Pt)
	U = 100-130 kV x 45	C4 (PT-5M)	Front and back screens 0.150-1.5 (Pt) Back screen 0.300-1.5 (Pt) Back screen 0.300-1.5 (Pt)
Ytterbium-169 (Yb-169) Иттербий-169	U = 150-250 kV x 45	C4 (PT-5M)	Front and back screens 0.150-1.5 (Pt) Back screen 0.300-1.5 (Pt) Back screen 0.300-1.5 (Pt)
	U = 150-250 kV x 75	C4 (PT-5M)	Front and back screens 0.150-1.5 (Pt) Back screen 0.300-1.5 (Pt) Back screen 0.300-1.5 (Pt)
Thulium-170 (Tm-170) Тулий-170	U = 250-400 kV x 45	C4 (PT-5M)	Front and back screens 0.150-1.5 (Pt) Back screen 0.300-1.5 (Pt) Back screen 0.300-1.5 (Pt)
	U = 250-400 kV x 75	C4 (PT-5M)	Front and back screens 0.150-1.5 (Pt) Back screen 0.300-1.5 (Pt) Back screen 0.300-1.5 (Pt)
Selenium-75 (Se-75) Селений-75	U = 100-150 kV x 45	C4 (PT-5M)	Front and back screens 0.150-1.5 (Pt) Back screen 0.300-1.5 (Pt) Back screen 0.300-1.5 (Pt)
	U = 100-150 kV x 75	C4 (PT-5M)	Front and back screens 0.150-1.5 (Pt) Back screen 0.300-1.5 (Pt) Back screen 0.300-1.5 (Pt)
Cesium-137 (Cs-137) Цезий-137	U = 100-150 kV x 45	C4 (PT-5M)	Front and back screens 0.150-1.5 (Pt) Back screen 0.300-1.5 (Pt) Back screen 0.300-1.5 (Pt)
	U = 100-150 kV x 75	C4 (PT-5M)	Front and back screens 0.150-1.5 (Pt) Back screen 0.300-1.5 (Pt) Back screen 0.300-1.5 (Pt)
Accelerators Ускорители	U = 1-4 MV x 45	C3 (PT-4M)	Back screen < 0.5 mm (Pt, Cu)
	U = 1-4 MV x 75	C3 (PT-4M)	Back screen < 0.5 mm (Pt, Cu)

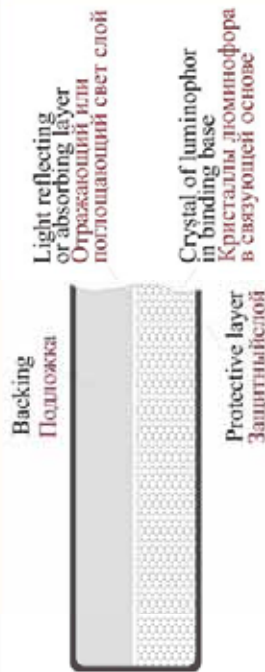
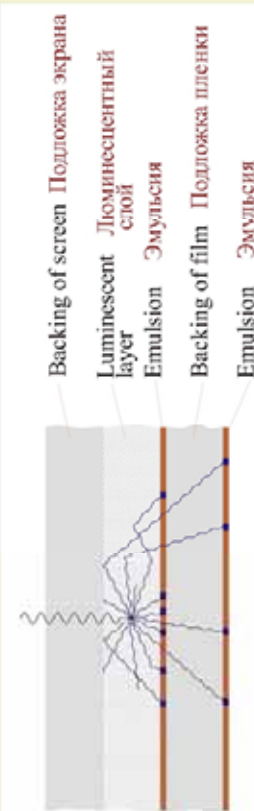
Comparison of the USA-films with Europe and Russian ones. Сравнение пленок США с европейскими и российскими.

USA film (USA) Пленка (США) ASTM (D54)	Class of accelerators with EN 584 Класс по EN 584	"AGFA-Gevaert" "Kodak" "Fujifilm"	"Kodak" "Kodak"	Russia X-ray film Виды пленки пленки
1	C1	DQ	DR	-
	C2	D3	M	PT-K
2	C3	D4	MC	PT-4M
	C4	D5	T	PT-5M
3	C5	D7	AJAX	PT-1
	C6	D8	CX	PT-2, PA-1

Main construction characteristics of luminescent screens Основные конструктивные характеристики люминесцентных экранов



1. The increase of luminescent layer thickness increases the sensitivity and light scattering.
Увеличение толщины люминесцентного слоя увеличивает чувствительность и светорассеяние.
2. Addition of reflecting layer or backing increases sensitivity and improves the spreading of light.
Добавление отражающего слоя или подложки увеличивает чувствительность и улучшает распространение света.
3. Addition of absorbing layer or backing reduces sensitivity and light scattering.
Добавление поглощающего слоя или подложки снижает чувствительность и светорассеяние.
4. Addition of light absorbing dye into the luminescent layer reduces the sensitivity and light scattering.
Добавка светопоглощающего красителя в люминесцентный слой снижает чувствительность и светорассеяние.
5. The decrease of luminophor particles size reduces the sensitivity and light scattering.
Уменьшение размеров частиц люминофора уменьшает чувствительность и светорассеяние.



COMPARATIVE CHARACTERISTICS OF DETECTORS

Qualitative coupling between some characteristics of registered radiation and parameters of electric signal of detector
 Качественная связь некоторых характеристик регистрируемого излучения и параметров электрического сигнала детектора

Radiation characteristics Характеристики излучения	Kind of detector Тип детектора		Analogue Аналоговые
	Discrete Дискретный	Proportional Пропорциональный	
Energy of particles or quanta Энергия частиц или квантов	Charge current pulse height Высота импульса зарядного тока	Discrete pulses Дискретные импульсы	-
Kind of particles Вид частиц	Form of current pulse Форма импульса тока	-	-
Moving trajectory Траектория движения	Form of current pulse Форма импульса тока	-	-
Time of passing through detector Время прохождения через детектор	Moment of current pulse zeroing Момент нулевания импульса тока	-	-
Flow density of particles or quanta Плотность потока частиц или квантов	Sum of current pulses Суммарный заряд за время t	-	Average current Средний ток
Dose power Мощность дозы	Average current Средний ток	-	Average current Средний ток
Dose during t period Доза за время t	Sum charge during t period Суммарный заряд за время t	-	Sum charge during t period Суммарный заряд за время t

Electric signal's data for some kinds of detectors

Kind of detector Тип детектора	Dimension factor (electron/MeV) Коэффициент преобразования (электрон/МэВ)	Charge (Coulomb/MeV) Заряд (кулумбы/МэВ)	Height (V/MeV) Высота (В/МэВ)
Pulse ionization chamber Импульсная ионизационная камера	$3 \cdot 10^8$	$5 \cdot 10^{-14}$	$0.25 \cdot 10^4$ E MeV (МэВ)
Proportional counter at $M = 10^4$ proportional Счетчик Гейгера-Мюллера	$3 \cdot 10^6$	$5 \cdot 10^{-14}$	0.25 E MeV (МэВ)
Geiger-Müller counter Счетчик Гейгера-Мюллера	-	$4 \cdot 10^{-14}$	30
Halogen filled Галогенный	-	$5 \cdot 10^{-14}$	80
Scintillation counter with photodiode (P) Сцинтилляционный счетчик с фотодиодом (ФД)	$3 \cdot 10^8$ M	$5 \cdot 10^{-14}$	1.0 E MeV (МэВ)
Scintillation counter (P-n) Детектор П-Н сцинтилляционный (P-n)	$3 \cdot 10^8$	$5 \cdot 10^{-14}$	$1 \cdot 10^4$ E MeV (МэВ)

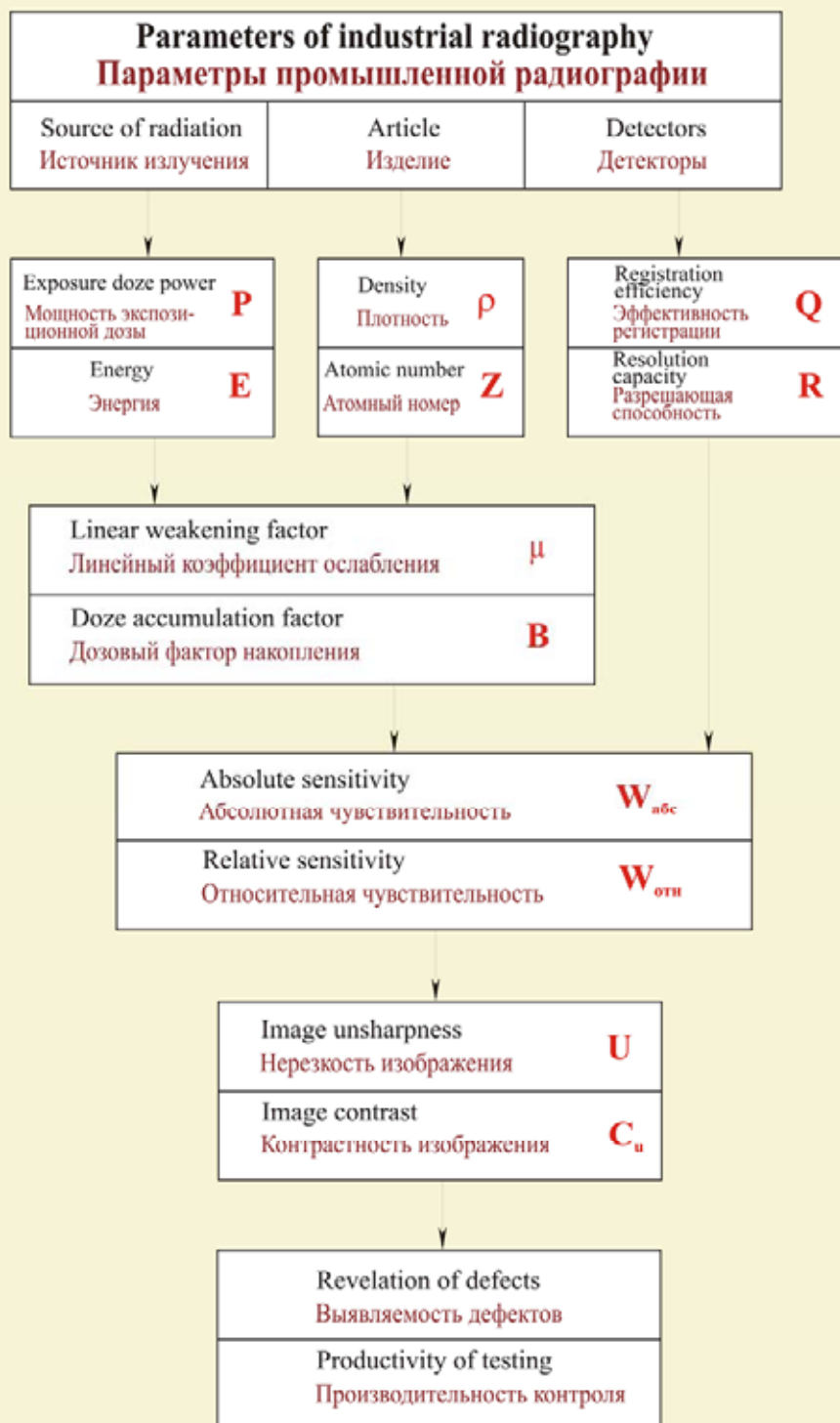
Comparison of detectors from the view of achieved volume of information

Сравнение детекторов по объему информации

Type of detectors Тип детектора	Kind of registered radiation Вид регистрируемого излучения										Energy distribution data Данные об энергетическом распределении										Temporal distribution data Данные о временном распределении									
	α	β	γ	X	n	α	β	γ	X	n	α	β	γ	X	n	α	β	γ	X	n	α	β	γ	X	n					
Pulse ionization chamber Импульсная ионизационная камера	+	+	+	+	+	+	+	+	+	+	+	+	+	+	+	+	+	+	+	+	+	+	+	+	+					
Current ionization chamber Токовая ионизационная камера	+	+	+	+	+	+	+	+	+	+	+	+	+	+	+	+	+	+	+	+	+	+	+	+	+					
Scintillation counter Сцинтилляционный счетчик	+	+	+	+	+	+	+	+	+	+	+	+	+	+	+	+	+	+	+	+	+	+	+	+	+					
Geiger-Müller counter Счетчик Гейгера-Мюллера	+	+	+	+	+	+	+	+	+	+	+	+	+	+	+	+	+	+	+	+	+	+	+	+	+					
gas газовый	+	+	+	+	+	+	+	+	+	+	+	+	+	+	+	+	+	+	+	+	+	+	+	+	+					
liquid жидкостный	+	+	+	+	+	+	+	+	+	+	+	+	+	+	+	+	+	+	+	+	+	+	+	+	+					
plastic пластиковый	+	+	+	+	+	+	+	+	+	+	+	+	+	+	+	+	+	+	+	+	+	+	+	+	+					
single crystal однокристаллический	+	+	+	+	+	+	+	+	+	+	+	+	+	+	+	+	+	+	+	+	+	+	+	+	+					
monocrystal монокристаллический	+	+	+	+	+	+	+	+	+	+	+	+	+	+	+	+	+	+	+	+	+	+	+	+	+					
p-n p-n	+	+	+	+	+	+	+	+	+	+	+	+	+	+	+	+	+	+	+	+	+	+	+	+	+					
intrinsic type пропороводящего типа	+	+	+	+	+	+	+	+	+	+	+	+	+	+	+	+	+	+	+	+	+	+	+	+	+					

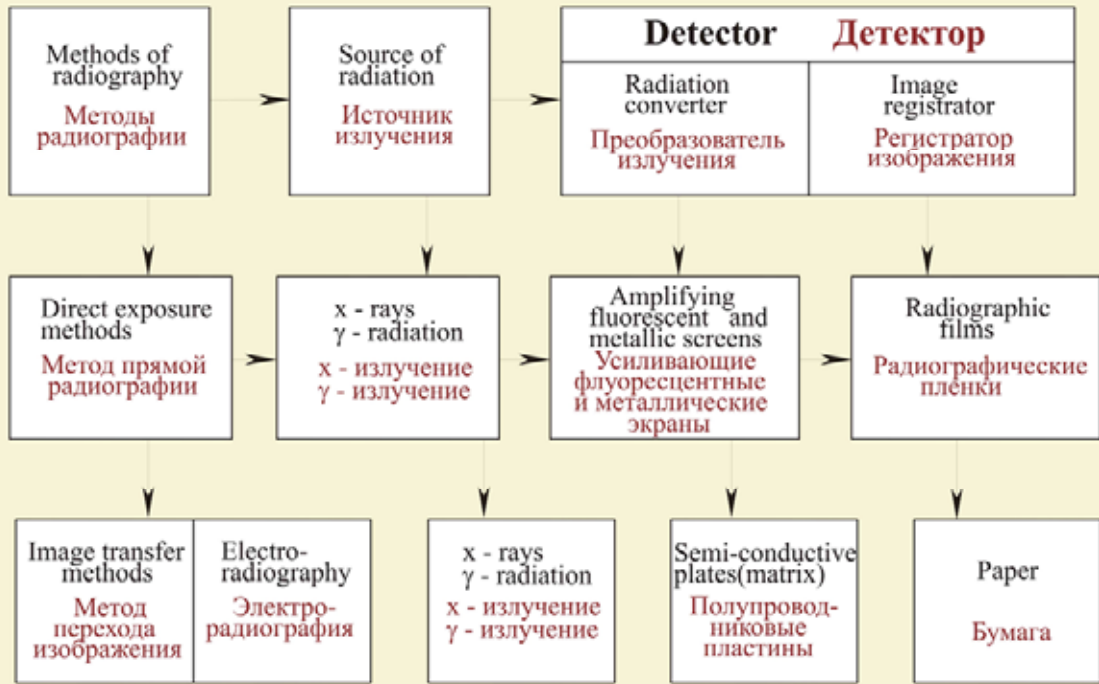


Main parameters of industrial radiography Основные параметры промышленной радиографии



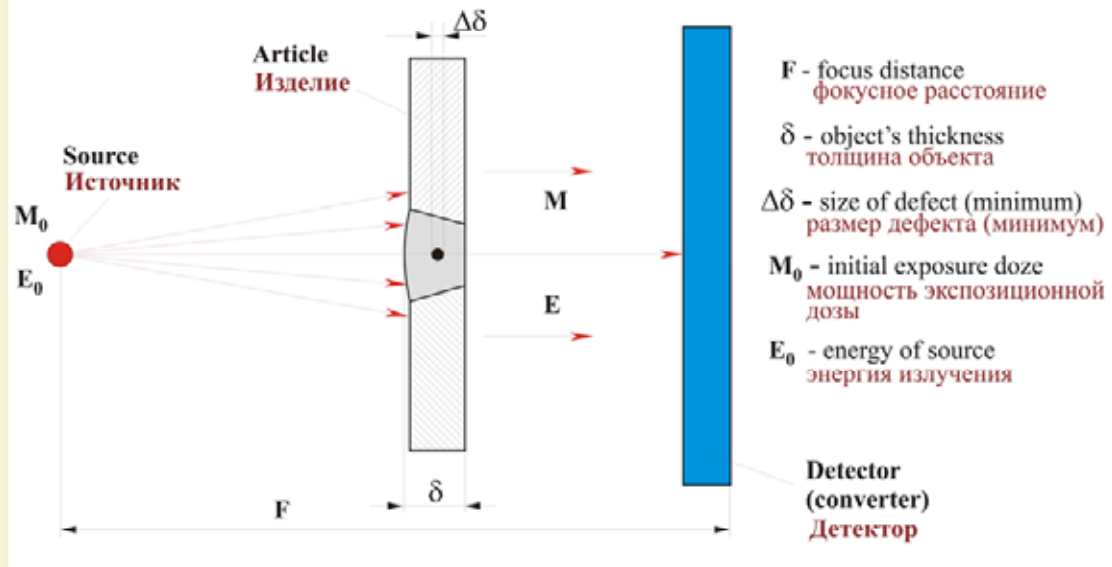
Industrial radiography methods

Классификация методов промышленной радиографии

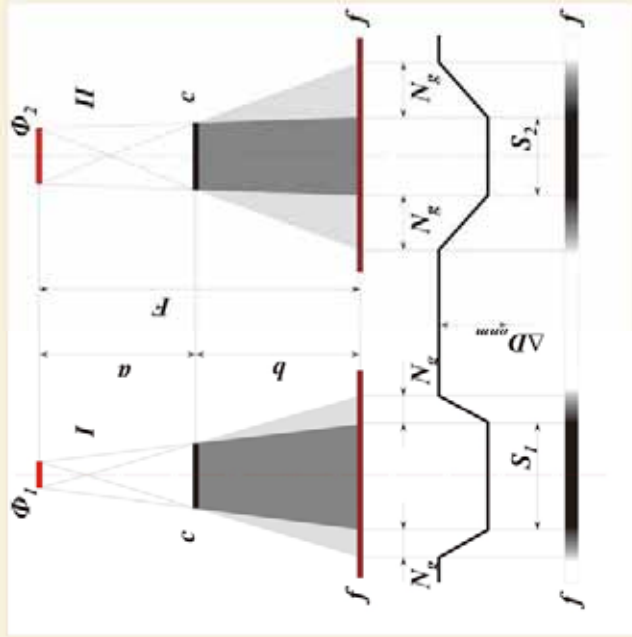


Examining scheme

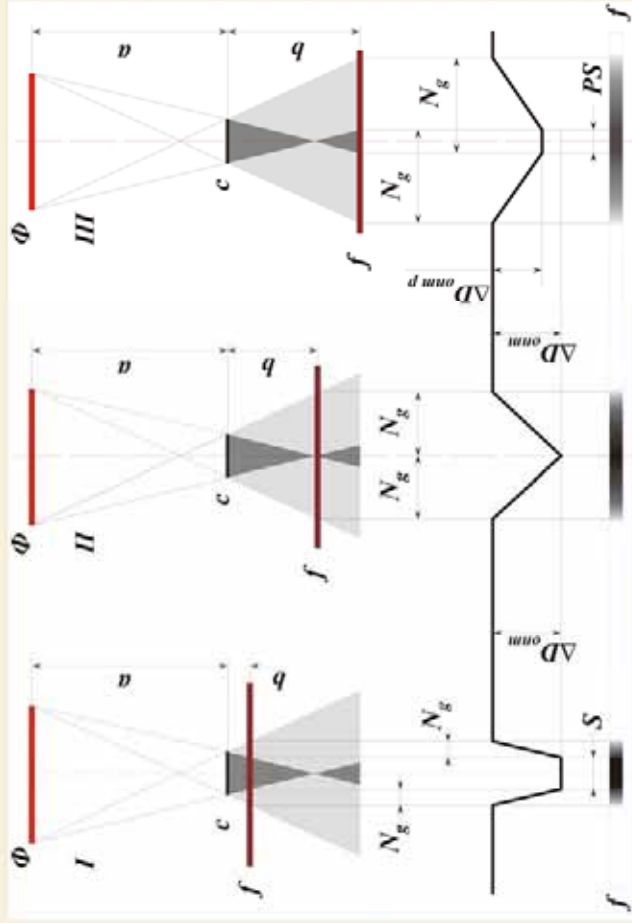
Схема просвечивания



Necessary conditions of clear shoots receiving
Условия получения четких снимков



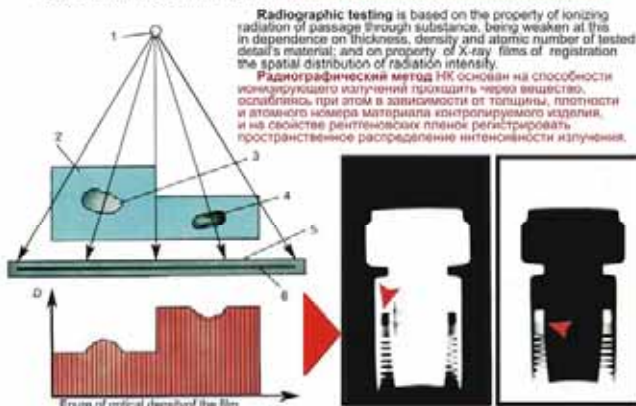
- Φ_1 and Φ_2 - foci of X-ray tube (фокусные пятна рентгеновской трубки);
- C - plate for defect simulation (предмет, имитирующий дефект);
- f - X-ray film (рентгеновская пленка);
- N_g - border (geometrical) unsharpness (граничная нерезкость);
- S_1 and S_2 - total blackening (полное затемнение);
- ΔD_{omn} (ΔD_{omn}) - image contrast (контрастность);



- Φ - focus of X-ray tube (фокусное пятно рентгеновской трубки);
- C - plate for defect simulation (предмет, имитирующий дефект);
- f - X-ray film (рентгеновская пленка);
- N_g - border (geometrical) unsharpness (граничная нерезкость);
- S - total blackening (полное затемнение);
- PS - pseudo-shadow (псевдотень);
- ΔD_{omn} (ΔD_{omn}) - image contrast (контрастность);
- ΔD_{opr} (ΔD_{opr}) - pseudo-shadow image contrast (контрастность псевдотени).

BASES OF RADIOGRAPHIC TESTING ОСНОВЫ РАДИОГРАФИЧЕСКОГО КОНТРОЛЯ

SCHEME OF IMAGE FORMATION / СХЕМА ФОРМИРОВАНИЯ ИЗОБРАЖЕНИЯ



Radiographic testing is based on the property of ionizing radiation of passage through substance, being weakened at this in dependence on thickness, density and atomic number of tested detail; and on property of X-ray films of registration the spatial distribution of radiation intensity.

Радиографический метод НК основан на способности ионизирующего излучения проходить через вещество, ослабляясь при этом в зависимости от толщины, плотности и атомного номера материала контролируемого изделия, и на свойстве рентгеновских пленок регистрировать пространственное распределение интенсивности излучения.

X-ray shot of defective zone. The maximum gap between trivette duct and tubular head is shown by the arrow.
Рентгеновский снимок дефектного шва. Стрелочками указан максимальный зазор между трубной головкой и дуговой трубкой.

DEFECTOSCOPIC CHARACTERISTICS OF RADIOGRAPHY METHOD / ДЕФЕКТОСКОПИЧЕСКИЕ ХАРАКТЕРИСТИКИ МЕТОДА

DEFECTOSCOPIC CHARACTERISTICS	X-RAY TESTING (РЕНТГЕНОВСКИЙ КОНТРОЛЬ)	GAMA TESTING (ГАММА-КОНТРОЛЬ)
Maximum examining thickness, mm. for steel	20 - 70* 100 - 350	60 - 120* 100 - 350
Maximum examining thickness, mm. for aluminum	20 - 70* 100 - 350	60 - 120* 100 - 350
Typical exposure	2 - 10 min	1 - 3 hour
Technical resolution	2 - 10 mm	1 - 3 +
Character of defects explored (within range of method's sensitivity)	Surface, subsurface and internal cracks, pores, inclusions, fusion, faulty welding, corrosion coverage, shifting inside of metal's elements.	Surface, subsurface and internal cracks, pores, inclusions, fusion, faulty welding, corrosion coverage, shifting inside of metal's elements.
Control panel	Электронный	Механический

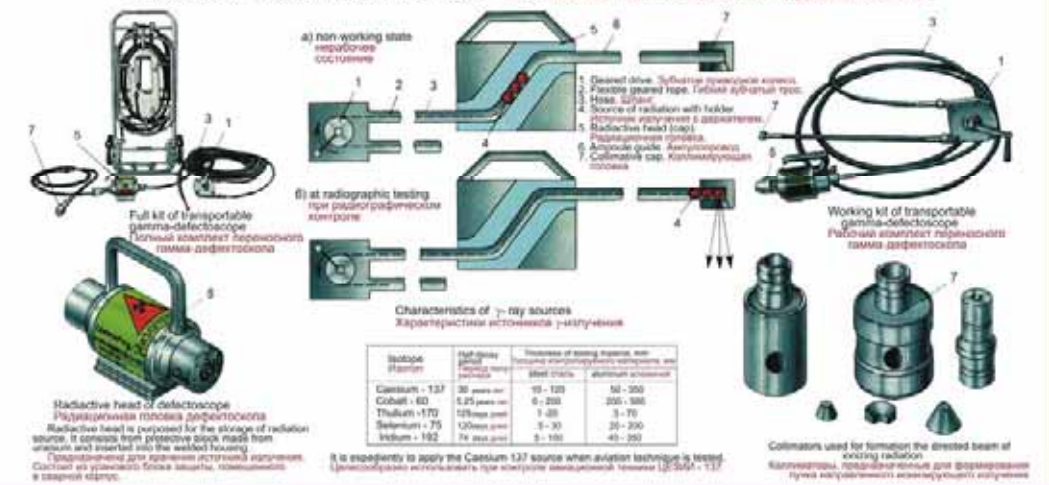
*Based on the technical characteristics of gamma X-ray apparatus and gamma-defectoscope. Прибор, оборудованный электронным управлением.

At testing the aggregates consisting from details with different mass density and having such examining thickness more than 20 mm, the radiographic method is preferable.
At testing the single details, the X-ray radiography is preferable.
При контроле агрегатов, состоящих из деталей с различной плотностью деталей и имеющих такую же или большую толщину более 20 мм, предпочтительнее использовать радиографический метод.
При контроле деталей предпочтительнее использовать рентгеновский метод.

STRUCTURE OF X-RAY APPARATUS / УСТРОЙСТВО РЕНТГЕНОВСКОГО АППАРАТА



STRUCTURE OF HOSE GAMMA-DEFECTOSCOPE / УСТРОЙСТВО ШЛАНГОВОГО ГАММА-ДЕФЕКТОСКОПА



ESTIMATION OF OBJECT'S TECHNICAL CONDITION BY RADIOGRAPHY ОЦЕНКА ТЕХНИЧЕСКОГО СОСТОЯНИЯ ОБЪЕКТОВ РАДИОГРАФИЧЕСКИМ МЕТОДОМ

ONE CAN REVEAL: ВЫЯВЛЯЮТСЯ:

**Mutual position of details
Взаимное положение деталей**



Fuel pump
Топливный насос

Circuit protection automatic device
Автомат защиты сети


**Form and sizes of details
Форма и размеры деталей**




Fuel burner
Топливная форсунка

Roller
Вал

**Strange subjects
Посторонние предметы**

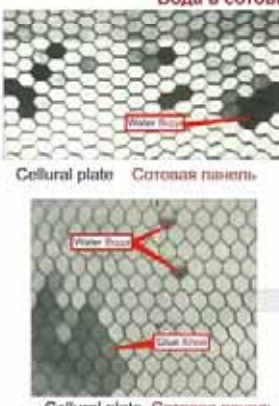


Terminal board of electroconnectors
Колodka электроразъемов



Hydraulic amplifier
Гидроусилитель

**Water in cellural constructions
Вода в сотовых конструкциях**

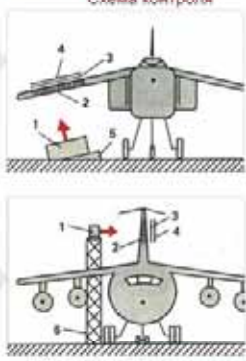


Cellural plate
Сотовая панель

Cellural plate
Сотовая панель

Sensitivity of radiographic testing of cellural constructions (height of water pole in a cell) - 1.5 - 3 mm depending upon the material and plate wall thickness.
Чувствительность рентгенографического контроля сотовых конструкций (высота столба воды в ячейке) - 1,5 - 3 мм в зависимости от материала и толщины стенки.

**Testing scheme
Схема контроля**



1. X-ray apparatus. Рентгеновский аппарат.
2. Cellural plate. Сотовая панель.
3. Cassette with X-ray film. Кассета с пленкой.
4. Protective screen. Защитный экран.
5. Appliance. Приспособление.

**Air pores, inclusions, cracks, corrosive coverages
Воздушные поры, включения, трещины, коррозионные поражения**



Brace of chassis leg
Подкос стойки шасси

Pores
Поры

Sensitivity of radiography at exposure of defects of welding and bonding in steel alloys.
Чувствительность рентгенографического контроля сварных соединений и соединений стальных сплавов.

Kind of connection	Depth	Width	Length
Welding	0.5 mm	0.2 mm	1 - 3 mm
Bonding	0.5 mm	0.2 mm	1 - 3 mm
Welding	0.5 mm	0.2 mm	1 - 3 mm
Bonding	0.5 mm	0.2 mm	1 - 3 mm
Welding	0.5 mm	0.2 mm	1 - 3 mm
Bonding	0.5 mm	0.2 mm	1 - 3 mm
Welding	0.5 mm	0.2 mm	1 - 3 mm
Bonding	0.5 mm	0.2 mm	1 - 3 mm

At 1 - 1.5 mm range, the testing sensitivity is 1.5 - 2 times more than at X-ray control.

Скорость дефектов при эксп. при контроле дюралюминия и магния не более 2 раз выше чем при рентгенографическом контроле.

При контроле дюралюминия и магния чувствительность контроля более 1.5 - 2 раз выше, чем при контроле рентгенографическим методом.

Чувствительность контроля при эксп. при контроле дюралюминия и магния более 1.5 - 2 раз выше, чем при контроле рентгенографическим методом.



Housing of combustion chamber
Корпус камеры сгорания

Crack
Трещина



Fire bottle (balloon)
Пожарный баллон

Rising corrosion
Язвенная коррозия



Stringer of wing
Стрингер крыла

Shearing corrosion
Расслоивающая коррозия

Sensitivity of roentgenographic testing at exposure the coverages of duraluminum articles by the shearing corrosion is within 10 - 13 % of the examining thickness, but not less than 0.6 - 0.9 mm.
Чувствительность рентгенографического контроля при выявлении расслоивающей коррозии дюралюминиевых деталей 10 - 13 % просвечиваемой толщины, но не менее 0.6 - 0.9 мм.

TECHNOLOGY OF RADIOGRAPHIC TESTING ТЕХНОЛОГИЧЕСКИЕ ОПЕРАЦИИ РАДИОГРАФИЧЕСКОГО КОНТРОЛЯ

1 PREPARING OF TESTING OBJECT, APPLIANCES AND ACCESSORIES ПОДГОТОВКА К КОНТРОЛЮ ОБЪЕКТА, ПРИНАДЛЕЖНОСТЕЙ И ПРИБОРОБЛАГОВЕНИЙ

Finally, the two-side access to testing object is provided. Sludge details that can shade the testing zone must be eliminated. The object is cleaned from solutions and wastes. Then tested zones are marked, working appliances and accessories, lead marking signs are chosen at once with sensitivity standards and amplifying screens.

Обеспечивают двусторонний доступ к контролируемому объекту (детали), демонтируют детали, затеняющие объект. Очищают от загрязнений и отходов объект. Размечают зоны контроля. Подбирают принадлежности, стандарты чувствительности, экраны усиления.

Marking of oil block. Разметка маслоблока на участке контроля



In order to reveal the defects of material, one must perform the testing using the sensitivity standards. Контроль с целью выявления дефектов материала выполняется с использованием чувствительности.



The wire standard is used at cracks and faulty holes exposure. Проволочный эталон используют при выявлении трещин и дефектов.

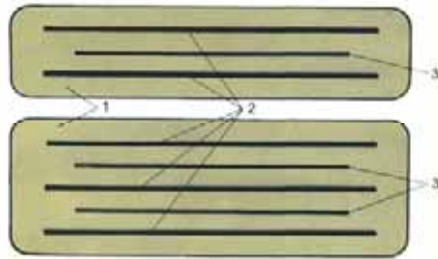
Slab standard is used at joints, welds and fissures exposure. Кладочный эталон применяют при выявлении стыков, швов, трещин.

2 CASSETTE LOADING ЗАГРУЗКА КАССЕТ

At radiographic testing the PT-5 film is used in: at gamma-graphic testing - the PCT-5 film. The film is charged (loaded) in light protected cassette at conditions of dark or non-acting dark red light. At cassette sizes choosing, one must provide film overlapping not less than 20 mm of adjacent zones of testing sections.

При радиационном контроле используют пленку ПТ-5 при гаммаграфическом контроле - пленку ПКТ-5. Пленку заправляют в радиационнозащищенные кассеты при отсутствии или слабом красном свете. При выборе формата кассеты должны быть обеспечены перекрытия соседних зон зоны контроля не менее 20 мм.

Loading variants Варианты загрузки



1. Cassette or back paper. Кассета или задняя бумага.
2. Amplifying screen. Усиляющий экран.
3. X-ray film. Радиационная пленка.

Usage of two films inside single cassette make it easy the separation of film defects from real defects of testing object at interpretation. Использование в кассете двух пленок облегчает при расшифровке снимков отделение дефектов пленки от дефектов объекта контроля.

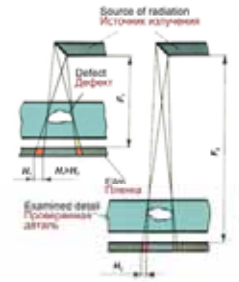
The usage of fluorescent amplifying screens is not recommended. Не рекомендуются флуоресцентные экраны.

3 CHOICE OF EXAM REGIME ВЫБОР РЕЖИМА

Focus distance F Фокусное расстояние F

At X-ray testing, the focus distance $F > 750$ mm is expedient. At gamma-graphic testing $F > 500$ mm. The decrease of focus distance can lead to the increase of geometric unsharpness M .

Целесообразно выбирать при рентгеновском контроле $F > 750$ мм, при гаммаграфическом контроле - $F > 500$ мм. Уменьшение фокусного расстояния ведет к росту геометрической нерезкости M .



Anode tension U and current I (for X-ray apparatus) Анодные напряжения U и ток I (для рентгеновского аппарата)

Thickness of material, mm Толщина материала, мм	Fe	St	Al	Mg	U, kV, not more U, кВ, не более
1,5	5	29	46		80
6	14	66	92		120
12	29	60	150		150
20	45	97	160		200
40	90	180	270		400
130	230	370			1000

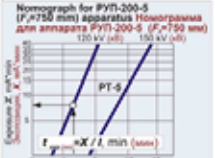
Anode current is chosen to be maximum with account of permissible loading on X-ray tube. Анодный ток выбирают максимально с учетом допустимых нагрузок на рентгеновскую трубку.

Permissible loadings on X-ray tube of PPT-200-5 apparatus Допустимые нагрузки на трубку аппарата PPT-200-5

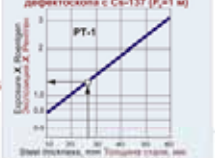
Tension on tube, kV Напряжение на	Current, mA Амперы, мА	Time, min Время, мин
120 - 200	3	5
70 - 130	5	5

X-raying length t_{exp} Продолжительность просвечивания t_{exp}

t_{exp} is calculated with a help of nomographs 1 and 2.

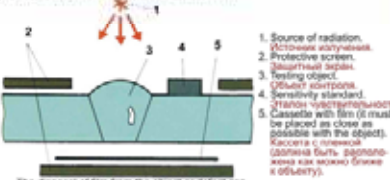


Nomograph for defectoscope with Cs-137 Номаграмма для дефектоскопа с Cs-137

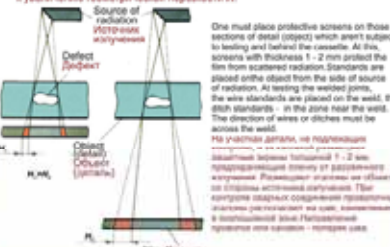


P_{max} is exposure dose power on distance F in focus source of radiation. P_{max} - мощность экспозиционной дозы на расстоянии F от источника.

4 PLACING OF RADIATION (SOURCE), OBJECT, CASSETTE AND ACCESSORIES РАЗМЕЩЕНИЕ ИСПУЩАТЕЛЯ, ОБЪЕКТА, КАССЕТЫ И ПРИНАДЛЕЖНОСТЕЙ



The disposal of film from the object or defect can lead to increase of geometric unsharpness M . Удалять пленку от объекта ведет к увеличению геометрической нерезкости M .



One must place protective screens on those sections of detail (object) which aren't subject to testing and behind the cassette. At the screens with thickness 1 - 2 mm arched the film from scattered radiation standards are placed on the object from the side of source of radiation. At testing the welded joints, the wire standards are placed on the weld, the slits standards - in the zone near the weld. The direction of wires or slits must be across the weld.

5 X-RAYING ПРОСВЕЧИВАНИЕ

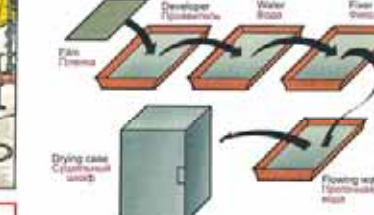


At exposure time the personnel is near the control panel, looks after the readiness of devices and corrects the exposure regime if need. Radiation dose power in area close to apparatus panel or panel of gamma-defectoscope must not be more than 2.8 mR/hour.

Во время экспозиции персонал находится у пульта управления, следит за готовностью приборов и при необходимости корректирует режим просвечивания. Мощность дозы излучения у пульта аппарата или гамма-дефектоскопа не должна превышать 2.8 мР/час.

6 PHOTOTREATMENT ФОТООБРАБОТКА

Phototreatment is performed at nonactinic dark-red light. Фотообработку проводят при неактивном темнокрасном свете.



Regimes of phototreatment Режимы фотообработки

Parameter Параметр	Developer Развиватель	Intermediate fixing Промывка	Fixing Фиксирование	Final washing Полоскание	Drying Сушка
Temperature, °C Температура, °C	18-22	18-22	18-22	18-22	18-22
Length, min Длина, мин	4-8	0.5-1	10-20	20-30	30-120

7 INTERPRETING OF RADIOGRAPH РАСШИФРОВКА СНИМКОВ

Estimation of quality of image (grade) is carried out. The contrast and sharpness of image must meet the standard radiograph. The value of optical density must be from 1.3 to 1.8 units of actual density. Recommended equipment: densitometer for optical density measurement; magnifying glass for radiograph; filter; magnifying glass; magnifying glass; magnifying glass.

Recommended equipment: densitometer for optical density measurement; magnifying glass for radiograph; filter; magnifying glass; magnifying glass; magnifying glass.



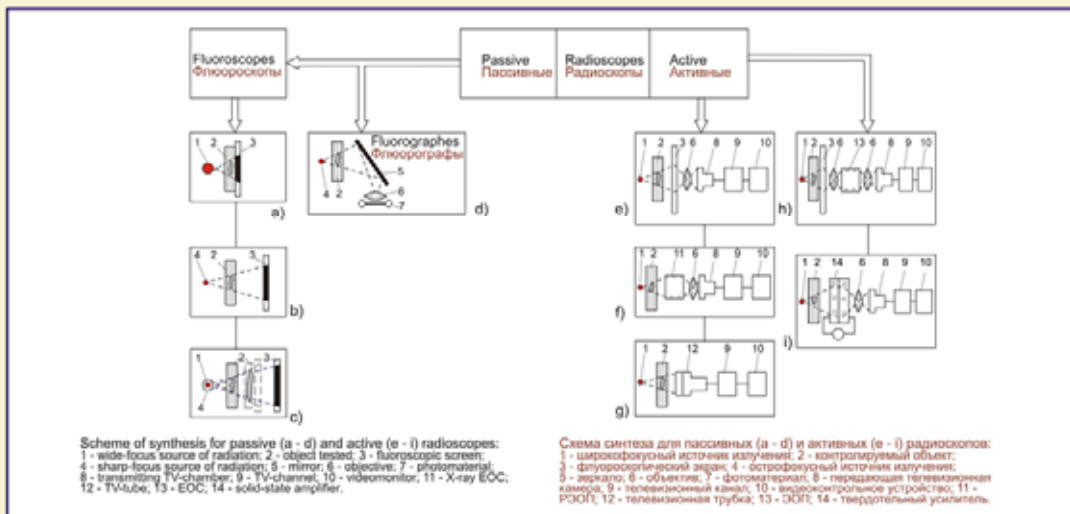
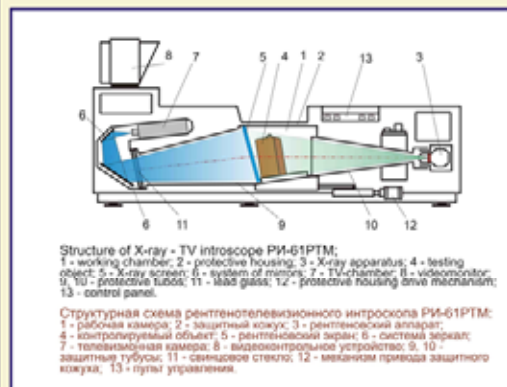
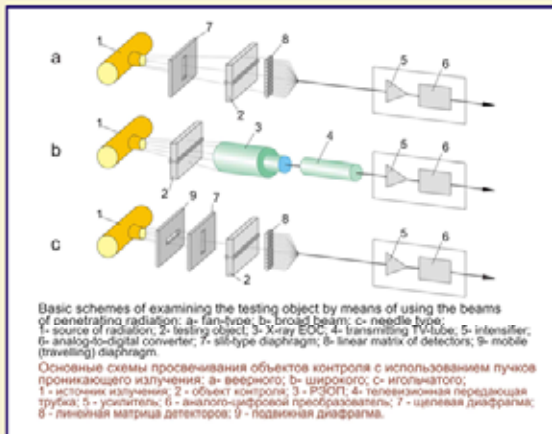
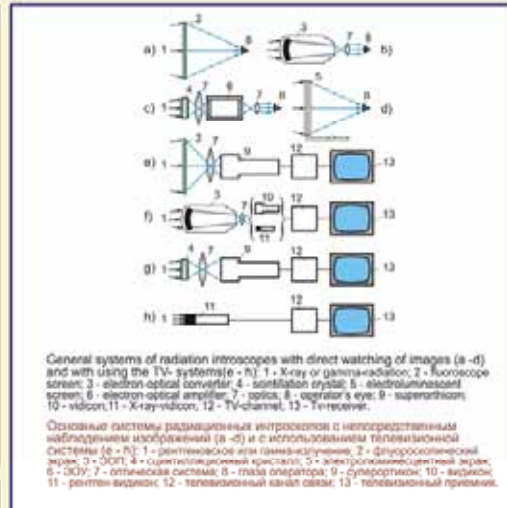
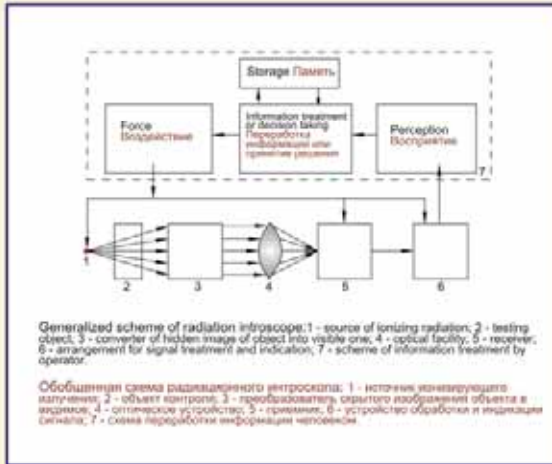
Recommended conditions: starting point, grade of radiograph with adjusting brightness of screen within (200 - 300) cd/m², maximum film-edge distance 40 mm. At determination the real sizes of defects, gaps of it, the values measured on the radiograph must be multiplied by the factor $k = \frac{F}{F-d}$, where F is distance between source and defect (detail); d is defect.

Recommended conditions: starting point, grade of radiograph with adjusting brightness of screen within (200 - 300) cd/m², maximum film-edge distance 40 mm. При определении реальных размеров дефектов, щелей их значения, измеренные на радиограмме, должны быть умножены на коэффициент $k = \frac{F}{F-d}$, где F - расстояние от источника до исследуемого объекта (детали), d - фактическое расстояние от дефекта до пленки.

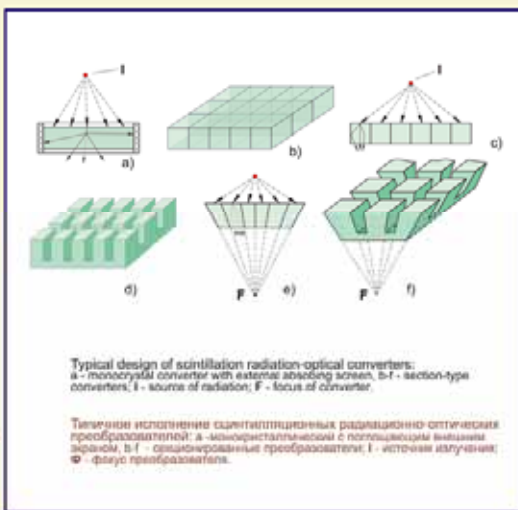
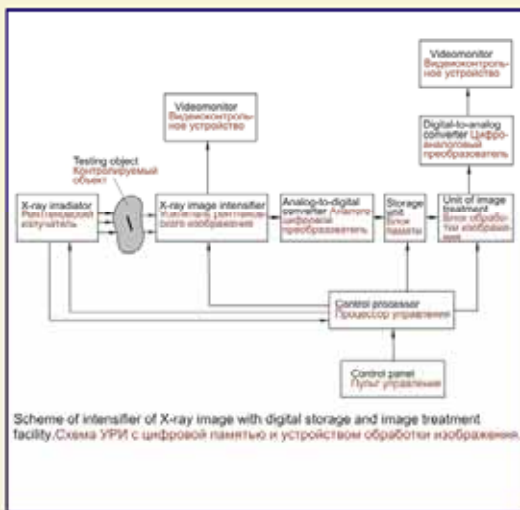
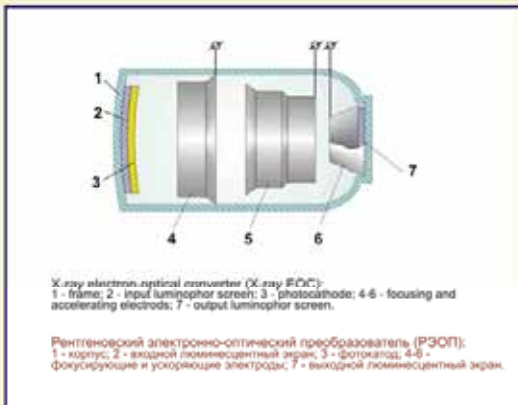
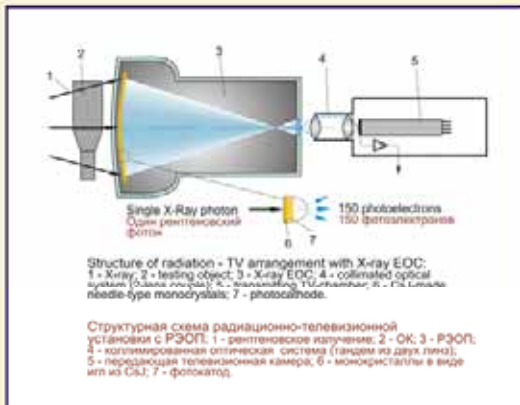
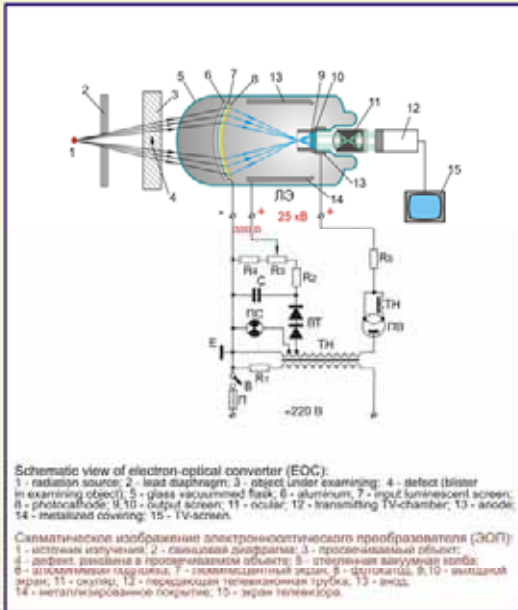
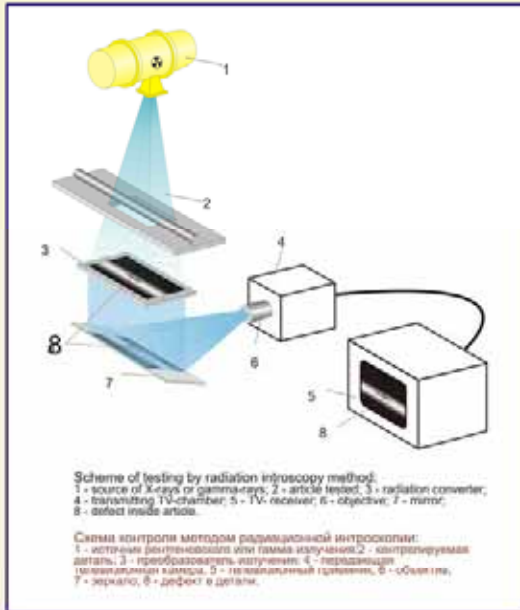
RADIOSCOPY (RADIATION INTROSCOPY) РАДИОСКОПИЯ (РАДИАЦИОННАЯ ИНТРОСКОПИЯ)

Radioscopy is based on the examining of object tested by the penetrating radiation, converting the hidden radiation image of the object into the visual light-shadow or electronic image, and transmitting those images on certain distance by means of optic facility or TV-receiver. At this, it is foreseen that an operator participates actively in the process of analysis the achieved light-shadow picture of the internal structure of the object tested.

Радиоскопия основана на просвечивании объекта контроля проникающим излучением, преобразовании скрытого радиационного изображения объекта контроля в видимое светотеневое или электронное изображение и передаче этих изображений на расстояние с помощью оптического устройства или телевизионного приемника. При этом предусматривается активное участие оператора в процессе анализа светотеневой картины внутреннего строения объекта контроля.



RADIOSCOPY (INTROSCOPES STRUCTURE'S ELEMENTS) РАДИОСКОПИЯ (ЭЛЕМЕНТЫ СТРУКТУР ИНТРОСКОПОВ)

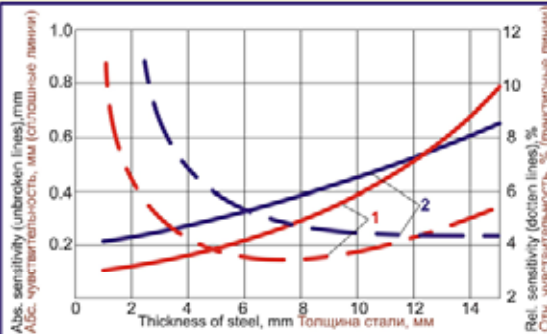


RADIOSCOPY (SENSITIVITY OF METHOD) РАДИОСКОПИЯ (ЧУВСТВИТЕЛЬНОСТЬ МЕТОДА)

Formulae for absolute and relative sensitivity of radiography method Формулы для абсолютной и относительной чувствительности метода радиоскопии

$$\Delta l = \frac{\Delta S \times B}{S \times \mu} \quad (\text{mm}) \qquad \frac{\Delta l}{L} = \frac{\Delta S \times B}{S \times \mu \times L} \quad (\%)$$

- μ - linear coefficient of weakening of X-ray and gamma-radiation in testing object's material линейный коэффициент ослабления рентгеновского и гамма-излучения в материале контролируемого объекта;
- L - object thickness in examining zone толщина объекта в месте просвечивания;
- B - accumulation factor of radiation scattered inside the testing object's material фактор накопления излучения, рассеянного в материале контролируемого объекта;
- $\frac{\Delta S}{S}$ - threshold contrast of eye пороговый контраст глаза.

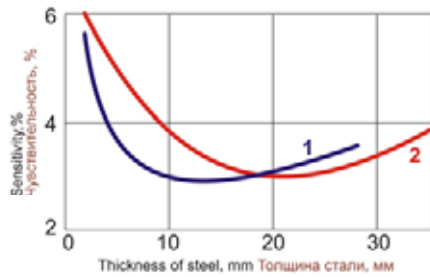


Sensitivity of method (using stepped standards with holes) at steel testing by X-ray apparatus РУП-150-150-10-1 with X-ray tube of 0.3 БПВ6-type and different convertes:

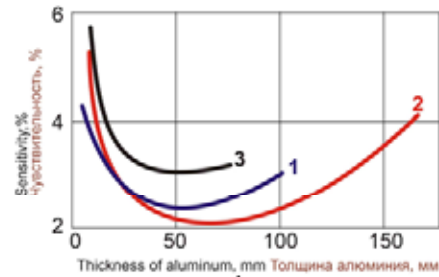
- 1 - X-ray-TV system with X-ray-vidicone tube ЛИ-417;
- 2 - scintillation crystal CsI and TV arrangement with superortikon ЛИ-17.

Чувствительность метода (по ступенчатым эталонам с отверстиями) при контроле стали с использованием рентгеновского аппарата типа РУП-150-10-1 с трубкой 0.3 БПВ6 и различных преобразователей:

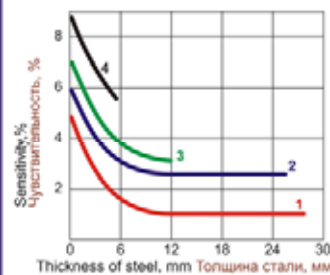
- 1 - рентгено-телевизионная система с рентген-видикомом ЛИ-417;
- 2 - сцинтилляционный кристалл CsI телевизионная установка с суперортиконом ЛИ-17.



Sensitivity of method at steel examining (a) and aluminum examining (b):
1 - fluoroscopic screen and optimal magnification 3x-6x;
2 - electron-optical converter, magnification 2x; 3 - fluoroscopic screen, magnification 2x.



Чувствительность метода при просвечивании стали (а) и алюминия (б):
1 - флуороскопический экран, оптимальное увеличение 3x - 6x;
2 - ЭОП, увеличение 2x; 3 - флуороскопический экран, увеличение 2x.



Comparative data concerning sensitivity of method at steel examining: 1 - radiography; 2 - EOC with additive optics; 3 - EOC with TV-system; 4 - fluoroscopic screen.

Сравнительные данные по чувствительности метода при просвечивании стали: 1 - радиография; 2 - ЭОП с дополнительной оптикой; 3 - ЭОП и телевизионная система; 4 - флуороскопический экран.

Sensitivity at aluminum testing Чувствительность при контроле алюминия

Tube voltage, kV Напряжение на трубке, кВ	Tube current, mA Ток трубки, мА	Al thickness, mm Толщина алюминия, мм	Sensitivity, % Чувствительность, %	Tube voltage, kV Напряжение на трубке, кВ	Tube current, mA Ток трубки, мА	Al thickness, mm Толщина алюминия, мм	Sensitivity, % Чувствительность, %
50	40	6.2	2	90	40	38.0	1.5
60	40	12.6	2	100	40	50.8	1.5
70	50	18.8	1.5	110	35	63.4	1.5
80	50	25.4	1.5	120	33	76.2	1.5

CONTENTS

PREFACE	3
CHAPTER 1. PRINCIPLES OF THE RADIATION TESTING	5
1.1. The spectrum of the electromagnetic radiation.....	5
1.2. The formation and properties of the X-radiation	6
1.2.1. The formation.....	6
1.2.2. Properties	10
1.3. X-ray and gamma–radiation interaction processes	10
1.3.1. X-ray and gamma-radiation	10
1.4. Physical principles of the radiation image formation and basic characteristics.....	15
1.4.1. Radiation contrast	15
1.4.2. Geometrical unsharpness	18
1.4.3. Dynamic unsharpness	20
1.4.4. The screen or own unsharpness	21
1.4.5. Other sources of the image unsharpness. The sum unsharpness	22
1.4.6. The frequency-contrast characteristics	24
1.4.7. Quantum fluctuations of the ionizing radiation and their influence on the threshold contrast.....	29
1.4.8. The information capacity of the image formation system	31
1.5. Control tasks.....	33
CHAPTER 2. RECEIVING AND REGISTRATION OF ROENTGEN AND GAMMA-RADIATION	39
2.1. Sources of X-ray and gamma-radiation	39
2.1.1. X-ray apparatus	39
2.1.2. Radioisotopic sources	41
2.1.2.1. Isotopes for the materials testing.....	41
2.1.2.2. Equipment for the testing by isotopes	43
2.1.3. Betatrons	44
2.1.4. Linear accelerators	51
2.1.5. Microtrones	55
2.2. The receiving of the examining picture by means of the X-ray film.....	58
2.3. Fluoroscopy and the roentgen radiation intensifiers	62
2.4. Detectors of the X-radiation.....	64
2.4.1. The semi-conductive detector	64

2.4.2. The gas ionization detectors.....	73
2.4.2.1. Impulsed ionization chamber	73
2.4.2.2. Gas-filled proportional detector	78
2.4.2.3. The Geiger-Muller counter.....	81
2.4.3. Scintillation detector	86
2.5. coNtrol tasks.....	92
2.6. set of tests on sections: “Principles of radiation testing; sources of radiation; detectors of ionizing radiation”	95
CHAPTER 3. RADIOGRAPHY	100
3.1. Bases of radiography	100
3.2. TYPE METHODS OF RADIOGRAPHIC TESTING	107
3.2.1. Types regimes	108
3.2.2. Selection of radiation energy (tension between electrodes of X-ray tube, accelerator energy or energy of radionuclidic source)	111
3.2.3. Choice of type of radiation source (X-ray equipment, gamma-defectoscope, accelerator).....	116
3.2.4. Determining of radiation intensity (anode current of X-ray tube, radiation yield of pulse X-ray apparatus, radionuclidic sources and electron accelerators).	117
3.2.5. Choice of X-ray films and amplifying screens	117
3.2.6. Choice of focus distance or distance between source and object	122
3.2.7. Optical density of shots.....	125
3.2.8. Choice of size of tested section and evaluation of number of sections tested	126
3.2.9. Calculation of exposure time	127
3.2.10. Chemical – photographic development of exposed X-ray film and its storage.....	133
3.2.11. Interpreting of shots and rejection of joints, patterns and articles	135
3.3. Control tasks.....	137
3.4. SET OF TEST QUATIONS ON SECTION “RADIOGRAPHY”	139
CHAPTER 4. RADIATION INTROSCOPY (RADIOSCOPY).....	143
4.1. Introduction	143
4.2. Choice of radiation sources	150
4.3. Choice of energy of radiation.....	151
4.4. Fluoroscopy	153
4.5. Brightness of screen luminescence	156
4.6. Screen’s unsharpness	156
4.7. Spectral structure of luminescence.....	156
4.8. Interpreting of fluoroscopic images	160
4.9. Determination of defect’s sizes	161

4.10. Fluorography	162
4.11. Amplifiers of radiation images.....	162
4.12. Radiation image amplifiers	164
4.13. TV – arrangements	165
4.14. Usage of fluoroscopy	166
4.14. Type methods of selection of regimes of radioscopy	170
4.15. Control tasks.....	173
4.16. Set of test quations on section “Radioscopy”	174
CHAPTER 5. WORK SAFETY IN THE RADIATION DEFECTOSCOPY	178
5.1. Dosimetric values in the radiation safety	178
5.1.1. Ionizing radiations.....	178
5.1.2. Parameters of the ionizing radiation field.....	180
5.1.3. Coefficients of the ionizing radiation interaction with the material	181
5.1.4. Penetrating capacity of the ionizing radiation and the linear energy transfer.....	183
5.1.4.1. Alpha – radiation	184
5.1.4.2. Beta – radiation.....	185
5.1.4.3. Gamma – radiation	185
5.1.5. Dosimetric values.....	187
5.1.5.1. Kerma	187
5.1.5.2. The exposure dose	187
5.1.5.3. The absorbed dose	188
5.1.5.4. The equivalent dose.....	189
5.1.5.5. Effective dose	191
5.1.5.6. The additional dosimetric values.....	193
5.1.6. Radioactivity parameters.....	194
5.2. Complex of technical means and measures for the labour safety provision in radiation defectoscopy	197
5.2.1. Danger factors and the safety system structure in radiation defectoscopy	197
5.2.2. Protection from the ionizing radiations.....	200
5.2.3. Providing of the safety at the conducting of the radiation defectoscopy	210
5.3. Control tasks to the section “Work safety in the radiation defectoscopy”	214
REFERENCES	217
APPENDIX 1	219
APPENDIX 2	237
APPENDIX 3	270

Educational Edition

Томский политехнический университет

ЕФИМОВ Павел Васильевич

КУЛЕШОВ Валерий Константинович

РАДИАЦИОННЫЙ КОНТРОЛЬ

Учебное пособие

Издательство Томского политехнического университета, 2008

На английском языке

Typesetting

K.S. Chechel'nitskaya

Cover design

O.Yu. Arshinova

O.A. Dmitriev

Signed for the press 15.12.2008. Format 60x84/16. Paper "Snegurochka".

Print XEROX. Arbitrary printer's sheet 13.67. Publisher's signature 12.36.

Order 739. Size of print run 200.



Tomsk Polytechnic University
Quality management system
of Tomsk Polytechnic University was certified by
NATIONAL QUALITY ASSURANCE on ISO 9001:2000



TPU PUBLISHING HOUSE. 30, Lenina Ave, Tomsk, 634050, Russia